A bioinformatic analysis of the role of mitochondrial biogenesis in human pathologies

Robert Bentham

A dissertation submitted in partial fulfillment

of the requirements for the degree of

Doctor of Philosophy

of

University College London.

Department of Cell and Developmental Biology

University College London

Monday 11th July, 2016

Declaration

I, Robert Bentham, confirm that the work presented in this thesis is my own. Where information has been derived from other sources, I confirm that this has been indicated in the work.

July, 2016

Robert Bentham

Abstract

Disease states are often associated with radical rearrangements of cellular metabolism; suggesting the transcriptome underlying these changes follows a distinctive pattern. Identification of these patterns is complicated by the hugely heterogeneous nature of these diseases, such as cancer, and the patterns remain hidden within noise of large datasets. A new biclustering algorithm called Massively Correlating Biclustering (MCbiclust) was developed to identify these patterns. Taking a large gene set such as those known to be associated with the mitochondria, samples are selected in which these genes are highly correlated. Rigorous benchmarking of this method with other biclustering methods on synthetic gene expression data and an *E. coli* data set show it to be superior in finding these patterns.

This method was used to identify the role mitochondrial biogenesis plays in cancer; applied on the Cancer Cell Line Encyclopedia (CCLE) it identified differences in mitochondrial function based on the different tissue of origin of the cell line. In patient breast tumour samples a change in mitochondrial function was identified and linked to differences in known breast cancer subtypes.

Breast cancer cell lines were identified that matched this pattern. Experimentally testing these cell lines confirming the significant difference in gene expression expected and also showed significant changes in mitochondrial function demonstrated by measurements in oxygen consumption, proteomics and metabolomics.

MCbiclust has been developed into an R package. Using this method, new cancer subtypes can be identified, based on fundamental changes to known pathways. The benefit is twofold: first to increase understanding of these complex systems and second to guide treatment using drug compounds known to target these pathways. The methods described here while applied to cancer and mitochondria, are versatile and can be applied to any large dataset of gene expression measurements.

Acknowledgements

First, I would like to express my utmost thanks to my supervisors Professor Gyorgy Szabadkai and Dr. Kevin Bryson; without their support, guidance, expert knowledge, kindness, and access to the Department of Computer Science coffee machine, this work could have never been completed.

I would like to thank the British Heart Foundation for funding my research and giving me the financial backing that I vitally needed.

I would like to thank Professor Michael Duchen and everyone involved with the Szabadkai Lab both past and present: Drs. Jose Vicencio, Zhi Yao, Ronan Astin, Will Kotiadis, Thomas Blacker and Nicoletta Plotegher for their patience in helping me with experimental techniques and welcoming me to the lab. I would also like to thank my fellow PhD students: Julia Hill, Jenny Sharpe, Pedro Dias, Stephanie Sundier, Neta Amior and Gauri Bhosale, all of whom helped me enormously and better than that made the entire experience fun! I would also like to thank Sam Ranasinghe for his work in maintaining much of the equipment in the lab and teaching me how to use the microscopes.

I would like to thank everyone involved in CoMPLEX, a department whose existence made possible my transition from mathematics to biological research, and without which I certainly would never have embarked on this work.

I thank my fellow Szabadkai lab PhD student Michella Menegollo at the University of Padova who greatly contributed to the experimental work of this project, and Dr. Mariia Yuneva of the Crick Institute for her collaboration and help on this project.

Finally, I would have never been able to complete this huge undertaking without the constant support of my family and friends.

List of my publications

The following publications were produced during my PhD but not related to the topic of this thesis:

Astin, R., Bentham, R., Djafarzadeh, S., Horscroft, J. A., Kuc, R. E., Leung, P. S., Skipworth, J. R., Vicencio, J. M., Davenport, A. P., Murray, A. J. et al. (2013), 'No evidence for a local renin-angiotensin system in liver mitochondria', *Scientific reports* **3**.

Tosatto, A., Sommaggio, R., Kummerow, C., Bentham, R. B., Blacker, T. S., Berecz, T., Duchen, M. R., Rosato, A., Bogeski, I., Szabadkai, G. et al. (2016), 'The mitochondrial calcium uniporter regulates breast cancer progression via hif-1α', *EMBO molecular medicine* **8**(5), 569–585.

Contents

List of Figures

List of Tables

Abbreviations

ADP adenosine diphosphate.

ANOVA analysis of variance.

ATP adenosine triphosphate.

BAT brown adipose tissue.

cAMP cyclic adenosine monophosphate.

CCLE Cancer Cell Line Encyclopedia.

cDNA complementary DNA.

CoRR co-location for redox regulation.

CREB cAMP response element binding protein.

DBD DNA-binding domain.

ER estrogen receptor.

ERR estrogen-related receptor.

ERRα estrogen-related receptor α.

ERRβ estrogen-related receptor β.

ERRγ estrogen-related receptor γ.

ETC electron transport chain.

FABIA Factor Analysis for Bicluster Acquisition.

FPR false positive rate.

GABP GA-binding protein.

GISTIC genomic identification of significant targets in cancer.

GO gene ontology.

GSEA gene set enrichment analysis.

HCM hypertrophic cardiomyopathy.

HER2 human epidermal growth factor receptor 2.

ICD implantable cardioverter-defibrillator.

ICT1 immature colon carcinoma transcript 1.

KEGG Kyoto encyclopedia of genes and genomes.

MCbiclust Massively Correlating Biclustering.

MEF2A myocyte-specific enhancer factor 2A.

MELAS mitochondrial encephalomyopathy, lactic acidosis, and stroke-like episodes.

miRNA micro RNA.

mRNA messenger RNA.

mtDNA mitochondrial DNA.

mTOR mammalian target of rapamycin.

NAD+ nicotinamide adenine dinucleotide (oxidised).

NADH nicotinamide adenine dinucleotide (reduced).

NCoR1 nuclear receptor corepressor 1.

NPI Nottingham prognostic index.

NRF-1 nuclear respiration factor 1.

NRF-2 nuclear respiration factor 2.

OXPHOS oxidative phoshporylation.

PAM prediction analysis for microarrays.

PC1 the first principal component.

PCA principal component analysis.

PD Parkinson's disease.

PGC peroxisome proliferator-activated receptor gamma coactivator.

PGC-1 peroxisome proliferator-activated receptor gamma coactivator 1.

PGC-1α peroxisome proliferator-activated receptor gamma coactivator 1-α.

PPAR peroxisome proliferator-activated receptor.

PPAR δ peroxisome proliferator-activated receptor δ.

PPARα peroxisome proliferator-activated receptor α.

PPARγ peroxisome proliferator-activated receptor γ.

PPI protein-protein interaction.

PR progesterone receptor.

PRC PGC-1 related coactivator.

q-PCR quantitative polymerase chain reaction.

RMA robust multi-array average.

ROC receiver operator characteristics.

ROR risk of recurrence.

ROS reactive oxygen species.

RPKM reads per kilobase per million mapped reads.

SNP single nucleotide polymorphism.

SSD signal sensing domain.

TAD trans-activating domain.

TCA tricarboxylic acid.

TF transcription factor.

TFAM transcription factor A mitochondrial.

TPR true positive rate.

tRNA transfer RNA.

YY1 Yin Yang 1.

Chapter 1

Introduction

1.1 Mitochondria

1.1.1 The basics of mitochondrial function

Mitochondria are compartments within the cell, cellular organelles, separated from the rest of the cell by an outer membrane and divided within itself by an inner membrane. This double membrane organelle thus has two subspaces, the inter-membrane space and the mitochondrial matrix.

The basic structure of a mitochondrion is given in Figure 1.1 and is remarkably complex. The inner membrane contains numerous folds called cristae that are utilised to maximise its surface area used for performing important biological reactions.

Inside the mitochondrial matrix there are multiple copies of mitochondrial DNA (mtDNA) as well as mitochondrial ribosomes for the protein synthesis of 13 protein encoding genes and 22 transfer RNAs (tRNAs). This is a system for the synthesis of specific proteins that is separate from the normal protein synthesis pathway in the nucleus and cytosolic ribosomes. Numerous proteins assemble into pores in both the inner and outer membrane and are involved in the transport of biological molecules across the membranes, composing part of a vast cellular transport and signalling networks. In addition to the complexity of mitochondrial structure, their organisation is highly regulated, with mitochondria fusing and dividing with the many others, forming complex networks.

Regarding the complexity of the structure and organisation of mitochondria, it is perhaps surprising that the function they are widely known for is merely energy production. This suggests that provision of energy for the cell is not a simple process,

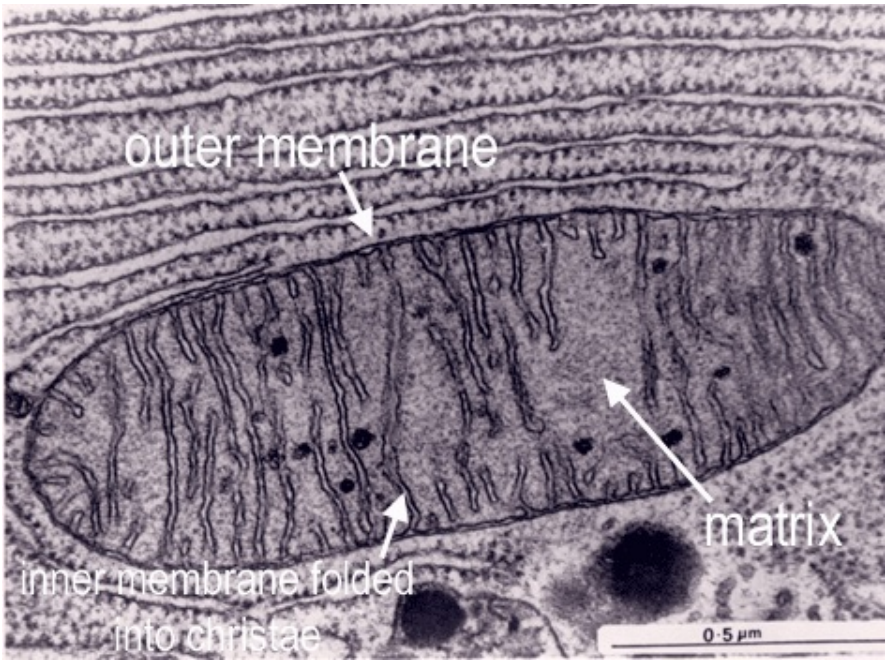

Figure 1.1: The basic stucture of a mitochondrion, electron microscope image taken from *The Histology Guide University of Leeds* (2016).

and depends on many forms of regulation.

The standard eukaryotic cell has a basic energetic problem; the transport and storage of energy. The cell can use energy from catabolism, the breaking down of organic matter through metabolic pathways. However the processes that use this energy in the cell (e.g. the synthesis of DNA, RNA and proteins as well as mechanical, signalling and transport functions) will not always take place at either the same rate as the energy made available by catabolism or in the same physical location. Thus for this release of energy from catabolism to be useful to the cell, it must be able to be stored and transported to where it is needed. This is the role adenosine triphosphate (ATP) play in the cell and mitochondria are the organelles primarily responsible for its production. Therefore mitochondria need to be regulated to adjust the rate of ATP production and meet the energetic needs of the cell.

ATP stores energy in the form of chemical potential energy, the molecule contains two phosphoanhydride bonds which when cleaved through the process of hydrolysis release energy. This energy released then can be used to drive numerous reactions throughout the cell.

The method mitochondria use to create ATP is through a process called oxidative phoshporylation (OXPHOS). The process starts within the citric acid cycle (also known

as the tricarboxylic acid (TCA) cycle), a 9 step process that converts pyruvate to oxaloacetate. In the final step from malate to oxaloacetate, a coenxyme called nicotinamide adenine dinucleotide (reduced) (NADH) is produced. NADH is the reduced form of this molecule, and as such it is able to donate two electrons converting it to nicotinamide adenine dinucleotide (oxidised) (NAD+). In this case the electrons are donated to the first member of the electron transport chain (ETC), complex I.

The ETC is a series of 5 enzyme complexes on the inner mitochondrial membrane, that pass along electrons. In doing so a proton gradient is formed with protons being pumped from the mitochondrial matrix to the inter-membrane space. Complex V, or ATP synthase, makes use of the potential energy from the pH gradient and electrical potential energy by pumping protons back into the mitochondrial matrix and in doing so coverts adenosine diphosphate (ADP) to ATP (Mitchell 1961). A diagram explaining this process is given in Figure 1.2

1.1.2 The role of mitochondria in apoptosis and their evolutionary history

Much more recently after the discovery of mitochondria being responsible for the energy production in the cell, a second key role was found: apoptosis. Apoptosis is a type of programmed cell death. In a multi-cellular organism there is often a need for certain cells to die. This occurs during development, but it also takes place when a cell is damaged in some way and is an essential process for homeostasis.

Mitochondrial outer membrane permeabilisation (MOMP), is considered the point of no return for apoptosis (Chipuk et al. 2006), at this point proteins that are normally only present in the mitochondrial inter-membrane space are released to the entire cell. One of these proteins released during MOMP is cytochrome c. Cytochrome c, normally part of the ETC, once released into the cell forms a cofactor with the apoptosis protease-activating factor-1, a transcription factor that initiates the formation of the apoptosome that causes a cascade of actions in the cell resulting in apoptosis.

MOMP is primarily regulated by family of BCL-2 proteins that act as sensors of cellular stress and interact with proteins on the outer mitochondrial membrane. Some such as Chipuk et al. (2006) argue that while being integral to this apoptosis pathway, mitochondria are themselves innocent bystanders in the decision to undergo apoptosis.

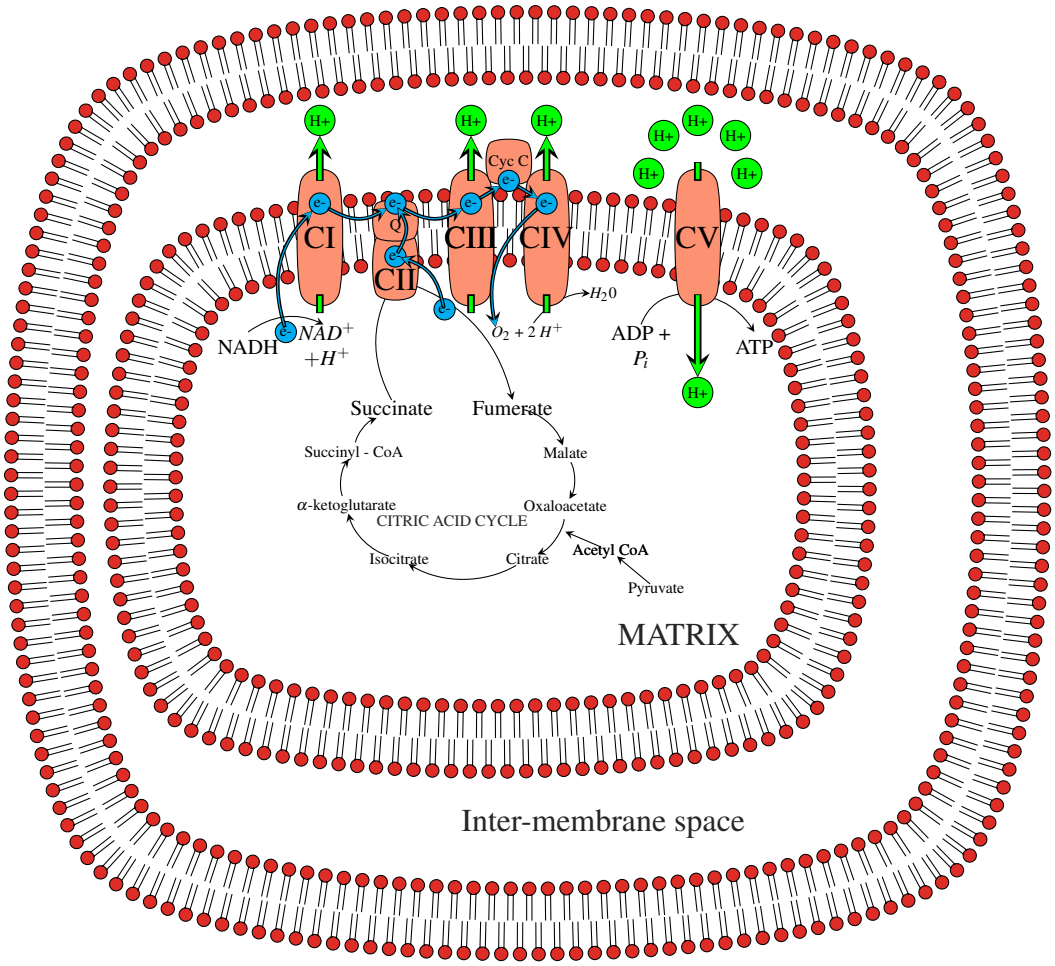

Figure 1.2: OXPHOS system and citric acid cycle within the mitochondrion. The blue arrows represent the flow of electrons in the ETC, electrons enters the respiratory chain at either complex I via NADH being oxidised to NAD+ or originating from succinate via complex 2, succinate dehydrogenase, which catalyzes the oxidation of succinate to fumarate in the citric acid cycle. Electrons leave the ETC at complex IV to reduce oxygen to H_2O. Throughout the electron chain, electrons are passed from donors to acceptors and at each stage this releases energy, used to pump protons across the mitochondrial membrane, creating a proton gradient, which is then used to power the phosphorylation of ADP to ATP at complex V, or ATP synthase. NADH itself is produced from the citric acid cycle. The green arrows in the diagram show the flow of protons in the OXPHOS system. Note this is a schematic drawing and not representative of the structure of the mitochondrion.

Stress in the mitochondria however can also lead to apoptosis, with mtDNA damage causing superoxide generation also shown to cause MOMP (Ricci et al. 2008). mtDNA have been further shown to be involved during apoptosis, with released oxidised mtDNA causing activation of the inflammasome, and hence inflammation of the cell during apoptosis (Shimada et al. 2012).

Maintaining this fine balance between cell growth and cell death is not the only

purpose of the mitochondria within the cell and they are at the centre of many other pathways. For example mitochondria take up calcium from the cell and are responsible for the regulation of number of free calcium ions. In this way they are highly involved in the calcium-signalling pathway (Szabadkai 2008).

Mitochondria have some unique properties due to their evolutionary history, and this should be understood when attempting to understand their regulation. Mitochondria are thought to be ancestors of what were once independently living prokaryotic cells. It is believed that roughly 2 billion years ago a prokaryotic cell thought to be closely related to *Rickettsia prowazekii* entered a host Archaea cell (Andersson et al. 1998). This endosymbiotic event gave rise to the entire domain of the Eukaryota (Lane 2005). Since this event occurred mitochondria are no longer free-living and possibly parasitic bacteria, but form an essential component of the eukaryotic cell. They no longer have a completely independent genome with the vast majority of their genes now encoded in the cellular nucleus. They do however retain a small amount of their own DNA, the reason for which is currently unknown. One theory called the co-location for redox regulation (CoRR) hypothesis explains this is so certain genes will be under direct regulatory control of the individual mitochondria, allowing them to quickly react to the specific redox state of the organelle (Allen 1993). This DNA is also not subjected to normal Mendelian transfer across generations but is inherited from the mother to child.

1.2 Mitochondrial heterogeneity

1.2.1 The mitochondrial proteome

An important feature about mitochondria is their heterogeneity, between tissues, following adaption to changing cellular conditions and even between different mitochondria in a single cell. This is especially relevant when studying disease states in which there has been a detrimental change in their function. One way of studying mitochondrial heterogeneity is by examining changes in the mitochondrial proteome between these different conditions. But to do this the proteins involved in mitochondrial function must first be identified.

High throughput profiling of the mitochondrial proteome by Lopez et al. (2000) initially suggested that the mitochondrial proteome may contain up to 1500 proteins. Since then there have been two main projects that aim to build a comprehensive mitochondrial

proteomic database.

The first is MitoCarta (Pagliarini et al. 2008, Calvo et al. 2015), released in 2008, that identified 1098 mouse genes with strong support for mitochondrial localisation. Recently in 2015 this dataset was updated in MitoCarta 2.0 and now contains 1158 human and mouse genes with strong support of mitochondrial localisation.

The original MitoCarta determined genes using three approaches to determine what proteins were specific to the mitochondria.

First, seven datasets that were predictive of genes with mitochondrial function were combined with a naive bayes integration method called Maestro originally described by Calvo et al. (2006). The datasets described protein domain, induction, co-expression, yeast homologues, ancestry, predicted cellular location (Emanuelsson et al. 2007) as well as proteomics of isolated mitochondria from 14 different mouse tissues. This predicted 951 genes with estimated sensitivity of 84% and a false discovery rate of 10%.

This predicted mitochondrial gene set was then combined with two further approaches 591 genes previously identified as having strong experimental evidence for being mitochondrial from the literature and 131 genes identified as being localised to the mitochondria from microscopy following being tagged by fluorescent molecule GFP. Combining these three methods the 1098 mitochondrial proteins were identified.

MitoCarta 2.0 uses the same strategy but constructed an inventory separately for mouse and human, using updated and newly available datasets.

The other main project is MitoMiner (Smith 2009, Smith et al. 2011). MitoMiner uses a similar strategy to MitoCarta in integrating information from various sources, including mass spectrometry and GFP tagging studies with large genome-scale datasets such as from Uniprot and gene ontology (GO).

Alternatively to these two main mitochondrial databases there are also the mitochondrial gene sets on databases such as GO and Uniprot. The issue with these datasets however is that they provide no measure of confidence for any individual gene actually being within the set, with much of the genes being electronically added based on a single controversial mention in literature, or based on evidence from a distant species.

1.2.2 Variation across tissues and in disease

One of the most interesting results in studies on the determination of the mitochondrial proteome is the high level of variation between mitochondria from different tissues. Pagliarini et al. (2008) examined the protein expression across 14 different mouse tissues and in many cases found that among different tissues there was a large variation in protein expression (Figure 1.3).

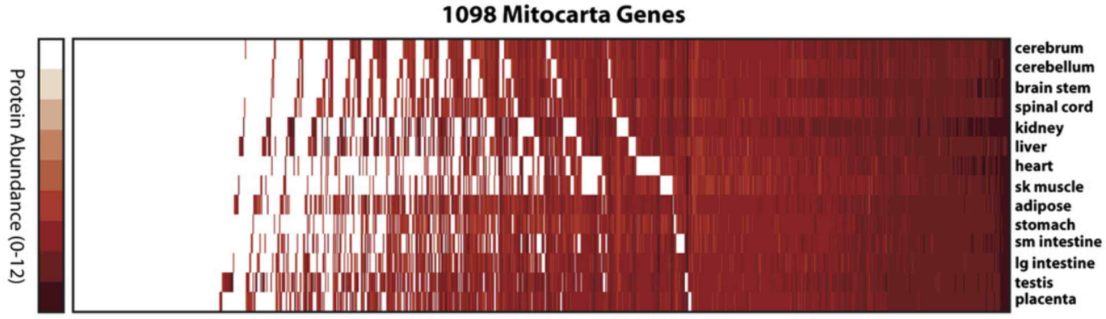

Figure 1.3: Pagliarini et al. (2008) measured protein abundance across 14 different tissues using mass spectometry, with protein abundance measured as log_{10} (total MS peak intensity). They found that the majority of mitochondrial genes were not present in all 14 tissues, and that a large number of known mitochondrial gene's protein products could not be detected by mass spectometry. Figure taken from Pagliarini et al. (2008).

While a core group of mitochondrial proteins involved in OXPHOS and the TCA cycle was found, a large number of the mitochondrial proteome appears to be tissue specific. In any given tissue, mitochondria were found to express an average of 760 MitoCarta genes, and between pairs of tissue types around 75% of their mitochondrial proteins is typically shared. This means that in any given cell the entire known mitochondrial proteome is not expressed at one time, and the mitochondrial proteome has a large tissue specific component.

Not just the protein make-up of the mitochondria was found to widely vary but also the quantity, with a 30-fold difference being found between levels of cytochrome c, an essential part of the ETC, across 19 different types of tissues (Pagliarini et al. 2008).

In addition to alterations in mitochondrial number and proteome, mitochondrial variation encompasses physiological changes to mitochondrial function and role. Mitochondria vary widely in dynamical terms between different tissue types (Kuznetsov et al. 2009); they can be static organelles or be constantly undergoing fusion and fission with each other to form complex networks such as is seen in cardiomyocytes, or they

can exist as discrete fragmented units uniformly covering the cell as is typically seen in hepatocytes within the liver. While these variations must be linked to the function of the cell type, it is not clear how various morphologies and arrangement of mitochondria contribute to the cellular function (Hoitzing et al. 2015).

A final area of mitochondrial variation is that of mtDNA itself. Due to its closeness to the electron transport chain, mtDNA is susceptible to mutations caused by reactive oxygen species (ROS). Unlike with nuclear mutations there are numerous copies of mtDNA in the cell, and a single mutation in one mitochondrion has little affect on the overall physiology of the cell.

Mitochondrial heteroplasmy refers to the existence of variations in mtDNA in a cell from these mutations. Since there are hundreds of copies of mtDNA there can be distinct populations with different mutational differences. It has been shown that a single mitochondrial mutation is usually present in only 1-2% of all mitochondrial genomes, though there can be hundreds of these unique mutations meaning that the majority of mitochondrial contain mutations (Smigrodzki 2005). This has been described as microheteroplasm and has been hypothesised to be linked with ageing and age-related diseases.

With mitochondrial heteroplasmy there is often a 'phenotypic threshold effect' where disease symptoms only become apparant when the percentage of the mitochondrial genomes carrying a certain mutation, referred to as the mutant load, reaches a critical value (Rossignol et al. 2003). Defective mitochondria are routinely turned over in mitophagy, and this process means that normally the mutant load remains very low (Kim et al. 2007). High mutant load is usually due to genetically caused mitochondrial diseases, although high levels of mtDNA mutations also occur in cancerous cells as both a driver and sustainer of cancer (Wallace 2012). mtDNA mutations are passed from mother to child and the child will have varying levels of mutant load in the different cells of their body.

Mitochondrial disease usually refer to genetic disorders caused by a mutation in either the mtDNA or the nuclear encoded mitochondrial genes. The phenotypes for these disorders vary enormously, with severity of the mtDNA mutational diseases also being affected by the mutant load. These disorders show the hallmarks of mitochondrial variability being very tissue specific in both the symptoms and the severity. There is

also a variety of different symptoms originating from mutations in different genes which on malfunction you might assume would have the same overall effect. For instance a mutation in one complex I subunit (*ND1, ND4* or *ND6*) causes Leber's Hereditary Optic neuropathy (Yu-Wai-Man et al. 2009), a condition that leads to optic atrophy and vision loss, while a mutation in a gene encoding a different subunit of complex I, *ND5* causes mitochondrial encephalomyopathy, lactic acidosis, and stroke-like episodes (MELAS), a much more severe condition which is progressive and fatal (McKenzie et al. 2007). The relationship between a mutation in a single mitochondrial gene and the phenotype the mitochondrial disease represents is clearly very complicated, and demonstrates the importance of mitochondrial variability in treating and understanding these disorders.

The origins of mitochondrial disorders can be divided into two categories: primary where the disorder is due to genetic mutations in the mtDNA or nuclear DNA encoding mitochondrial proteins, such as in Complex I deficiency (Fassone 2012); and secondary where there is an important mitochondrial component in the disorder but the cause is due to extramitochondrial genetic mutations or other effects. Secondary mitochondrial disorders include neurodegeneration, heart disease and cancer and will be discussed in Section 1.4.

In many of these cases mitochondrial variability is important in understanding the cause, progression and possible treatment of the disease. While mitochondria defects may not necessary be the etiological cause of these disorders, understanding how mitochondria are altered in their key central role maintaining energy for the cell may be critical for treatment.

1.3 Mechanisms of regulation of the mitochondria

The key to understanding the cause of mitochondrial heterogeneity and its role in disease is to understand the system that regulates the mitochondria. Regulation here refers to the regulation of all factors varying in mitochondria heterogeneity, this includes controlling the quantity of mitochondria as well as their dynamics and proteome make-up.

There are two main types of natural variation to be concerned about, one the difference between populations of mitochondria of two different cell types and the other is the difference between populations originating from the same cell type, but under different environmental conditions. Along with these, the mechanisms that create and

maintain these differences will be of interest.

An understanding of these natural variations in mitochondrial function will be vital in understanding pathological variations that result in dysfunctional mitochondria and disease.

In this section, all mechanisms that determine the regulation of mitochondria will be discussed. First in Section 1.3.1, I will describe the role epigentics and retrograde signalling plays, then in Section 1.3.2 the mitochondrial degradation processes will be described particularly with a reference to how they contribute to quality control, mitochondrial turnover and hence mitochondrial heterogeneity when altered. Finally in Section 1.3.3 the large topic of the regulation of mitochondrial biogenesis will be introduced and Section 1.3.4 will give an in depth study of the transcription factor network that regulates it.

1.3.1 Epigenetics

Many of the differences in mitochondria between different differentiated cell types can be assumed to originate from epigenetic changes. Feinberg (2008) defines epigenetics as 'modifications of the DNA or associated proteins, other than DNA sequence variation, that carry information content during cell division'. One example of this is DNA methylation, where methyl groups are attached to strands of DNA and conserved upon cell division by the enzyme DNA methyltransferase I.

While methylation has long been identified in being important for cellular differentiation, little is known about how methylation particularly changes mitochondrial protein gene expression during this process. It has however been shown that methylation occurs in some mitochondrial related diseases; for instance in type 2 diabetes there is hypermethylation of the cofactor PGC-1α, a key regulator of mitochondrial biogenesis, leading to decreased mitochondrial density (Barrès et al. 2009).

Whatever the process of how these modifications of the DNA sequence are preserved in cell division, they serve an important role in regulating gene expression and allowing the formation of different cell types from the same underlying genome.

While epigenetics certainly play an important role in mitochondrial function it is not one way, there is evidence of retrograde signalling where changes in mitochondrial function alter the epigenetics. Mitochondria typically have a varying number of copies

of mtDNA in the cell, referred to as the mtDNA copy-number (Satoh 1991). Smiraglia et al. (2008) discovered that cells with low mtDNA copy-number are susceptible to certain methylational changes in the nuclear genome which are reversed upon restoration of normal mtDNA copy-number.

This type of signalling could be expected to be common, with a major role of the epigenome being to respond to a cell's environment (Feinberg 2008). Dysregulation of the mitochondria can happen for a variety of reasons; due to genetic mutations or failure to adapt quickly to the changing environmental state. In either scenario these changes result in signalling changes from within the mitochondria resulting for example changed ROS levels or NADH/NAD+ ratio.

Recent studies confirm the importance of this signalling; Martínez-Reyes et al. (2015) found that the oxidative TCA cycle is necessary for histone acetylation as well as membrane potential dependent ROS generation being required for cellular proliferation and HIF-1 activation in response to hypoxia. In cancer, Hirschey et al. (2015) reviews the increasing evidence that dysregulation involving this retrograde signalling can contribute to tumorigenesis, with mutations in many cytosolic and mitochondrial metobolism enzymes being linked to both hereditary and sporadic classes of cancer. With this there are emerging links between metabolim and epigenetic changes, in cancer this is especially important as numerous epigenetic changes occur during tumorigenesis (Jones 1999, Feinberg 2004).

1.3.2 Mitochondrial degradation, quality control and turnover

Heterogeneity between mitochondrial populations of the same cell type must originate from alterations in the regulation of mitochondria. With these alterations occurring for either an adaptive or dysfunctional purpose. The two most important of these processes are the elimination/degradation of existing mitochondria and the generation of new mitochondria via mitochondrial biogenesis.

There are two main processes that control the degradation of mitochondrial proteins, one is the degradation of individual mitochondrial proteins by mitochondrial proteases (Quirós et al. 2015) and the other is the degradation of an entire mitochondrion by a specific autophagy pathway that has been coined mitophagy (Lemasters 2005). An overview of these two pathways is given in Figure 1.4.

(a)

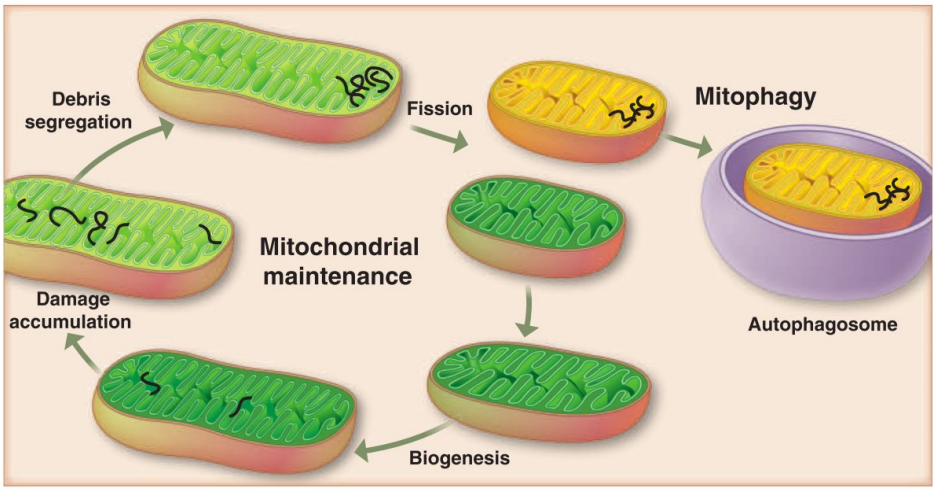

(b)

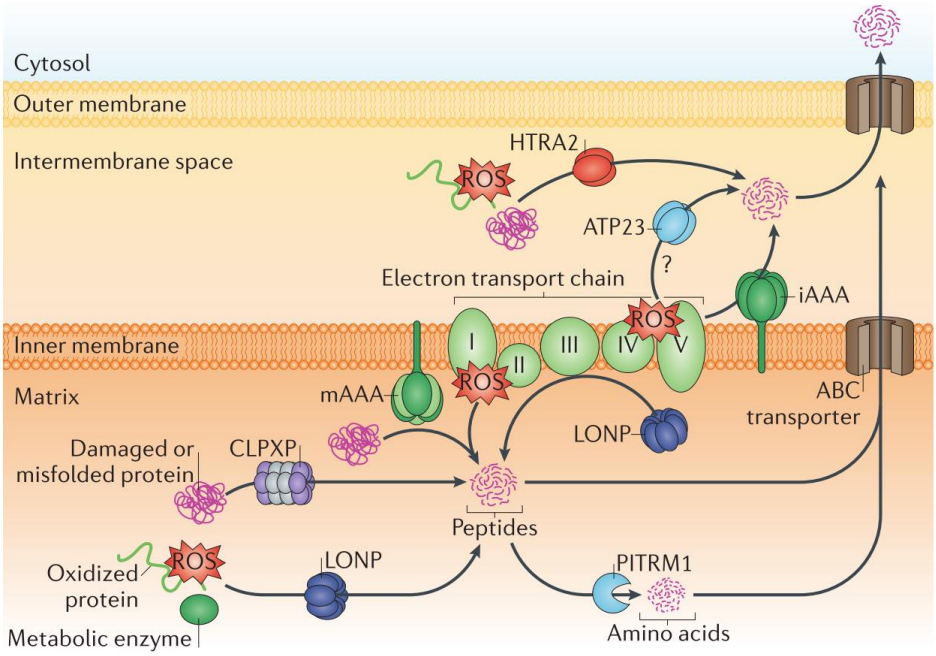

Figure 1.4: Two mechanisms of quality control within the mitochondria. **(a)** is taken from Youle (2012) and shows how fission can separate damaged and functional mitochondrial components, leaving the dysfunctional mitochondrion to be eliminated by mitophagy. **(b)** is taken from Quirós et al. (2015) and shows how mitochondrial proteases are involved in eliminating damaged mitochondrial proteins.

Autophagy is the cellular process that catabolises cellular components through the encapsulation of them by a double membrane structure called the autophagosome (Yang 2010). Mitophagy is the form of autophagy that targets mitochondria. Autophagy is known to occur in two situations: in nutrient deficient conditions where organelles are

catabolised for energetic purposes; and in nutrient rich conditions where the process serves more of a quality control purpose. In regards to selective mitophagy for quality control purposes it has been identified in both yeast and mammalian cells (for a review see Youle (2011)).

It is known that mitophagy is important for regulating the mitochondrial number (Kissová et al. 2004), and also required for a steady state turnover of mitochondria (Tal et al. 2007). In particular it has been shown that mitophagy plays an important role in eliminating damaged mitochondria through the PINK1/parkin pathway (Narendra et al. 2010) but it is also very important during development and cell differentiation.

During cell differentiation the proteome of mitochondria is known to change (Pagliarini et al. 2008) so it would be expected that mitophagy would play an increased role in fast elimination of the old population of mitochondria.

Importantly, any small change is the rates of mitophagy versus mitochondrial biogenesis could be expected to result in an exponential change of the mitochondria population levels, and as such these rates must be highly regulated. This is done through two pathways. First, SIRT1, a deacetylase enzyme, activitates not only various autophagy proteins but the cofactor stimulating mitochondrial biogenesis, PGC1-α (Andres et al. 2015). Secondly, there is a co-repressor of PGC1-α, parkin interacting substrate (PARIS) that is in turn repressed by parkin an essential protein in the mitophagy pathway (Shin et al. 2011). Both of these pathways ensure that with increased mitophagy there is an increase in mitochondrial biogenesis.

There are some extreme examples of mitophagy that have been well studied such as in red blood cell development where all mitochondria are removed (Schweers et al. 2007, Kundu et al. 2008), or in fertilised oocytes of *C. elegans* where paternal mitochondria are targeted for elimination (Sato 2011). Overall however, not much is known of the role of mitophagy in cell differentiation.

Studies have shown an important role for autophagy in the differentiation of adipose tissue and this appears to have a mitochondrial component. Zhang et al. (2009) showed that mice with a targeted deletion of a vital autophagy gene in adipose tissue contained only 20% of white adipose tissue as wild-type mice and had a cytosol that contained more mitochondria. It has therefore been suggested that mitophagy plays an important role in adipocyte differentiation (Lu et al. 2013).

Cellular senecense is the phenomenon in which ageing cells cease to divide and it is known that autophagy is involved in this process. Like cell differentiation mitochondrial changes occur, but the role of mitophagy in this process is not clear. Though recently García-Prat et al. (2016) demonstrated that autophagy is vital for preventing muscle stem cell senescence with mitophagy in particular being shown as important for preventing premature ageing.

Overall regulation of mitochondrial content via both mitophagy and mitochondrial biogenesis is important in determining cell behaviour. Mitochondrial mass along with mitochondrial biogenesis has been shown to increase during the G(1) phase of the cell cycle, in which the cell increases in size before DNA replication (Lee et al. 2007), presumably for the increased energy requirements during cell division. Additionally during senescence mitochondrial mass has been shown to increase (Lee et al. 2002), though in this case it most likely acts as a compensation for decreased mitochondrial function in senescent cells.

Instead of degrading entire mitochondrion as is done in mitophagy, mitochondrial proteases target for degradation individual proteins within a functioning mitochondria (Quirós et al. 2015). This is however not their main and only role, for instance they are involved in protein trafficking into the mitochondria, with peptidase PMPCP responsible for the removal of mitochondrial import signals from many proteins (Gakh et al. 2002).

Mitochondrial proteases form the most immediate pathway that can respond to mitochondrial damage, this can be induced from stress or proteins damaged from ROS. They are also responsible for the degradations of non-assembled proteins resulting from a stoichiometric imbalance between synthesis of the nuclear and mitochondrial genome. There is a small group of proteases involved in this process, they include ATP-dependent proteases that are present in the mitochondrial matrix or inter-membrane, collectively they are called inter-membrane/matix ATPases associated with diverse cellular activities proteases (i/mAAAs) (Quirós et al. 2015).

For this pathway to function efficiently there must be some mechanism for damage sensing, AAA proteases for instance have the ability to recognise the folding state of proteins and are thus selective for degrading misfolded proteins (Gerdes et al. 2012).

Mitophagy and mitochondrial proteases together with the process of mitochondrial biogenesis control the quantity of mitochondria in the cell. The functioning and co-

ordination together of these processes control mitochondrial turnover in the cell, although their precise modes of interaction are not entirely known there are many links between mitochondrial proteases and mitochondrial biogenesis (Quirós et al. 2015).

Mitochondrial turnover can be measured by radioactive labelling of mitochondrial proteins. This was first done over 50 years ago and identified that mitochondria in different tissues have different turnover rates (Fletcher 1961, Menzies 1971); more recently these results have been verified with an advanced labelling of nearly 500 mitochondrial proteins by Kim et al. (2012). Different tissues were found to have on average different rates of mitochondrial turnover; for example the average half life for mitochondrial proteins in the heart is 17.2 days but in the liver is 4.26 days. Different protein in the mitochondria were found to have different half lives, which can vary from a factor of hours to months. Nor was the difference in half lives between the different tissues just a simple shift; Kim et al. (2012) found that heart and liver mitochondria have distinct protein kinetics adding another level to mitochondrial heterogeneity.

These finding indicate that the entire mitochondrial proteome does not follow the same life cycle in the cell, and this life cycle can change between different tissues. This effect shows either that the role of mitochondrial proteases in degrading mitochondrial proteins is incredibly important or a similar effect is achieved through the process of fusion and fission of mitochondria allowing some segregation between damaged and functional components before mitophagy. Fusion allows damaged mitochondria to be rescued by functional mitochondria, while mitochondria forming through fission with mainly damaged components are quickly targeted for mitophagy (Youle 2012).

Asymmetric segregation of damaged mitochondrial proteins during fission and then elimination of the damaged mitochondria through mitophagy would indeed be a sensible method of quality control. This process has been observed to occur in mitochondria (Twig et al. 2008) though the exact mechanism behind it is currently unknown (Youle 2012).

It has been speculated that any dysfunction in mitochondrial quality control and turnover over time will lead to the proliferation of many dysfunctional mitochondria in a cell. The break down of this process has been hypothesised to be responsible for ageing and age related diseases (Terman et al. 2010).

A key piece of evidence supporting this hypothesis is the identification of an

interface between mitochondrial biogenesis, mitophagy and longevity in *C. elegans*. Palikaras et al. (2015) found that impairment of mitophagy in *C. elegans* triggers a signalling pathway that results in enhanced DCT-1 expression. DCT-1 is the *C. elegans* homologue of BNIP3, and is known to be involved in apoptosis as well as mitophagy. This DCT-1 activated signalling pathway in turn regulates both mitochondrial biogenesis and mitophagy. and knock down of DCT-1 was found to significantly reduce the life span of long lived mutant *C. elegans*.

While mitophagy and mitochondrial proteases are undoubtedly important for mitochondrial quality control and turnover, they have no direct control on the contents of the mitochondrial proteome which are uniquely controlled by the mitochondrial biogenesis pathway. Thus to understand mitochondrial heterogeneity and how it can be altered, mitochondrial biogenesis must be examined in depth.

1.3.3 Mitochondrial biogenesis

A major component of mitochondrial biogenesis is the process in which new proteins are synthesised that in turn makes up new mitochondria. More generally it also refers to protein import, lipid biosynthesis and transport as well as DNA/RNA synthesis that must accompany this. To maintain a healthy population of mitochondria, this has to be a continuous process, replacing mitochondrial components as they are damaged and degraded by either mitophagy or mitochondrial proteases.

Mitochondria are not synthesised *de novo* but are created from the division of existing mitochondria. Mitochondria biogenesis therefore describes the process replicating the mtDNA, and the synthesising and import of mitochondrial proteins from the cytosol, as well as synthesis of mitochondrial proteins within the mitochondria themselves. Of these coinciding processes the synthesis of mitochondrial proteins within the mitochondria is likely the first pathway that can respond to environmental changes such as physiological signals, but due to the limited number of proteins in this pathway large mitochondrial changes can only be achieved with coordination of the full mitochondrial biogenesis pathway.

New individual mitochondria can only be created though the process of fission, but this is just a segregation of the components of a pre-existing mitochondrion. Even if fission is not occurring there is still a constant turnover of proteins resulting from the

activity of mitochondrial proteases and here mitochondrial biogenesis can still be said to occur but with no corresponding increase in mitochondrial content in the cell. Despite this mitochondrial biogenesis in the literature almost exclusively refers to a changed level of mitochondrial content in a cell, typically an increase.

Besides having a main housekeeping role in maintaining healthy mitochondria, the mitochondrial biogenesis pathway must importantly respond to the needs of the cell, increasing the mitochondrial content if needed and altering the mitochondrial proteome as happens during cellular differentiation. The most obvious sign of changes in mitochondrial biogenesis however is when there is an increase in mitochondrial content and several pathways where this has occurred have been found and described.

1.3.3.1 Physiological signals causing mitochondrial biogenesis

It has been found that mitochondrial biogenesis increases in response to various physiological signals. One of the first identified was an increase in mitochondrial biogenesis in response to cold (Puigserver et al. 1998, Wu et al. 1999). These studies identified the co-factor peroxisome proliferator-activated receptor gamma coactivator 1 (PGC-1)α which has been since dubbed by some 'the master regulator of mitochondrial biogenesis', though it is just one part of a much bigger transcription factor network. This cold response up-regulates mitochondria in brown adipose tissue (BAT). In this tissue mitochondria contain an additional trans-membrane protein called UPC1 or thermogenin, this is an uncoupling protein that pumps protons back into the mitochondrial matrix, but instead of the energy being used to generate ATP it is used to generate heat. It has been shown by Lin et al. (2004) that PGC-1α null mice have striking sensitivity to the cold, meaning this mitochondrial biogenesis response is essential for survival.

The other main signal causing increased levels of mitochondrial biogenesis is the response to exercise. There are numerous studies that show in response to exercise there is an up-regulation of PGC-1α in skeletal muscle tissue (Baar et al. 2002, Pilegaard et al. 2003, Terada 2004). Wright et al. (2007) show that this up-regulation is initiated first by activation of PGC-1α in which it is translocated into the nucleus and only later causes a subsequent increase in the levels of PGC-1α itself.

In both these cases the tissue in question has a greater demand for mitochondria, whether for its role for generating heat or an increased demand for ATP caused by

exercise. There have however been studies linking animals undergoing calorie restriction to an increase in mitochondrial biogenesis (Nisoli et al. 2005, Civitarese et al. 2007).

Nisoli et al. (2005) reported that 30% caloric restriction for 3 months in mice resulted in significant increases in mitochondria in various tissues in the brain, heart, liver and adipose tissue, which was evidenced by increased mtDNA, cytochrome c and co-factor PGC-1α. This is slightly paradoxical as under caloric restriction in which cells are said to be undernourished but not malnourished there is no obvious need for additional mitochondrial biogenesis. Indeed these results have been questioned primarily by Hancock et al. (2011).

Hancock et al. (2011) argued that it was additionally surprising that increased mitochondrial biogenesis was observed in heart tissue, since this has previously been shown to be maladaptive (Russell et al. 2004) and calorie restriction is known to benefit the heart. Upon attempting to replicate the data presented by Nisoli et al. (2005), Hancock et al. (2011) found no evidence of increased mitochondrial biogenesis in any tissue. Civitarese et al. (2007) reported increase in muscle mtDNA during calorie restriction in humans, however Hancock et al. (2011) argues that these results occured without an increase in key mitochondrial enzymes without which it is not possible to have an increase in functional mitochondria.

It is certainly true that calorie restriction has a strong protective effect on mitochondria especially in response to ageing (Lee et al. 1999, McKiernan et al. 2007), and that upon calorie restriction there are some proteomic changes as Hancock et al. (2011) noted with a significant increase in long-chain acyl-CoA dehydrogenase protein. A further study by Lanza et al. (2012) has shown that this protective effect occurs with no increase in mitochondrial biogenesis.

What is likely occurring in the case of calorie restriction is not a huge increase in mitochondrial biogenesis, but a subtle change in its regulation leading to mitochondria that are protective against age-related loss of function of mitochondria. This process has been described by Baltzer et al. (2010) who analysed microarray studies involving calorie restriction. The overall interpretation of this analysis is difficult. The literature concerns mitochondrial changes in different animal models, under different protocols of calorie restriction and starvation. The results show that different mitochondrial pathways are up and down regulated in various tissues, for example adipose tissue has a

down-regulation of the energy producing pathways.

Another simple example of this is the effect of the fasting response in liver tissue. Upon fasting, there is a large release of fatty acids from adipose tissue that are transported to the liver for oxidation. To cope with this there must be an up-regulation of certain mitochondrial genes and this is largely accomplished through the up-regulation of the transcription factor of mitochondrial genes peroxisome proliferator-activated receptor (PPAR)α. Kersten et al. (1999) found that PPARα null mice had massive accumulation of lipids within their livers and upon fasting had severe hypoglycaemia, hypoketonemia and hypothermia.

It is suspected that the transcription factor network controlling mitochondrial biogenesis has many nutrient sensing pathways, for example PGC-1 related coactivator (PRC) is a serum inducible co-factor and appears to be a direct link between adjustments to the mitochondrial biogenesis network and nutrient availability (Baltzer et al. 2010, Andersson 2001).

A final physiological signal regulating mitochondrial biogenesis is the immune response to inflammatory processes (Piantadosi 2012). The reason for this is that the innate immune response leads to mitochondrial damage, this has been observed as long as 40 years ago by Mela et al. (1971) but has been now linked to molecular damage from cytokines such as the tumour necrosis factor alpha (Schulze-Osthoff et al. 1992). Due to this, increased mitochondrial biogenesis along with the clearance of damaged mitochondria is an important process during the immune response.

Besides the need to repair damaged mitochondria during the immune response, mitochondria have recently been found to be central to regulating the immune response itself. ROS generated by the mitochondria has been identified as being an important signal to modulate the activity of macrophages (Arsenijevic et al. 2000, Rousset et al. 2006), and ERRα and PGC-1β two important members of the transcription factor (TF) network involved in mitochondrial biogenesis have been found to be vital in producing increased ROS production during host defence (Sonoda et al. 2007a). PPARγ another member of the mitochondrial biogenesis TF network is required for alternative activated macrophages (Odegaard et al. 2007).

1.3.4 The transcription factor network underlying mitochondria biogenesis

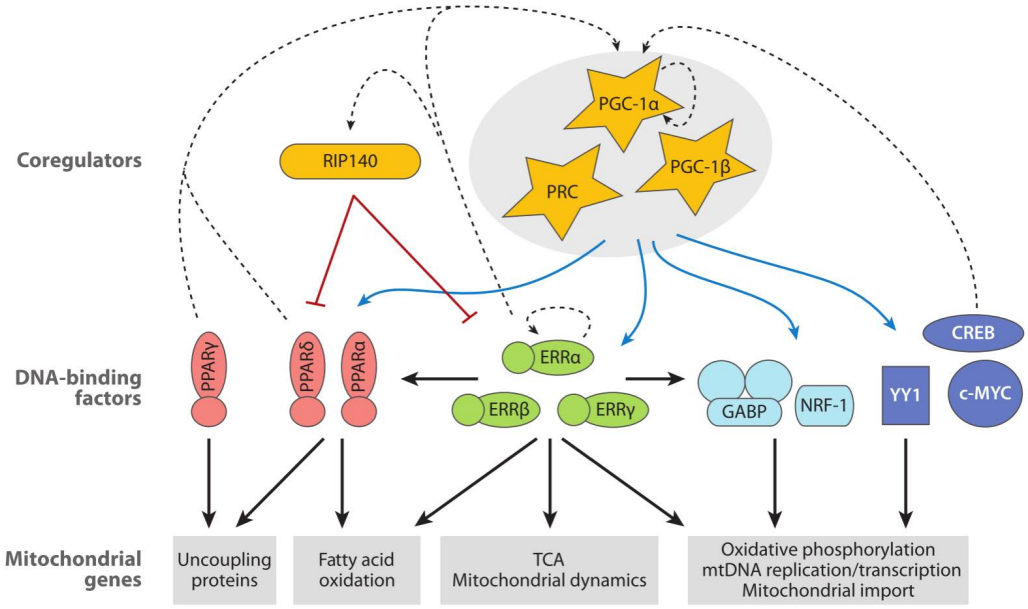

Figure 1.5: Overview of the mitochondrial biogenesis transcription factor network, with cofactor PGC-1α being central in the regulation. Figure taken from Scarpulla (2008).

The central dogma of molecular biology first stated by Crick (1970) is that genetic information flows in one direction, from DNA to RNA to proteins. The control of the proteome of the mitochondria therefore must be primarily achieved at the DNA level and this is largely achieved by TFs, coactivators and corepressors together making up a complicated TF network. The components of this network are highly regulated by post translational modifications and the targets of many signalling networks.

TFs are proteins that bind to specific DNA sequences and control the rate of transcription of genes in the proximal region where they have bound. A TF can either act to increase or repress the transcription rate of a gene, which is also often refered to as an up or down-regulation of that gene. TFs operate by binding to the promoter region of the gene, located upstream of the gene itself, this is the site where RNA polymerase initially binds to begin transcription. The action of the TF binding to the promoter either helps the RNA polymerase binding, causing an up-regulation of that gene, or blocks it causing down-regulation.

To do this TFs must have what is known as a DNA-binding domain (DBD) but they also have other important domains, a trans-activating domain (TAD) and optionally a

signal sensing domain (SSD). A TAD is a region which has a binding site to which other proteins can bind. These proteins are termed coactivators or corepressors which either act to increase or decrease the rate of transcription of the genes targeted by the TF.

A SSD is a region where ligand-binding can occur possibly changing the conformation and targets of the TF. This is also the region where the TF can be phosphorylated or bind to other TFs. In this way along with coactivators, corepressors, microRNAs and also epigenetic changes in the actual structure of the DNA, the actions of a TF are highly modulated.

In what follows the most important members of the transcription factor network controlling mitochondrial biogenesis will be described. First I will describe the transcription factors that are known to regulate mitochondrial genes and function then I will discuss the important role that cofactors play in regulating these transcription factors. Finally I will describe the role microRNAs play in regulating this network as well as the important role signalling and post-translational modification have in modulating it.

A general review of the transcription factor network can also be found in Hock (2009) and a simplified overview of this process is given in Figure 1.5.

1.3.4.1 DNA binding transcription factors

Nuclear respiration factor 1 (NRF-1) is a transcription factor that was first identified as binding to the site of the cytochrome c promoter (Virbasius et al. 1993*a*). Since then it has also been identified as regulating numerous other mitochondrial genes encoding members of the OXPHOS pathway, mitochondrial transporters and mitochondrial ribosome proteins (Scarpulla 2008). It is also involved in regulating transcription factor A mitochondrial (TFAM), a transcription factor that regulates genes on the mtDNA and participates in mtDNA replication.

In this way NRF-1 has a very clear mitochondrial function, but it also regulates many non-mitochondrial genes in particular those related to the cell-cycle and proliferation (Cam et al. 2004). In itself it is not sufficient for mitochondrial biogenesis since increased expression does not lead to increased respiratory capacity (Baar et al. 2003). Knockout of NRF-1 is lethal in early stage embryonic mice (Chan et al. 1998) and it is thought that it is required for normal basal expression level of its mitochondrial targeted genes since silencing leads to a significant suppression (Cam et al. 2004).

NRF-1 has many well described interactions with other proteins, it has been shown that members of the PGC family of coactivators including PGC-1α enhance NRF-1 expression (Andersson 2001, Puigserver et al. 1998). In addition to this it is strongly repressed by cyclin D1, a protein involved in regulating the cell cycle (Sakamaki et al. 2006, Wang et al. 2006) as well as regulated by phosphorylation (Gugneja 1997).

Nuclear respiration factor 2 (NRF-2) alternatively known as GA-binding protein (GABP) was identified by Virbasius et al. (1993*b*) as binding and activating the CoxIV promoter, a subunit of cyctochrome c oxidase or Complex IV in the ETC. Like NRF-1 it was found to regulate many mitochondrial genes involved in OXPHOS, mitochondrial import, and the transcription factor TFAM. GABP also regulates a large number of non-mitochondrial genes and was first identified as a regulator of genes for important viral pathogens and has additionally been found to be involved in the cell cycle, including the regulation of cytosolic ribosomal genes (Rosmarin et al. 2004, Yang et al. 2007).

GABP is notable among transcription factors for being made up of a tetrametric complex made up of two unrelated genes, GABPα and GABPβ, with GABPα containing the DBD and GABPβ containing the TAD. In addition to this there are two distinct but homologous genes encoded on different chromosomes for GABPβ, known as GABPβ1 and GABPβ2, of which GABPβ1 has four different isoforms arising from alternative mRNA splicing. These different variations of GABP components have been found to be differently expressed across different tissues and conditions leading to variations in function (Rosmarin et al. 2004).

Mootha et al. (2004) found that PGC-1α induces GABP expression along with estrogen-related receptor α (ERRα) with which it forms a double positive feedback loop that greatly enhances mitochondrial gene expression. It was also found to be induced by Ca^{2+} signalling and by exercise (Ojuka et al. 2003).

The Estrogen-related receptor (ERR) family of transcription factors contain three members ERRα, estrogen-related receptor β (ERRβ) and estrogen-related receptor γ (ERRγ) and all are involved in the regulation of mitochondrial biogenesis. As the names suggest ERRα and ERRβ, the first members of the family discovered, were found by being structurally similar to estrogen receptors of the nuclear receptor TF family (Giguère et al. 1988). Nuclear receptors are TFs that are mainly transcriptionally active when ligands bind to their SSD domain, despite their structural similarity to estrogen

receptors, neither estrogen, estrogen-like molecules nor any other known ligands bind to members of the ERR family, thus they were some of the first known members of what are now known as orphan nuclear receptors (O'Malley 1990).

Instead of becoming transcriptionally active upon ligand-binding members of the ERR family were found to become transcriptionally active upon interaction with coactivators such as those in the PGC family (Kallen et al. 2004).

ERRα is by far the most well studied of the ERR family, with it being known to regulate genes involved in lipid oxidation, OXPHOS, the TCA cycle, mitochondrial import and dynamics as well as response to oxidative stress (Hock 2009). It has been recognised as being vital for PGC-1α-induced mitochondrial biogenesis (Mootha et al. 2004, Schreiber et al. 2004), in particular in response to cold, with which ERRα-null mice fail to adapt to temperatures of 13°Celsius (Villena et al. 2007). In a complex with PGC-1β it has also been shown to be vital for macrophage activation in the immune response to bacterial pathogens through increased ROS signalling (Sonoda et al. 2007a).

While ERR members are known to interact with other coactivators such as nuclear receptor coactivators 1, 2 and 3, their transcriptional activity seems to be dependent on their relationship with PGC-1α and PGC-1β (Huss et al. 2015). Besides this they are known to interact with transcriptional corepressor RIP140 and NCoR1 to form complexes and repress target gene expression (White et al. 2008, Pérez-Schindler et al. 2012).

Of the other two members of the family ERRγ has been found to be strongly associated with ERRα (Dufour et al. 2007), both targeting many of the same promoters. ERRβ however is the least known, though it is recognised to be important in development, with ERRβ mutant mice embryos not surviving to birth (Luo et al. 1997), and stem cells treated with RNAi molecules targeting the gene encoding ERRβ negatively affecting self-renewal properties (Ivanova et al. 2006).

ERRα has been found to be expressed across all tissues while ERRβ is not present in the immune system, and both ERRβ and ERRγ are absent in adult skin and bones (Bookout et al. 2006). In addition to the difference in expression across different tissues more mitochondrial variety arises from different splice variants of ERRβ and ERRγ as well as the regulation effects of phosphorylation and sumoylation (Huss et al. 2015).

The PPAR family of transcription factors are like the ERR family, being a group

of nuclear receptors highly involved in the regulation of mitochondria biogenesis. The PPAR family contains three isoforms, PPARα, PPARδ also referred to as PPARβ and PPARγ, all of which have distinct tissue distributions as well as physiological functions.

Peroxisome proliferator-activated receptor α (PPARα) was first identified by Issemann (1990) as regulating peroxisomal proliferation after binding chemicals known to induce peroxisome proliferation in rodent liver. Since then PPARα has been shown to be involved in regulating fatty acid oxidation (Evans et al. 2004), the enzymes of which are located in the mitochondrial matrix. PPARα has also been shown to be induced in liver during the fasting response in which fatty acids have been transported from adipose tissue (Evans et al. 2004).

In contrast to PPARα, peroxisome proliferator-activated receptor δ (PPARδ) has a broader role in oxidative metabolism within the mitochondria being a regulator of lipid oxidation as well as promoting glucose oxidation (Hock 2009). PPARδ has also been shown to be linked to more general mitochondrial biogenesis. Mice lacking PPARδ have a decrease in mitochondrial gene expression as well as in oxidative capacity (Schuler et al. 2006), while PPARδ ligands have been shown to induce mitochondrial biogenesis (Bastin et al. 2008). These results can be explained due to PPARδ directly regulating the co-activator PGC-1α via a PPAR response element within it's promoter.

Peroxisome proliferator-activated receptor γ (PPARγ) primarily regulates lipid synthesis and storage and as such is most abundant in adipose tissue, though it is also present in lower levels within macrophages, muscle and liver (Evans et al. 2004). Like PPARδ, PPARγ is also thought to regulate co-activator PGC-1α via a PPAR response element, this has been shown due to increased mitochondrial biogenesis occurring with treatment of PPARγ ligands such as pioglitazone (Bogacka et al. 2005, Hondares et al. 2006).

The PPAR family has become an important therapeutic target for metabolic diseases, especially those related to obesity and diabetes (Evans et al. 2004, Willson et al. 2000). Agonists such as hypolipidemic fibrates bind to PPARα and by promoting the lowering of lipid levels in the blood, provides a treatment for hyperlipidemia. Agonists for PPARγ include the thiazolidinedione (TZD) class of insulin sensitizers commonly used for treatment of type 2 diabetes (Willson et al. 2000). In addition, a polymorphism in the PPARγ gene has been shown to possibly be protective for ischemic stroke with

type 2 diabetes (Lee et al. 2006). With the links between the PPARs and mitochondria biogenesis clearly established it is clear that mitochondrial biogenesis defects are often involved in diabetes and other metabolic diseases.

CAMP response element binding protein (CREB) is a transcription factor that regulates genes in response to cyclic adenosine monophosphate (cAMP), a second messenger derivative of ATP used for intracellular signalling. It is known that CREB is involved in regulating certain key mitochondrial genes including subunits of cytochrome c oxidase in the ETC (Scarpulla 2008). In addition, it has been found that CREB binds to the PGC-1α promoter and directly regulates it (Herzig et al. 2001). For these reasons CREB is certainly an important part of the mitochondrial biogenesis TF network but it has a much wider biological function being also involved in general processes such as cell proliferation, differentiation and adaptive responses and much more specific roles such as in the development of memory (Shaywitz 1999).

Yin Yang 1 (YY1) is a transcription factor, that has been implicated in regulation of cyctochrome c oxidase subunits (Scarpulla 2008). Importantly it has been shown by Cunningham et al. (2007) to form a complex with PGC-1α in muscle to regulate mitochondrial gene expression. It is striking that to fulfil this role YY1 requires activity of the protein mammalian target of rapamycin (mTOR), a protein that regulates many cellular processes involved in cell growth. mTOR is often described as a nutrient sensor, and YY1 appears to be a link between the nutrient sensing pathways and that of mitochondrial biogenesis.

c-Myc also commonly referred to as *Myc* is a transcription factor involved in the cell cycle, apoptosis and cellular transformation and has been identified as an oncogene being commonly mutated in many types of cancer (Dang 2012). Myc also plays an important role in mitochondrial biogenesis being shown to bind to the promoter region of 107 mitochondrial genes including the mitochondrial DNA TF, TFAM (Kim et al. 2008, Li et al. 2005). Myc has been identified as an important transcription factor in the Warburg effect, a common metabolic change within mitochondria that occurs in cancer (Wise et al. 2008).

TFAM is an important transcription factor for the mitochondrial genome originally identified by Parisi (1991). It has been found to be essential for the regulation of the 13 genes on the mtDNA as well as being essential for maintenance of the mtDNA (Larsson

et al. 1998). The promoter site for TFAM contains binding sites for other TFs in the mitochondrial biogenesis network such as NRF-1 and Myc, ensuring the coordination of the transcription of the nuclear and mitochondrial encoded genes.

Myocyte-specific enhancer factor 2A (MEF2A) is a transcription factor in the MEF2 family involved in cellular differentiation, notably it has been found to regulate cytochrome c oxidase subunits and the coactivator PGC-1α, as well as itself being regulated by NRF-1 (Ramachandran et al. 2008). Mice lacking MEF2A have mitochondrial deficiencies and are susceptible to sudden cardiac death (Naya et al. 2002).

The E2F family have relatively recently been identified as being involved in mitochondrial function. They are most widely known for their role in the cell cycle but are also known to be involved in the induction of apoptosis (Benevolenskaya 2015). Significantly Ambrus et al. (2013) found in Drosophila that E2F defective mutants were resistant to irradiation-induced apoptosis, not due to an inability to induce the apoptotic program but due to a mitochondrial dysfunction, this showed the E2F family's importance in maintaining mitochondrial function, a result that has been demonstrated to be conserved in humans. Another of the main indicators of the E2F family role in mitochondrial biogenesis is the great overlap in E2F binding sites with binding sites of known mitochondrial biogenesis transcription factors (Yeo et al. 2011). E2F-1 has been shown to repress genes that regulate energy homeostasis and mitochondrial function and has been hypothesised to act as a metabolic switch from oxidative to glycolytic metabolism (Blanchet et al. 2011). It is thought that E2F regulates mitochondria not only by direct binding to promoter regions of mitochondrial genes but via interactions with other members of the mitochondrial biogenesis transcription factor network (Benevolenskaya 2015).

1.3.4.2 Coregulators

Coregulators are proteins that directly interact with transcription factors by binding to their TAD domain, and act to either enhance or repress the expression of their target genes. They typically act by recruiting other proteins such as histone acetyl-transferases, which by transferring acetyl groups to the histones which wrap DNA, make the DNA more accessible to transcription factors. Coregulators do not always do this in a direct manner; PGC1α, an important mitochondrial biogenesis coregulator, acts by inducing

a confirmational change that increases the affinity of the transcription factor complex to recruit other coregulators that do act as histone acetyl-transferases (Liang 2006). Coregulators that function by this or similar methods to enhance gene expression are known to as coactivators.

Alternatively coregulators can recruit proteins such as histone deacetylase that have the opposite function of removing these acetyl groups and making the DNA less accessible to transcription factors. These coregulators are known as corepressors.

Coregulators can interact with a large number of different transcription factors and can thereby regulate a large number of genes and initiate large gene expression programs, such as the ones necessary for mitochondrial biogenesis. For this reason there has been much focus on coregulators and particularly the peroxisome proliferator-activated receptor gamma coactivator (PGC) family of coactivators in the control of mitochondrial biogenesis, with many mentions in the literature referring to them as the 'master regulators' of mitochondrial biogenesis.

The PGC family of coactivators are composed of three members PGC-1α, PGC-1β and PRC, of these PGC-1α was the first to be identified by Puigserver et al. (1998) with PGC-1β and PRC being discovered by their molecular similarity (Lin et al. 2002, Andersson 2001). These coregulators function by having a protein surface that enables interaction with numerous transcription factors, such as NRF-1, GABP, ERRα and PPARγ, and all contain sites of post-translational modifications to allow interactions with regulatory proteins (Hock 2009).

Due to its role in mitochondrial biogenesis, the PGC family and particularly PGC-1α act as a signalling hub controlled by post-translational modification. These pathway have been extensively reviewed (for instance by Scarpulla et al. (2012)) and it is worth discussing well known examples of signalling pathways that lead to altered function of PGC-1α.

Caloric excess has been shown to cause the coactivator SRC-3 to induce GCN5 expression that causes acetylation of PGC-1α repressing its activity (Dominy et al. 2010). Energy deprivation leads to two signalling pathways: in one decreased glucose levels leads to elevates levels of NAD+ this activates SIRT1 activity that through deacetylation promotes PGC-1α activity (Gerhart-Hines et al. 2007); in the other decreased levels of ATP and increased levels of AMP lead to the activation of AMPK that through

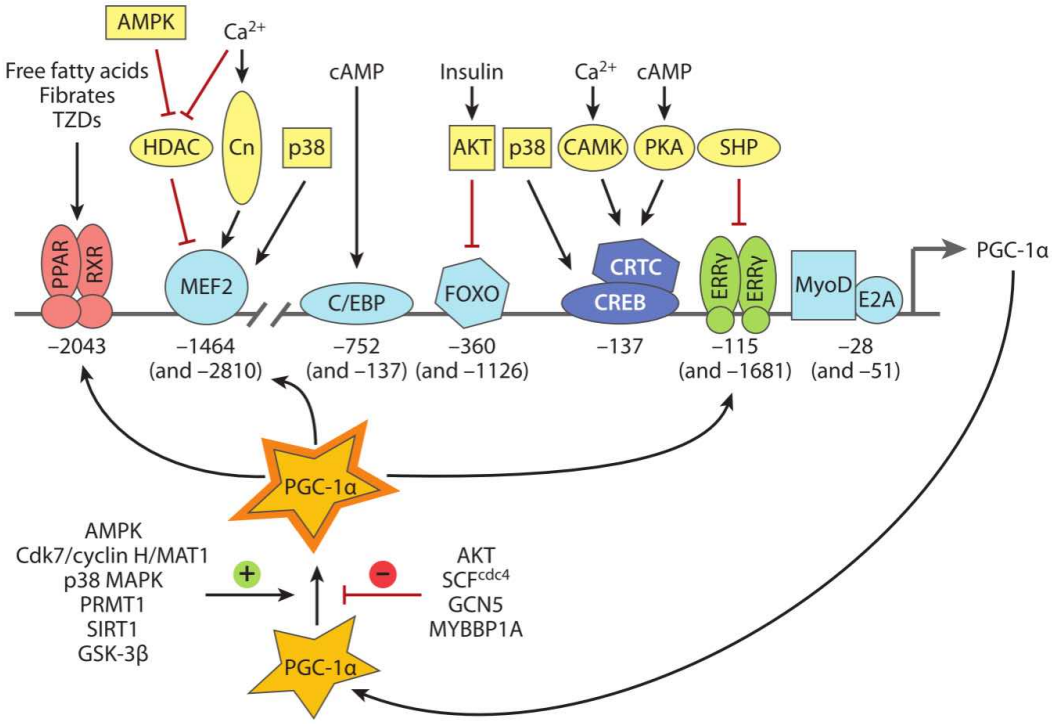

Figure 1.6: Cofactor PGC-1α is central in the regulation of mitochondrial biogenesis, and is also a main signalling hub for regulation. Figure taken from Scarpulla (2008).

phosphorylation also promotes PGC-1α activity (Jäger et al. 2007).

PGC-1α itself is a target for rapid degradation by the proteasome via ubiqitination with a half life in the nucleus of 0.3 hours (Trausch-Azar et al. 2010). Additionally, Rasbach et al. (2008) showed that proteasome degradation of PGC-1α occurs under basal conditions, but under stress conditions oxidants and Ca^{2+} induce PGC-1α degradation via calpain, a calcium dependent cysteine protease.

Of the three coactivators, PGC-1α and PGC-1β are the most studied and confirmed to have a role in initiating mitochondrial biogenesis (Hock 2009). Overexpression of both PGC-1α and PGC-1β will lead to increased mitochondrial biogenesis, and knockout mouse models of either lead to a mild mitochondrial deficient phenotype, with mice unable to cope with any large physiological stimulus such as the response to cold and exercise (Lin et al. 2004, Sonoda et al. 2007b). It is supposed that this relatively mild phenotype is due to compensation of PGC-1α for PGC-1β and vice versa when one is knocked out, and indeed a double knockout mouse model is much more severe with mice dying shortly after birth due to defects in high energy tissues such as the heart and BAT (Uldry et al. 2006).

Though both PGC-1α and PGC-1β have similar effects both interacting with many of the same transcription factors, it is thought that they represent different programs of increased mitochondrial biogenesis (St-Pierre et al. 2006). For instance they have both been found to induce distinct muscle contractile proteins (Arany et al. 2007), and have certainly different functions such as PGC-1β's role in macrophage activation (Sonoda et al. 2007a).

PRC is the third member of the PGC family and while overexpression has been linked to an induction of OXPHOS it is not thought to be sufficient by itself to initiate a mitochondrial biogenesis program. Instead it seems to be more involved in cellular proliferation with expression correlation with the proliferative status of the cell (Vercauteren et al. 2006) and inhibition affecting the proliferation of a cancer cell line in not only glucose but galactose only media (Vercauteren et al. 2009), meaning that this effect is not solely based on mitochondrial function.

RIP140 is a corepressor that has been described as the 'antithesis of the PGC-1 coactivators' (Hock 2009). Like the PGC family it interacts with many of the transcription factors known to be involved in mitochondrial biogenesis, but importantly represses their function.

Experimental work has shown that without RIP140 there is an increased expression of mitochondrial genes both in silencing experiments and null animal models (Powelka et al. 2006, Leonardsson et al. 2004). This corepressor adds another layer of complexity to the regulation of mitochondrial biogenesis, it has been suggested by Hock (2009) that together with PGC-1α it provides a switching function via PRMT1 mediated methylation which enhances the activity of PGC-1α but suppresses RIP140 (Teyssier et al. 2005, Huq et al. 2006).

In addition to this there seems to be a natural brake inherent in the mitochondrial biogenesis program with ERRα being shown to regulate RIP140 (Hock 2009).

Nuclear receptor corepressor 1 (NCoR1) was identified as an additional corepressor of mitochondrial function by Pérez-Schindler et al. (2012). They found that there was a high degree of overlap in the effect on global gene expression by NCoR1 deletion and PGC-1α activation, and it was found that PPARδ and ERRα are both regulated by PGC-1α and NCoR1.

Catic et al. (2013) found the NCoR1 is itself a key target for proteolysis suggesting

that its protein levels are tightly controlled and continually need to be reduced to maintain normal transcript levels. NCoR1 was found to especially interact with CREB and inhibition of this proteolysis process was found to greatly diminish mitochondrial function.

A summary of all the transcription and cofactors is given in Table 1.1.

1.3.4.3 Micro RNAs (miRNAs)

MiRNAs are short RNA molecules typically only 18 to 24 nucleotides in length, which are not translated into proteins, but play a role in the regulation of gene expression typically by interacting with messenger RNA (mRNA). The effect of miRNAs is usually a repressive one, binding to mRNA to inhibit their translation or promoting their degradation (Li et al. 2012), though there are recent examples of miRNAs driving up-regulation of their target genes (Vasudevan 2012).

The role miRNAs play in terms of regulating mitochondrial biogenesis is not completely clear, this is partly due to how individual miRNA have relatively few mRNA targets and relatively few miRNA have been studied in detail. There is however growing evidence that miRNA form a major part of the transcriptional network regulating mitochondrial biogenesis, the mechanisms of which are only in recent years becoming known.

It has been known for some years that the TF Myc in addition to regulating mitochondrial biogenesis is involved in regulating a large number of miRNA (Chang et al. 2008). The majority of miRNA that Myc regulates it represses, this includes miR-23a/b which targets mitochondrial glutaminase expression. This repression of miR-23a/b results in a greater expression of mitochondrial glutaminase which is vital for increased glutamine metabolism in proliferating cells (Gao et al. 2009). Myc also suppresses miR-17-5p and miR-20a, these two miRNAs in turn negatively regulate another TF involved in regulating mitochondria, E2F1, which itself is also positively regulated by Myc (O'Donnell et al. 2005). It seems that through these means Myc is a major hub for regulating miRNAs and as such can finely control mitochondrial function.

There are other individual miRNA that have been found to regulate mitochondrial function, these include miR-388 targeting the gene COXIV (Aschrafi et al. 2008), miR210 repression of iron-sulphur cluster assembly proteins ISCU1/2 (Chan et al. 2009)

TF	Regulates	References
NRF-1	ETC and OXPHOS proteins, mitochondrial ribosomes, mitochondrial transporters, TFAM, cell cycle and proliferation genes, MEF2A.	Scarpulla (2008), Cam et al. (2004), Baar et al. (2003), Chan et al. (1998)
NRF-2/GABP	ETC and OXPHOS proteins, mitochondrial import, TFAM, cell cycle genes, cytosolic ribosome genes.	Virbasius et al. (1993*b*), Rosmarin et al. (2004), Yang et al. (2007)
ERRα	lipid oxidation, OXPHOS, TCA cycle, mitochondrial import and dynamics and response to oxidative stress, macrophage activation, PGC-1α and itself.	Hock (2009), Mootha et al. (2004), Schreiber et al. (2004), Villena et al. (2007), Sonoda et al. (2007a)
ERRβ	Development, stem cell self renewal.	Luo et al. (1997), Ivanova et al. (2006)
ERRγ	Very similar targets to ERRα.	Dufour et al. (2007)
PPARα	peroxisomal proliferation, fatty acid oxidation, fasting response.	Issemann (1990), Evans et al. (2004)
PPARδ/β	peroxisomal proliferation, fatty acid oxidation, PGC-1α.	Bastin et al. (2008), Evans et al. (2004)
PPARγ	lipid synthesis and storage, PGC-1α.	Bogacka et al. (2005), Hondares et al. (2006), Evans et al. (2004)
CREB	ETC, peroxisome proliferator-activated receptor gamma coactivator 1-α (PGC-1α)	Herzig et al. (2001)
YY1	cytochrome c oxidase (Complex IV of ETC)	Scarpulla (2008)
Myc	TFAM, 107 mitochondrial genes, cell cycle, apoptosis.	Dang (2012), Kim et al. (2008), Li et al. (2005), Wise et al. (2008)
TFAM	Replication and maintenance of mtDNA.	Larsson et al. (1998)
MEF2A	Cellular differentiation, Complex IV and PGC-1α.	Ramachandran et al. (2008)
E2F-1	Cell cycle, apoptosis, overlapping binding sites with other mitochondrial biogenesis transcription factors.	Yeo et al. (2011), Blanchet et al. (2011), Benevolenskaya (2015)
Coregulators	**Regulates**	**References**
PGC-1α	NRF-1, GABP, ERRα, PPARγ, etc.	Lin et al. (2002), Andersson (2001), Hock (2009)
PGC-1β	Similar to PGC-1α	Hock (2009)
PRC	Induction of OXPHOS, cellular proliferation.	Vercauteren et al. (2006)
RIP140	Similar to PGC-1α but repressive.	Powelka et al. (2006), Leonardsson et al. (2004)
NCoR1	Similar to PGC-1α but repressive.	Pérez-Schindler et al. (2012).

Table 1.1: Transcription factors and coregulators in the mitochondrial biogenesis network.

that are critical for the function of the electron transport chain and the miR-30 family which is involved in regulating mitochondrial dynamics (Li et al. 2010). Besides this miRNA have been found to be involved with regulation of mitochondrial-mediated apoptosis and mitophagy (Li et al. 2012).

In addition to this, Barrey et al. (2011) identified miRNA within the mitochondria itself, regulating the transcription of the mitochondrial genome. Zhang et al. (2014) found that one of these miRNA, miR-1 is specifically induced during muscle differentiation and stimulates the translation of specific mitochondrial genome-encoded transcripts.

While there is a lot of recent evidence for miRNAs playing an important role in regulating mitochondria, considering the large number of miRNAs not studied in detail, our total understanding of the full role it plays is likely incomplete. This, while especially true for understanding the functional role of miRNAs, also holds for the rest of the transcription network regulating mitochondrial function previously described. In regards to the complexity of the system it should be understood that even the most up to date and detailed description is still a very simplified account.

1.3.4.4 Signalling and mitochondria-nuclear crosstalk

The entire transcriptional network described in detail so far in Section 1.3.4 is not a static process based on a few inputs, but is dynamically altering in response to various signals. It is a network made up of many component parts situated mainly in the nucleus and the mitochondrion, and to function as a single efficient system, there must be an extensive signalling system. This system must exist so mitochondria can react to external stimuli such as the response to cold, but there must also be signalling within the cell between the nucleus and mitochondria itself, modulating mitochondrial function based on the current state of the mitochondria themselves. This is known as mitochondria-nuclear crosstalk.

Regarding external stimuli there are several important molecules, such as AMPK which acts as a cellular energy status sensor, for example becoming activated in endurance exercise and in turn activating PGC-1α, and SIRT1 which becomes active in states such as fasting and also induces PGC-1α (Hock 2009).

Besides this cellular calcium plays a big role, the mitochondrion being central in the cellular calcium signalling network. Calcium release from the mitochondria is

associated with exercise and being known to induce PGC-1α and other members of the mitochondria transcriptional network (Hock 2009).

Regarding crosstalk, changes to the epigenome, mentioned in Section 1.3.1, in response to mitochondrial state is just one example. Crosstalk has been known to take place for some time, it could be said to be obvious due to the need to coordinate mitochondrial biogenesis between both the nuclear and mitochondrial genomes (Poyton 1996). This type of crosstalk was first shown to exist in yeast (Parikh et al. 1987), but should not be assumed to contribute much to mitochondrial heterogeneity as this process is viewed as necessary for maintaining a cell in homeostasis, though changes in crosstalk could drive tissue specific differences.

While maintaining homeostasis, nuclear-mitochondrial crosstalk often occurs when the mitochondria are dysfunctional, such as in the epigenetic example with depleted mitochondrial copy number (Feinberg 2008). Jones et al. (2012) identified 4 primary signals from the dysfunctional mitochondria that activate a wide range of signalling pathways and downstream nuclear transcription pathways. These are the reduction of ATP levels, changes in the cellular NADH / NAD+ ratio, disequilibrium of free radical production and cellular oxidative defences and deregulation of cellular calcium.

The aims of these pathways upon dysfunction are either to promote cellular survival or the apoptosis pathway. Indeed mitochondrial dysfunction has been found to alter the global expression of the entire cell (Epstein et al. 2001). The need for this is clear since upon mitochondrial dysfunction the cell has perhaps to adapt to generate ATP from glycolysis instead of from OXPHOS, and if it is to survive alter its function to cope with its new energetic state.

Signalling is the final part of the mitochondrial biogenesis transcription network described here, but in many ways is the most important, since the entire network's main function could be said to be sensory allowing mitochondrial to adapt and the cell to survive in changing environments. It is only through these complex signalling networks linking outside stimuli such as a change of temperature to a change of mitochondrial gene expression, with feedback signals coming from the mitochondrion itself to modulate this process, that this entire system can work.

Now that the entire mitochondrial transcription network has been described in detail, what follows will be a description of how this system can become dysfunctional

and lead to many pathologies.

1.4 Mitochondria and disease

Mitochondria have long been known to be involved in human pathologies. This is perhaps not surprising considering the pivotal role mitochondria play in providing energy for the cell, any dysfunction of which could be expected to be severe. What is surprising is the sheer variety in clinical phenotypes associated to mitochondrial dysfunction, and this can only be caused by the huge heterogeneity of mitochondria between different tissues and environmental conditions.

In some of these cases, the mitochondrial dysfunction is the original etiological cause of the disease, as is the case of mitochondrial diseases discussed in Section 1.2.2. In others it is just one part of a much more complicated disorder, and may be one of many contributory factors, or a consequence of the disease phenotype itself. Whatever the case may be, mitochondria and its associated regulatory network are now recognised to be a major target for novel treatments for many diseases. As will be seen, it is dysfunctions in the mechanisms for control of mitochondria that cause many of these underlying disease phenotypes.

For a general review on mitochondria and disease see Duchen (2010).

1.4.1 Cancer

Cancer is a disease affecting millions, with 14.1 million new cases and 8.2 million deaths being reported worldwide in 2012 (Torre et al. 2015). The disease is primarily characterised by uncontrollable cell growth and huge heterogeneity between different cases. Much has been described about the hallmarks of cancer, originally by Hanahan (2000) and then developed by Hanahan (2011). The original hallmarks included uncontrollable cell growth and evasion of apoptosis as well as the induction of angiogenesis, activating invasion and metastasis and sustaining proliferative signalling. The updated hallmarks also include the deregulation of cellular energetics, showing the recent importance mitochondrial changes are recognised to have in tumorigenesis.

This importance of metabolism has been recognised partly due to the realisation the deregulation of proliferation can not be separated from a corresponding deregulation of energy metabolism (Hanahan 2011). In fact this is not a new observation, Otto Warburg

(a) **(b)**

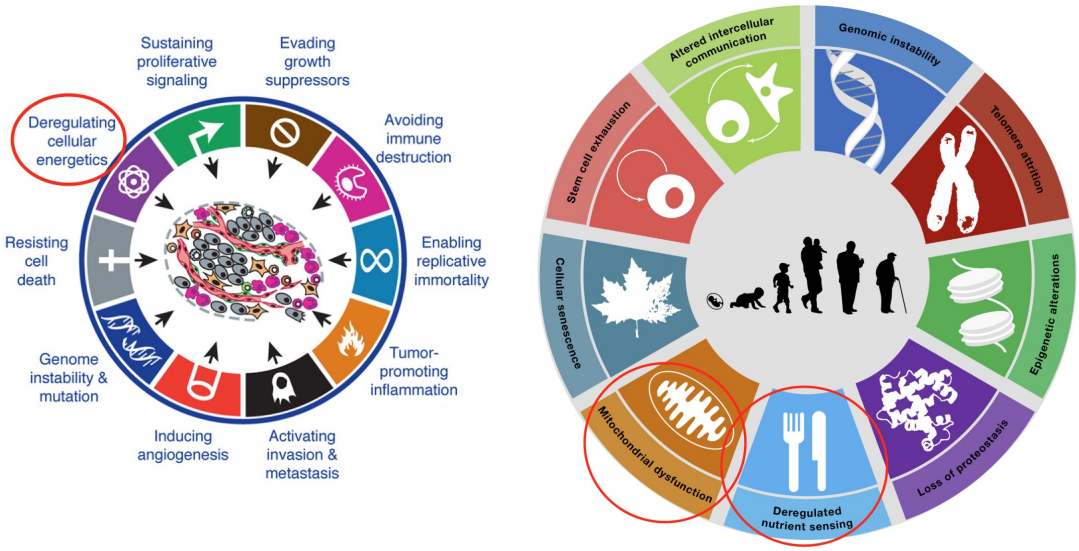

Figure 1.7: Figure **(a)** is adapted from Hanahan (2011) and shows the hallmarks of cancer, which include deregulation of cellular energetics. Figure **(b)** is taken from López-Otín et al. (2013) and shows that mitochondrial dysfunction is also considered a hallmark for ageing. In both figures the hallmarks related to mitochondrial function have been labelled with a red circle.

famously noted that in cancer cells there is often a metabolic switch from the normal mode of producing energy from the OXPHOS pathway to using glycolysis (Warburg 1956). Glycolysis is typically only used in the absence of oxygen but in cancer cells it is used even in the presence of oxygen, this has been called the Warburg effect.

Warburg hypothesised that this change in the metabolic state was the fundamental cause of cancer (Warburg 1956). This however is not necessary the case, with cancer being caused by numerous mutations affecting multiple pathways, the question is why does this metabolic change take place when the OXPHOS pathway is 18-fold more efficient at producing ATP.

One simple explanation could be down to the cancer's environment which is often lacking in oxygen, but Vander Heiden et al. (2009) proposes that the Warburg effect is in fact beneficial to proliferating cells as it facilitates the uptake and incorporation of nutrients. Unicellular organisms undergoing exponential growth are dependent on the glycolytic pathway for energy, as are rapidly growing embryoninc tissue (Hanahan 2011, Vander Heiden et al. 2009) suggesting that this is a pathway that has been conserved between unicellular and multicellular organisms and which cancer hijacks. It is still debated whether these metabolic changes are causal to the development of cancer

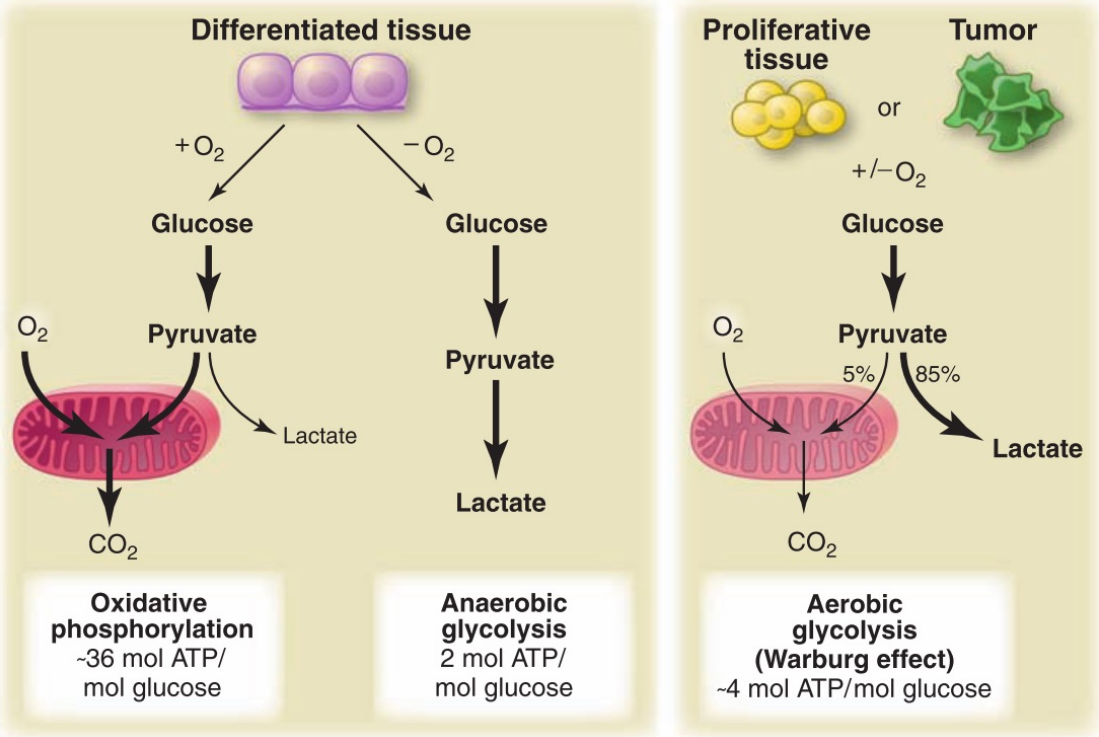

Figure 1.8: The Warburg effect describes the common metabolic deregulation occuring in cancer cells that switch from the normal mode of producing energy via the OXPHOS pathway to using glycolysis despite its inefficiency. Figure taken from Vander Heiden et al. (2009).

or simple a consequence of them, but they are still recognised as a great potential therapeutic target, even being referred in a recent review as "Cancer's Achilles' Heel" (Kroemer 2008, Gogvadze et al. 2008).

One of the original core hallmarks of cancer is the evasion of apoptosis, and often this occurs due to enhanced resistance to mitochondrial apoptosis. This often involves mutations and dysregulation of the mitochondria or proteins such as the pro-apoptotic BCL-2 family that are located on the outer mitochondrial membrane.

Considering the changes in both cancer metabolics and apoptosis, tumorigenesis must involve significant alterations in the mitochondrial transcriptome. Indeed it has been found that several members of the mitochondrial biogenesis transcription network are altered in cancer.

C-Myc is an important transcription factor involved in mitochondrial biogenesis but it is also an oncogene, commonly mutated in cancer leading it to have highly amplified expression (Dang 2012). This increased expression of Myc has been linked to increased genomic instability, presumably from increased ROS production caused by the up-

regulation of mitochondrial genes (Dang 2012). While due to the Warburg effect, the cancer cell is often less dependent on mitochondria for OXPHOS, mitochondria are still essential for other metabolic functions, one of these is glutamine metabolism, which Myc enhances via its suppression of miRNA miR-23a/b (Gao et al. 2009). Myc is in fact responsible for regulating a large number of miRNA, many like miR-23a/b involved in mitochondrial function, and it is clear to see the deregulation of Myc would cause deregulation of miRNAs which is known to occur in cancer (Garzon et al. 2009).

Mutations within cancer do not exclusively affect the nuclear genome but also affect mtDNA. Horton et al. (1996) first noted a deletion in mtDNA in renal cell carcinoma, but since then mtDNA mutations have been shown to be common in cancer (Wallace 2012). It has also been noted that there are populations with mtDNA variations with increased risks of developing cancer (Wallace 2012). These mutations are sometimes seen as only passenger mutations but alterations in the ETC have been linked to increasing ROS production thus increasing tumorigenesis (Ishikawa et al. 2008, Petros et al. 2005). They are not however just responsible for increased ROS production but can fundamentally alter the metabolism of the tumour cell (Wallace 2012).

One way this is done is through mtDNA mutations promoting an altered mitochondrial environment, which causes a direct signalling response in expression in the nuclear genome. Another way this occurs is through known mutations in mitochondrial enzymes, an example is a mutation in gene SDH, for succinate dehydrogenase or complex II on the ETC. Mutations in SDH increase the levels of succinate in the cell which in turn through signalling leads to a transcriptional change causing a more glycolytic energy metabolism (Wallace 2012). Such mutations are common in colon and kidney cancers as well as paragangliomas and pheochromocytomas (Bardella et al. 2011).

Other members of the transcriptional network for mitochondrial biogenesis are also involved in cancer. ERRα has emerged as both a prognostic marker of breast cancer and a potential therapeutic target (Stein 2006). Cyclin D1, known to repress transcription factor GABP, is typically overexpressed in human breast cancers (Sakamaki et al. 2006). Importantly, altered expression of the 'master regulators' of mitochondrial biogenesis, the PGC family of coactivators, is frequently seen in cancer (Jones et al. 2012).

These examples illustrate the changes that can occur within the transcriptional network controlling mitochondrial biogenesis. Accordingly, mitochondrial changes are

now recognised as a hallmark of cancer, and these changes must occur by modulation of the regulation of the mitochondria. The system controlling the regulation of mitochondrial biogenesis is very complex, and the nature of dysfunction in cancer seem heterogeneous, possibly affecting many different members of the network to achieve similar results. However, greater understanding of this network and the different ways it can be dysfunctional within cancer could lead to novel treatments.

1.4.2 Heart disease

Heart disease is a group of conditions that affect either the muscle of the heart or the coronary vessels. It is one of the leading causes of death worldwide, with 2% of the population of the USA suffering from heart disease and costing billions of dollars each year (Rosca et al. 2013). The heart is an organ with high energy requirements, displaying the greatest level of oxygen consumption, with the vast majority of the ATP production met by the OXPHOS pathway in the mitochondria (Rosca et al. 2013).

Accordingly, the mitochondria and hence mitochondrial biogenesis are essential for correct functioning of the heart. Double knockout of PGC-1α and PGC-1β, the master regulators of mitochondrial biogenesis, result in mice having early postnatal heart failure (Lai et al. 2008). Single knockouts while viable also have heart defects. Other members of the transcription factor network have also been shown to be involved with ERRγ being important in the development of the postnatal heart (Alaynick et al. 2007).

Besides being essential for correct function of the heart, mitochondria have been found to be especially important in cardiac hypertrophy, it often being caused by mitochondrial defects (Rosca et al. 2013). Cardiac hypertrophy refers to the thickening or enlargement of the heart muscles. Physiological cardiac hypertrophy does naturally happen in response to exercise, but the pathological phenotype leads to a permanent hypertrophy of the heart muscles that can lead to heart failure. Rosca et al. (2013) note that in cardiac hypertrophy there is either a preservation or up-regulation of mitochondrial pathways, which collapse in expression during heart failure. This indicates a failure of the mitochondrial biogenesis system to match energy demand, though the precise mechanism of this is not known (Rosca et al. 2013).

In some types of heart disease the etiological cause is directly linked to the mito-

chondria. For instance, hypertrophic cardiomyopathy is a form of pathological cardiac hypertrophy that is typically caused by a genetic mutation and can often result in sudden cardiac death. Many of these genetic alterations are linked to the mitochondria, for instance polymorphisms in PGC-1α are associated with higher likelihood of hypertrophic cardiomyopathy (Wang et al. 2007), as well as mutations in the mitochondrial ribosome gene MRSP22 (Smits et al. 2011).

While cardiac hypertrophy can occur due to genetic mutations, it can also take place when the heart is under stress from other conditions such as high blood pressure in hypertension. Even in these cases, defects in the mitochondria can be involved.

Through its ability to increase cellular antioxidant defences it is thought that the PGC-1α, and the rest of the mitochondrial biogenesis transcription network, have a protective effect (Jones et al. 2012). This has been shown in the vascular endothelium, the cells that line the blood vessels (Valle et al. 2005). Defects in the endothelium cells caused by excessive ROS production can lead to endothelial dysfunction which is closely linked to cardiovascular diseases. PGC-1α however up-regulated mitochondrial antioxidant proteins and helps prevent ROS damage (Valle et al. 2005).

Increased expression of mitochondrial biogenesis is protective in vascular endothelium cells but this is not always the case. Forced overexpression of PGC-1α can lead to cardiomyopathy (Russell et al. 2004) and increased cell death following anoxia (Lynn et al. 2010). Clearly mitochondria are carefully regulated in the heart, and any alterations in their regulation can be detrimental. While there are many factors that can lead to heart disease, such as smoking and lack of exercise, the mitochondria offer a possible target for managing and treating heart disease, as well as possibly aiding its prevention. This can only be done, avoiding any detrimental effects, by greater understanding of the role of mitochondrial biogenesis in the heart.

1.4.3 Neurodegeneration, diabetes and ageing

Although the focus of this thesis will be on defects in the mitochondrial biogenesis pathway in cancer and heart disease, these form just a subset of the pathologies mitochondrial dysfunction is involved in. Neurodegeneration and diabetes are two major disorders in which mitochondrial dysfunction also play an important role (Duchen 2010). Of these neurodegeneration describes a wide range of disorders affecting different parts

of the brain, sometimes being caused by genetic mutations, while diabetes is a metabolic disorder that can itself lead to among other things heart disease.

Ageing is often not thought of as a disease, but with ageing comes a variety of age-related diseases which include an increase likelihood of neurodegeneration, cancer and heart disease. All of these are thought to have an important mitochondrial component.

Neurodegeneration represents the widespread progressive loss of function and death of neurons in the brain. There are many different types of neurodegeneration ranging from Alzheimer's, Parkinson's, Huntington's and others. These diseases can either be familial caused by inherited mutations or sporadic appearing in later life from a more complex development. Notably however nearly all neurodegenerative diseased have been linked to mitochondrial dysfunction playing some role in causing loss of function or cell death (Duchen 2010).

It could be suspected that some of this dysfunction could be linked to malfunctions in the mitochondrial biogenesis network, and indeed knockout mouse models of PGC-1α present with symptoms of neuronal degeneration (Lin et al. 2004). Genetic studies have also identified variations in PGC-1α as well as transcription factors TFAM and NRF-1 with increased risk of neurodegeneration (Maruszak et al. 2011, Taherzadeh-Fard et al. 2011). There are also increasing amount of data showing that coactivators PGC-1α and PGC-1β could have protective functions in neurodegeneration, leading to attention as potential targets of treatment (Handschin 2009, Jones et al. 2012).

Of all neurodegeneration diseases, Parkinson's disease (PD) has been most strongly linked to mitochondrial function. PD is characterised by death of dopamine generating neurons in the substantia nigra region of the brain. Familial PD has been found to be caused by mutations in many genes with links to the mitochondria (Mandemakers et al. 2007). One of these is parkin, which has been shown to induce the proteasomal degradation of the parkin-interacting substrate which is a repressor of PGC-1α (Shin et al. 2011). This leads to the suppression of mitochondrial biogenesis following the loss of parkin. Additionally PD disease like symptoms occur upon exposure to drugs which target complex I of the ETC, these include MPTP, rotenone and annonacin (Exner et al. 2012).

Diabetes or diabetes mellitus is often described as a metabolic disease and as such it is not surprising that mitochondrial dysfunctions plays a role. Diabetes itself is

fundamentally linked with the hormone insulin and has two main types: type 1 diabetes in which insulin is not produced in enough quantity by the pancreas; and type 2 where the cells in the body become resistant to insulin. Insulin has an important role in human metabolism by stimulating the disposal of glucose in adipose and muscle tissue as well as inhibiting gluconeogenesis in the liver.

The link between diabetes and mitochondrial dysfunctions has been intensively studied (Patti 2010). The mitochondrial biogenesis transcription factor network has been found to be highly involved, particularly of the PPAR family which, as discussed in Section 1.3.4.1, have emerged as therapeutic targets for treating diabetes. In addition to this it has been shown that PGC-1α regulated genes are down-regulated in diabetes (Mootha et al. 2004) and large number of studies have found that mitochondrial function is diminished in diabetes (Patti 2010).

It is hypothesised that mitochondria play an important part in the development of insulin resistance in obesity-related type 2 diabetes (Patti 2010). The general hypothesis is that when excessive fuel load exceeds the oxidative capacity of the mitochondria, if this is not compensated by either increased exercise or decreased food intake, this chronic oversupply of fuel leads to an accumulation of lipid oxidative metabolites and it is this disordered lipid metabolism that is thought to lead to insulin resistance and the development of diabetes.

The role of mitochondria in ageing is much debated. Harman (1955) created the mitochondria free radical theory of ageing, in which ROS by-products of the ETC are responsible for causing damage which accumulate over time and cause ageing. This theory, though only one of many on the causes of ageing, has been hugely influential and seemingly supported by the well documented accumulation of mtDNA mutations and diminishing mitochondrial function with age (Bratic et al. 2013).

However, recent evidence has cast doubt on this theory, due to the recognition of ROS as being important in signalling and there being no clear correlation between oxidative damage and life span (Bratic et al. 2013, Hekimi et al. 2011). Importantly a genetic alteration in polymerase γ which introduce mutations in mtDNA at an increased rate, show animals ageing prematurely (Trifunovic et al. 2004), but recent evidence states that this effect seems to be related to the early onset of dysfunctional somatic stem cells, not increased ROS production (Ahlqvist et al. 2012).

Despite this, mitochondria are still recognised as being hugely important in the ageing process. López-Otín et al. (2013) describe mitochondrial dysfunction, as well as genetic instability which includes that of the mtDNA as being hallmarks of ageing, and it is believed that mitochondrial dysfunction contributes to ageing independently of ROS. It is instead thought that deficiencies in the control of mitochondrial biogenesis could be the cause of mitochondrial dysfunction associated ageing, and that perhaps mild mitochondrial toxic treatment, known as hormesis, could trigger a beneficial compensatory response in the transcriptional network that can help to increase lifespan (López-Otín et al. 2013). It has indeed been found that in *C. elegans* mild mitochondrial stress extends lifespan (Maglioni et al. 2014).

In summary, mitochondrial dysfunction is important in cancer, heart disease, neurodegeneration, diabetes and the general ageing process as well as being involved in other conditions such as mitochondrial diseases caused by genetic mutations. Together these pathologies affect millions of people worldwide, and cost many billions of dollars in health care. Mitochondrial targeted therapies offer new possible treatments but any new treatments can only be found by greater understanding of the regulation of mitochondria and especially that of the mitochondrial biogenesis transcription factor network.

1.5 Investigating the regulation of mitochondria

1.5.1 Experimental methods

So far, what is known of mitochondria and their regulation as well as their importance in disease have been discussed, but the experimental and bioinformatic methods used to study them have not. The purpose of this thesis is to use novel bioinformatics methods to investigate the regulation of mitochondria, but first it is worth discussing existing experimental methods and how they can either be used to generate data to apply bioinformatics techniques or support the results of a bioinformatics analysis.

Table 1.2 gives an overview of the main existing methods for assessing mitochondrial function, and those assessing mitochondrial biogenesis in particular are reviewed in Medeiros (2008). Often experimental methods can only measure one aspect of mitochondrial function at a time, microscopy can give us vital information about the dynamics of the mitochondrial network, as well as the number of mitochondria but say little of the

proteomic make-up itself.

Other methods such as the measurements of oxygen consumption are examining specific physiological properties of the mitochondrion and give us important information about the real effect of changes in expression of various mitochondrial proteins. A measurement of mitochondrial oxygen consumption, along with running a western blot can be seen as traditional experiments whose results lead to a few data points and need to be replicated. However with modern advances in biological technology, it is now possible from a single experiment to obtain many thousands or even millions of data points, with these advances simple statistical analysis is often not enough to understand results, and hence more complex bioinformatical tools are required.

In terms of measuring mitochondria, large transcriptomics datasets are now available that measure the expression of all the genes known from the mitochondrial proteome.

1.5.2 Bioinformatics

1.5.2.1 Transcriptomics

Transcriptomics involves simultaneously measuring the complete set of mRNA transcripts present in the cell, known as the transcriptome. For studying the regulation of mitochondria, the transcripts encoding mitochondrial related proteins are of particular interest, so it is this 'mito-transcriptome' that is the particular target of study in this work. By examining the 'mito-transcriptome', not only massive up-regulations of the mitochondrial biogenesis will be apparent but also subtler remodelling of the mitochondrial proteome. To do this, understanding of the technology behind transcriptomics and the bioinformatic methods associated with them is first needed.

1.5.2.2 Microarray and RNA-Seq technology

There are two main high throughput ways of measuring transcriptomics, either with microarray or RNA-seq technology. Of these microarray technology is the older (Schena et al. 1995). Microarray, or more precisely complementary DNA (cDNA) microarray, technology works by using the known cDNA sequences of an organism to produce probes. cDNA are double stranded DNA synthesized from mRNA templates, catalysed by the enzyme reverse transcriptase. DNA probes are produced to hybridise precisely to segments of these known existing cDNA sequences, and these probes are attached

Method	Purpose	Further information
Fluorescent microscopy	Using mitochondria targeting fluorescent dyes mitochondria quantity, structure and membrane potential can be measured.	Johnson et al. (1980) first used dye rhodamine 123 as a probe for localisation of mitochondria. Scaduto (1999) introduced the use of TMRM for measuring membrane potential. Additionally other dies such as Chloromethy-X-rosamine (MitoTracker Red) and MitoTracker Green are used to measure mitochondrial function (Pendergrass et al. 2004).
mtDNA copy-number	To measure the number of copies of mtDNA using real-time PCR	For a review of different PCR based methods see Rooney et al. (2015).
Western blots	Using protein antibodies measure the amount of specific mitochondrial related proteins.	Western blots are widely used in science and were first developed by Towbin et al. (1979). Companies such as Abcam market antibody cocktails targeting the different complexes of the ETC.
Oxygen Consumption	To measure the function of the ETC under different conditions, using specially made machines such as those produced by Seahorse Bioscience and Oroboros.	General theory behind cellular respiration experiments can be found in Brand (2011). For basics behind the use of Oroboros 2k for measuring oxygen consumption see Gnaiger (2007) and for Seahorse consult Divakaruni et al. (2014).
Metabolomics	To measure the precise metabolic state of the mitochondria, including that of the TCA cycle.	For review focusing on studying mitochondria see Nagrath et al. (2011).
qPCR	To measure accurately precise numbers of transcribed RNA of important mitochondrial genes.	A general review of qPCR is given in VanGuilder et al. (2008).
Transcriptomics	To measure the expression level of all the nuclear encoded genes, and using bioinformatics techniques examine those encoding mitochondrial genes, typically looking for significant up or down regulations between different conditions.	A general introduction to transcriptomic technology is given in this review of RNA-Seq by Wang et al. (2009), studies such as MitoCarta by Pagliarini et al. (2008) list all the known mitochondrial genes.

Table 1.2: Experimental methods for measuring regulation of mitochondrial biogenesis and function.

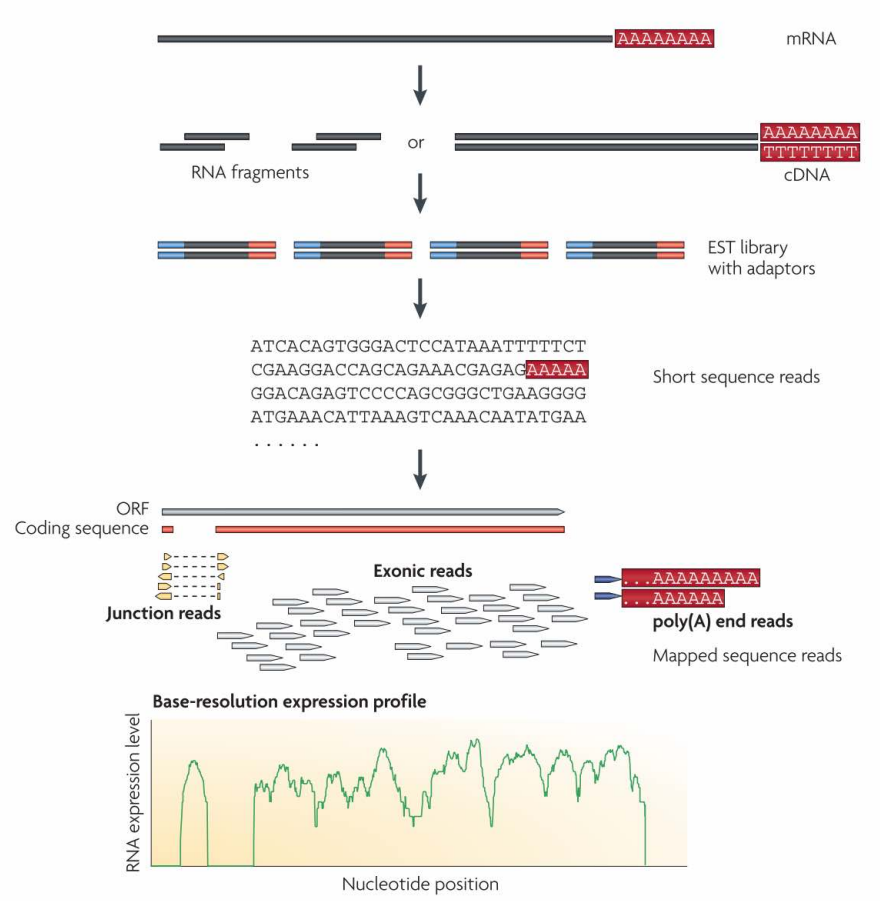

Figure 1.9: The basic steps of an RNA-seq experiment. Figure taken from Wang et al. (2009).

to a surface, making up the microarray. cDNA is then generated from prepared total mRNA from a biological sample and labelled with a fluorescent probe. When the sample fluorescent cDNA is hybridised with the DNA probes on the microarray, only those that match the sequence of one of the probes remain after washing. The resulting strength of the fluorescently labelled cDNA spot intensity can then be used as a measure of gene expression.

Using this technique microarray technology was the first to allow simultaneous measurements of tens of thousands of genes, enough to measure the transcription of the entire known human genome. There are however quite a few disadvantages to microarray data. First, microarrays are very noisy, with the hybridisation reaction depending on the temperature as well as the pH of the experiment (Wang et al. 2009). Due to the nature of the construction of the DNA probes, being short segments, microarrays are also susceptible to noise from cross-hybridisation, where a single DNA probe has multiple target cDNA (Okoniewski 2006). On top of this the dynamic range a microarray

measures is limited, due to background noise and saturation of the signals coming from fluorescence. Finally microarrays are unable to detect novel transcripts, with probes being created from the existing knowledge of cDNA sequences.

RNA-Seq technology answered many of these shortcomings (Wang et al. 2009). Instead of making use of a hybridisation reaction, RNA-Seq uses next generation sequencing technology to directly sequence cDNA produced from mRNA from a biological sample. Modern high-throughput sequencing technology can only sequence relatively short reads, so the cDNA is fragmented before sequencing can begin. Once the sequencing is complete, with the number of reads sequenced typically in the order of millions to ensure adequate coverage of all transcripts, the reads are matched up to a reference genomic sequence. Gene expression can then be measured by various normalisations such as the commonly used reads per kilobase per million mapped reads (RPKM) (Dillies et al. 2013).

1.5.2.3 Quality control and normalisation

An important part of working with transcriptomics data is normalisation. This is more important for microarray data, but though initially claimed by Wang et al. (2009) that RNA-Seq did not require any sophisticated normalisation it has been increasingly recognised as an important step in analysis (Dillies et al. 2013).

For microarrays, due to the high noise level and variation, it is first important to undertake quality control. Microarray chips could for example be scratched, or have uneven hybridisation effecting the signal intensity, and RNA degradation is also an issue. If the chip passes quality control, it then must be normalised to be comparable to other experiments. It is important to remember that the strength of fluorescent signals varies between experiments depending on the hybridisation and can not be used as an exact measure of gene expression.

One of the most popular methods of normalisation for microarray data is called robust multi-array average (RMA) (Irizarry et al. 2003). This method applies a background correction, normalises the arrays to have the same statistical properties with quantile-quantile normalisation and then fits a linear model to obtain the expression measure from each probe set targeting a gene.

Once normalisation has been done, it's effectiveness can be assessed by a MA-

plot between two different arrays (Bolstad et al. 2004). For the measurements of two different arrays $x \in X$ and $y \in Y$, M represents the log ratio of the two values $log_2(x/y)$, and A represents the mean average, $\frac{1}{2}log_2(xy)$. For two arrays that have been properly normalised, the LOESS line should be close to the $M = 0$ axis.

RNA-Seq technology has less of the quality control and normalisation issues associated with the hybridisation step used in microarrays, but instead have quality control issues associated with the sequencing process (Li et al. 2015). These include issues such as ensuring there is no contamination with rRNA or tRNA and ensuring that enough reads have been sequenced. For normalisation it has been shown that RPKM can introduce a bias for lowly expressed genes when running a differential gene analysis (Dillies et al. 2013). For this reason Dillies et al. (2013) recommend to use a method such as DESeq by Anders (2010) where the hypothesis that most genes are not differentially expressed is used. DESeq constructs a scaling factor, based on the median of the ratio, for each gene, of its total number of reads in that lane, with the geometric mean of the total number of reads for that gene across all lanes.

1.5.2.4 Differential gene expression analysis

Once all normalisations have been completed for either microarray or RNA-Seq data, running a differential gene expression analysis is standard. For microarray experiments, with a dataset with 2 or more well-defined classes of samples, it is a relatively simple task to use techniques such as LIMMA (Smyth 2005), to calculate the genes with significant log fold changes in expression between the classes.

LIMMA, or linear models for microarray data, is a package for the statistical programming language and environment R, that fits linear models to the expression data for each gene, to calculate the log fold change of gene expression between different conditions along with their associated p-values.

Finding differential gene expression with RNA-Seq data has the advantage of working directly with count data. Sequencing a number of reads could be viewed as a Poisson process, where the probability of sequencing a particular gene has a specific probability. It has been shown by Marioni et al. (2008) that RNA-Seq data from technical replicates match a Poisson distribution, suggesting that this distribution could be the basis of a statistical test. However the Poisson distribution does not account for the

variation seen in biological replicates, where over-dispersion occurs at large count numbers with variation growing faster than the mean (Anders 2010). Because of this, many differential gene expression methods for RNA-Seq data, such as DESeq (Anders 2010), use a negative binomial distribution model for gene counts and to calculate significance.

1.5.2.5 Gene set enrichment

Using the results of say a differential gene expression, the next step of analysis is to study gene set enrichment. A gene set is a group of genes that share a similar function such as all being involved in the same biological process. There is an increasing number of gene set databases such as GO (Ashburner et al. 2000), which has ontologies describing eukaryotic genes involved in numerous terms related to biological process, molecular function and cellular components.

Other databases include Kyoto encyclopedia of genes and genomes (KEGG) (Kanehisa 2000), a widely used collection of terms listing genes involved in various biological pathways, and more specific databases such as TRANSFAC (Matys et al. 2003) for genes regulated by transcription factors and miRBase (Griffiths-Jones et al. 2006) for genes regulated by various microRNAs. In addition to these databases terms can be manually constructed for example by using the BioGRID protein-protein interaction network (Stark et al. 2006), and selecting all the genes that interact with a protein of interest.

One example of a gene set enrichment system is DAVID (Dennis Jr et al. 2003), which has been widely used but is now no longer being updated, which takes gene lists and uses a modified version of Fisher's exact test (Fisher 1922) to find significant terms. In general Fisher's exact test is a common technique for finding significant terms from a discrete list of genes.

With an ordered list of genes, other enrichment methods can be used. One of these is gene set enrichment analysis (GSEA) developed by Subramanian et al. (2005), that from the ordered gene list calculates an enrichment score. This score gives a higher significance when genes from a specific term, are at the top of the list.

Gene set enrichment can use more than just ranked list but actually incorporate continuous values such as the log fold change values from a LIMMA analysis. This is

the procedure used by many enrichment methods such as generally applicable gene set enrichment, or GAGE (Luo et al. 2009), which finds significant terms by using a two sample t-test of the log-fold change values.

There are a wide number of methods that can be used for gene set analysis of varying statistical complexity. One of the more esoteric methods is HotNet (Vandin et al. 2011), which uses concepts from the physics of heat diffusion to find modules of the protein-protein interaction network that are significantly enriched.

It should be noted that there are several problems with using gene set enrichment analysis. Firstly any method is only as good as our knowledge of the biological pathways involved. To take the GO database as an example, many genes are added to a pathway based on automatic electronic annotation, where the evidence for association has not be reviewed by a curator and may not be valid. In general our knowledge of biological pathways is noisy, incomplete and lacks detail, and this certainly affects results. As has been noted there are a number of competing methods that are possible to use, however there is a general lack of consensus over which method is best (Maciejewski 2013). Simpler techniques may ignore relevant biological knowledge, for instance how gene work together, but complex techniques are difficult to create, interpret and understand.

1.5.2.6 Clustering and biclustering

The above description of analysing transcriptomic data using differential gene expression and then gene set enrichment analysis, works well if the experimental design has two clear conditions, but less well with big datasets that are more of a mass data collection project for heterogeneous clinical samples. Examples of these datasets are those from the Cancer Cell Line Encyclopedia (CCLE) (Barretina et al. 2012) and The Cancer Genome Atlas (CGAN 2012).

In clinical data it is unclear on how to divide the samples into classes, as there are many factors involved distinguishing them from each other, some of which will likely be unknown. Further difficulties can arise from imperfect information, in many diseases differences are often due to mutational variations, however this data is itself evolving and previously different variants have been wrongly associated with a disease (Rehm et al. 2015). Thus since there are no well-defined classes, different approaches to the analysis of gene expression data must be used.

The approach used in the analysis of these datasets often can only be one of data mining and pattern discovery. For this there is thankfully a deep literature of possible approaches that have been used successfully. Clustering and machine learning techniques have been successfully applied to gene expression data, a case model for this is the development of the PAM50 gene-set for diagnosing breast cancer subtype (Parker et al. 2009).

Clustering of gene expression data was first notably practiced by Eisen et al. (1998). They used hierarchical clustering, computing a dendrogram containing all the samples in a tree. This clustering can be applied on either the samples or the genes and can divide them into groups or clusters based on similarities of their expression values. Hierarchical clustering of this kind can be used to classify samples into different subtypes, as was done with breast cancer samples by Perou et al. (2000). Importantly Tibshirani et al. (2002) developed a nearest centroid classifier algorithm to classify cancer samples into the different known clusters types from a minimal gene-set in the gene expression data. This approach was extended for breast cancer by Parker et al. (2009) who devised a method to classify breast cancer into its intrinsic subtype using only 50 genes. These 50 genes form the PAM50 genetic test now widely used in a clinical setting for diagnosing breast cancer subtype.

Standard clustering techniques while successful at identifying relevant subtypes of samples are often only useful at spotting global patterns within the data. Often modes of regulation only effect a subset of samples, leading genes to be conditionally coregulated only on specific cellular or environmental signals (Gasch 2002). Indeed regulation of transcription needs to be dynamic for the organism to adapt to its environment and survive. The problem is that when this process occurs only a subset of the samples would have a particular subset of genes coregulated, and standard clustering techniques would not detect this coregulation in the noise of the data. Solving this problem and finding these samples with coregulated genes is the aim of biclustering algorithms.

1.6 Overview and aims of thesis

The aim of this thesis is to introduce novel bioinformatic methods to specifically investigate the role of mitochondrial biogenesis in human pathologies. Transcriptomic datasets will be the main target of bioinformatics methods developed in this thesis, though it

should be noted that alternative bioinformatic methods could and can be applied to both genomic data as well as increasingly proteomic data to understand mitochondrial function.

Chapter 2 will introduce a novel biclustering algorithm applied to transcriptomic data that is designed to be ideal in identification of different regulation patterns of the 'mito-transcriptome'. It will be shown that this algorithm is superior to existing biclustering methods on a synthetic dataset and that it finds biologically relevant biclusters in a test bacterial *Escherichia coli* dataset.

Chapter 3 will demonstrate the use of this biclustering algorithm in two disease datasets, one for hypertrophic cardiomyopathy and the other for cancer cell lines.

Chapter 4 will involve a more in depth study of breast cancer using this bioinformatic algorithm. Patient samples with different mitochondrial regulation will be identified and breast cancer derived cancer cell line that match these samples will be used as a experimental model to study of these differences. This final results chapter will thus present a pipeline for the identification and experimental study of a novel mode of mitochondrial regulation.

Through all this work I will demonstrate that these novel bionformatic methods have the potential to greatly further our understanding of mitochondrial biogenesis and its role in disease.

Chapter 2

A novel biclustering algorithm

2.1 Introduction

Figure 2.1 shows the general idea of applying biclustering algorithms to investigate the regulation of mitochondrial biogenesis, that is to identify subsets of samples in disease conditions that have a similar regulation of mitochondrial genes. There are however issues with this approach due to the limits of existing biclustering techniques which shall be explained.

Biclustering techniques were first applied to gene expression by Cheng (2000), but the technique itself dates back to the 1970's in the work of Hartigan who referred to it as direct clustering (Hartigan 1972). In its essence, biclustering algorithms select a subset of the rows and columns of a data matrix in such a way that a particular measurement describing the quality of the bicluster is maximised.

It is not known *a priori* how many significant biclusters there are within a data matrix. The exact number will depend on the method of measuring a biclusters quality as well as determining its significance. Additionally the method of search used will determine how many biclusters are found, since it is impractical to exhaustively check every possible bicluster.

Different biclustering algorithms take different approaches to these issues, with some only capable of detecting certain types of bicluster. The various models, described in a review by Madeira (2004), for the different types of bicluster found are shown in Figure 2.2.

The simplest type of bicluster is the constant value bicluster, where all values in a subset of the rows and columns have exactly the same value. Hartigan's direct clustering

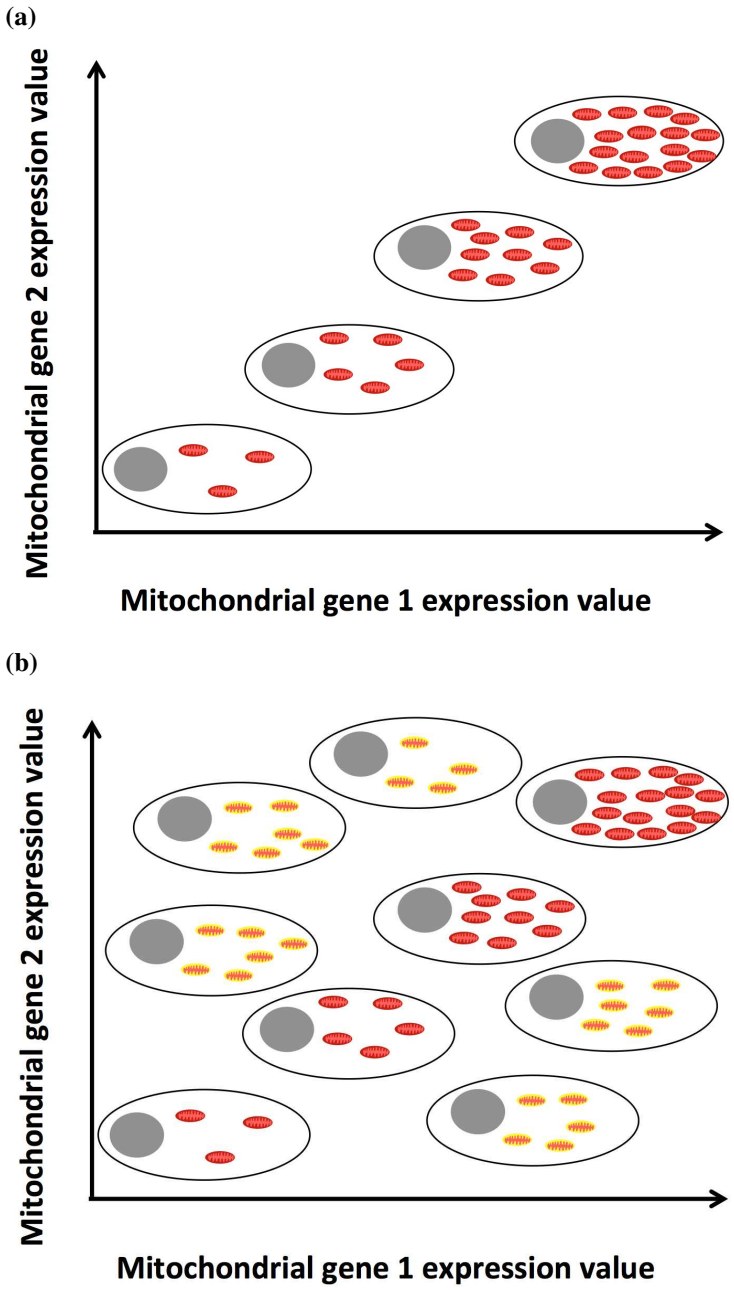

Figure 2.1: Two models of mitochondrial biogenesis in gene expression data, showing scatter plot of the expression of two mitochondrial genes where cartoons of cells with different number of mitochondria replace sample points. In Figure **(a)** there is only one mode of mitochondrial biogenesis in the sample cells, shown by only red mitochondria existing in each cell, and there is a strong correlation between between mitochondrial genes. In Figure **(b)** however there are two modes of mitochondrial biogenesis, represented by the yellow and red mitochondria in the cells, and without knowing which samples belong to which modes, all traces of correlation from the samples with the red mitochondria are lost. In heterogeneous gene expression datasets from clinical data it could be expected that there are multiple modes representing different regulations of mitochondrial biogenesis. A biclustering algorithm can discover these modes by finding the subset of the samples and mitochondrial genes that have many highly correlated mitochondrial genes.

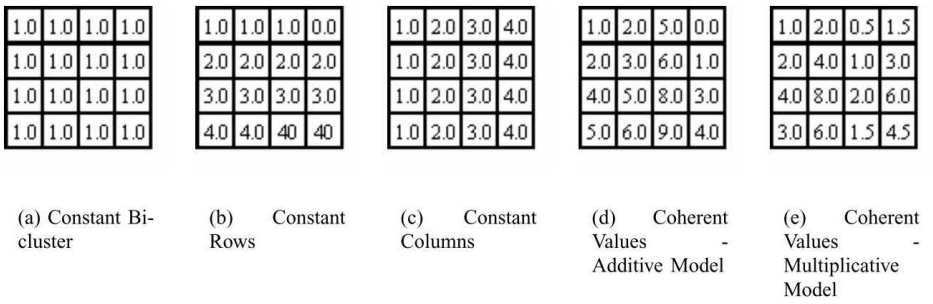

Figure 2.2: Different types of biclusters, figure taken from Madeira (2004).

technique searched for these by developing an algorithm that looked for subsets of the rows and columns with a low variance score. For gene expression data these constant value type of bicluster are not of great biological interest.

Biologically relevant biclusters were first found in gene expression data by Cheng (2000) who developed the Cheng-Church algorithm and introduced the mean square residue score for evaluating biclusters. This method of evaluation has since been used by numerous other biclustering techniques such as MSB (Liu 2007), FLOC (Yang et al. 2005) and BiHEA (Gallo et al. 2009).

Due to the influence the mean square residue has had over many biclustering techniques it is useful to understand its workings.

Definition 1 *Let X represent the set of gene probes, and Y the set of samples, a_{ij} an element in expression matrix A, $I \subset X$ and $J \subset Y$ are subsets of the probes and samples respectively. Then define the mean square residue as*

$$H(I,J) = \frac{1}{|I||J|} \sum_{i \in I, j \in J} (a_{ij} - a_{iJ} - a_{Ij} + a_{IJ})^2 \tag{2.1}$$

Where

$$a_{iJ} = \frac{1}{|J|} \sum_{j \in J} a_{ij}, \qquad a_{Ij} = \frac{1}{|I|} \sum_{i \in I} a_{ij} \qquad \text{and} \qquad a_{IJ} = \frac{1}{|I||J|} \sum_{i \in I, j \in J} a_{ij} \tag{2.2}$$

A submatrix is called a δ-bicluster for some $\delta \geq 0$ if:

$$H(I,J) \leq \delta \tag{2.3}$$

is the maximum acceptable mean square residue score for a bicluster. A higher

value for δ corresponds to a larger bicluster.

This mean square residue approach does find biological relevant biclusters but is limited in the type of bicluster it finds. It is good at finding what is called shifting patterns but less efficient at finding biclusters with scaling patterns (Aguilar-Ruiz 2005).

Here, shifting refers to the type of co-regulation where the gene probes increase or decrease by similar amounts under different conditions while scaling refers to where increases or decreases for the gene probes are more pronounced in some probes than others. This lack of finding scaling patterns means that mean square residue based techniques are unable to find many biologically relevant patterns. However, a logarithm transform on gene expression data will transform scaling patterns to shifting patterns. As gene expression data is commonly logged before analysis, a bicluster that searches for these shifting patterns still has biological merit.

The mean square residue is just one of many methods for assessing bicluster quality, many of these are reviewed in Pontes et al. (2015b). One of these alternative methods would be to examine Pearson's correlation coefficient between probes, and this has been used successfully in some biclustering methods (Pontes et al. 2015b).

Biclustering has been shown to be an NP-complete problem (Tanay et al. 2002), much more difficult than normal clustering. NP here refers to the set of problems that while the solution can be verified in polynomial time there is no known method for finding the answer in polynomial time. Practically this means that for any large dataset an exhaustive test of every possible bicluster is impossible and some kind of heuristic technique must be used to search for potential biclusters.

A summary of the different heuristic methods used in existing biclustering techniques is given in Pontes et al. (2015a), these include methods based in iterative greedy searches, nature inspired techniques and non metric graph based approaches.

There are several problems with using these methods for examining mitochondrial biogenesis. Practically there is the issue that these techniques may fail to be computationally efficient on very large datasets of interest. More importantly though, these existing biclustering algorithms are adept at finding biclusters involving relatively few genes but often will not find biclusters involving a large number of genes. This is particularly relevant when wishing to examine biclusters involving regulation of large pathways accounting for hundreds if not thousands of genes involved in mitochondrial

function.

For the study of mitochondrial biogenesis, there is therefore a need for a new biclustering method that is capable of finding biclusters involving large gene sets within datasets with a large number of samples in a computationally efficient manner. This chapter will describe such a method, demonstrate its superiority over existing techniques using a simulated dataset and test the algorithm on a real gene expression dataset for *Escherichia coli*.

Simulated datasets are essential when aiming to build new bioinformatic tools. A new biclustering method ideally will be tested on a simulated gene expression dataset where all the biclusters are already known. Real biological datasets do not have this advantage.

There are a number of established methods for generating simulated gene expression data, such as GeneNetWeaver (Schaffter et al. 2011), GRENDEL (Haynes 2009), and SynTReN (Van den Bulcke et al. 2006). Simulated data however has a major disadvantage in being unrealistic compared to real biological data. Maier et al. (2013) recently reviewed popular methods of generating synthetic data and showed that simulated datasets are statistically very different from real biological datasets. Despite this, synthetic datasets are a powerful tool for analysing different biclustering techniques.

As well as the many advantages real data has over synthetic, the motivation for testing the biclustering method on a bacterial *E. coli* dataset, came from the hope that due to its smaller genome and transcriptional regulation the results would be more easily understandable. From these results the utility of this new biclustering algorithm could more easily be demonstrated. Additionally, for relevance to the study of mitochondrial biogenesis, *E. coli* could be seen as a good test case due to the mitochondrion's bacterial ancestry.

2.2 Massively correlated biclustering (MCbiclust)

The aim of developing this biclustering algorithm is to find biclusters, composed of large numbers of gene probes, within datasets. The hypothetical bicluster that is sought will have probes whose expression is highly correlated across the subset of samples in the bicluster, and it should not be viewed as important whether these correlations are positive or negative. To achive this a novel bioinformatic method called Massively

Correlating Biclustering (MCbiclust) has been developed which will be described in detail in this section.

A general data pipeline of the full method is given in Figure 2.3 and 2.4 but the first step to creating a method to achieve this is to define a suitable quality metric.

2.2.1 Defining a method of measuring bicluster quality

An obvious and simple way of measuring the quality of the bicluster will be as the mean absolute average value of the probe-probe Pearson's correlation coefficient matrix of the subset of probes calculated from the subset of samples.

A correlation based scoring metric has been used in previous biclustering methods as can be seen in Pontes et al. (2015b). The exact formulation of this correlation score will be defined as follows:

Definition 2 *From a gene expression dataset measuring multiple gene probes across multiple samples, let*

$$X = \textit{Set of all probes, } Y = \textit{Set of all samples} \tag{2.4}$$

Then define two subsets of X and Y, I and J repectively

$$I \subset X \textit{ and } J \subset Y \tag{2.5}$$

Subsets I and J form a bicluster on sets X and Y, and the strength of this bicluster measured is based on measuring the correlations between pairs of probes in set I across all samples in set J. The correlation between a probe $i \in I$ to a probe $k \in I$ across the samples in J is denoted as $C^J_{i,k}$. Then the strength of the bicluster is measured as having a score α based on these correlations, defined as:

$$\alpha^J_I = \frac{1}{|I|^2} \sum_{i \in I} \sum_{k \in I} abs(C^J_{i,k}) \tag{2.6}$$

where the function $abs()$ refers to the absolute value. In words the score α is the average of the absolute values of the gene-gene correlation matrix for gene-probe set I across the samples in sample set J.

It should be noted that in this definition, the value of i is allowed to equal that of k,

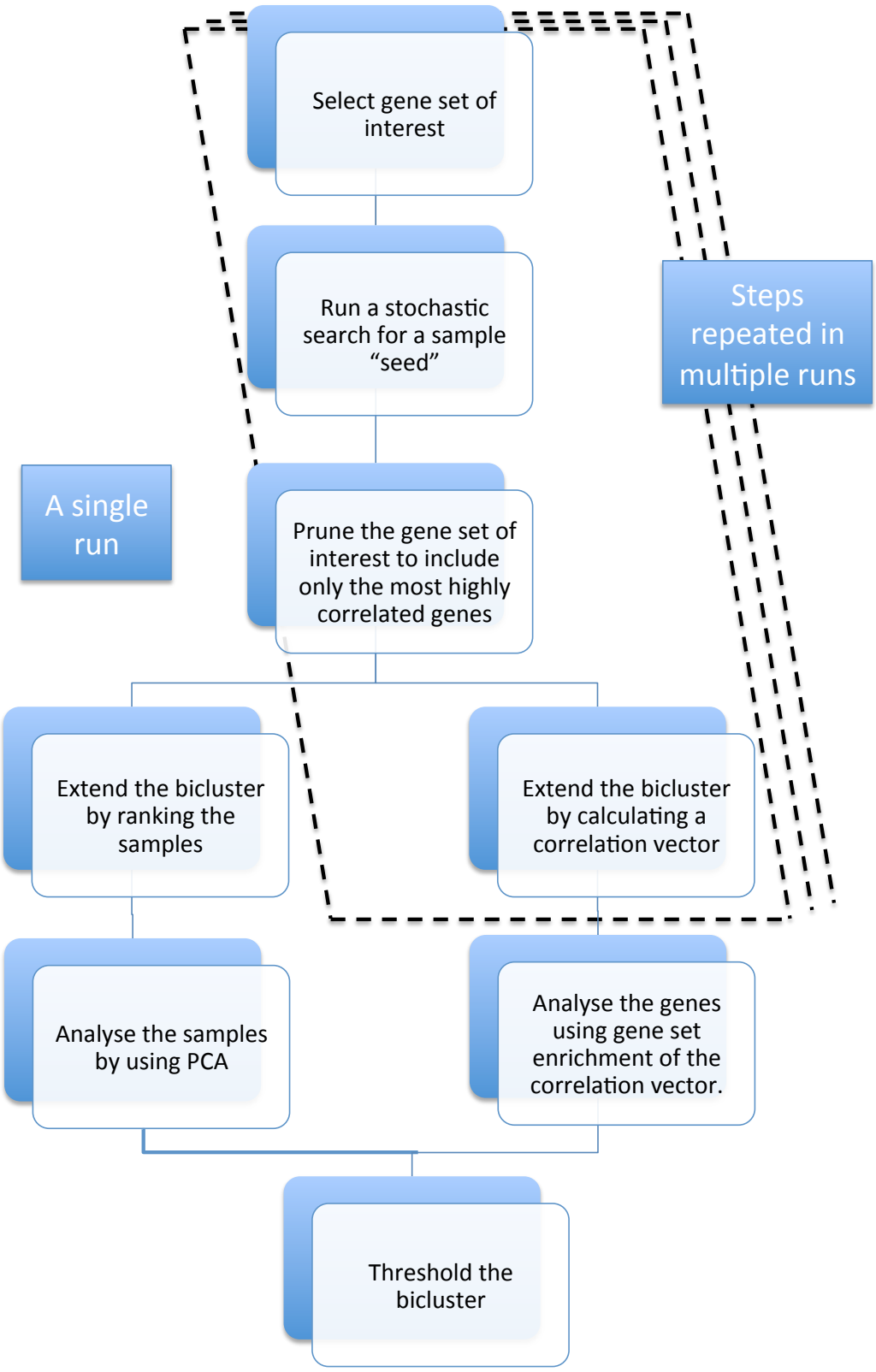

Figure 2.3: The data pipeline of using MCbiclust to analyse a dataset from a single run.

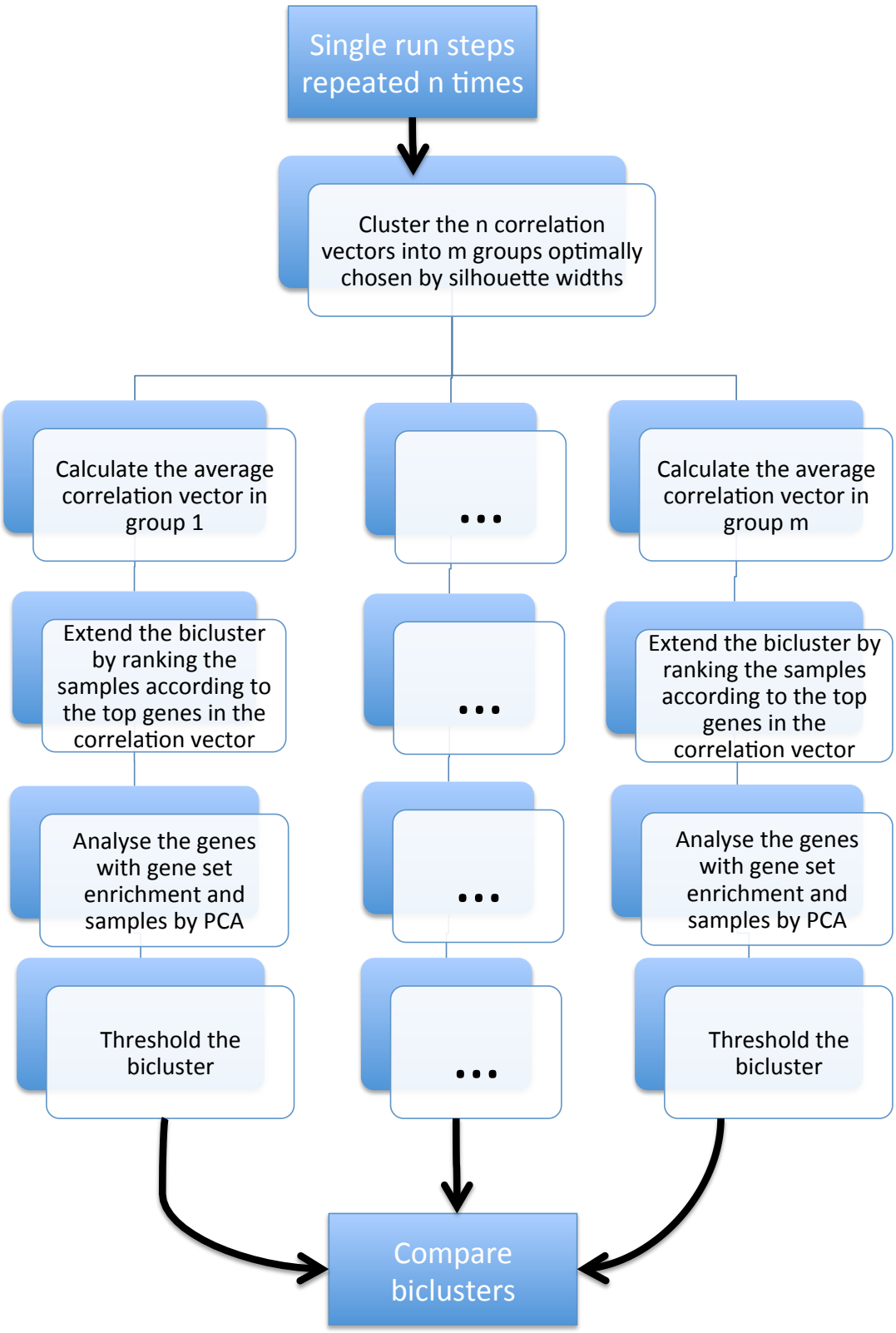

Figure 2.4: The data pipeline of using MCbiclust to analyse a dataset from multiple runs.

this means that the diagonal values in the correlation matrix which will always equal 1 are used to calculate the score. More properly a quality score would not include these values but with large gene sets the overall effect is relatively small and identical in size between two biclusters containing the same number of probes. Since the method is designed to work with large gene sets, and all comparisons of score will be done on biclusters with the same probe length this difference is not important and the score is kept like this due to its computational efficiency.

A high α_I^J value indicates that the probes in set I are being strongly co-regulated across the samples in set J. As α_I^J is calculating using the absolute values of $C_{i,k}^J$, these probes could be in either in correlation or anti-correlation with each other.

2.2.2 A stochastic greedy search for biclusters

Initially n samples are chosen at random for J and the value for α_I^J calculated, the algorithm then undergoes a stochastic greedy search to find the optimum n samples to maximise α_I^J. In each step of the algorithm, the sample set J is altered with one of the n samples randomly chosen and replaced with one of the $N - n$ samples. If after the replacement the value for α is higher then the new set J is kept, if not then J reverts to the old set before replacement. In this way after thousands of steps a bicluster is found. Typically n is set to be much smaller than the total number of N samples in the dataset, such that the greedy search can find a local maximum more easily in the possible sample space.

It is also important to note that the probe set I is not altered during this process. This has been deliberately made this way to ensure that the algorithm in its greedy search is forced to find biclusters affecting a large number of genes. I can be chosen at random or to represent a particular pathway of interest such as genes involved in the mitochondrial proteome. Computationally the size of probe set I is limited to roughly 1500 probes due to the expense of calculating large correlation matrix in this and further steps.

The n samples chosen by the algorithm after a set number of steps T is called the seed of the bicluster and is used in further steps to both extend the bicluster and elucidate its biological function. The details of how this initial algorithm functions is presented in Algorithm 1.

Algorithm 1 Find a sample subset which has maximal correlation for a chosen probe subset.

Precondition: J is a subset of the samples Y. I is a subset of the probes X. $C^J_{i,k}$ is the correlation between the ith and kth probe in set I across the samples in set J. Q is the number of iterations of the greedy search.

function FINDSEED(J, Y, I, Q)
  $n \leftarrow |J|$ ▷ $||$: size of set, typically $|J| << |Y|$
  $N \leftarrow |Y|$
  $J' \leftarrow J$
  $\alpha \leftarrow \frac{1}{|I|^2} \sum_{i \in I} \sum_{k \in I} abs(C^{J'}_{i,k})$
  for $l \leftarrow 1$ to Q **do**
    $r_1 \leftarrow$ a random integer between 1 and n
    $r_2 \leftarrow$ a random integer between 1 and $N - n$
    $J^* \leftarrow J'$
    $J^*[r_1] \leftarrow \overline{J}[r_2]$ ▷ $\overline{J'} : Y - J'$
    $\alpha^* \leftarrow \frac{1}{|I|^2} \sum_{i \in I} \sum_{k \in I} abs(C^{J^*}_{i,k})$
    if $\alpha^* > \alpha$ **then**
      $\alpha \leftarrow \alpha^*$
      $J' \leftarrow J^*$
    end if
  end for
  return J'
end function

2.2.3 Pruning the bicluster

Once the bicluster seed n has been found, with an associated high value for α, the correlation matrix, M^J_I of the bicluster can be examined. α^J_I may be further maximised by selecting only a fraction of the probes, that is by taking out some of the rows in M^J_I. It is possible to find a very high α from a bicluster with very few probes but this is not desirable as it puts a bias against finding biclusters involving many genes. The solution to pruning the number of probes in the bicluster without only leaving a small number is by using hierarchical clustering, as discussed in Section 1.5.2.6.

By separating the probes into m groups $I_1, I_2, ...I_m$ using hierarchical clustering, the probes which are most strongly correlated in the bicluster and those that are not will belong to separate groups. These probe groups can then be scored to judge their bicluster quality $\alpha^J_{I_i}$ for $i \in 1, 2, ..., m$. Those groups that score less than the original α^J_I are then judged to be not contributing to the strength of the bicluster and omitted. After omitting these groups of probes, a new probe-set is created I'. Complete details of this

procedure is given in Algorithm 2.

Algorithm 2 Find the most highly correlating probes within a bicluster.

Precondition: m is the number of groups to divide the probes into. *hclust* an algorithm that computes the dendrogram result from hierarchical clustering. J' is an output of Algorithm 1 and I is the same as was used for the input of that algorithm,. All other variables as defined in Algorithm 1

1: **function** HICORGENES(J', Y, I, m)
2: $Dend \leftarrow hclust(C_I^{J'})$ ▷ *hclust* performed on the correlation matrix of probe-set I across samples J
3: $I_m \leftarrow Dend$ cut at a height to have m groups. ▷ $I_{m(i)}$ will refer to the probes in the ith group
4: $I^* \leftarrow \emptyset$
5: $\alpha \leftarrow \frac{1}{|I|^2} \sum_{i \in I} \sum_{k \in I} abs(C_{i,k}^{J'})$
6: **for** $l \leftarrow 1$ to m **do**
7: $\alpha_l \leftarrow \frac{1}{|I_{m(l)}|^2} \sum_{i \in I_{m(l)}} \sum_{k \in I_{m(l)}} abs(C_{i,k}^{J'})$
8: **if** $\alpha_l > \alpha$ **then**
9: $I^* \leftarrow I^* \cup I_{m(l)}$
10: **end if**
11: **end for**
12: **return** I^*
13: **end function**

2.2.4 Extending the bicluster

2.2.4.1 Samples

After finding the sample seed of n samples and highly correlating probe set I' of the bicluster, it is possible to extend these to find the full bicluster. For samples this is done by finding the ranking that most conserves the correlation found. Precisely, the remaining $N-n$ samples in $\overline{J}$ can be ranked in terms of how well they preserve the correlation strength of the correlation matrix.

Let $J_n = J$, the $n+1$st sample is chosen as the sample for which $\alpha_{I'}^{J_{n+1}}$ is maximum with $J_{n+1} = J_n \cup \overline{J_{ni}}$ for some $i \in 1,2,...,N-n$. This process is repeated until all N samples have been ranked. In this way each sample in the dataset can be ranked by how well it fits in to the chosen bicluster. The details are explained in Algorithm 3.

2.2.4.2 Genes

A slightly different approach can be used to rank every probe measured in the gene expression database, not just the probes in set I. A different approach is necessary due

Algorithm 3 Rank samples according to strength of bicluster

Precondition: All variables as defined before in Algorithms 1 and 2, with J' being an output of Algorithm 1 and I^* being an output of Algorithm 2.

function SAMPLESORT(J', I^*)
  $J_{ord} \leftarrow J'$
  while $length(J_{ord}) < length(J') + length(\overline{J'})$ **do**
    $\alpha^* \leftarrow \emptyset$
    for $i \leftarrow 1$ to $length(\overline{J})$ **do**
      $J^* \leftarrow J_{ord} \cup \overline{J}[i]$
      $\alpha \leftarrow \frac{1}{|I|^2} \sum_{i \in I^*} \sum_{k \in I^*} abs(C^{J^*}_{i,k})$
      $\alpha^* \leftarrow \alpha^* \cup \alpha$
    end for
    $MaxLoc \leftarrow which.max(\alpha^*)$
    $J_{ord} \leftarrow J_{ord} \cup \overline{J'}[MaxLoc]$
  end while
  return J_{ord}
end function

to the large number of probes present within the highly correlating probe set that would not be ranked, as well as the large computational cost in ranking all the gene-probes.

The probes within the probe-set are again divided into m groups using hierarchical clustering, the gene group I_m with the largest $\alpha^J_{I_m}$ is chosen as that which represents the bicluster best. The average gene expression for this probe-set is then calculated for the first n ranked samples. Using this, the correlation of every probe to that of the bicluster can be calculated, and this will be referred to as the correlation vector, CV. The details of this are given in Algorithm 4.

Conversely this approach would not be suitable to rank the samples, as due to their small number within the sample seed it is not practical to use hierarchical clustering to separate them into different groups, and it would lose the direct interpretation the ranking method has in terms of preserving correlation strength.

2.2.5 Analysing the bicluster

2.2.5.1 Genes

Using the correlation vector it is possible to run gene-set enrichment analysis to see all the pathways that are involved in the regulation identified by the bicluster. This can be done by using any of the methods described in Section 1.5.2.5, but as the values of the correlation vector are not normally distributed being bounded between -1 and 1 a

Algorithm 4 Rank probes according to strength of bicluster

Precondition: All variables as defined before in Algorithms 1, 2 and 3, with J' being an output of Algorithm 1 and I^* being an output of Algorithm 2.

function GENERANK(J', I^*, m, M)
  $Dend \leftarrow hclust(C^{J'}_{I^*})$
  $I_m \leftarrow Dend$ cut at a height to have m groups.
  $S \leftarrow \emptyset$
  for $l \leftarrow 1$ to m **do**
    $\alpha_l \leftarrow \frac{1}{|I_{m(l)}|^2} \sum_{i \in I_{m(l)}} \sum_{k \in I_{m(l)}} abs(C^{J'}_{i,k})$
    $S \leftarrow S \cup \alpha_l$
  end for
  $S.MaxLoc \leftarrow which.max(S)$
  $I^*_m \leftarrow I_{m(S.MaxLoc)}$
  $M^* \leftarrow M^{J'}_{I^*_m}$ ▷ Gene expression matrix of samples J' and probes I^*_m
  $D_{J'} \leftarrow$ Average of probes in I^*_m for samples in J'.
  $C.vec \leftarrow \emptyset$
  for $i \leftarrow 1$ to $length(X)$ **do**
    $\beta \leftarrow Cor(D_{J'}, M^{J'}_i)$
    $C.vec \leftarrow C.vec \cup \beta$
  end for
  return $C.vec$
end function

Mann-Whitney test (Mann 1947) can be used to test significance between genes in a particular gene set and those that are not.

2.2.5.2 Samples

Primarily for plotting purposes but also for sample classification it is beneficial to run a principal component analysis (PCA) on the samples. PCA is a statistical procedure initially developed by Pearson (1901) (for a more modern review see Wold et al. (1987) or Abdi (2010)),that undertakes a dimensional reduction on a dataset. PCA transforms a multi-dimensional dataset by converting it to a new set of variables, this transformation is reversible and the new set of variables are known as principal components. These principal components are calculated as a linear combination of the original variables and are chosen under two main restraints. Firstly they are chosen such that the first component explains the most variation within the dataset, the second component the second most and so on. Secondly all components must be at right angles or orthogonal to each other, that is they are all lineally uncorrelated to each other.

Since the components are ranked by how much variance in the dataset they explain, PCA is effective at dimensional reduction since the first few principal components can explain the majority of the variance within the data.

This is done using the gene-probes which have been found to be highly correlated in Algorithm 2 and the ordering of the samples calculated in Algorithm 3 (See Figure 2.3 and 2.4). PCA is run on a sub-matrix of the entire gene expression matrix containing the top ranked n samples from the calculated ordering and the highly correlating probes. With this the calculated eigenvectors from the principal component analysis are used to fit a value for the first principal component (PC1) to every sample. When plotting the fitted PC1 value against the sample ordering, a fork like pattern is often seen separating the highly correlated samples into two distinct groups. Details of this are given in Algorithm 5.

Algorithm 5 Calculate the first principal component for all the samples

Precondition: n is the number of samples to calculate the initial PC1 values, and I^* is an output of Algorithm 2 and J_{ord} is an output of Algorithm 3. $pcfun$ is a function that perfoms a principal component analysis and returns the matrix of eigenvectors. $lsfit(x,y)$ is a function that performs the least square estimate of b in the model $y = x*b+e$. All other variables as defined before in Algorithms 1, 2, 3 and 4

1: **function** PC1VEC(M, I^*, J_{ord}, n)
2: $ts \leftarrow J_{ord}[(1,2,3,...,n)]$
3: $PC.eig \leftarrow pcfun(M^{ts}_{I^*})$
4: $PC.vec \leftarrow \emptyset$
5: **for** $i \leftarrow 1$ to $length(Y)$ **do**
6: $\gamma \leftarrow lsfit(PC.eig, J_{ord}[i])[1]$ ▷ The fitted value for the first principal component
7: $PC.vec \leftarrow PC.vec \cup \gamma$
8: **end for**
9: **return** $PC.vec$
10: **end function**

2.2.6 Thresholding the bicluster

This biclustering method outputs a ranking of all the probes and the samples, however this is not typical of alternative methods. It is common for methods to clearly define exactly which samples and which probes are within the bicluster found. To generate comparisons and provide a level of certainty that any individual sample or probe is within the bicluster a threshold function is needed. The aim of this function is to take the

ranked list of samples and probes and return those that are definitely within the bicluster.

For probes the correlation vector values are used and k-means clustering is run to divide these values into two groups. A probe should either be regulated in the bicluster or not, and k-means separates the values into two, one with higher and lower average absolute correlation vector values. It is this higher group that is said to be definitely in the bicluster.

For the samples, a ranking exists but not according to simple numerical values but to the strength of the entire correlation matrix. To classify the samples, instead the ranking and the calculated PC1 values for each sample are used. The samples towards the last 10% of the ranking are taken, where it is assumed that no samples are present in the bicluster. From these samples the associated PC1 values are examined and a suitable interval range chosen, e.g the 2.5 and 97.5 percentiles. The first ranked sample within this interval is the first of the ranked sample not within the bicluster, and no other samples ranked after it will be within the bicluster. In this way a precise set of probes and samples are chosen to be present in the bicluster. Details of this method are given in Algorithm 6.

2.2.7 Methods for dealing with multiple runs

Since the biclustering algorithm performs a greedy stochastic search, the outcome of different runs of the algorithm will produce different results. The dataset may contain multiple different biclusters and to find them the algorithm will need to be run multiple times. Each run of the algorithm finds only a single bicluster sample and highly correlating gene-probe set, different seeds may correspond to very similar biclusters, and thus the seeds themselves are not suitable for comparison.

Instead of seeds it is best to compare the correlation vectors from multiple runs, this compares the strength of each individual probe to the bicluster found and whether it is positively or negatively correlated. If the results of two runs are similar, the probes involved will be the same and thus the correlation vectors should closely match.

Therefore identifying the number of distinct biclusters found is equivalent to finding the number of distinct clusters of correlation vectors. This can be done with the concept of cluster silhouettes first described by Rousseeuw (1987). Silhouettes show how well each object lies in their cluster, and therefore can judge the optimum number of clusters.

Algorithm 6 Threshold function to define probes and samples in bicluster

Precondition: $C.vec$ is an output of Algorithm 4. J_{ord} is an output of Algorithm 3 and $PC.vec$ is an output of Algorithm 5. $samp.sig$ is the threshold p-value for determining which samples and probes are within the bicluster. pb is the percentage of samples ranked at the end of the ordering to use for the threshold calculation. $kmeans(x,n)$ is a function the clusters set x into n groups using k-means clustering and returns a vector of length the same as x classifying the members of the set into the groups $1,2,...,n$. $quantile(x,n)$ is a function that calculates the n quantile of x. All other variables as defined before in Algorithms 1, 2, 3 ,4 and 5

1: **function** THRESHBIC($C.vec, J_{ord}, PC.vec, samp.sig, pb$)
2: $genes.kmeans \leftarrow kmeans(C.vec, 2)$
3: $g.group1 \leftarrow which(genes.kmeans == 1)$
4: $g.group2 \leftarrow which(genes.kmeans == 2)$
5: **if** $mean(abs(C.vec))[g.group1] > mean(abs(C.vec))[g.group1]$ **then**
6: $bic.genes \leftarrow g.group1$
7: **else**
8: $bic.genes \leftarrow g.group2$
9: **end if**
10: $pn \leftarrow ceiling(\frac{length(J_{ord})}{pb} * 100)$
11: $pc1.min \leftarrow quantile(PC.vec[length(J_{ord}) - pn, ..., lenght(J_{ord})], samp.sig/2)$
12: $pc1.max \leftarrow quantile(PC.vec[length(J_{ord}) - pn, ..., lenght(J_{ord})], 1 - samp.sig/2)$
13: $first.no.samp \leftarrow which(PC.vec > pv1.min \& PC1.vec < pc1.max)[1]$
14: $bic.samples \leftarrow J_{ord}[1,2,..., first.no.samp - 1]$
15: **return** $bic.genes, bic.samples$
16: **end function**

To do this, the average dissimilarity to other objects both within and in other clusters is used. For an object i in a cluster A, $a(i)$ is defined as the average dissimilarity of i to all other objects in A. Similarly in relation to another cluster C, $d(i,C)$ is defined as the average dissimilarity of i to all objects in C, and $b(i)$ is defined as the minimum $d(i,C)$ for all $C \neq A$. Using these definitions, $s(i)$ the silhouette width of object i can be defined as follows:

$$s(i) = \frac{b(i) - a(i)}{max(a(i), b(i))} \tag{2.7}$$

In this way when $s(i)$ is very close to 1, the object i's dissimilarity to other objects in the same cluster is much smaller than its dissimilarity to objects in other clusters. A value of $s(i)$ close to 0 indicates the object i would have been just as well-clustered if placed in cluster C, while a negative value indicates it would have been better clustered

if in C.

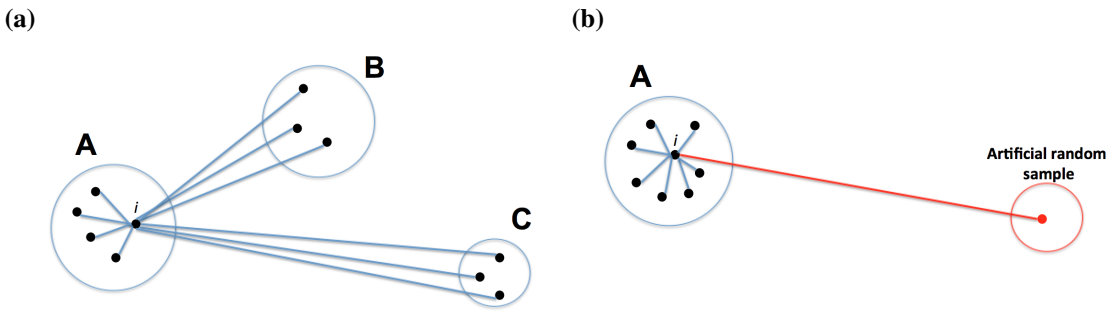

Figure 2.5: A visual explanation of silhouette widths. In Figure **(a)** the computation of $s(i)$ is illustrated, there are three clusters A, B and C and object i is in cluster A, the larger the length of the lines connecting the objects the larger the dissimilarity between those objects, $a(i)$ is calculated as the average dissimilarity of all objects in A to i, while $b(i)$ is the minimum of the dissimilarity between object i and all the objects in cluster B or cluster C. Figure **(b)** graphically illustrates the case where all objects are very similar and how an artificial sample can be added to calculate the silhouette width for keeping all the original data in a single cluster.

Using silhouette widths, how well objects can be clustered can be easily visualised, as seen later in Figure 2.11 on page 101. What is more useful is the optimum number of clusters can be found by maximising the average silhouette width of all objects.

When judging how many distinct biclusters have been found, the dissimilarity score used between two gene-probe correlation vectors, CV_1 and CV_2 is:

$$1 - |cor(CV_1, CV_2)| \tag{2.8}$$

That is 1 minus the absolute correlation between the two gene-probe correlation vectors.

It may be the case that the correlation vectors are best kept as a single cluster, as all biclusters found are highly similar and may even be near identical. With the silhouette method this poses a problem, as silhouette width is calculated by how well a sample belongs in its cluster compared to being placed in an alternative cluster. This means that an average silhouette width can not be calculated if there is only one cluster, and that the correlation vectors will 'optimally' be split into two clusters even if there is little difference between those clusters.

To get around this problem an artificial correlation vector can be added to the data. This artificial correlation vector contains random noise, sampled from a normal

distribution with mean 0 and standard deviation 1, and will be so different from the other correlation vectors, as under clustering to form its own cluster. Therefore splitting this data into two clusters will separate the artificial correlation vector from the real ones. Using this two group clustering, an average silhouette width can be calculated that gives an indication if all the correlation vectors are best kept as a single cluster. This value can then be compared to the average silhouette width for the real correlation vectors divided into multiple clusters allowing the optimum number of clusters to be chosen. A visual illustration of silhouette widths is given in Figure 2.5.

Following the identification of the number of distinct biclusters, an analysis of the distinct biclusters can be made more efficient by averaging all correlation vectors describing the same distinct biclusters together. Using this average correlation vector for each distinct bicluster, gene set enrichment analysis can be performed to help understand the functional role of the bicluster, and the average correlation vectors can be directly compared with each other, identifying modules of genes with the same regulation in both. Further gene set enrichment analysis can then be done on these distinct gene modules.

Ranking of the samples can also be done using the average correlation vectors, by taking the top probes in the average correlation vectors, identifying the bicluster sample seed n which has the maximum correlation score α associated with those top probes, and then calculating the ranking as in Section 2.2.4.1 from those initial n samples.

In practice the difference between sample rankings from the different runs identifying the same bicluster is very small and since it is a computationally expensive task, it is sufficient to only be done once for each distinct bicluster found from multiple runs.

2.3 Benchmarking of massively correlated biclustering on a simulated dataset

2.3.1 Generation of artificial data

A synthetic dataset was created using an adapted version of the method used by Hochreiter et al. (2010) for the biclustering method Factor Analysis for Bicluster Acquisition (FABIA), using the R package 'FABIA'. This method implants a set number of multiplicative biclusters that match the FABIA model, into a dataset.

The FABIA model is a multiplicative model. According to the model, two vectors are similar if one is a multiple of the other, biclusters without noise can therefore be represented as the outer product of two sparse vectors, $\lambda_i z_i^T$. A dataset containing p biclusters can therefore be modelled as the summation of the outer product of p different sparse vectors plus a matrix containing additive noise, Y.

$$X = \sum_{i}^{p} \lambda_i z_i^T + Y = \Lambda Z + Y \tag{2.9}$$

Where Λ is a matrix containing the λ_is as columns and Z is a matrix containing vectors z_i^T as rows. Using this model of biclusters, FABIA uses factor analysis to identify biclusters within the dataset. To generate synthetic data Hochreiter et al. (2010) assumed $n = 1000$ genes and $l = 100$ samples and implanted $p = 10$ biclusters using Equation 2.9 as a model.

This method was adapted to assure that there were no overlap of samples belonging to different biclusters, meaning that each sample belonged to one and only one bicluster.

This was done by creating 8 separate synthetic datasets, using the FABIA model by Hochreiter et al. (2010) described in Equation 2.9. Each dataset contained only 1 bicluster, on average containing approximately 500 genes and 130 samples, and each dataset was mean centered according to the genes before being combined. Eight biclusters were chosen so that there would be over 1000 samples in the combined synthetic dataset, meaning the final synthetic dataset contained 1000 genes and 1059 samples.

Enforcing sample exclusiveness to a single bicluster was done primarily to make the comparison between the different bicluster algorithms simpler. If a sample belonged to two or more biclusters, due to each bicluster affecting a large number of the genes, there would be a significant number of genes belonging to both biclusters and this overlap of genes could potentially confound the classification of samples to their correct bicluster.

While biologically it is feasible for a sample to belong to multiple biclusters, the biclusters aimed to be found by MCbiclust are very large biclusters, composed of many genes, e.g. all the nuclear encoded mitochondrial proteins. It is perhaps less likely that multiple of these large biclusters would be present in the same sample and for the means of creating a synthetic dataset discounting this possibility is a reasonable assumption to

make. It can also be justified as the purpose of the synthetic dataset is not to model real data but to compare different biclustering algorithms.

2.3.2 Means of comparison between different biclustering methods

A sample or gene is either a part of a found bicluster or not, in this way methods used in the evaluation of binary classifiers can be used to compare different biclustering methods. Sets of biclusters discovered by different biclustering methods will be compared in various ways by using receiver operator characteristics (ROC) curves, the F1 score and a calculated consensus score, as used by Hochreiter et al. (2010).

A ROC curve plots the true positive rate (TPR), also known as the recall, on the y-axis against the false positive rate (FPR) on the x-axis. The TPR is the ratio of the number of true positives in the binary classifier by the total number of the true positives (TP) plus the number of false negatives (FN), or:

$$TPR = TP/(TP+FN) \tag{2.10}$$

The FPR is the ratio of the number of false positives in the binary classifier over the total number of false positives (FP) plus the number of true negatives (TN), or:

$$FPR = FP/(FP+TN) \tag{2.11}$$

A TPR of 1 refers to the binary classifier identifying correctly all the positive samples, while a false positive rate of 1 refers to the classifier identifying incorrectly all the negative samples as positive. If a binary classifier is better than random it will have a significantly higher TPR than FPR.

A ROC curve is typically calculated for different thresholds of the classifier. This can be done for the results of MCbiclust, which give a ranked list of the genes and samples, for which the TPR and FPR can be calculated along the entire ranked list. Other biclustering methods typically do not give a ranked list but a set of samples or genes calculated to be in the bicluster, these can be plotted as points on the ROC plot. Using the threshold bicluster algorithm, Algorithm 6, that calculates a threshold to determine which of the top samples and genes are within a given bicluster, the MCbiclust method can be more directly compared with others.

Besides from ROC curves which use the TPR and FPR, another important measure is precision, that is the number of correct positive results divided by the number of all positive results:

$$\text{Precision} = TP/(TP+FP) \tag{2.12}$$

Taking into account precision when assessing a binary classifier, allows the identification of classifiers that while possibly having a high TPR, fails to identify the majority of the positive samples. Of course a good binary classifier should have both a high TPR and high precision, the F1 score is a measure that can judge whether this is so by calculating the harmonic mean TPR and precision:

$$F1 = 2\frac{precision \times TPR}{precision + TPR} \tag{2.13}$$

Providing the known set of synthetic biclusters and a set of predicted biclusters, the consensus score, ROC curves and F1 score are calculated using the following steps (an overview of which is given in Figure 2.6:

1. For the results of each biclustering algorithm compute the similarities between all possible pairs of the known and predicted biclusters using the Jaccard index. The Jaccard index is a measure of similarity between two sets A and B which is equal to the ratio of the size of the intersection with the size of the union of sets A and B, defined as:

   $$J(A,B) = \frac{|A \cap B|}{|A \cup B|} \tag{2.14}$$

   A high Jaccard index indicates a high degree of similarity between the two sets.

2. Assign each of the predicted biclusters to one of the known synthetic biclusters using the Munkres algorithm. The Munkres algorithm, also known as the Hungarian algorithm, was developed by Kuhn (1955) and is an algorithm that solves the assignment problem. The assignment problem refers to a case when there is a number of agents and a number of tasks that these agents can perform, each task has some cost associated to each agent. An algorithm solving the assignment problem assigns one agent to each task in a way that the total cost is minimised.

   In the case of assigning the found biclusters from the biclustering algorithms

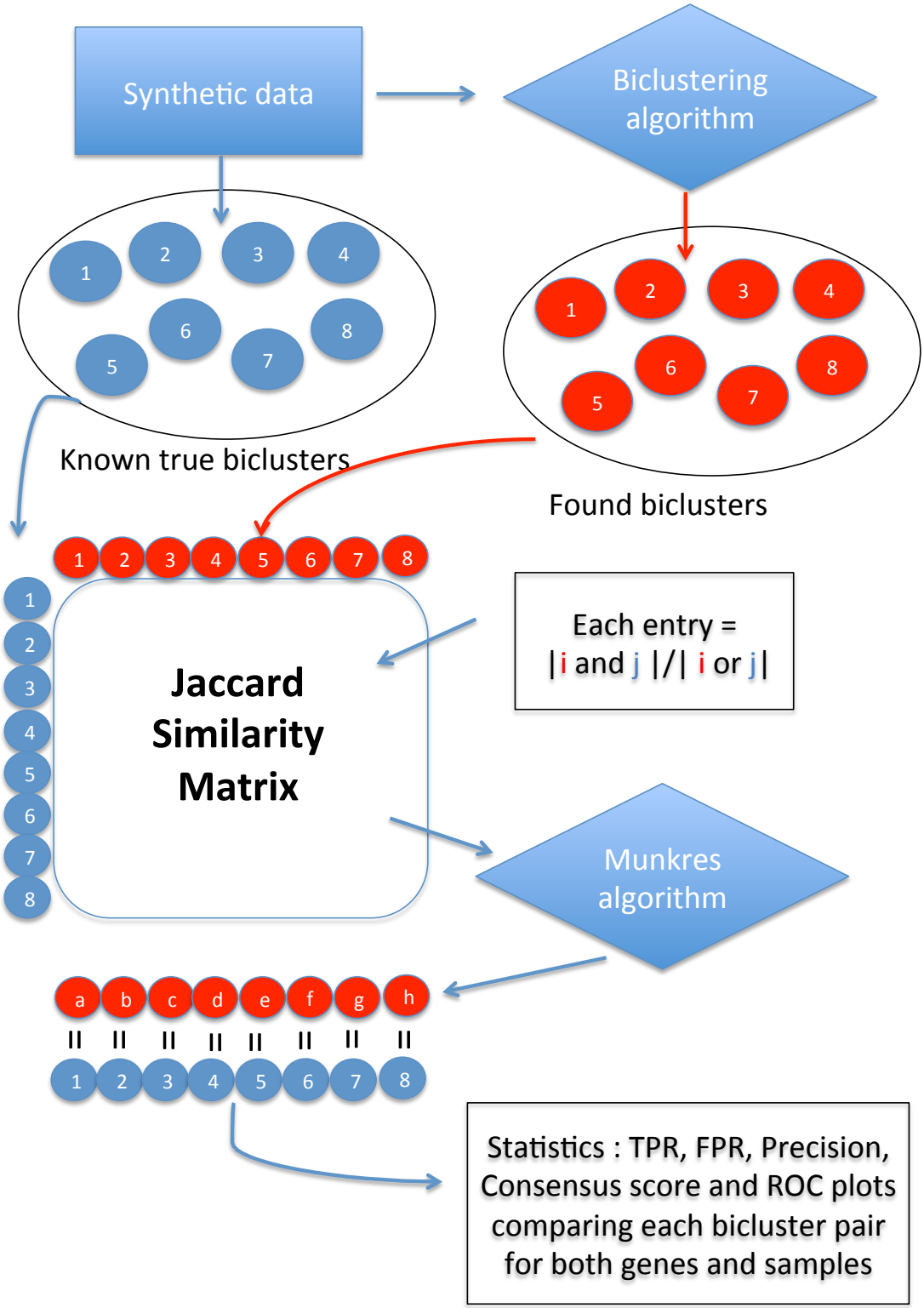

Figure 2.6: Pipeline used to compare different biclustering algorithms on the synthetic data.

to the known synthetic biclusters, the found biclusters are the agents while the known synthetic biclusters are the tasks and the cost to be minimised between found bicluster A and synthetic bicluster B is $1 - J(A,B)$.

3. Finally with the found biclusters assigned to synthetic biclusters, statistics can be calculated. The consensus score, as used by Hochreiter et al. (2010), is calculated as the sum of the Jaccard index similarities of the predicted biclusters to their matched known biclusters and dividing by the size of the larger set. This final division by the size of the larger set penalises any difference in the number of predicted and known biclusters. This consensus score gives a measure of how well the different biclustering methods identified all the synthetic biclusters.

   Statistics like TPR, FPR, precision and the F1 score, previously defined, can be calculated using the number of true/false positive/negative samples correctly classified into each bicluster. These with the consensus score can assess how well each found bicluster matches its assigned synthetic bicluster. From the TPR and FPR, ROC curves can be made using the ranked gene and sample lists from the results of the MCbiclust algorithm and the other methods represented as points.

In addition to the threshold bicluster method of determining the precise bicluster described, in Section 2.2.6 on page 83, an optimum bicluster from the ranked list can also be calculated as the number of n top genes and m top samples that maximises the Jaccard Index to the known bicluster.

To calculate this optimum MCbiclust bicluster the Jaccard Index must be calculated for every possible top n genes and m samples so that the maximum value can be chosen, before the Munkres algorithm assigns the found patterns to the synthetic biclusters. By doing this a Jaccard Index matrix can be constructed from the calculated values, this in turn can be visualised as a heat map. Two examples of this Jaccard index heat map are given in Figure 2.7, and show the Jaccard index matrix for one of the synthetic bicluster being calculated for two different orderings found from the MCbiclust method. One of these patterns clearly matches the synthetic bicluster while the other does not.

2.3.3 Biclustering methods

Using the methods from Section 2.3.2, 10 different biclustering methods were compared on the synthetic dataset. A summary of these methods is given in Table 2.1.

Method	Description	References	Software
MCbiclust	The method developed in this Chapter, outputting a ranked list of the genes/probes and samples		Run with R package 'MCbiclust' for details see Appendix A.
FABIA	Factor analysis for bicluster acquisition.	Hochreiter et al. (2010)	Run with R package 'fabia'
FABIAS	A variation of the FABIA method using a different prior distribution in the model.	Hochreiter et al. (2010)	Run with R package 'fabia'
biMax	Assuming a binary data model, uses a fast divide and conquer strategy to find biclusters, originally designed as a reference method to compare different biclustering techniques.	Prelić et al. (2006)	Run with R package 'biclust' (Kaiser 2008).
CC	Landmark method that originally applied biclustering methods to gene expression data, strategy is to find biclusters which minimise the mean square residue.	Cheng (2000)	Run with R package 'biclust' (Kaiser 2008).
Plaid	Biclusters form layers that are superposed to form the data matrix, the algorithm aims to minimise the sum of square errors matching the model to the data.	First Proposed by Lazzeroni et al. (2002), the actual implementation used is that of the improved version by Turner et al. (2005)	Run with R package 'biclust' (Kaiser 2008).
ISA	Iterated Signature Algorithm, designed to work on very large datasets, and decomposes them into modules.	Bergmann et al. (2003)	Run with R package 'isa2' (Csárdi et al. 2010).
FLOC	Flexible Overlapped biClustering, uses a stochastic iterative greedy search, to find possible overlapping biclusters.	Yang et al. (2003)	Run with R package 'biCARE' .
QUBIC	Qualitative biclustering algorithm is a non-metric method that uses ideas from graph theory to find biclusters.	Li et al. (2009)	Run with R package 'rqubic'.
CPB	Correlated Patterns Biclustering, a method utilising Pearson's correlation as its quality measurement score.	Bozdağ et al. (2009)	Run with python script.

Table 2.1: Summary of the different biclustering algorithms compared. Python script for CPB is available from: http://bmi.osu.edu/hpc/software/cpb/index.html

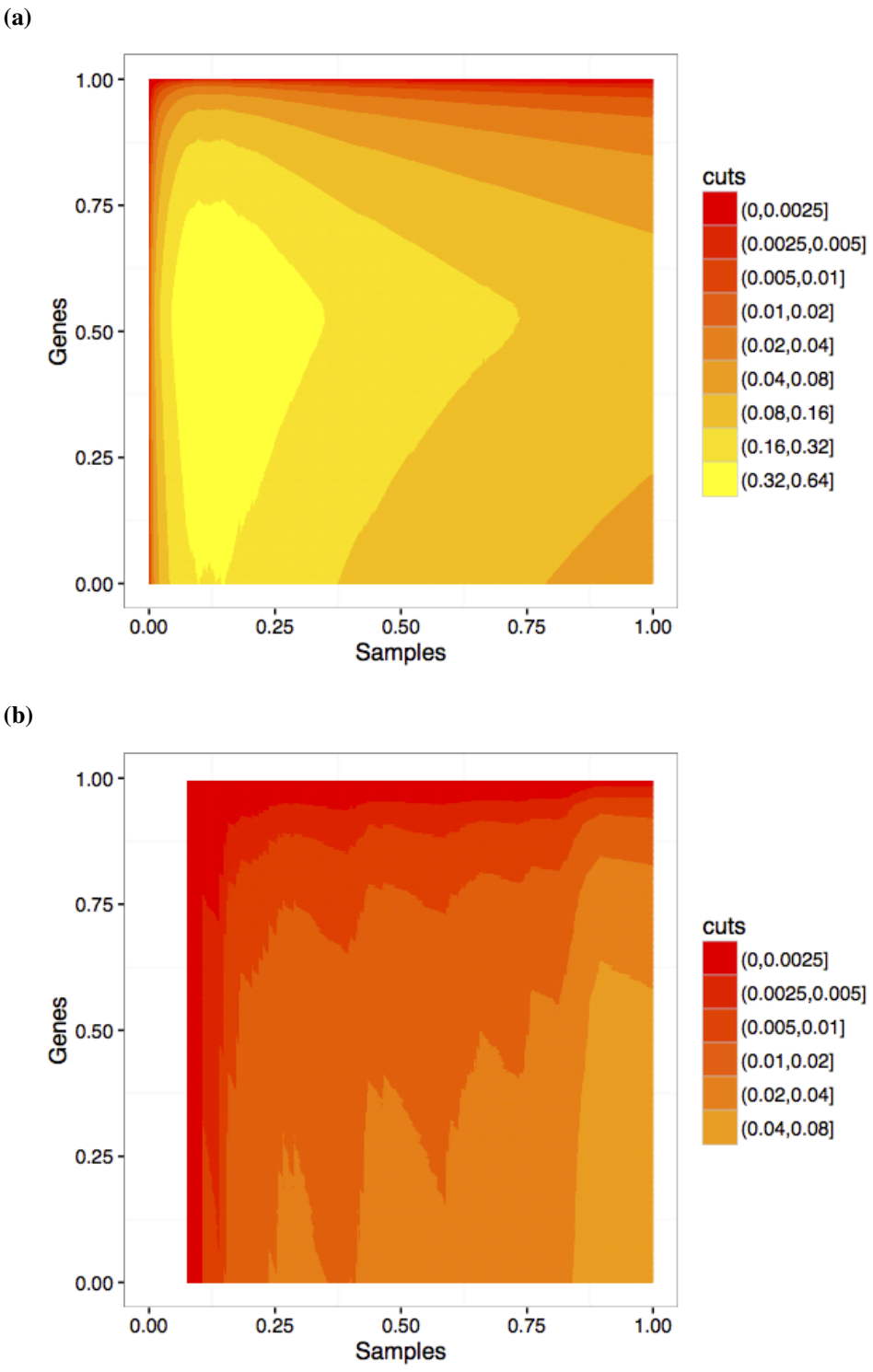

Figure 2.7: Jaccard index matrix from two different discovered MCbiclust patterns compared to the same synthetic bicluster. **(a)** shows a pattern that strongly matches the synthetic bicluster, while **(b)** shows a pattern that has almost no relation to the synthetic bicluster.

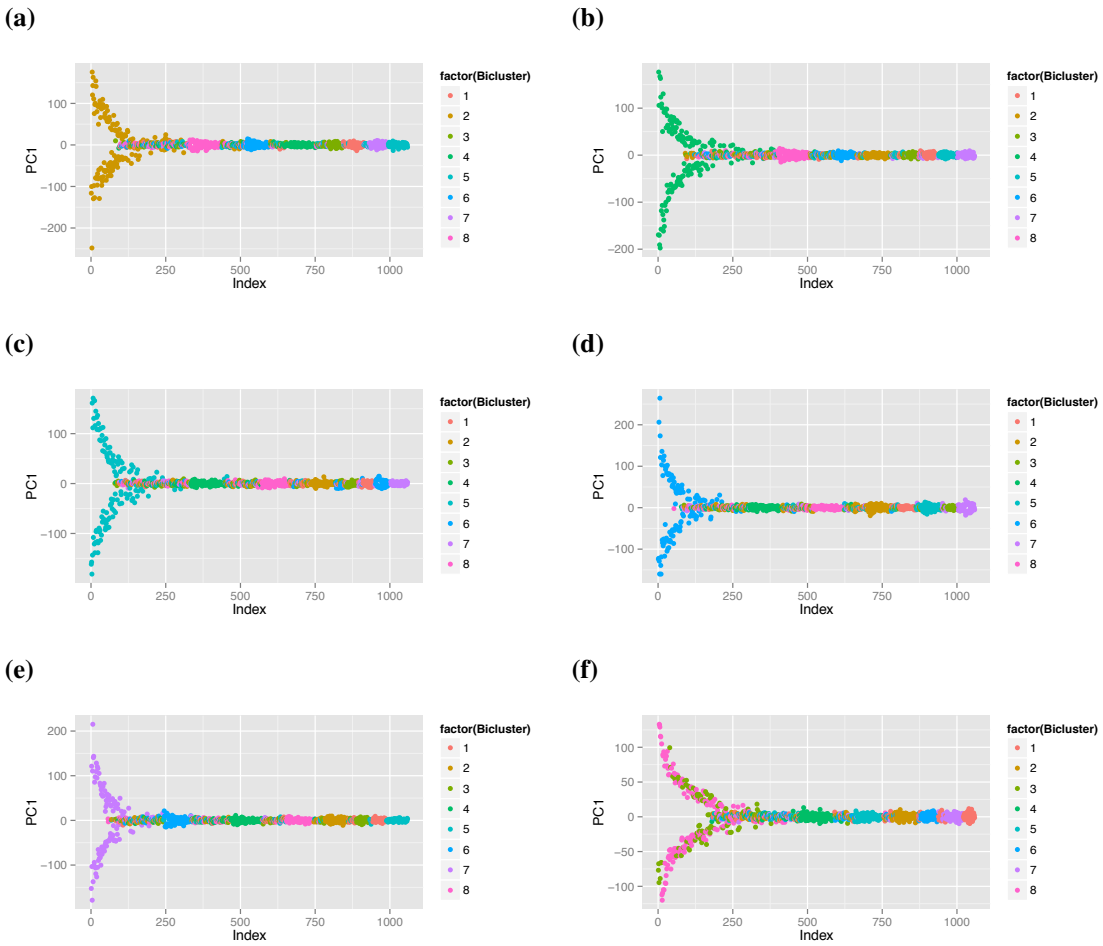

Figure 2.8: Principal component plots from synthetic data results. The *x*-axis show the samples ordered by how well they preserve the correlation identified in the bicluster and the *y*-axis plost the values for the first principal component describing the bicluster. Using MCbiclust 6 patterns were found, and the samples coloured according to the known synthetic biclusters clearly show that MCbiclust is indeed capable of finding these biclusters.

2.3.4 Comparison of different biclustering methods

MCbiclust when applied to the synthetic data found 6 biclusters. This can be seen in Figure 2.8, which plots the first principal component calculated from the found biclusters, against the samples ordered by how well they preserve the correlation pattern present in the bicluster. These plots have the samples colour coded to the known synthetic biclusters in the data, and show that MCbiclust correctly identifies the known synthetic biclusters.

For the other biclustering methods, when possible the parameters were set to find 8 biclusters the same number of embedded biclusters within the synthetic data. This was the case for the FABIA, FABIAS, biMax, CC and FLOC methods. MCbiclust however

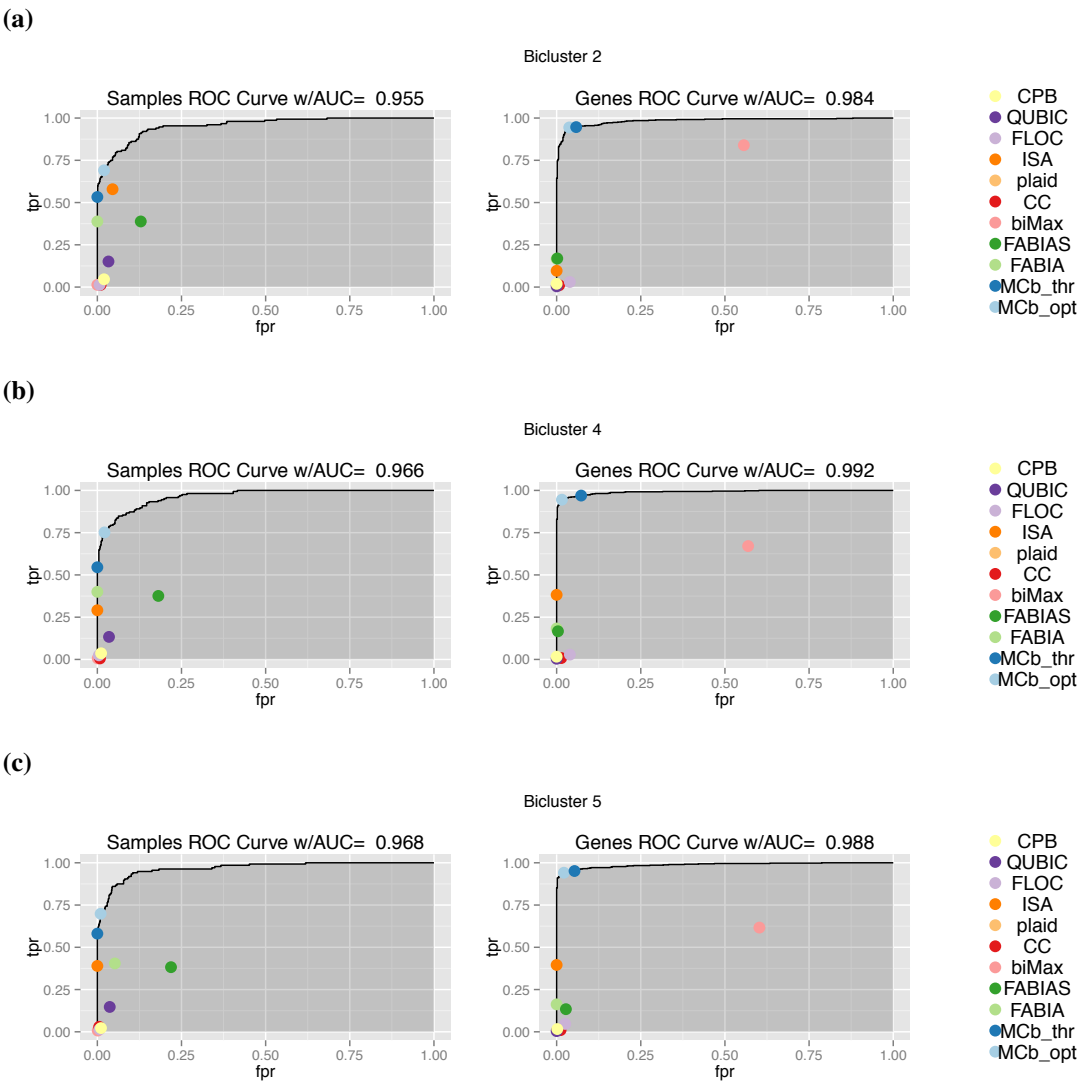

Figure 2.9: ROC plots comparing 3 of the 6 found biclusters using MCbiclust with their matched synthetic bicluster, assessing both genes and samples separately. The coloured points show the matched bicluster found from other methods. Figure continued on page 97.

does not have this capability and only found 6 distinct biclusters. Five of these identified nearly all the genes and samples in the biclusters with a 0 false positive rate. While one pattern was a mix of two of the known biclusters, and the difference can clearly be seen on the ROC plots in Figure 2.9. This means that MCbiclust failed to identify one of the known synthetic biclusters.

In contrast to this the alternative methods struggled to identify any large biclusters within the data, often only identifying very small biclusters containing relatively few genes and samples. This is likely due to these methods being designed when datasets were much smaller and contained relatively few samples.

Of the other methods besides MCbiclust, the two that most stood out was FABIA

(d)

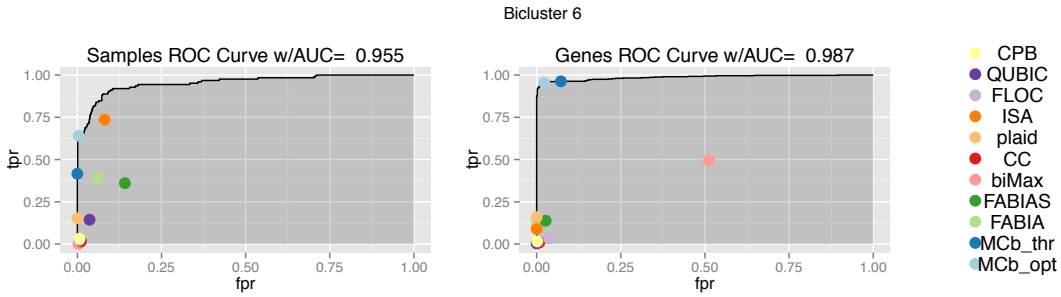

(e)

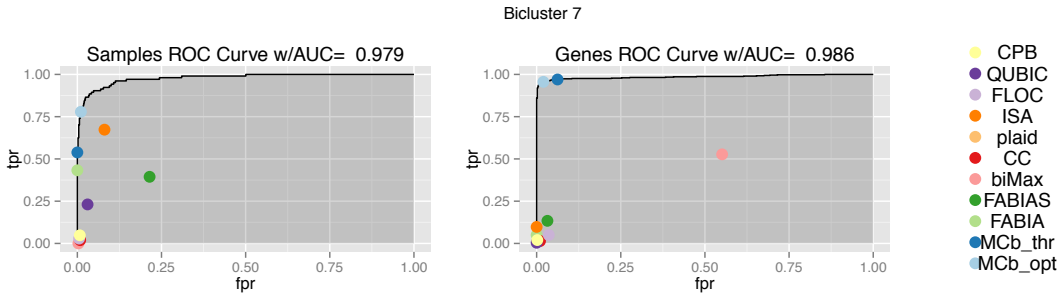

(f)

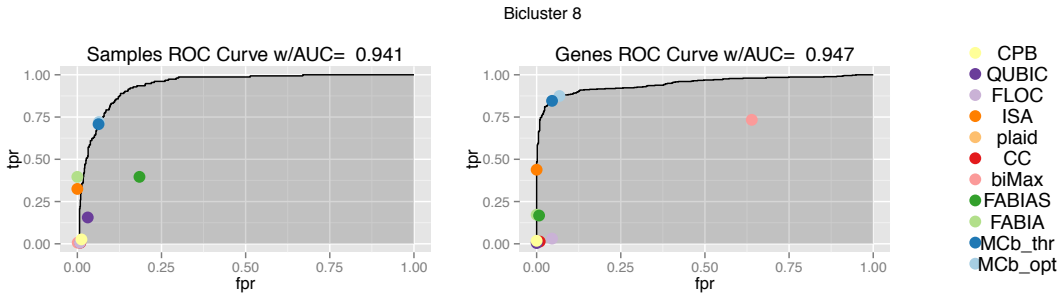

Figure 2.9: Figure continued from page 96. ROC plots comparing the 3 of the 6 found biclusters using MCbiclust with their matched synthetic bicluster, assessing both genes and samples separately. The coloured points show the matched bicluster found from other methods.

and ISA. FABIA had the advantage that the synthetic data was generated according to the model FABIA uses to identify biclusters, but still the method failed to find the complete bicluster in all cases and included false positives.

ISA is designed for use on large datasets so may also be expected to perform better. Its biggest downfall however was the sheer number of biclusters identified, well over 500. Out of these 500, 8 were however reasonable matches for the 8 synthetic biclusters. Despite this, even if all the erroneously identified biclusters are ignored, the set of the best 8 still have a lower consensus score than MCbiclust and only slightly better than the consensus score for FABIA. This is with the penalisation MCbiclust has on the

Method	Biclusters Found	Consensus Score	Genes F1	Samples F1
MCbiclust optimum	6	0.4368	0.8145	0.6634
MCbiclust threshold	6	0.3462	0.8043	0.5864
FABIA	8	0.04106	0.1962	0.549
FABIAS	8	0.02475	0.2498	0.2878
biMax	8	0.002343	0.5697	0.01672
CC	8	0.0001895	0.02177	0.03344
Plaid	2	0.004164	0.1299	0.1747
ISA	504	0.001191	0.3256	0.5459
FLOC	8	0.0006008	0.06603	0.03746
QUBIC	9	0.0003819	0.008219	0.2113
CPB	24	0.0001685	0.02989	0.06277
ISA best	8	0.07504	0.3256	0.5459

Table 2.2: Comparison statistics of different biclustering methods

consensus score from only finding 6 out of the 8 patterns.

Examining the consensus score with other metrics such as the F1 score for genes and samples as can be seen in Table 2.2 on page 98, MCbiclust clearly outperforms the other biclustering methods. This demonstrates MCbiclust's unique potential to identify large scale biclusters within large datasets.

2.4 Case study: *Escherichia coli* expression data

2.4.1 Rationale

Escherichia coli is a gram negative bacteria that is used as a model for prokaryotic organisms. In comparison to eukaryotic cells *E. coli* has a very small genome, the K-12 strain commonly used in labs having 4290 protein encoding genes. As stated in Section 2.1, the purpose of testing the biclustering algorithm on an *E. coli* dataset is that due to its smaller genome it may prove a simpler initial model than eukaryotic cells, and thus an easier test case to demonstrate that the biclustering algorithm works on real data.

Thus it is hoped that any analytical results concerning transcriptomic patterns of *E. coli* may be better understood and that these results may even have some relevance to examining mitochondrial biogenesis due to the many similarities between bacteria and mitochondria.

Despite this reduction in simplicity from considering the entire eukaryotic cell, the complexity of regulation of *E. coli*, like the mitochondria in the cell, is not without difficulty and still very high. There is however enough known about the regulation

of genes within *E. coli* to provide a suitable test for the workings of the biclustering algorithm.

Proteins such as sigma factors are used to initiate RNA synthesis, with different sigma factors known to regulate different bacterial genes. A biclustering algorithm may be able to pick up samples showing increased or decreased activity levels of sigma factor regulation, depending on the level of noise in the data. The genes that are regulated by particular sigma factors are known from databases such as RegulonDB (Gama-Castro et al. 2011).

The *E. coli* dataset used is from the Many Microbes Microarray database (Faith et al. 2008). This dataset includes 907 samples with 7459 probes, which include many probes for non-coding intergenic regions. These intergenic regions have been classified by Tjaden et al. (2002) as being operon elements, 5'-UTRs, 3'-UTRs, small RNAs, new ORFs or transcripts of unknown function. The samples within the dataset are from a wide variety of conditions, mostly involving different growing media conditions with the addition of various drug compounds. In this way the biclustering algorithm is also able to identify differences in regulation caused by different environmental conditions.

Overall this dataset is ideal for test purposes and has been used previously for benchmarking bioinformatic algorithms such as by Maier et al. (2013). With this data the biclustering algorithm was run 1000 times, each time with 1000 randomly chosen probes. From these runs the output of the correlation vector for each found bicluster was recorded.

2.4.2 Finding the number of distinct biclusters

After 1000 runs of the biclustering algorithm, the correlation vectors found must be analysed to obtain the number of distinct biclusters. This is done using the silhouette width method described in Section 2.2.7.

First however the relation between the correlation vectors can be initially visualised by plotting a heatmap of the correlation between the correlation vectors where the correlation vectors have been ordered according to the structure of a dendrogram calculated by hierarchical clustering. This can be seen in Figure 2.10.

Using the hierarchical clustering as calculated on the heat map in Figure 2.10, the dendrogram can be cut at various places to form k distinct clusters. To find the optimum

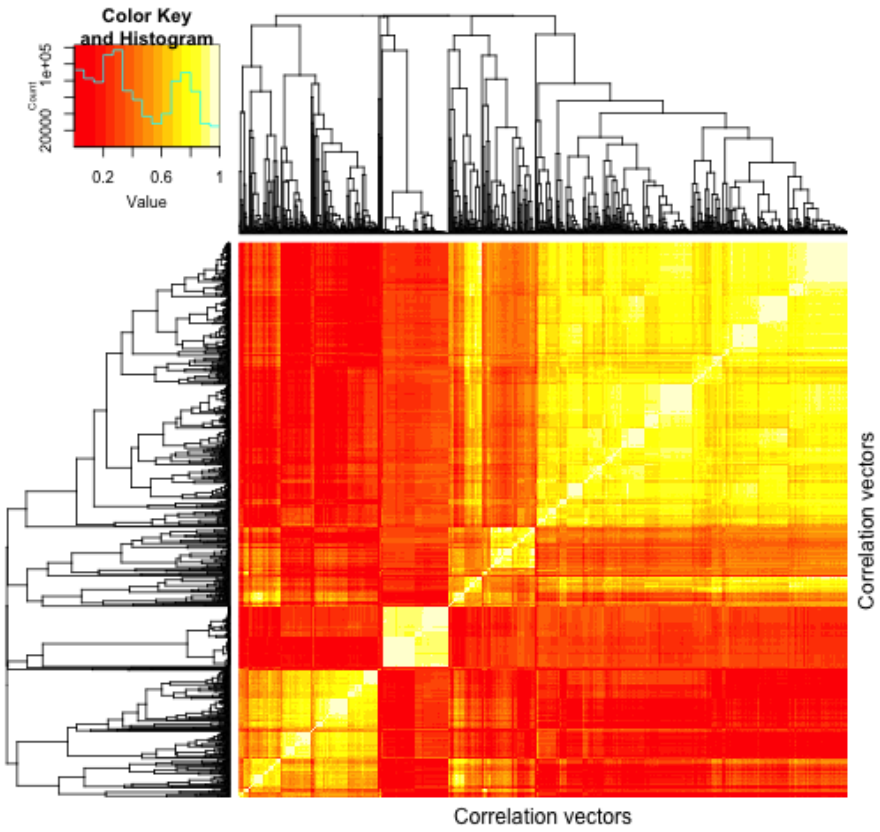

Figure 2.10: Heat map of the correlation matrix of correlation vectors, where correlation vectors are vectors containing the correlation of every probe measured to the pattern found in the bicluster. 1000 biclusters were found by running MCbiclust 1000 times on *E. coli* data initialised with random probe-sets, and each bicluster found has an associated correlation vector, describing the correlation of every probe to the pattern found in the bicluster. The correlation vectors have been rearranged according to a dendrogram calculated by hierarchical clustering.

number of distinct clusters, the average silhouette width is calculated for 1 to 20 clusters and as can be seen in Figure 2.11 the number of optimum clusters is 3.

Using these 3 distinct bicluster groups, which will be denote as $E1$, $E2$, and $E3$, containing correlation vectors from 656, 229 and 115 runs respectively, the averages of the correlation vectors can be calculated and from these an attempt made to understand what these biclusters represent. These biclusters are all large, after thresholding with a sample p-value of 0.05 they were found to contain 4822, 4700 and 6086 probes and 131, 130 and 96 samples respectively.

(a)

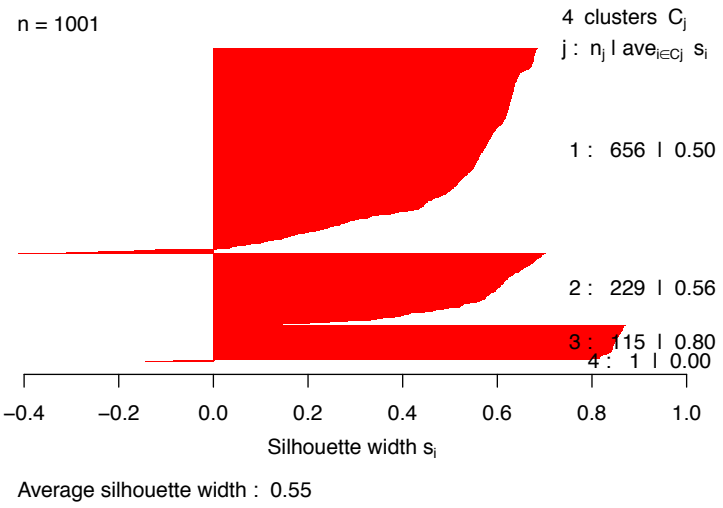

(b)

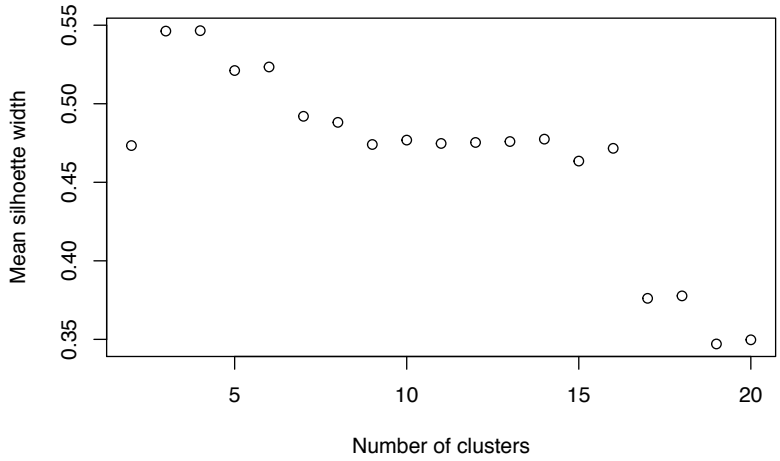

Figure 2.11: Output from silhouette width analysis on *E. coli* data, **(a)** shows the silhouette plot when the data is divided into 3 clusters, the 4th cluster of size 1 contains the artificial correlation vector used to judge whether the correlation vectors are better not divided into multiple clusters and can be ignored from further analysis. **(b)** shows the mean average silhouette width as the number of clusters varies.

2.4.3 Analysis of different bicluster patterns

The first thing that can be done to understand these 3 patterns is to run a gene set enrichment analysis, to see if there are any significant pathways. This was done in the manner described in Section 2.2.5.1 using a Mann-Whitney test on the average gene-probe correlation vector associated with each distinct bicluster. The terms tested

included GO terms related to *E. coli* as well as manually chosen terms of genes regulated by Sigma factors and other *E. coli* transcription factors from RegulonDB (Gama-Castro et al. 2011), additionally terms for probes that are examining genes or the intergenic regions were added.

Tables B.1 to B.3 in Appendix B give the full results of these gene set enrichment studies. For patterns $E1$, $E2$ and $E3$, 175, 25 and 196 significant terms were found respectively, of these there is a large overlap of 132 terms which are significant in both $E1$ and $E3$. These terms seem mostly related to biosynthetic processes but also include terms such as ribosome biogenesis and transcription factor NanR and overall seem to be related to *E. coli* proliferation.

This however does not explain the difference between $E1$ and $E3$, the difference seems primarily related to the terms for intergenic and non-intergenic probes, both being extremely significant in $E3$ with adjusted p-values of $2.355E-299$ and $1.076E-187$ respectively, comparatively in $E1$ the adjusted p-values were still very significant but only $6.670E-29$ and $8.284E-18$ respectively.

Upon examining the values of the intergenic and non-intergenic regions in the average correlation vectors, it is clear that this is the driving force of the pattern $E3$ along with the significant pathways regulated similarly to $E1$. This can be seen in Figure 2.12**(b)**, which shows a strong anti-correlation between the average expression of the intergenic and non-inter-genic regions, with one outlier sample always selected in the seed for $E3$ samples responsible for finding the pattern.

With the $E3$ pattern there is an extremely highly significant effect from the difference in expression between intergenic and non-intergenic genes, which must be assumed to have some regulatory function possibly from microRNAs. Both $E1$ and $E3$ patterns have multiple significant GO terms, it is not at all clear from the gene set enrichment analysis what is driving the $E2$ pattern.

There are only 25 significant terms for $E2$, and compared to $E1$ and $E3$, these have relatively small p-values. Interestingly some of the most significant terms are those related to the Sigma factors, indicating that these may be driving the pattern. However if this is the case it is odd that there are relatively few GO terms that are found significant.

One variable not tested for significance in the gene set enrichment is position on the genome, when this is analysed the meaning of pattern $E2$ immediately becomes

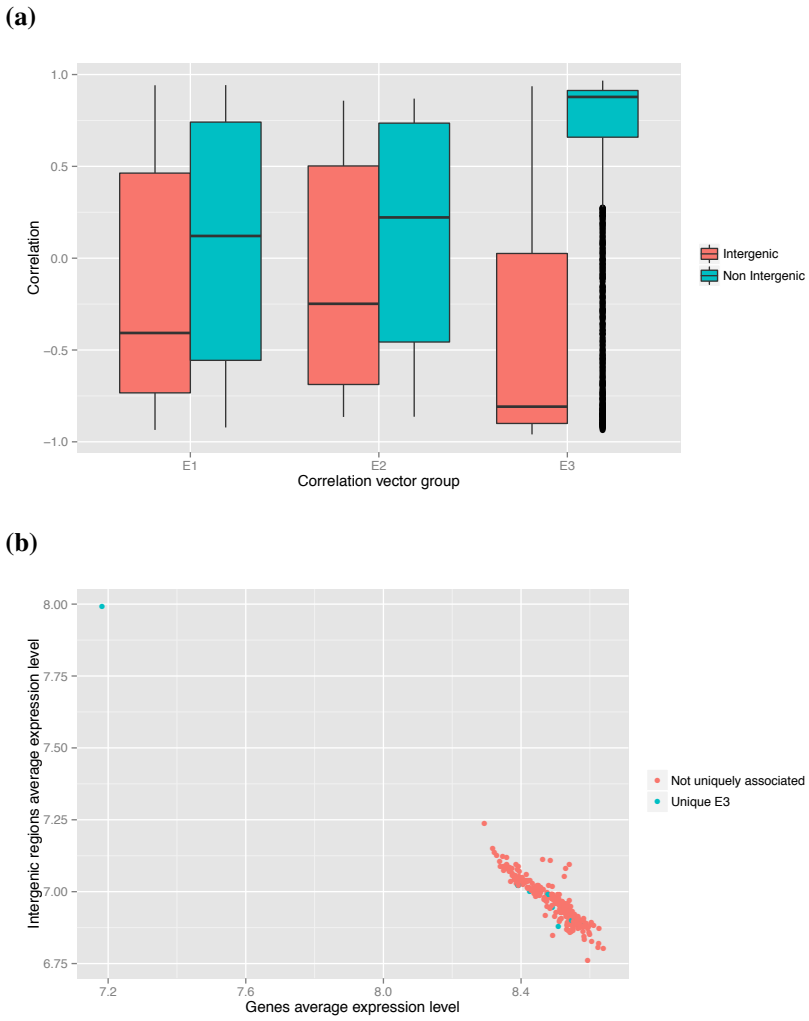

Figure 2.12: **(a)** shows box plots of the values of the intergenic and non-intergenic regions within the average correlation vectors for the three distinct biclusters, showing just how big this difference is in $E3$. **(b)** shows for every sample in the dataset a scatter plot of the average expression value of the intergenic regions versus the average expression value of all the probes. There is a significant negative correlation between the two, with a linear model fitted between the two having a r^2 value of 0.609, and a p-value of $9.02e-187$. The inter-genic regions on a whole seem to have a repressive effect on the expression of the genes and there is one clear outlier which was always and only found in the sample seed for pattern $E3$, though even without this outlier the relationship is highly significant with a r^2 value of 0.554, and a p-value of $2.53e-159$, the effect size is however much smaller and therefore harder to detect with the biclustering algorithm over the noise of the data.

clear, with some samples having a major up-regulation of genes close to the origin of replication. Figure 2.13 shows the genome presented as a heat-map, and then using a sine wave as a model of the strength of the correlation vector showing that the minimum is approximately at the origin of replication.

Further, by examining the conditions of the samples in the dataset, many have been

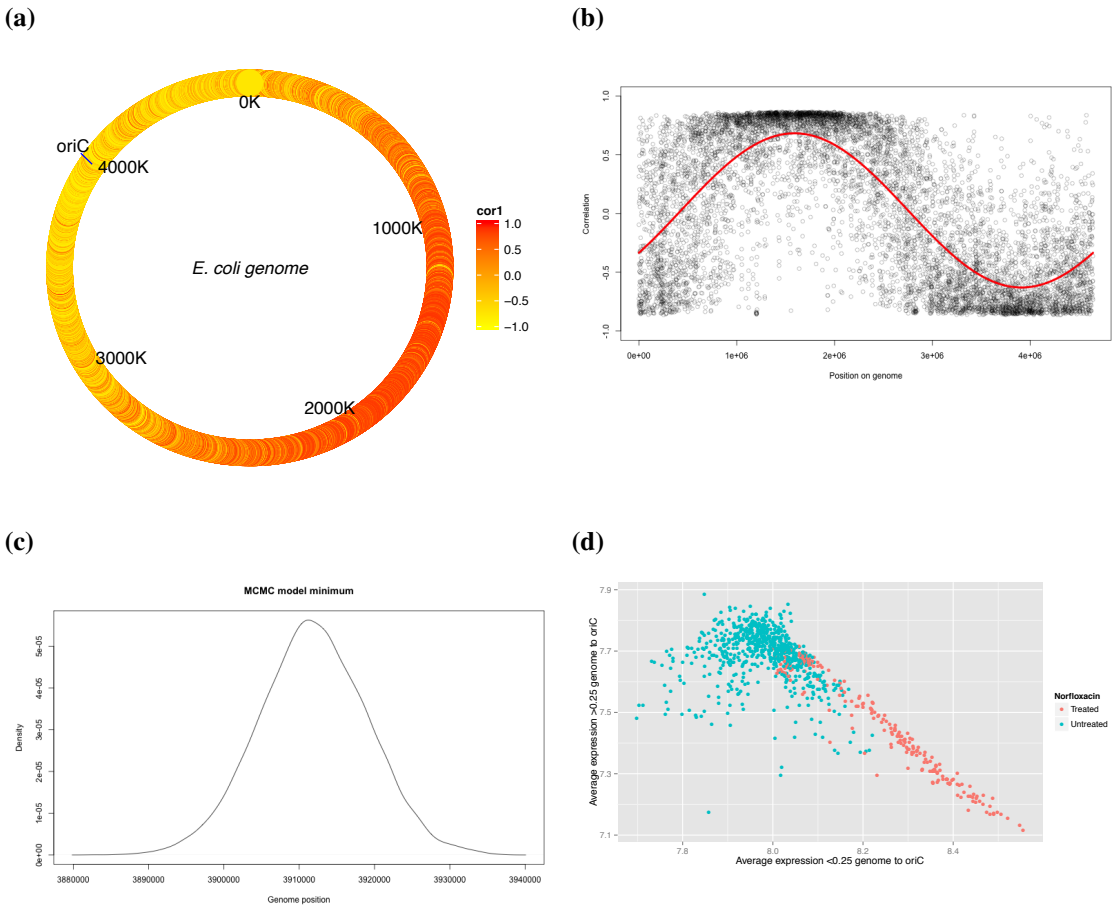

Figure 2.13: **(a)** Heat map of average correlation vector of $E2$ pattern plotted by genome position, there is a clear link to strength of the correlation and position on the genome, with an up-regulation of those gene-probes close to the origin of replication. **(b)** A linear model was used to fit a sine function of the genome position to the values of the average correlation vector. The fitted sine wave is shown in red, and the fit is highly significant with a reported p-value $< 2.2e-16$. Additionally the minimum of the sine wave is at position 3911817, close to the origin of replication at 3923k. **(c)** The probability distribution of the minimum of the sine wave was recalculated using a Markov chain Monte Carlo, showing that there is a significant probability of the minimum occurring on the origin of replication. **(d)** Scatter plot showing the average expression of genes close to the origin of replication, and those genes far from the origin. The samples with the highest expression of genes close to the origin of replication and low expression of genes far from the origin have all been treated with a drug called Norfloxacin, a DNA gyrase inhibitor that prevents the division of DNA strands during replication. The relationship is highly significant with a fitted linear model between the two having a p-value of $4.304e-197$, even excluding the Norfloxacin treated samples this relationship still seems to exist with a p-value of $5.24e-09$.

grown in the presence of Norfloxacin, a DNA gyrase inhibitor, that prevents the division of the strands of *E. coli* DNA during replication, and indeed as shown in Figure 2.13 this effect is greater in those samples treated with Norfloaxin. This same effect has been

previously shown to exist in *Streptococcus pneumoniae* by Slager et al. (2014) who showed that upon treatments with antibiotics that stall bacterial DNA replication, there is a up-regulation of genes close to the origin of replication. Interestingly *Streptococcus pneumoniae* has evolved so that genes close to the origin of replication when up-regulated trigger bacterial competence in response to antibiotics.

The biclustering algorithm has therefore found 3 distinct biclusters within the *E. coli* data, these biclusters represent complex regulatory patterns resulting from either transcriptional programs or response to environmental conditions.

2.4.4 Analysis of random probe sets

It can be noticed from Figures 2.12**(b)** and 2.13**(d)**, that the biclusters identified both are represented by the identification of two probe sets which are anti-correlated to each other. That is there are two probe sets, in which when one is up-regulated, the other is down-regulated.

It can however be observed that this is not the general case. Upon randomly dividing the measured probes into two sets, it is relatively easy to take an average of these two probe sets and plot in a similar manner the samples as was done in Figures 2.12**(b)** and 2.13**(d)**. This can in fact be done computationally 1000 times, and Figure 2.14 shows an example of this being done along with the distribution of the correlation between the two probe sets.

As can be seen from 1000 randomly generated pairs of probe sets all had a strong positive correlation and none had a correlation less than 0.86. Two things need to be explained, why random probe sets have such a strong positive correlation and why the probe sets found from the biclustering analysis have such strongly negative correlations?

To explain the strong positive correlation, these probe sets being random, it would be highly unlikely if they were to share a functional role. It is possible that these average values therefore only reflect the average value of all probes being measured of which there is some variation across the samples. The fact that this variation exists in this dataset, could potentially highlight an issue with normalisation as on average some samples have a higher average gene expression value than others. These differences however are generally small, and natural variation may indeed be expected to exist in the average gene expression values between different biological samples.

(a)

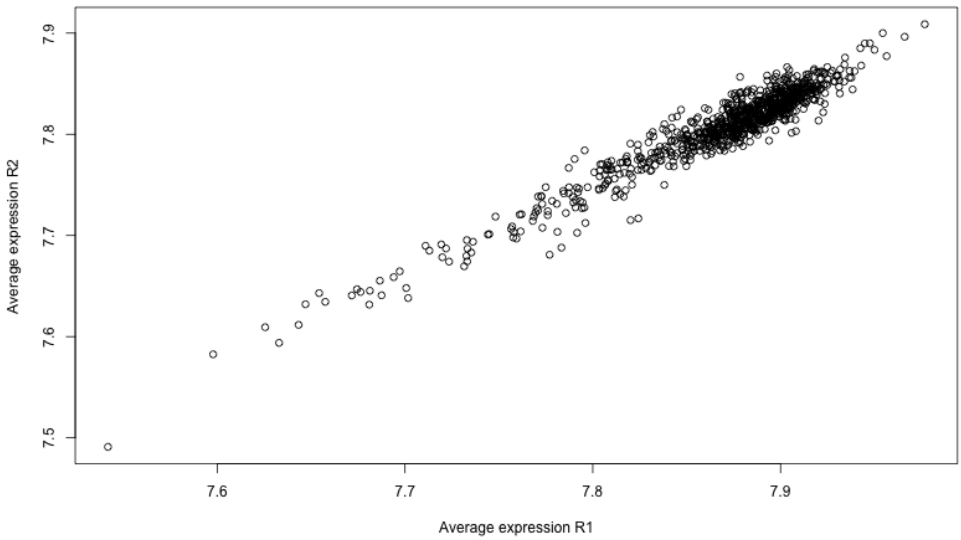

(b)

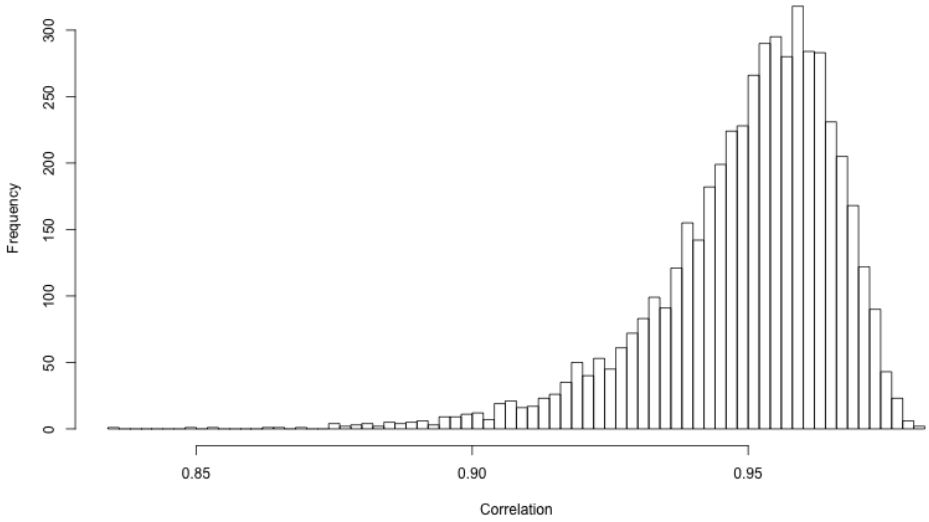

Figure 2.14: **(a)** A scatter plot showing the average of two random probe sets for all the samples in the *E. coli* dataset. The two random probe sets were created one of size 3720 and the other of size 3719, to cover all of the 7439 probes measured. **(b)** A frequency histogram plot of the correlation between two randomly generated probe sets created in the manner of **(a)** repeated 999 more times.

The biclustering analysis however has not picked out random probes but biologically relevant patterns. In transcriptional programs, genes are only up or down-regulated in relation to other non-changing genes, comparing the two up and down-regulated gene sets will therefore always result in a strong negative correlation and such a negative

correlation is the hallmark of a non-random regulation effect.

2.5 Conclusion

The aim of this chapter was twofold, firstly to introduce a novel bioinformatic technique, MCbiclust, that can be used to investigate mitochondrial biogenesis in disease, and secondly to demonstrate its validity and usefulness for this role.

The first task of this was accomplished by the development of a novel biclustering algorithm specifically designed to study mitochondrial biogenesis. The development in detail is described in Section 2.2. Additionally information of the implementation of this algorithm and associated methods in R will be given in Appendix A.

Once the method was fully introduced the next major task was to demonstrate its validity in tackling the problem set of studying mitochondrial biogenesis. To do this it had to be shown to be superior to other existing biclustering methods that were not designed to examine such large regulation patterns exclusively.

For this aim a synthetic dataset was created that reproduced the size of a bicluster representing mitochondrial biogenesis as well as the scale of the large datasets that are available to study. On achieving this by various measures such as the F1 score and examining ROC plots, MCbiclust was found to be superior to alternative methods even though it only found 6 of the 8 synthetic biclusters.

Finally MCbiclust was demonstrated on a real dataset, containing bacterial *E. coli* samples. Due to mitochondria's bacterial origin, *E. coli* can be thought of as a similar transcriptional complexity to an investigation of mitochondrial biogenesis. The method was extremely successful in identifying biological relevant patterns, including some involving very novel effects such as a compound causing inhibition of division of DNA during replication leading to an up-regulation of genes close to the origin of replication.

There are perhaps some weaknesses in the current method, this mainly involves there being one or more biclusters that dominate the results such that any other biclusters are not found. This appears to be the case for the two synthetic biclusters that were not identified, and was apparent in the *E. coli* analysis where the bicluster involving intergenic regions was only identified due to one outlier sample, where the signal was much stronger. It may be possible in future to build an adapted version of the method described here which can identify these weak signal patterns.

Despite this, overall the method developed is a great improvement over existing techniques and seems absolutely suitable for the investigation of mitochondrial biogenesis in disease. While potentially it will not be able to find all the different modes of regulation for mitochondrial biogenesis, it has the potential to identify the major modes of regulation present in the data. This will be the focus of the next chapter, specifically focusing on the regulation of mitochondrial biogenesis in hypertrophic cardiomyopathy and different cancer cell lines.

Chapter 3

Bioinformatic analysis of mitochondrial biogenesis in disease

3.1 Introduction

Following the establishment in Chapter 2 of the Massively Correlating Biclustering (MCbiclust) as a method for finding large scale biclusters in transcriptomic data, it is time to attempt to use these methods for their intended aim of studying alterations of mitochondrial biogenesis in disease.

The focus of this chapter will be on two pathologies: cancer and heart disease. These two diseases and their relationship to mitochondrial function were previously discussed in Section 1.4.1 on page 52 for cancer and Section 1.4.2 on page 56 for heart disease. Both cancer and heart disease are conditions that describe a large number of clinically distinct disorders; in both these cases MCbiclust will only be run on a single dataset. This is so that the utility of MCbiclust in investigating mitochondrial function can be demonstrated, as well as its suitability for a more extensive investigation of the variety of mitochondrial biogenesis regulation in these disorders.

It has been previously shown that MCbiclust is capable of finding these patterns, but precise knowledge of its statistical power to do so is hard to define. Say, for example if a bicluster contains 50% of the known mitochondrial genes, roughly 500, and includes 10% of all samples, so 100 samples in a dataset containing 1000 in total; then the total number of possible biclusters matching this is roughly 1.7×10^{439}. How many of these possible mitochondrial related biclusters represent a true biologically significant pattern? It is not computationally possible to check them all. While MCbiclust certainly finds

relevant mitochondrial related biclusters it is not possible to say all relevants biclusters have been found without checking all possibilities.

According to this purpose, for heart disease, MCbiclust will be applied to a dataset concerning hypertrophic cardiomyopathy from Hebl et al. (2012). While for cancer MCbiclust will be applied to a dataset from the Cancer Cell Line Encyclopeadia (Barretina et al. 2012).

3.1.1 Hypertrophic Cardiomyopathy (HCM)

Hypertrophic cardiomyopathy (HCM) is a genetic cardiac disease, characterised by a thickening of the myocardium, the muscle tissue of the heart.

HCM is more precisely characterised by a disordered arrangement of myocytes and asymmetric patterns of left ventricle wall thickening (Maron 2015). Pathologically the course of the disease varies considerably, and Figure 3.1 shows the possible outcomes of which a large percentage of patients have a benign form of HCM and will not require treatment. It is important to note that this benign form is distinct from the condition known as athletic heart syndrome, which is a non-pathological condition in which the heart is enlarged from regular exercise.

Overall HCM can be divided into two main subtypes, obstructive and non-obstructive with the obstructive patients having a significantly worse prognosis if untreated. Obstructive here refers to a blocking of the left ventricle outflow tract caused by wall thickening. This is a serious condition that can lead to progressive heart failure or a stroke; it is also easily treated by surgery with a myectomy that removes a small amount of the muscle to increase the left ventricle outflow. Patients treated with a myectomy in a sense are fully recovered with long-term survival post operation being equivalent to the general population.

Besides surgery, the likelihood of heart failure for both obstructive and non-obstructive cases can be reduced through treatment by beta-blockers (Maron 2015). In a few extreme cases neither drug treatment or surgery avoid advanced heart failure but in even these cases, patients can receive a heart transplant and expect a full recovery.

HCM is perhaps most widely known for the minority of cases in which the patients remain asymptomatic until undergoing sudden cardiac death, and this is one of the leading causes of sudden death in the young and has been notable in the media for being

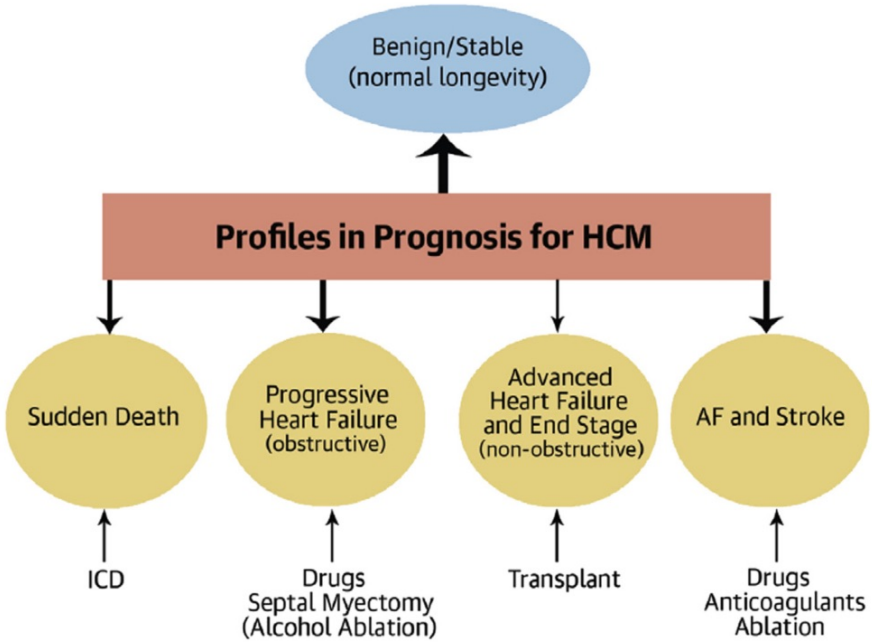

Figure 3.1: Possible clinical outcomes of HCM. Figure is taken from (Maron 2015), most cases of HCM are benign, however for pathological outcomes they can be treated by various means such as septal myectomy surgery, the use of an implantable cardioverter-defibrillator (ICD), drug treatment or in extreme cases a heart transplant. AF in the diagram refers to atrial fibrillation.

the cause of death of otherwise healthy young athletes (Maron 2003). Even in these cases however if the risk of sudden death can be identified a treatment option is possible with the use of an implantable cardioverter-defibrillator (ICD) which can detect and treat potentially fatal arrhythmias in HCM patients (Maron 2015).

Therefore, there are possible modes of treatment for all pathological outcomes of HCM, though in the case of preventing sudden death it is essential to determine those patients at high risk. Due to the large rate of progress in treating HCM it has been recently declared to be a contemporary treatable disease (Maron 2012).

It has been previously estimated that HCM effects 1 : 500 of the population (Maron et al. 1995) though recently it has been thought that the population effected is higher and this has recently been revised upward to 1 : 200 (Semsarian et al. 2015). This has partly come about due to the greater use of genetic screenings, and an appreciation that there are individuals who have a mutation causing HCM who are at risk of but not developed the phenotypic symptoms.

HCM is best known for occurring from mutations in sarcomere proteins, proteins

that form the basic unit of striated muscle tissue. With more than 1000 individual mutations causing HCM identified in 11 sarcomere protein genes (Maron et al. 2012). In addition to this sarcomere connection there are possible reasons to suggest that the mitochondria may play a role in the development of HCM. This is mainly due to the apparent occurrence of HCM in various mitochondrial diseases.

Smits et al. (2011) reported a case where a mutation in the mitochondrial ribosome gene MRPS22, caused brain anomalies as well as hypertrophic cardiomyopathy. More generally Holmgren et al. (2003) found that out of 101 patients with mitochondrial diseases 17 were discovered to have HCM of the non-obstructive type, suggesting that on a whole patients with mitochondrial defects are more likely to have HCM. Additionally Wang et al. (2007) noted that patients with polymorphisms of mitochondrial master regulator peroxisome proliferator-activated receptor gamma coactivator 1-α (PGC-1α) are more likely to develop HCM.

Despite this known association with mitochondrial defects, little is known about the exact role mitochondria plays in HCM. For these reasons HCM is a good case model for studying the role of mitochondrial biogenesis using the novel biclustering technique developed in Chapter 2. Greater understanding of the role mitochondria plays in HCM has the potential to lead to better determination of a patients risk of sudden death and aid clinical decisions as well as understanding what differentiates the benign and pathological versions of the disease.

3.1.2 Cancer cell lines

Cancer cell lines are derived from tumours taken from patients; these cells have then gone through a process called immortalisation such that they can be grown continuously in the lab. The first cancer cell line to be produced were HeLa cells that were taken from a woman called Henrietta Lacks who died from cervical cancer in 1951 (Skloot 2010). Since then HeLa and other cancer cell lines have been widely cultured and used by scientists as an easily available model to study cancer and molecular cellular function.

Cancer cell lines are sometimes criticised for not being representative of the tumour they derive from (Masters 2000). In some senses this is true since they are grown *in vitro* in an environment very dissimilar to a real tumour, and additionally the cancer cell line has had to undergo immortalisation involving selective pressure for certain genetic

changes to continuously grow in lab conditions.

Despite this they are still valuable tools; research into the gene expression profiles of cancer cell lines reveal a distinct correspondence to their tissue of origin (Ross et al. 2000), this suggests the cancer cell lines can be used as a relevant model for studying cancer.

What is more, studies such as Barretina et al. (2012) use cancer cell lines as a pre-clinical model to test for drug sensitivity. Such research therefore has the potential to identify important biomarkers in cancer, such as distinct gene expression patterns or copynumber changes, present in both cancer cell lines and patient tumours. For this reason cancer cell lines are an ideal model to use to investigate the role alterations in mitochondrial biogenesis plays in cancer.

3.2 Bioinformatic analysis of mitochondrial biogenesis in hypertrophic cardiomyopathy

3.2.1 The data

The dataset from Hebl et al. (2012) contains 107 RNA-Seq samples from patients with HCM and 39 control samples. The disease tissue RNA was extracted from tissue collected following septal myectomy, a surgery treatment for HCM that removes a portion of the septum obstructing blood flow, while the control samples were collected from healthy donor hearts. As all the patients representing HCM in this dataset have undergone septal myectomy, the dataset only represents patients with one of the possible pathological outcomes of the disease. This leads to some bias within the data and it is not possible to study how differences in mitochondrial biogenesis cause some cases to be benign and others not.

For both the HCM samples and controls $37,846$ genes were measured using the Illumina HumanHT-12 v3 Expression BeadChip. Unfortunately the publicly available dataset (Gene Expression Omnibus accession number GSE36961) contains no additional clinical data of interest.

The original analysis undertaken by Hebl et al. (2012) examined the differentially expressed genes between the HCM tissue and the controls, and not whether there are any distinct subtypes of HCM samples with a different expression profile. For this

reason, this dataset is ideal to search for biclusters that find distinct modes of regulation occurring in only a subset of the samples.

The novel biclustering method MCbiclust described in Chapter 2 therefore was applied to the HCM data. Two sets of initial runs were done, on both the control and disease samples together. The first was a set of 1000 runs aiming to find biclusters involving the mitochondrial genes described by MitoCarta (Pagliarini et al. 2008). The second was a set of 1000 runs where each run used a different random gene set containing 1000 genes.

The rationale behind the runs with the random gene sets is to find general biclusters that affect a large proportion of the transcriptome. These biclusters may be the same as the ones found with the MitoCarta gene set, indicating significant mitochondrial change also coincide with large scale changes affecting non-mitochondrial genes.

3.2.2 Silhouette plots and ranking the samples

The first step in the analysis for both the MitoCarta and random gene set runs is to identify how many distinct biclusters are found, and this is done using a silhouette plot analysis. For the MitoCarta gene runs, examining the silhouette plot seen in Figure 3.2 **(a - b)** shows that the optimum number of clusters is 1, with the highest silhouette width occurring when all 1000 correlation vectors are clustered together compared against the randomly generated correlation vector. This bicluster was named Mito.1. Similarly for the set of random gene runs, the result from the silhouette analysis is that the optimum number of clusters is 1, this can be seen in Figure 3.2 **(c - d)**. This bicluster was named Random.1.

For each of the runs, one of the sample seeds was chosen such that the correlation score was maximum for the top 1000 genes in the average correlation vector from the clustered groups. Using this sample seed and the top 1000 genes in the average correlation vector, all the samples could be ranked by how well they matched the correlation pattern.

Following the ranking of the samples, the correlation pattern can be summarised using principal component analysis, and have the strength of the correlation in each sample numerically quantified by the value for the first principal component. Figure 3.3 shows the first principle component plotted against the ranked samples for both biclusters

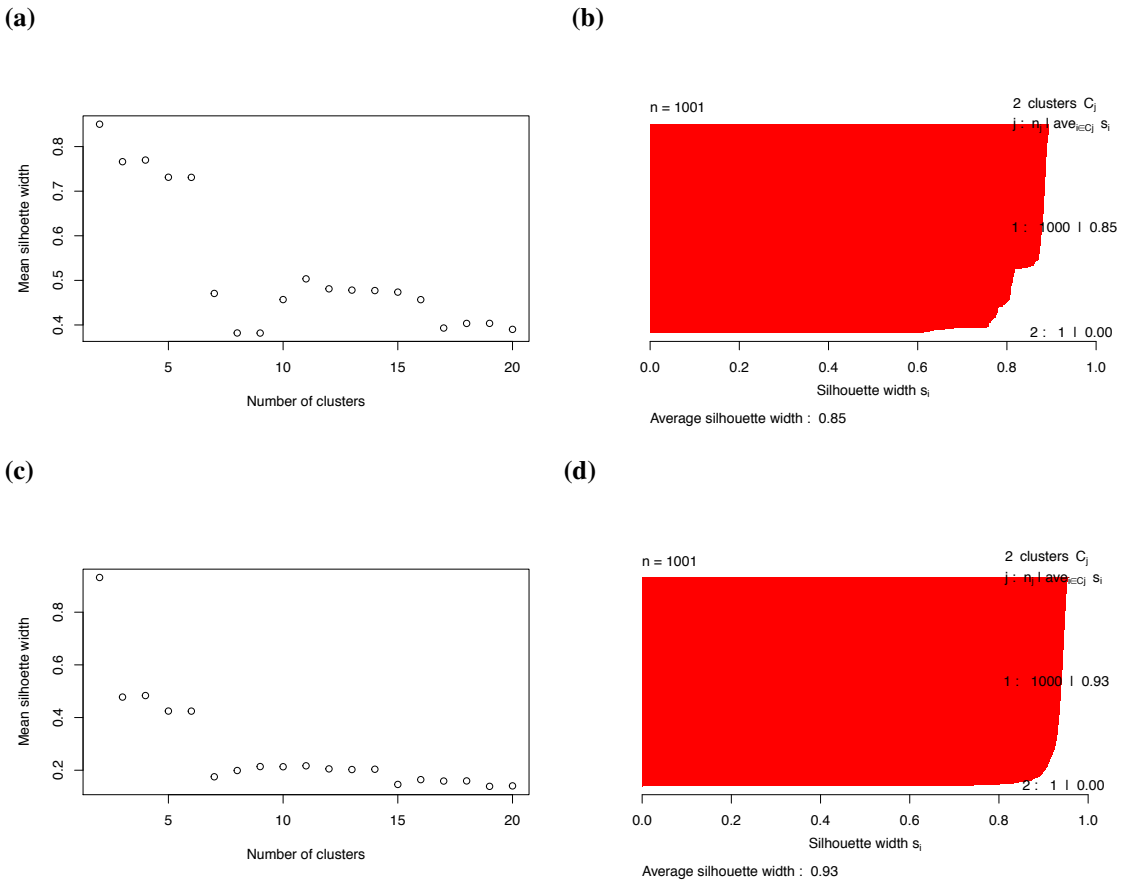

Figure 3.2: Silhouette analysis of two sets of runs in the HCM data. Figures **(a)** and **(b)** show the mean silhouette width for different numbers of clusters and the silhouette plot for the correlation vectors from the run on the MitoCarta genes while Figures **(c)** and **(d)** show the same but for the runs from the random gene sets. In both cases the data was best grouped into a single cluster when ignoring the randomly generated correlation vector inputted into the analysis for comparison. A single cluster is narrowly the optimum way of clustering for the MitoCarta runs while for the random gene set runs it is by far the best.

found.

Figure 3.3 clearly shows two distinct 'forks' representing the biclusters. The Mito.1 fork from the MitoCarta gene set is especially of interest as the upper fork is made up entirely of control samples. It can be checked by examining a plot of the average expression value of the mitochondrial genes (shown in Figure 3.4) that this signifies that the pattern represents a down-regulation of the mitochondria in these control samples compared to the rest of the samples in the dataset. Conversely it can be viewed that in the disease samples there is a up-regulation of mitochondrial genes compared to this healthy control subset. This is interesting as it represents a mode of regulation involving the mitochondria that only occurs in healthy samples and not disease.

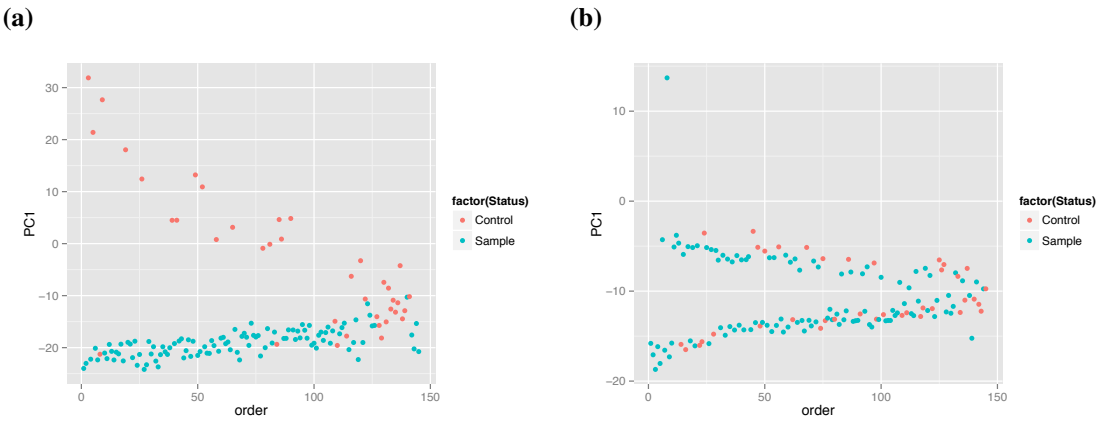

Figure 3.3: PC1 plots of two sets of runs in the HCM data. Figure **(a)** shows the PC1 plotted against the ranked samples from the bicluster found with the mitochondrial gene set (Mito.1 bicluster). This clearly separates control and disease samples across the ranking, though there is one control sample grouped with the disease samples at the beginning of the ranking, possibly indicating an unknown mitochondrial defect in either that control sample or the control samples making up the upper fork. The PC1 plot against the ranked samples from the bicluster found with the random gene sets is given in Figure **(b)** (Random.1 bicluster). This shows a difference that seems to affect both control and disease samples, with the effect being notably stronger in a single disease outlier sample.

Another notable point from this is that the biclustering algorithm found no biclusters representing different types of regulation of mitochondria in any HCM samples. For this reason it was thought important to have one more set of runs with the mitochondrial genes but no control samples.

This was done and a silhouette analysis (Figure 3.5) was found to identify 3 distinct biclusters, named Mitonc.1, Mitonc.2 and Mitonc.3. As done on the other two biclusters previously found, a sample ranking was made for these 3 new biclusters as well as a principal component analysis to summarise the correlation pattern found with the first principal component. In the ranking of the samples, control samples were allowed back in, since their absence from the sample seed was enough to ensure that distinct biclusters showing mitochondrial differences between disease samples were found. PC1 plots can be seen in Figure 3.6.

3.2.3 Comparing the biclusters

Overall from the three sets of runs, 5 biclusters were identified. These can be directly compared with each other by three means:

1. The ranking order of the samples.

(a)

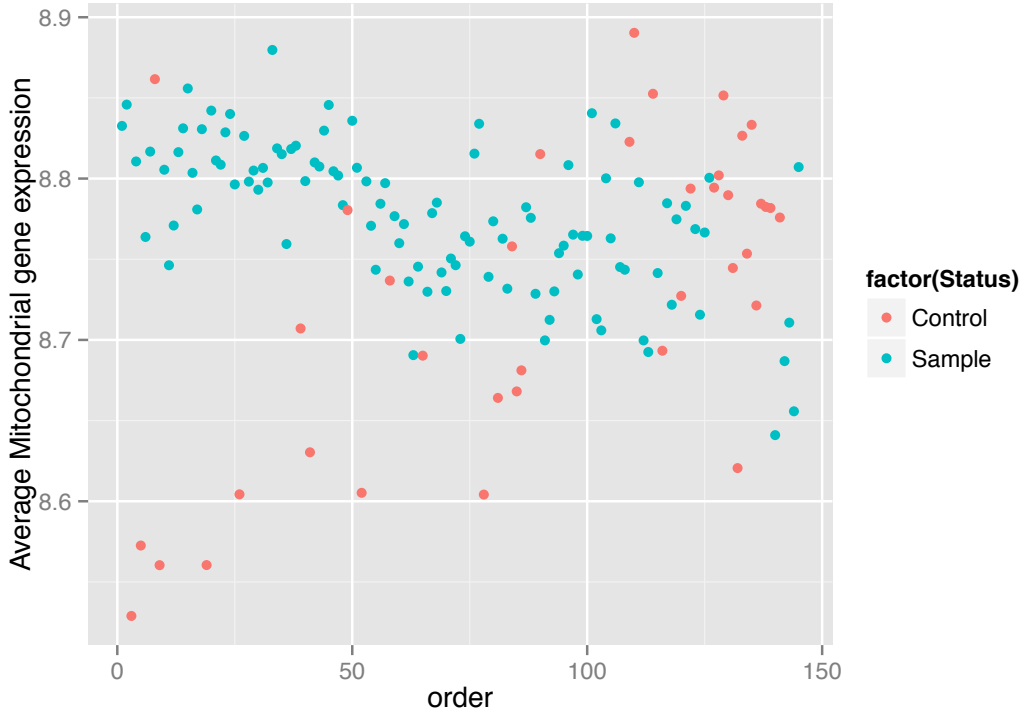

Figure 3.4: Average mitochondrial expression plot of Mito.1 pattern reveals that mitochondria expression is downregulated in a subset of the control samples compared to the rest of the samples in the dataset.

(a) **(b)**

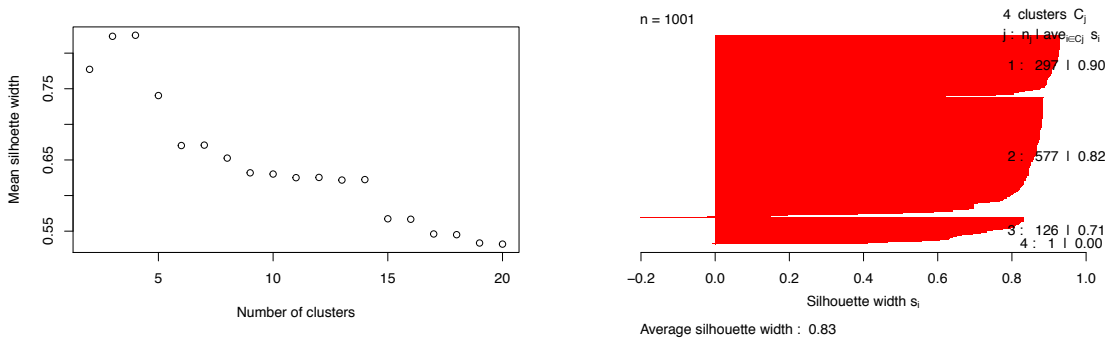

Figure 3.5: **(a)** and **(b)** show the silhouette analysis set of runs in the HCM data on mitochondrial genes without the controls revealing three distinct biclusters. These biclusters were not found previously when the controls were included, indicating that the overall strength of the correlations involved must be weaker.

2. The individual values of the correlation vectors.

3. Gene set enrichment of the correlation vectors.

(a) Mitonc.1

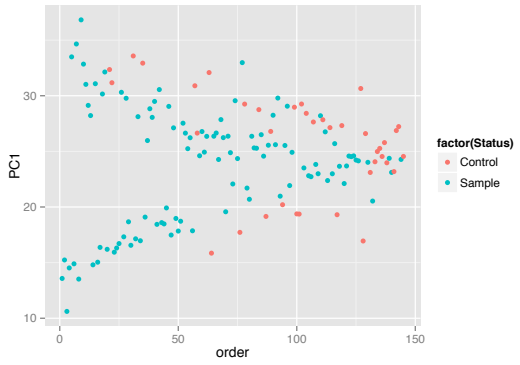

(b) Mitonc.2

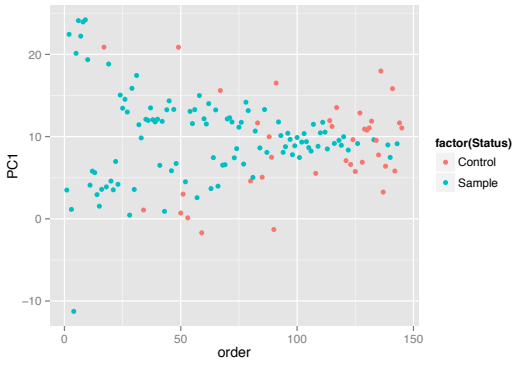

(c) Mitonc.3

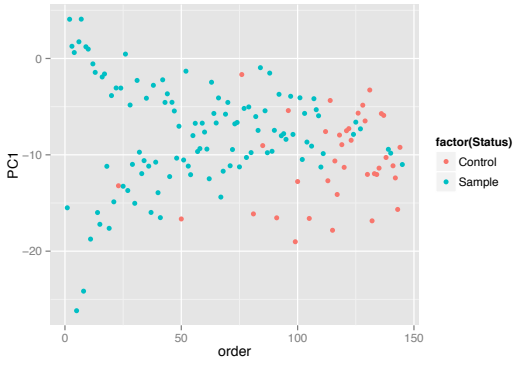

Figure 3.6: PC1 plots of biclusters from set of runs in the HCM data on the mitochondrial genes without controls.

Since there is limited clinical information for the samples besides whether they are a control or not, all comparisons must be done using the correlation vectors themselves. The simplest way to do this is to numerically compare the values in the correlation vectors themselves. Two correlation vectors describing a similar pattern will be strongly correlated. Therefore if any of the 5 distinct correlation vectors identified are strongly correlated to each other, it is enough to say that they are describing the same pattern.

Figure 3.7 shows all 5 bicluster correlation vectors compared by using scatter plots, examining mitochondrial and non-mitochondrial genes separately. From this it is apparent the bicluster identified from the random gene sets, Random.1, is highly similar to one of the biclusters identified from the MitoCarta gene set run with no controls, Mitonc.1. This therefore shows that there are only 4 distinct biclusters found from the 3 sets of runs that need to be examined in detail.

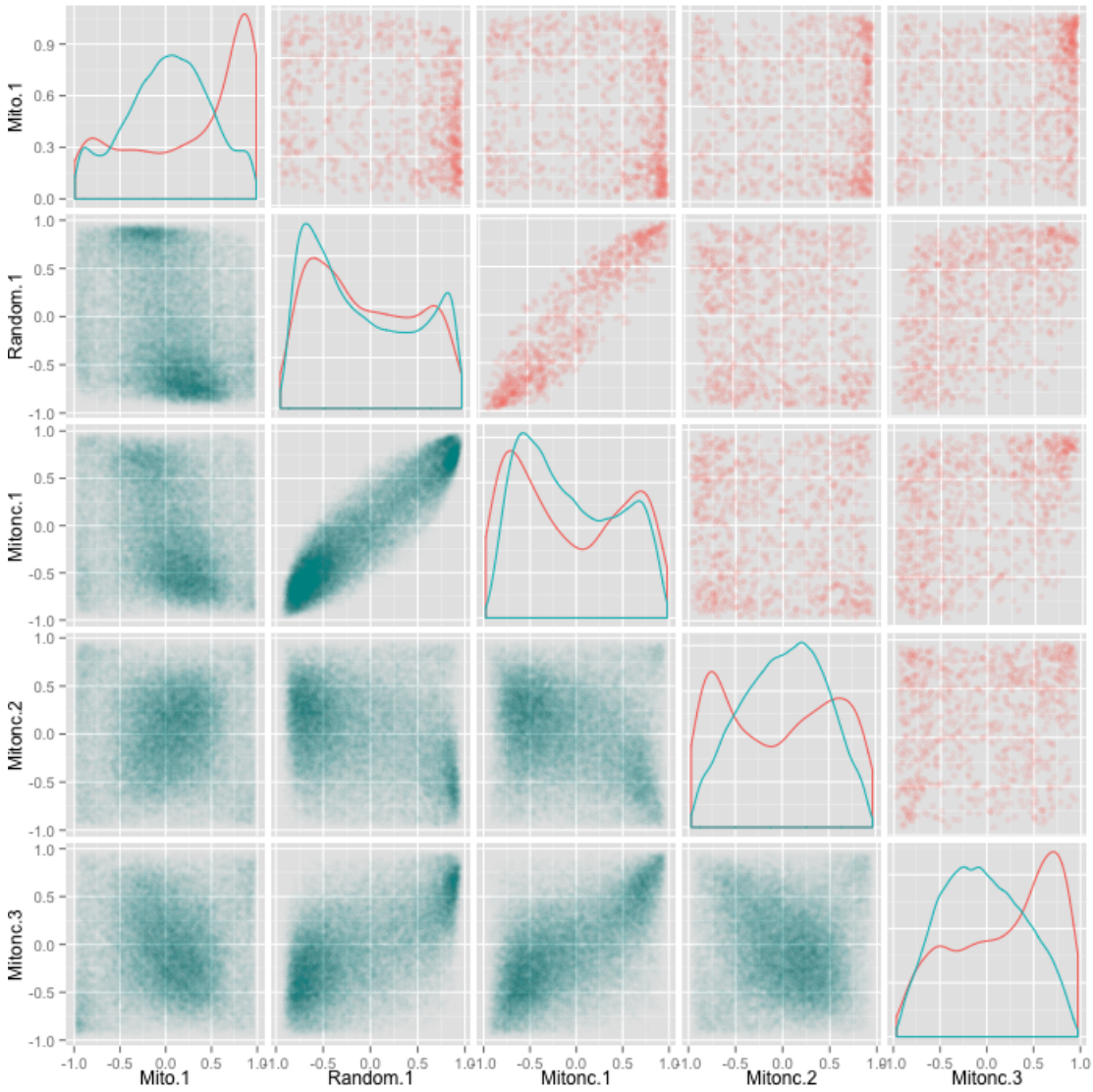

Figure 3.7: Comparison plot of the correlation vectors from the 5 biclusters found in the HCM data. Each distinct bicluster that has been identified has an average correlation vector associated with it, that describes how each gene measured correlates with the bicluster. These different correlation vectors can compared against each other in a scatter plot. If there is a strong correlation between the different correlation vectors as can be seen between bicluster Random.1 and Mitonc.1this indicates that the two biclusters are highly similar. In this figure the lower diagonal scatter plots in blue represent the non-mitochondrial genes, while the upper diagonal scatter plots in red represent the mitochondrial genes. The plots on the diagonal show the mitochondrial and non-mitochondrial histogram for each bicluster. Two correlation vectors can be distinct, yet contain large modules of genes that are regulated in the same way, this can be seen between the Mito.1 and Mitonc.3 biclusters that contain a high density of mitochondrial genes regulated similarly in both biclusters.

It is also possible that while two correlation vectors are distinct, they share gene modules that are regulated in similar ways. For instance, on closer examination of Figure 3.7 between Mito.1 and Mitonc.3 there appears to be a small module of mito-

chondrial genes that are similarly regulated despite the majority of the mitochondrial genes not being similarly regulated between the different biclusters.

This gene module can be examined, as can be seen in Figure 3.8, the genes in the identified modules were selected as those that have a correlation vector greater than 0.75 in both the Mito.1 and Mitonc.3 biclusters.

168 of the total 900 mitochondrial genes measured in the HCM had a correlation vector greater that 0.75 for the Mitonc.3 pattern, while 352 genes had a correlation vector greater than 0.75 for the Mito.1 pattern. The intersection of these 2 groups was 86 genes, the number of genes in this intersection can be modelled using the hypergeometric distribution, considering genes belonging to both gene sets a success.

In general with a gene set of size N with two subsets selected of size a and b and $b > a$ the probability of the size of the intersection being x will follow a hypergeometric distribution:

$$P(x) = \frac{\binom{N-a}{b-x}\binom{a}{x}}{\binom{N}{b}} \tag{3.1}$$

In this case $N = 900$, $a = 168$ and $b = 352$. Using this the mean expected size of the intersection can be calculated as $b\frac{a}{N} = 352\frac{168}{900} \approx 65.7$, and $P(X \geq 86) = 0.00029$. Thus the size of this gene module is larger than expected if they were selected randomly, and indicates that there are genes in the module that are co-regulated. While this is not a huge module of co-regulated genes it is statistically significant and demonstrates the ability of this method to find these modules of co-regulated genes between distinct biclusters.

The group of genes in the module are given in Table 3.1 along with the correlation vector values in the relevant biclusters, the gene list includes genes that very well may be coregulated such as members of the electron transport chain (ETC) notably for ATP synthase, Complex I, the fatty acid beta oxidation pathway and genes encoding the mitochondrial ribosome.

The discovery of these co-regulated mitochondrial modules give some indication to how the regulation of mitochondrial biogenesis functions. Presumably these modules exist due to some effect of members of the transcription factor network controlling mitochondrial biogenesis. Importantly the existence of these differences in the mitochondrial

	Mito.1	Mitonc.3		Mito.1	Mitonc.3
ABHD11	0.94	0.77	ME2	0.84	0.81
ACAA2	0.86	0.85	MIPEP	0.91	0.76
ACADM	0.94	0.90	MLYCD	0.88	0.80
ACADSB	0.95	0.76	MOSC2	0.95	0.85
ACAT1	0.97	0.88	MRPL16	0.80	0.84
ACN9	0.85	0.88	MRPL39	0.79	0.92
ACOT2	0.92	0.84	MRPS10	0.77	0.80
AFG3L2	0.85	0.84	MRPS7	0.87	0.84
AIFM1	0.97	0.87	MRRF	0.90	0.76
AKAP1	0.89	0.93	MTX2	0.88	0.80
ALDH5A1	0.98	0.94	MUT	0.92	0.78
AS3MT	0.91	0.92	NDUFA10	0.90	0.88
ATAD1	0.88	0.88	NDUFAF1	0.77	0.90
ATP5F1	0.93	0.96	NDUFB3	0.90	0.82
ATP5G3	0.94	0.79	NDUFB5	0.86	0.85
ATPAF1	0.96	0.84	NDUFB6	0.84	0.78
AUH	0.93	0.92	NDUFS2	0.85	0.90
BCKDHB	0.94	0.91	NNT	0.98	0.94
BDH1	0.93	0.76	OMA1	0.98	0.90
CHCHD4	0.94	0.88	OSGEPL1	0.96	0.93
CHCHD7	0.96	0.86	OXCT1	0.93	0.81
COQ3	0.97	0.88	PACRG	0.88	0.88
DCI	0.80	0.80	PCBD2	0.95	0.79
DHTKD1	0.79	0.90	PCCA	0.91	0.86
DLAT	0.89	0.86	PECI	0.87	0.88
DLD	0.84	0.97	PET112L	0.96	0.87
EARS2	0.82	0.83	PHYH	0.92	0.86
EHHADH	0.96	0.83	PINK1	0.89	0.80
GFM2	0.93	0.88	PMPCB	0.91	0.81
GPAM	0.90	0.79	PRDX2	0.90	0.83
GTPBP8	0.94	0.91	PRDX3	0.96	0.87
HADH	0.98	0.87	PTCD2	0.98	0.80
HIGD1A	0.80	0.91	PTGES2	0.86	0.77
HRSP12	0.85	0.93	QDPR	0.97	0.90
HSDL2	0.94	0.83	SARS2	0.76	0.78
IARS2	0.87	0.86	SCO1	0.91	0.79
IMMP2L	0.83	0.89	SDSL	0.94	0.80
IMMT	0.81	0.88	SIRT5	0.97	0.89
LDHB	0.79	0.96	SLC25A20	0.91	0.86
LIAS	0.95	0.85	SUCLA2	0.97	0.94
MAOB	0.98	0.95	TATDN3	0.97	0.92
MCCC2	0.95	0.83	TOMM20	0.83	0.82
MCEE	0.95	0.86	UQCRC2	0.85	0.96

Table 3.1: Mitochondrial co-regulated gene module identified in two different biclusters

transcriptional program between different HCM samples also confirms that there are subtypes with different mitochondrial regulation.

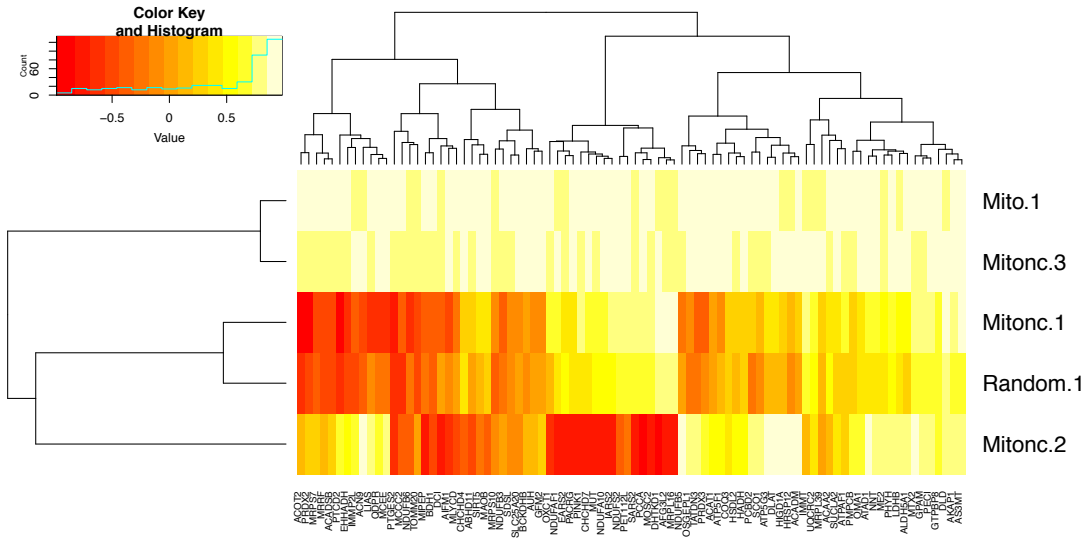

Figure 3.8: Heat map showing a module of similarly regulated mitochondrial genes in the correlation vector values. Mitochondrial genes that had correlation values greater than 0.75 in both the Mito.1 and Mitonc.3 biclusters were selected, this revealed a large subgroup that has many terms related to the ETC.

3.2.3.1 Gene set enrichment

The final method of comparing the different biclusters is by using gene set enrichment. By applying this on the correlation vectors this will find not only the significant mitochondrial terms, but all the significant non-mitochondrial terms as well. Although our primary interest is the regulation of mitochondrial biogenesis in disease models, mitochondria have to react to changes in the cellular environment. The significant non-mitochondrial terms therefore tell us of what wider cellular transcriptional program the change in mitochondrial regulation is related to.

There are 998 significant gene ontology (GO) terms found from the Mito.1 pattern. A table of the top 200 terms by significance is given in Table B.4. The vast majority of significant terms have a negative average correlation vector value, the exceptions are terms related to the mitochondria that have positive average correlation vector values. This implies that when the healthy samples have a large number of downregulated mitochondrial genes compared to the disease samples, as is seen in Figure 3.4, all these other terms are upregulated. These up-regulated terms include strongly those related to the immune system, ribosome biogenesis and cell proliferation. Since only the healthy control samples had their mitochondria down-regulated during this up-regulation

of cellular proliferation, while the disease samples conversely had their mitochondria up-regulated during down-regulation of cellular proliferation, it is tempting to form a hypothesis that the switch in this regulation could lead to HCM.

The other biclusters seem to describe either different regulation between different HCM samples or a type of regulation that exists in both HCM and control samples.

For the Random.1 and Mitonc.1 biclusters the significant terms are similar to eachother, with 200 of the 213 significant terms of Mitonc.1 also being significant for *Random*.1, and do not seem to be much related to mitochondrial function, with only the 13 terms only significant in Mitonc.1 being related to mitochondrial function. It is hard to see a general functional role for all these significant terms, 482 for the Random.1 pattern and 213 for the mitonc.1 pattern, with many generic high-level terms describing broad biological processes such as binding being significant. A full table of these significant terms is given in Table B.5 and B.6.

The Mitonc.2 and Mitonc.3 bicluster were identified as being potentially related to mitochondrial function but not involving the control samples. The Mitonc.3 significant terms seems to be exclusively related to the mitochondria with very few non-mitochondrial terms being highly significant. There are relatively few Mitonc.2 significant terms and these also are fairly general and do not give much of an indication of what the pattern in Mitonc.2 represents. The significant terms for Mitonc.2 and Mitonc.3 are given in Tables B.7 and B.8 respectively.

While not a lot is known about these biclusters due to the absence of additional clinical data, all identified biclusters represent a real biological effect. Strikingly one of these biclusters separated the control and disease samples, and seems to suggest a mode of regulation not existing in either the control or disease samples. With the additional discovery of modules of co-regulated mitochondrial genes, this demonstrates that this technique can be used to study the role of the regulation of mitochondrial biogenesis in disease.

3.3 Bioinformatic analysis of mitochondrial biogenesis in cancer cell lines

3.3.1 The data

The Cancer Cell Line Encyclopedia (CCLE) (Barretina et al. 2012) is a dataset created by the Broad Institute to provide detailed characterisations of a wide range of human cancer cell lines on the gene expression level. In addition to this, the data includes the chromosomal copy number across 947 human cancer cell lines, and has the pharmacological profiles for 24 anticancer drugs across 479 cancer cell lines. Within this dataset, due to the heterogeneous nature of cancer, it is expected that there is large variations in the modes of regulation. This is especially true as the total collection of cell lines come from 36 different tumour types (Barretina et al. 2012).

For the data generated by Barretina et al. (2012), the gene expression levels were measured from messenger RNA using Affymetrix U133 plus 2.0 arrays, while DNA copy number was measured using high-density single nucleotide polymorphism arrays. To measure the pharmacological profile of the cell lines, a 8-point dose-response curve for 24 anticancer compounds was generated for 479 of the cell lines.

By using the biclustering algorithm different regulations of mitochondrial biogenesis as well as other pathways can be investigated in much the same way as was done for hypertrophic cardiomyopathy. Any biclusters found can then additionally be understood using the copy number and the pharmacological data.

Like the HCM dataset, two sets of runs were done, one using the MitoCarta genes (Pagliarini et al. 2008) and the other using random probe sets. Both included 1000 runs of the biclustering algorithm.

3.3.2 Silhouette plots and comparison

Once both of the sets of runs were completed, silhouette width analysis was used to determine the number of distinct biclusters. For the MitoCarta set, it was shown that there was only one distinct bicluster, as can be seen in Figure 3.9**(a - b)**. For the random probe set, the silhouette results showed that there were two distinct biclusters, this can be seen in Figure 3.9**(c - d)** with three biclusters being identified from the silhouette analysis, and no reason to include an additional set of runs as was required for the

analysis of the HCM dataset, the next step is to compare all the biclusters found to judge their similarity. This is done in the same manner as in Section 3.2.3, with the different correlation vectors being plotted against each other separately for mitochondrial and non-mitochondrial probes, this is given in Figure 3.10.

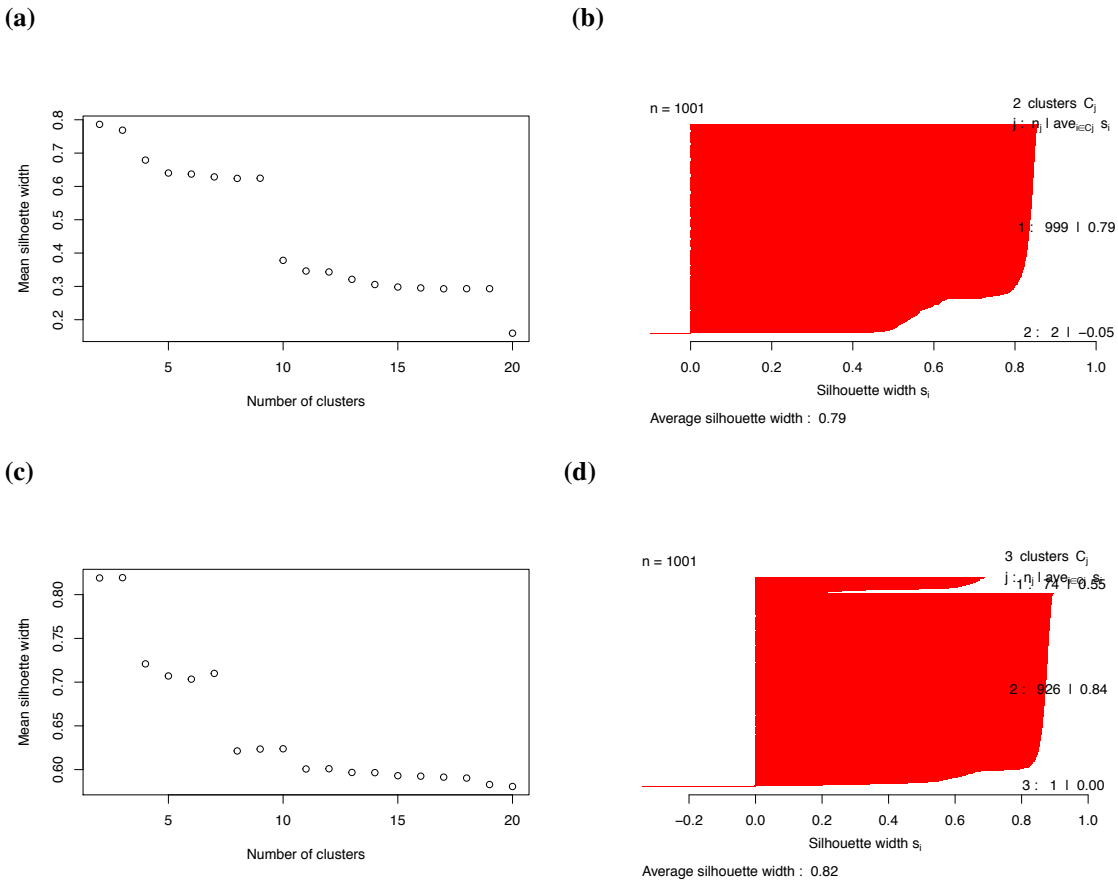

Figure 3.9: Silhouette analysis of two sets of runs in the CCLE data. **(a)** and **(b)** show the silhouette analysis for the correlation vectors from the run on the MitoCarta genes finding one main cluster ignoring the randomly generated correlation vector group. **(c)** and **(d)** show the silhouette analysis for the correlation vectors from the run on the random probe sets finds two optimal clusters of correlation vectors, again ignoring the group from the randomly generated correlation vector.

It can be easily seen from this that pattern Mito.CV1 and Random.CV2 are very similar and are likely representing the same type of regulation.

3.3.3 Understanding the biclusters

3.3.3.1 Sample ordering

The samples from all the biclusters identified were ordered by the same method used in Section 3.2.3, that is for each distinct bicluster group identifying the sample seed

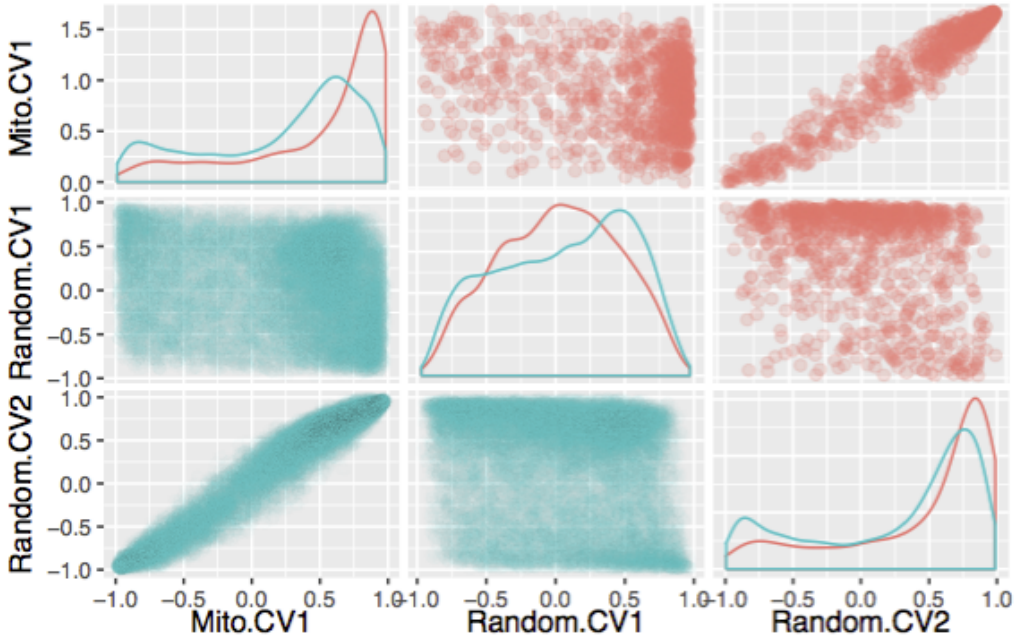

Figure 3.10: Comparison plot of the correlation vectors from the 3 found biclusters in the CCLE data. In the scatter plots red represents mitochondrial genes and blue represents non-mitochondrial genes. It is easy to see that the correlation vectors for Random.CV2 and Mito.CV1 are extremely similar.

that maximises the correlation score with the top 1000 probes in the average correlation vector. Once this was done the first principal component could be calculated and plotted against the ranking of the samples.

Unlike the hypertrophic cardiomyopathy dataset there is plenty of clinical data to examine for significance in the ranking of the samples. One of the most obvious things to examine is the tissue of origin of the cancer cell line. Since cancer can derive from various tissues, tissue of origin variation is one of the major sources of heterogeneity in cancer cell lines.

The ordering of the Mito.CV1 can be seen in Figure 3.11**(a)** and there is a clear dependence on tissue of origin with most of the cell line samples in the upper fork being derived from haematopoietic and lymphoid tissue. The lower fork however is a mix of samples from different derived tissue.

The ordering of the Random.CV1 seems to have a complicated relationship with tissue of origin apart from haematopoietic and lymphoid tissue being at the back of the ranking, as can be seen in Figure 3.12**(a)**. This can be clarified by examining the

(a) Mito.CV1

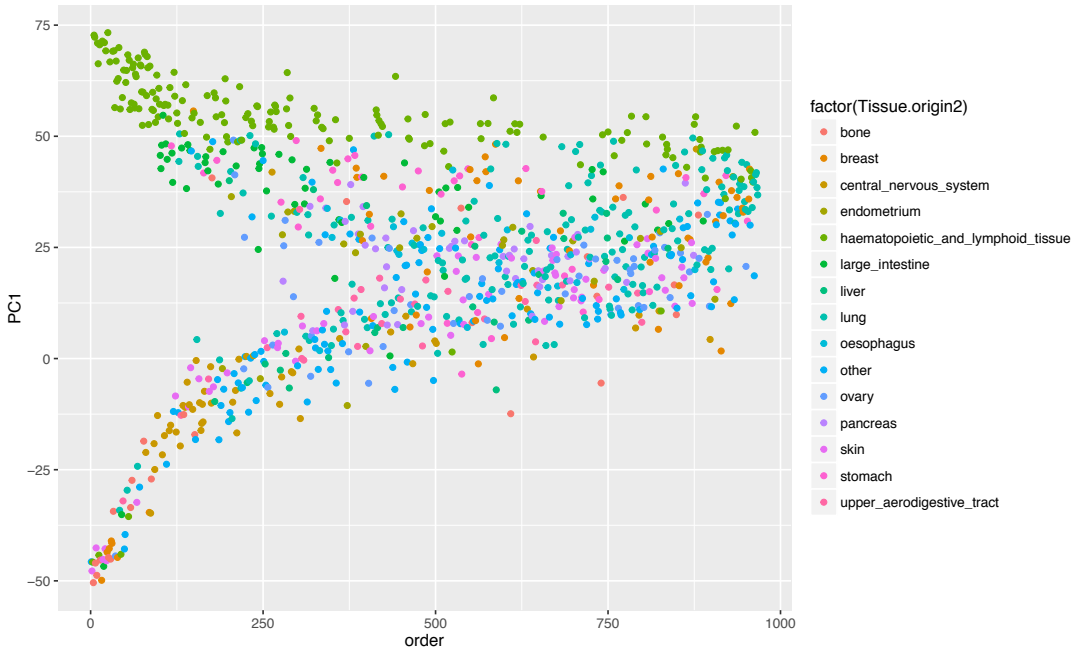

(b) Random.CV2

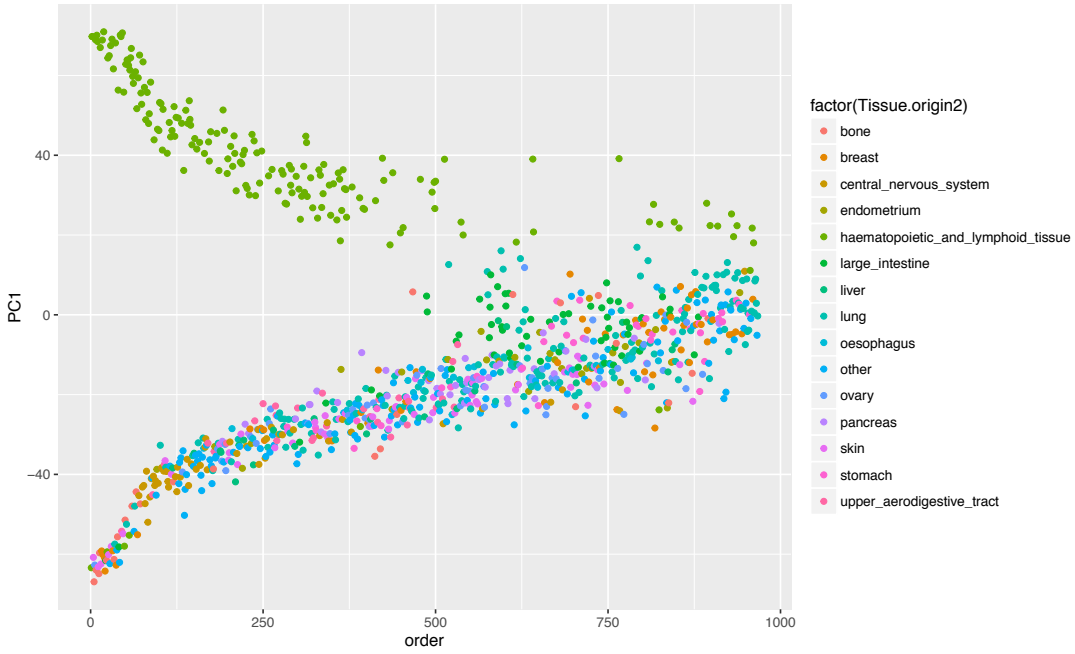

Figure 3.11: PC1 plots of Mito.CV1 and Random.CV2 biclusters from set of runs in the CCLE data, both plots show the tissue of origin of the samples.

histology of the sample instead of the tissue of origin, that reveals the majority of the samples in the bicluster to be carcinomas, as can be seen in Figure 3.12**(b)**.

Histology of the cancer cell line here describes the structure of the cancer cell, and the general origin of the cancer cell line. For instance carcinomas that make up the

(a) Random.CV1 tissue of origin

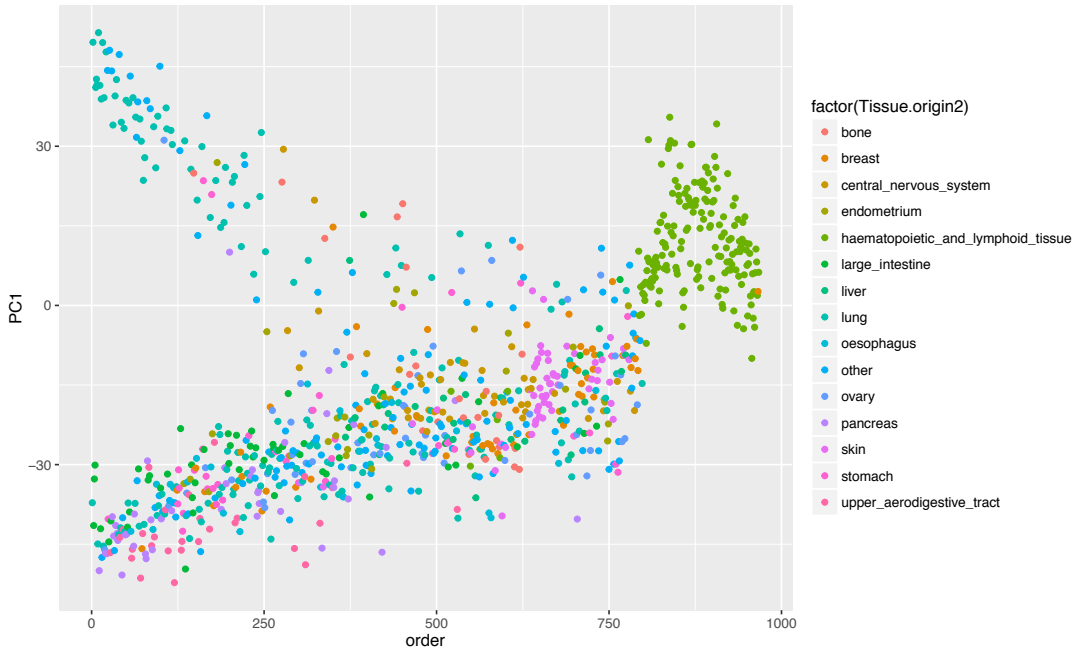

(b) Random.CV1 histology

Figure 3.12: PC1 plots of bicluster, Random.CV1 from set of runs in the CCLE data, plots **(a)** shows the tissue of origin of the samples while plot **(b)** shows the histology of the samples.

majority of all cancers originate in epithelia cells, the cells that make up the lining of the skin and organs. Other types such as neuroblastomas originate from the cells in the peripheral nervous system, and frequently originate in the adrenal gland. There are many other types of histological subgroups that can be clearly seen in Figure 3.12**(b)** which

include types such as lymphomas that originate from cells from the immune system and leukaemia that origin from the bone marrow.

The ordering of Random.CV2 should be expected to be highly similar to that of Mito.CV1 as the gene-probe correlation vectors themselves are highly correlated. However the resulting plot of the first principal component shown in Figure 3.11**(b)** gives a much clearer separation between the upper and lower fork. The Random.CV2 clearly distinguishes haematopoietic and lymphoid derived cell lines from others, this distinction is not as clear in the Mito.CV1 bicluster. This indicates that while there is a significant mitochondrial component to this bicluster in a large number of the haematopoietic and lymphoid derived cell lines, it is perhaps more clearly defined in terms of its non-mitochondrial components.

3.3.3.2 Gene set enrichment

To further compare the biclusters the gene set enrichment of the correlation vectors can be studied. For the Mito.CV1 pattern the top 200 of 1219 significant terms are given in Table B.9. From this it can be seen that mitochondrial, cytosolic ribosome and general cellular proliferation terms are all up and down-regulated together.

The Random.CV1 pattern does not seem to be related much to mitochondrial regulation but instead seems much more related to differences in the immune system as can be seen from examining the terms given in Table B.10. The Random.CV2 pattern unsurprisingly has significant terms that are very similar to those found from the Mito.CV1 pattern and are given in Table B.11.

3.3.4 Copy number differences

In addition to measuring the transcriptome, the CCLE dataset also contained information for copy number changes in the samples. In cancer there are often many copy number alterations across the genome. Knowing the sample ranking and from the principal component analysis which are in the upper and lower fork, it is relatively simple to search for regions of the genome with significant copy number differences between the upper and lower fork samples.

To do this the top 250 samples were selected, and then separated into two groups based on the value of the first principal component using k means clustering. The 250 samples were chosen as among these samples in all the biclusters described, there was

a clear separation between the upper and lower forks, while statistically being a large enough number to derive reliable p-values. Using these two groups representing the upper and lower fork the average copy number for each group was calculated as well as the difference between these averages.

To calculate which genes had a significant different copy number between the two groups, a permutation technique was used. The top 250 samples were divided randomly into two groups the same size as the groups representing the upper and lower forks. From these new random groups the average copy number was calculated as well as the difference. This process was done 100 times and the combined vector of the 100 differences between the random groups was used as the distribution for the difference in copy number between two random groups.

Using this distribution, it was then possible to calculate p-values for the copy number differences between the upper and lower fork. Since every single gene was tested for significance, it was essential to then do a multiple hypothesis adjustment on the calculated p-values.

After the multiple hypothesis adjustment, for the pattern Mito.CV1 there were two main regions of significant difference, one around gene FHIT and the other around gene CDKN2A. Full details of this are given in Table 3.2 and the copy number changes can be seen in Figure 3.13**(a)**.

Gene num	Genes (adj p-value)	Chr	Av copy-lower	Av copy-upper	Copy change
1	FHIT (0)	3	-1.13	-0.38	-0.74
4	C9orf53 (0.001), CDKN2A (0.001), CDKN2BAS (0), CDKN2B (0)	9	-0.75	-1.53	0.78

Table 3.2: Significant copy number change regions for the Mito.CV1 pattern between upper and lower forks. All genes are significant with adjusted p-value < 0.05.

Significantly both FHIT and CDKN2A are known tumour suppresors (Siprashvili et al. 1997, Foulkes et al. 1997), thus it would appear that in the upper fork samples FHIT is more likely to have a higher copy number while in the lower fork samples CDKN2A is much more likely to have a higher copynumber. These results are likely due to changed rates of gene deletion between the different forks, since there are only two small regions it seems unlikely there is any significant change in the diploid state as if this were the case larger regions would be significant.

Interestingly, both have links to the mitochondria, with FHIT having a mitochondrial isoform that regulates mitochondrial calcium uptake and apoptosis (Karras et al. 2014), and CDKN2A suppressing transcription factor E2F-1 activity (Hara et al. 1996), which involvement in the regulation of mitochondrial biogenesis was discussed in Section 1.3.4.1.

For the pattern Random.CV1 there were 12 regions of the genome with a significant difference in copy number between the upper and lower forks. There was a very large region on chromosome 18 containing 159 genes that has a significantly lower copy number in the upper fork samples indicating a loss in heterozygosity event or possibly a relative loss from a tetraploid genome for the upper fork samples. This region includes known oncogenes such as those in the SMAD family such as SMAD4, especially known to be associated with colorectal cancer (Miyaki et al. 1999) and gene DCC or Deleted in Colorectal Carcinoma (Shibata et al. 1996). Indeed chromosome instability in this region been associated with colorectal carcinogenesis (Takayama et al. 2006).

The full list of the copy number changes can be seen in Table 3.3, with a boxplot of the average result being shown in Figure 3.14**(a)**. Interestingly, similar to the the Mito.CV1 bicluster oncogenes FHIT and CDKN2A were both found to be significantly different between the upper and lower forks.

For the pattern Random.CV2, which shows a strong resemblance to the Mito.CV1 pattern, two regions of the genome were found to have significant copy number variations between the two forks. These regions however were different from the regions discovered in Mito.CV1, and were of the single genes TARP of chromosome 7 and ADAM6 on chromosome 14. TARP is a gene related to the T cell receptor gamma, and has been associated previously with cancer (Wolfgang et al. 2000) and has a significantly lower copy number in the lower fork samples. ADAM6 may be a false positive as it is a pseudogene with no known associations to cancer. It addition to this it is only just significant, with upper fork samples having a slightly higher copy number. Despite this it may have a functional role as other members of the ADAM family of genes have previously been identified to be involved in cancer (Mochizuki 2007) and in recent years there has been a wider appreciation of the role that pseudogenes play in cancer (Kalyana-Sundaram et al. 2012). The full list of the significant copy number changes can be seen in Table 3.4, with the boxplot shown in Figure 3.14**(b)**.

Gene num	Genes	Chr	Av copy-lower	Av copy-upper	Copy change
2	TRIT1, MYCL1	1	0.60	-0.05	0.65
2	MYCNOS, MYCN	2	0.72	0.01	0.71
1	FHIT	3	-0.65	-2.05	1.40
1	CSMD1	8	-0.38	-1.17	0.79
1	SLC25A37	8	-0.11	-0.76	0.65
5	MTAP, C9orf53, CDKN2A, CDKN2BAS, CDKN2B	9	-0.12	-1.25	1.13
1	WWOX	16	-0.43	-1.16	0.72
4	C18orf34, ASXL3, NOL4, DTNA	18	0.21	-0.43	0.64
2	ZNF397, ZSCAN30	18	0.18	-0.45	0.63
4	FHOD3, C18orf10, KIAA1328, CELF4	18	0.15	-0.50	0.65
159	LOC647946, hsa-mir-924, KC6, PIK3C3, RIT2, SYT4, SETBP1, MIR4319, SLC14A2, SLC14A1, SIGLEC15, KIAA1632, PSTPIP2, ATP5A1, HAUS1, C18orf25, RNF165, LOXHD1, ST8SIA5, PIAS2, KATNAL2, TCEB3C, TCEB3CL, TCEB3B, HDHD2, IER3IP1, SMAD2, ZBTB7C, KIAA0427, SMAD7, DYM, C18orf32, MIR1539, hsa-mir-1539, RPL17, SNORD58C, U58, U58C, SNORD58A, U58A, SNORD58B, U58B, LIPG, ACAA2, SCARNA17, mgU12-22/U4-8, U91, MYO5B, MIR4320, CCDC11, MBD1, CXXC1, SKA1, MAPK4, MRO, ME2, ELAC1, SMAD4, MEX3C, DCC, MBD2, SNORA37, ACA37, POLI, STARD6, C18orf54, C18orf26, RAB27B, CCDC68, TCF4, TXNL1, WDR7, BOD1P, ST8SIA3, ONECUT2, FECH, NARS, ATP8B1, NEDD4L, MIR122, hsa-mir-122, ALPK2, MALT1, ZNF532, LOC390858, SEC11C, GRP, RAX, CPLX4, LMAN1, CCBE1, PMAIP1, MC4R, CDH20, RNF152, PIGN, KIAA1468, TNFRSF11A, ZCCHC2, PHLPP1, BCL2, KDSR, VPS4B, SERPINB5, SERPINB12, SERPINB13, SERPINB4, SERPINB3, SERPINB11, SERPINB7, SERPINB2, SERPINB10, HMSD, SERPINB8, C18orf20, LOC284294, LOC400654, CDH7, CDH19, DSEL, LOC643542, TMX3, CCDC102B, DOK6, CD226, RTTN, SOCS6, CBLN2, NETO1, LOC400655, FBXO15, C18orf55, CYB5A, DKFZP781G0119, FAM69C, CNDP2, CNDP1, LOC400657, ZNF407, ZADH2, TSHZ1, C18orf62, ZNF516, LOC284276, ZNF236, MBP, GALR1, SALL3, ATP9B, NFATC1, CTDP1, KCNG2, PQLC1, HSBP1L1, TXNL4A, C18orf22, ADNP2, LOC100130522, PARD6G	18	0.10	-0.61	0.71
1	MACROD2	20	0.11	-0.70	0.81

Table 3.3: Significant copy number change regions for the Random.CV1 pattern between upper and lower forks. All genes are significant with adjusted p-value < 0.05.

What is most interesting about these results is the different copy number regions found significant between the Mito.CV1 and Random.CV2 biclusters. In Figure 3.10 it is clear that these two correlation vectors are describing something very similar, and both certainly have a strong mitochondrial component. Pattern Mito.CV1 however was found whilst seeking this mitochondrial effect while Random.CV2 was not. In addition

Gene num	Genes (adj p-value)	Chr	Av copy-lower	Av copy-upper	Copy change
1	TARP (0)	7	-0.84	0.26	-1.11
1	ADAM6 (0.001)	14	0.01	0.77	-0.77

Table 3.4: Significant copy number change regions for the Random.CV2 pattern between upper and lower forks. All genes are significant with adjusted p-value < 0.05.

(a) Mito.CV1

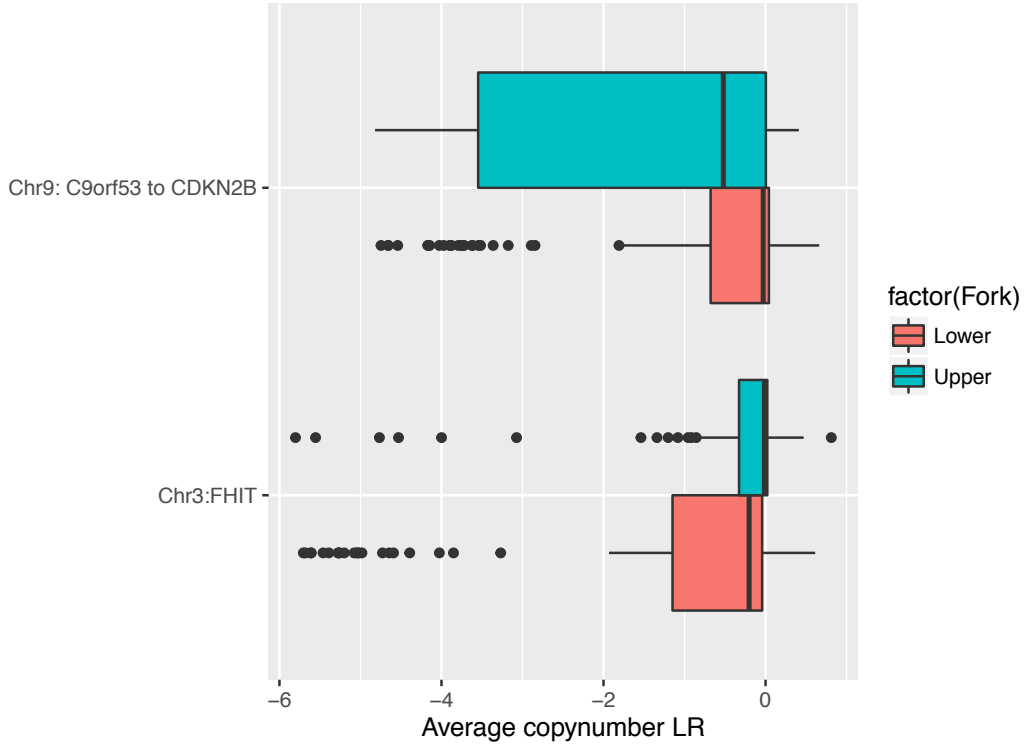

Figure 3.13: Boxplot for significant copy number differences between the upper and lower forks in Mito.CV1.

to this, the fork patterns look distinctly different in Figures 3.11**(a)** and 3.11**(b)**, with the Random.CV2 fork cleanly separately the haematopoietic and lymphoid tissue from the rest. The only difference between the two biclusters is the focus on mitochondrial expression for Mito.CV1, so it would appear that the difference between the forks and the significant copy number variations is due to the effect of focusing on mitochondrial function.

3.3.5 Pharmacology differences

An additional data resource in the CCLE dataset is of pharmacological profiles. 479 of the cell lines were treated with 24 anticancer drugs and for each cell line the high concentration effect level A_{max} was measured. A_{max} measures the maximum relative

(a) Random.CV1

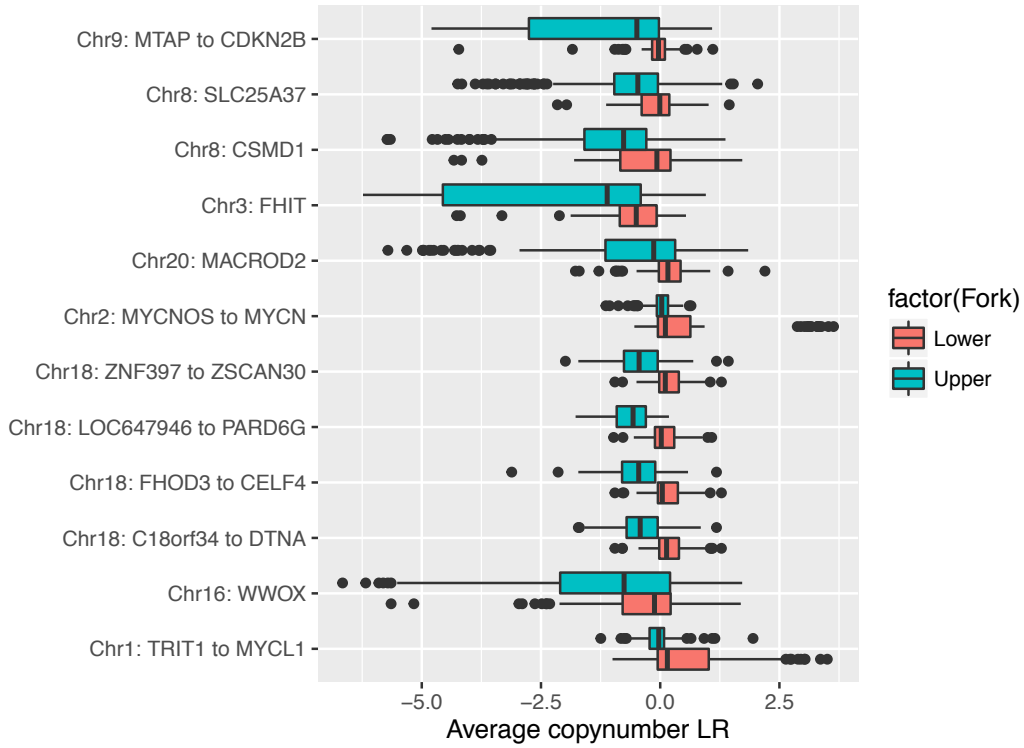

(b) Random.CV2

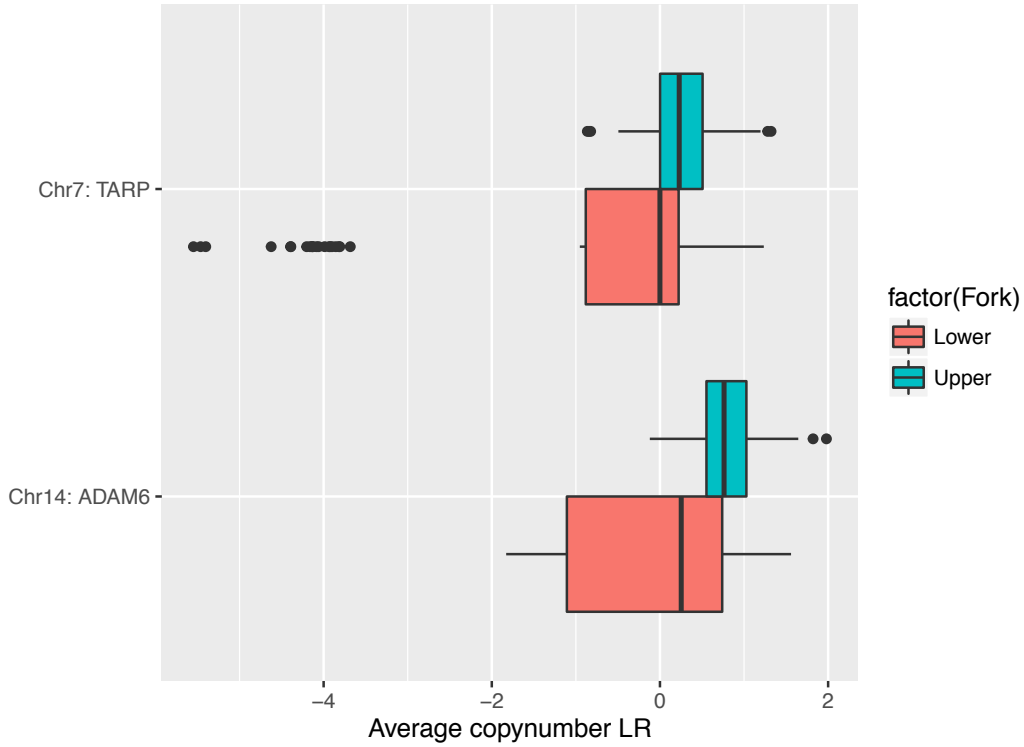

Figure 3.14: **(a - b)** Boxplots for significant copy number differences between the upper and lower forks in Random.CV1 and Random.CV2. As can be seen, Random.CV1 has numerous regions of significantly different copy number changes.

growth inhibition that occurs at high levels of drug concentration.

In the analysis done on the CCLE dataset, Barretina et al. (2012) identified various predictors to drug sensitivity, therefore it is hoped that the new groups identified could also be predictive of drug sensitivity.

As with analysing the copy number changes, for each pattern identified the top 250 samples were selected and then divided into two groups based on whether they belonged to the upper or lower fork. As not all the samples in the dataset were treated with the anticancer drugs, those that had not could not be included in the analysis.

Following the selection of the appropriate samples, the average difference in A_{max} was calculated between the upper and lower fork. To test for significance, as in Section 3.3.4 a permutation method was used. In this case the samples in the upper and lower fork were randomly reassigned into sets of the same size, and the values for A_{max} recalculated. This was done 10000 times, giving a distribution of the expected value of A_{max} for each of the 24 anticancer drugs across random sets identical in size to the upper and lower fork groups. Using this distribution it was then possible to calculate p-values and the multiple hypothesis adjusted p-values for every anti-cancer drug, and all adjusted p-values < 0.05 were deemed significant.

The results for Mito.CV1 showed that 6 of the anti-cancer drugs have statistically different values of A_{max}. This includes compounds 17-AAG, Irinotecan, L-685458, Paclitaxel, Sorafenib and Topotecan. Details of this can be seen in Table 3.5 and Figure 3.15**(a)**.

Compounds	Upper A_{max} mean	Lower A_{max} mean	A_{max} difference	adj p-value
L-685458	-34.00	-7.05	-26.95	0.002
Sorafenib	-36.47	-11.45	-25.02	0
Topotecan	-93.21	-70.18	-23.03	0
Irinotecan	-93.11	-79.06	-14.06	0
Paclitaxel	-89.79	-79.06	-10.73	0
17-AAG	-85.49	-77.79	-7.69	0.002

Table 3.5: Significant pharmacological high concentration effect level changes in the Mito.CV1 bicluster pattern between upper and lower forks.

The results for Random.CV1 showed 5 of the anti-cancer drugs with statistically different values of A_{max} between the upper and lower fork groups. These include AZD0530, Erlotinib, Lapatinib, PD-0325901 and ZD-6474. Details of this can be seen

in Table 3.6 and Figure 3.15**(b)**.

Compounds	Upper A_{max} mean	Lower A_{max} mean	A_{max} difference	adj p-value
Lapatinib	-7.56	-47.71	40.15	0
Erlotinib	-0.01	-37.01	37.01	0
PD-0325901	-24.78	-54.62	29.83	0.0088
AZD0530	-18.03	-46.05	28.02	0.0105
ZD-6474	-22.08	-46.61	24.53	0.0105

Table 3.6: Significant pharmacological high concentration effect level changes in the Random.CV1 bicluster pattern between upper and lower forks.

The results for Random.CV2 should be expected to be similar to that of Mito.CV1, but do show slight differences finding 9 compounds with statistically different values of A_{max}. These are 17-AAG, Irinotecan, L-685458, Paclitaxel, Sorafenib and Topotecan like the compounds significant for Mito.CV1, but also include PD-0325901, PD-0332991and PHA-665752. Details of this can be seen in Table 3.7 and Figure 3.15**(c)**.

Compounds	Upper A_{max} mean	Lower A_{max} mean	A_{max} difference	adj p-value
L-685458	-48.03	-5.35	-42.68	0
PD-0332991	-47.52	-20.52	-27.00	0
Sorafenib	-37.80	-11.19	-26.61	0.0020
Topotecan	-94.35	-69.78	-24.58	0
PHA-665752	-29.32	-6.49	-22.83	0.0020
PD-0325901	-20.69	-40.48	19.79	0.0051
Irinotecan	-94.81	-78.77	-16.04	0
Paclitaxel	-89.44	-78.50	-10.94	0.0036
17-AAG	-85.28	-76.33	-8.95	0.0176

Table 3.7: Significant pharmacological high concentration effect level changes in the Random.CV2 bicluster pattern between upper and lower forks.

3.4 Conclusion

In this chapter I applied a novel method for biclustering on disease-related dataset in order to elucidate the heterogeneity in the regulation of mitochondrial biogenesis. This has been a success in the way that both the HCM and CCLE dataset biclustering patterns were found clearly related to the mitochondria, with samples being identified with higher and lower mitochondrial biogenesis.

It is also clear that as well as identifying samples with different levels of mitochondrial biogenesis, it also has the potential to examine different modes of mitochondrial biogenesis. This was done to some extent in Section 3.2.1 where the identification of a

(a) Mito.CV1

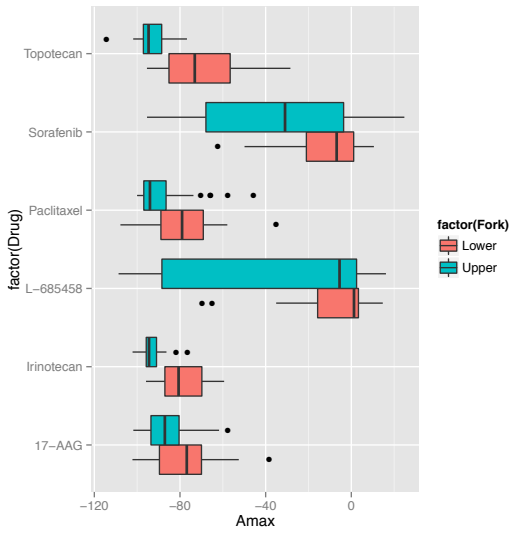

(b) Random.CV1

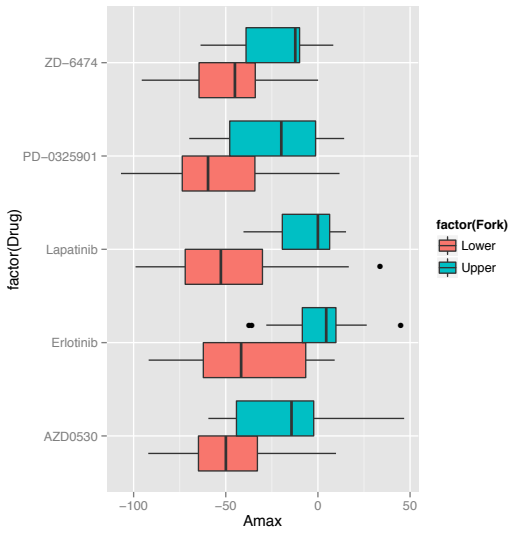

(c) Random.CV2

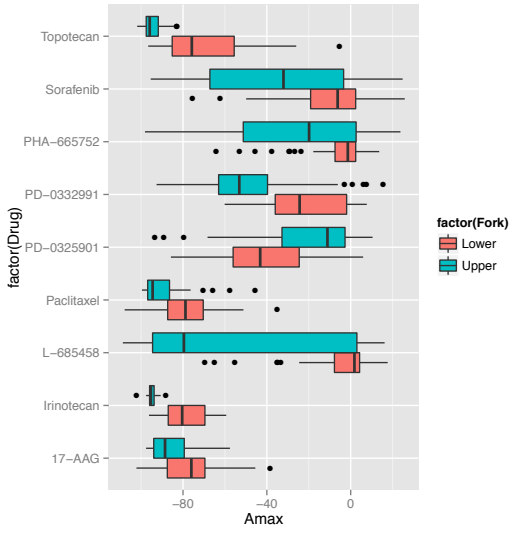

Figure 3.15: **(a - c)** Boxplots for the difference in high concentration effect level (A_{max}) for different pharmacological compounds, between upper and lower fork samples in each pattern found.

module of mitochondrial genes that are co-regulated in two distinct biclustering patterns were identified in the HCM data. This module was significantly bigger than it would be expected to be by chance and contained genes representing different functions within the mitochondria such as the ETC and the mitochondrial ribosomes.

It is easy to imagine with the further identification of many modes of mitochondrial biogenesis across different datasets involving different tissues, to identify many of these significant modules and use them to elucidate which mitochondrial genes are

co-regulated under different conditions perhaps bringing a greater understanding to the underlying transcription factor network.

The role of this chapter however was not to discover these mitochondrial co-regulated modules but to understand the role that mitochondria play in disease, specifically HCM and cancer.

For the HCM data there was a very promising result found in Figure 3.3**(a)** where a bicluster (Mito.1) was found with a significant difference in mitochondrial function between two groups of samples were identified. It is especially interesting that this bicluster was made up of two forks, one of which had mitochondrial genes down-regulated and was entirely made up of control samples and the other that had mitochondrial genes up-regulated and was almost entirely made up of disease samples with the exception of a single control sample.

It is tempting to speculate that this control sample could actually comes from a benign HCM sample that was undiagnosed, statistically this is not as unlikely as it may sound as if we are to take the prevalence of HCM at $1:200$ as is now reported (Semsarian et al. 2015) then upon screening 39 people at random the chance of at least one of them having HCM can be calculated as $1-\frac{199}{200}^{39} \approx 0.178$. It may be the case that there is donor screening to not allow donors with unknown or benign cases of HCM but if there was not, the probability that one or more of the control samples is in reality a HCM sample is nearly one in five.

It was unfortunately difficult to make further conclusions from the HCM dataset especially from the other biclusters identified, due to the lack of additional clinical data available. The dataset is not perfect only coming from patients who have undergone septal myectomy, which immediately has put a selection bias for a particular subtype of patient with HCM.

Further work on studying mitochondrial regulation in HCM is greatly hampered by this lack of further data. Therefore little more analysis on HCM can be made, without the availability of an experimental model, or access to additional clinical data across all forms of HCM. This is unlikely to be produced due to the very invasive procedure required to collect it.

In comparison to this, the CCLE data has much potential for further analysis, since cancer cell lines can be obtained and cultured. Like the HCM biclustering results, a

biclustering pattern was found within the CCLE data directly linked to mitochondrial function. With the additional information from the CCLE dataset, these could be directly linked to copy number changes and associated with the pharmacological profiles of anti-cancer drugs.

One interesting thing to note from the MCbiclust analysis on the CCLE data is just how few distinct biclusters were found. It could be expected in this dataset to find multiple biclusters related to different cancer signalling pathways, but this is not the case. The MCbiclust method is bias in selecting very large biclusters, indicating that the number of genes involved in the mitochondrial biogenesis and cellular proliferation bicluster found is much larger than the number of genes involved in cancer signalling pathways . Even using random gene sets with no relation to the mitochondria, this mitochondria related bicluster is frequently found, showing that a large number of non-mitochondrial genes must be regulated with it.

The only issue with the CCLE analysis is that the differences found were linked to samples from different origins. This while confirming that the alteration of mitochondrial function is biologically relevant, is a possible confounding factor. It is simply not possible to say whether the differences identified in copy number or the effect of anti-cancer drugs are due to altered mitochondrial function or the large number of differences between cancer cell lines with different histologies and tissues of origin.

For this reason further work on examining the regulation of mitochondrial biogenesis in cancer should exclusively look at a single type of cancer originating from the same tissue. This would have the benefit to spot unknown differences in mitochondrial function in seemingly similar cancers. It is also important to remember that cancer cell lines are only an experimental model used to study cancer. If this method is ever to be used in a clinical setting to help decide treatment, it must be demonstrated to work on patient samples. Both of these issues will be addressed in the next chapter.

Chapter 4

Bioinformatic analysis of mitochondrial biogenesis in breast cancer

4.1 Introduction

In Chapter 3 different regulations of the mitochondria within cancer cell lines were identified. It was however noted that many of these differences were found to be specific to cell lines originating from different tissue types, greatly limitting the possible clinical applications. To be of any possible use in prognosis and deciding clinical treatment, the biclustering method need to be demonstrated and find relevant biclusters from patient tumour samples.

To achieve this, this chapter will examine the regulation of mitochondria biogenesis within breast cancer, first by studying breast tumour samples and then by using breast cancer derived cell lines as a model to experimentally validate the mitochondrial differences.

4.1.1 Breast cancer

Breast cancer is one of the most common forms of cancer in woman. In the United States, in 2016 it is projected that there will be $246,660$ new cases of breast cancer. Breast cancer however has considerable better treatment available than other forms of cancer; in females in 2016, while 29% of all new cancer cases are projected to be breast cancer only 15% of all cancer deaths are projected to be due to it (Siegel et al. 2015).

Worldwide in 2012 it was estimated that there were $1,676,600$ new cases of female breast cancer and $421,900$ associated deaths (Siegel et al. 2012). While breast cancer mainly affects females, male breast cancer does occur but is rare with only 1500 new cases diagnosed yearly in the United States (Giordano et al. 2002). Due to these relatively small numbers the main focus of research for breast cancer treatment has been for woman.

Female breast cancer represents a disease affecting millions of woman worldwide, it also is a disease with a large degree of variation in both the clinical outcome and prognosis (Zardavas et al. 2015). Historically this disease was diagnosed and treatment decided purely on the clinical phenotypes, but today gene expression data is used to provide both a prognosis for the cancer and to cluster the disease into different groups with different clinical outcomes (Parker et al. 2009). The existence of these different subtypes of breast cancer has led to a paradigm shift and now breast cancer is thought of as group of different diseases that must be treated differently (Reis-Filho 2011).

While these new subtypes of breast cancer were discovered through the study of gene expression data, there has been no previous focus on searching for subtypes based on the expression of mitochondrial genes. In fact, these previous studies do not use functionally correlated genes to identify the subtypes, and the relation of the subtypes to metabolism has not been fully established. By using the biclustering algorithm, Massively Correlating Biclustering (MCbiclust) presented in Chapter 2, potentially new subtypes based on mitochondrial expression can be found and these can be compared to known existing subtypes.

4.1.1.1 Clinical and pathological features of breast cancer

Before the use of microarray technology, breast cancer prognosis was determined using the clinical and pathological features and first these must be understood to understand the impact gene expression data has had. The most important of the clinical features are a patient's age, the tumour size, the histological grade of the tumour and whether the cancer has spread to the lymph nodes.

Breast cancer has three different histological grades based on the appearance of the cancer cells, grade I refers to cells which look similar to normal cells and are slow growing, grade II refers to cells that are abnormal and are growing at an increased

rate, while grade III refers to cells that look very abnormal and are growing quickly. Examining the lymph nodes are important as breast cancer can easily spread there and once spread the chance of metastasis to other parts of the body is greatly increased.

The Nottingham prognostic index (NPI) (Haybittle et al. 1982) makes use of these clinical phenotypes to assign the probability of 5-year survival, the index is calculated following surgery and takes into account the tumour size, grade and the node status. The formula used is as follows:

$$NPI = [0.2 \times S] + N + G \tag{4.1}$$

Where S is the tumour size in centimetres, N is the node status with a score of 1 if the cancer has spread to no nodes, 2 if 1-4 nodes and 3 for more than 4 nodes. Finally G is the grade of the tumour, with Grade I scoring 1, II scoring 2 and III scoring 3. Different values of this index have different probability of 5 year survival.

Additionally to these simple to measure clinical features there are three main pathological markers of breast cancer. These are of three receptor, the estrogen receptor (ER), the progesterone receptor (PR) and the human epidermal growth factor receptor 2 (HER2), and each is responsible for driving a particular transcriptional program. The level of these receptors can be determined by immunohistochemistry to be significantly up-regulated, and these tumours are called positive for that receptor. This has lead to the sub-classification of breast cancer into groups such as ER positive and triple negative.

Standard treatment of breast cancer involves removing the tumour with surgery that can be preceded or followed with additional neoadjuvant or adjuvant therapy. Deciding on what course of adjuvant therapy to follow is where the sub-classifications of breast cancer become important.

For ER positive tumours, estrogen binding to ER is responsible for driving a proliferative program, so these cancers can be treated with hormone blocking therapies using drugs such as tamoxifen that block the estrogen receptor. The progesterone receptor has recently been found to act together with the estrogen receptor to drive a particular transcriptomic program (Mohammed et al. 2015) and when a cancer is both ER and PR positive the response to treatment is greater. HER2 positive cancers are traditionally associated with a poorer prognosis, these cancers however can be treated

with the drug Trastuzumab that blocks the HER2 receptor.

Cancers that are not positive for any of these receptors are known as triple negative breast cancer, in these cases the adjuvant options are only radiation therapy post surgery and a course of chemotherapy.

One of the difficulties of deciding treatment is weighting up the benefit of various adjuvant therapies. Patients with good overall prognosis post-surgery are less likely to receive any benefits from a course of chemotherapy. This is a major problem as many patients currently receive unnecessary chemotherapy after surgery, with only between 2 and 15% of patients actually receiving any benefit (Early Breast Cancer Trialists Collaborative Group 2005).

To help clinicians decide on an appropriate treatment the software Adjuvant! is commonly used (Ravdin et al. 2001). Adjuvant! uses an actuarial analysis by taking into account all relevant clinical and pathological features to calculate the statistical benefit a patient receives from different treatment options.

One clinical aim of studying gene expression data of breast cancer is that it can improve on these current methods of deciding adjuvant treatment, by finding a better method of determining which patients have good prognosis so to avoid unnecessary treatments and by discovering new subtypes of breast cancer that require different treatments.

4.1.2 Intrinsic subtypes of breast cancer

With the application of transcriptomics data to studying breast cancer, there are two main approaches. The first is to create a prognostic score, similar to the NPI, from the gene expression data. The other is to examine the gene expression data to find subtypes that represent fundamentally different kinds of breast cancer, which require different treatment options.

The creation of prognostic scores has been very successful, and many have been described in the literature (Reis-Filho 2011). A successful example of one scoring system is MammaPrint, which is available in a clinical setting and used to identify patients that need not undergo adjuvant chemotherapy (Mook et al. 2007). These scores however have a limited use, since the only option for ER negative tumours often is chemotherapy, and the prognosis is unlikely to ever be good enough to justify patients

not undergoing adjuvant chemotherapy (Weigelt et al. 2012). Therefore much of the hope of finding new novel treatments and better prognosis measures comes from the identification of previously unknown subtypes of breast cancer from gene expression values.

Perou et al. (2000) were the first to apply microarray data to search for breast cancer subtypes. They focusing on a set of genes that varied greatly in abundance between different tumour samples, this gene set is said to describe the intrinsic properties of the tumour and is referred to as the intrinsic gene set. Using this gene set, the tumour samples could be divided into distinct groups using hierarchical clustering, with each group representing a distinct biological program, these groups became known as the intrinsic subtypes of breast cancer.

There were originally four subtypes found by Perou et al. (2000) , basal-like, luminal, HER2-enriched and normal-like. In later work by Sørlie et al. (2001) the luminal group was found to be composed of at least 2 distinct subgroups, called luminal A and luminal B and possibly a third known as luminal C . A rare subtype within the basal group called claudin-low has also been identified and is characterised as having lower proliferation (Herschkowitz et al. 2007).

Of these groups, the basal and luminal were named due to their similarities with the expression of basal and luminal breast epithelia cells. Basal tumours often have worse prognosis, often being triple negative. The HER2-enriched group is notable for the over expression of genes linked to the HER2 receptor and has clear links with HER2 positive breast tumours. The normal-like group is named for having similarity in expression with normal non-cancerous tissue, and there has been some debate stating that this group may be an artefact from tumour samples contaminated with normal tissue (Prat 2011).

The difference between the luminal groups is based on particular gene sets. Luminal B tumours typically have higher expression of proliferation related genes than luminal A (Reis-Filho 2011), and as such luminal A samples have the better prognosis.

Parker et al. (2009) developed a 50 gene set predictor, based on the prediction analysis for microarrays (PAM) method (Tibshirani et al. 2002), called PAM50 for assigning samples to belonging to basal-like, luminal A, luminal B, HER2-enriched or normal-like tumours. The normal-like subtype is based on the expression of actual normal breast tissue, and as such tumour samples categorised as such are likely to be so

due to normal tissue contamination.

The 50 gene set was chosen from a list of genes previously used as intrinsic genes and also as being suitable for measurement from from formalin-fixed parafin-embedded tissue. The gene set was then further minimised by selecting the top *N* t-test statistics for each subgroup. In doing this the samples were then classified using a centroid-based prediction method. In additional to the intrinsic subtype classification, a risk of recurrence (ROR) score was trained based on the subtype classification.

The PAM50 method is now available to be used in a clinical setting to determine the intrinsic subtype of a sample (Nielsen et al. 2014), and it will be the method used to determine breast cancer intrinsic subtype within this chapter.

These 5 subtypes have some clear links to the clinical markers, such as HER2-enriched group being mainly HER2 positive. An overview of the relationship between the clinical and pathological features and the PAM50 groups can be seen in Figure 4.1. However Parker et al. (2009) made clear that while there are some clear trends in the distribution of ER and HER2 positive/negative status within the different subtypes, any given subtype could be found in any ER/HER2 positive/negative status sample.

The intrinsic subtypes have been shown to be related to different clinical outcome (Sørlie et al. 2001). It is therefore not surprising that use of the intrinsic subtypes offers prognostic information. Nielsen et al. (2010) using the PAM50 intrinsic subtypes identified the presence of a low risk luminal A group that received very little benefit from adjuvant chemotherapy, while Dowsett et al. (2013) showed that the ROR score from PAM50 offers greater prognostic information for patients following endocrine therapy.

Stein et al. (2016) recently completed a preliminary study for a clinical trial for patients suffering from ER-positive HER2 negative breast cancer, a group that is largely luminal A and luminal B. The study involved using a risk of recurrence score similar to Mamaprint in the test group to decide which patients were to receive chemotherapy. In addition to this multiple other tests were done on these tumours including identification of the intrinsic subtype. The preliminary study was a success and will be extended to a larger study with 4500 patients and will aim to determine if this technology can be used to safely reduce the number of patients receiving unnecessary chemotherapy.

One of the main outcomes of finding these intrinsic subtypes is the acceptance that

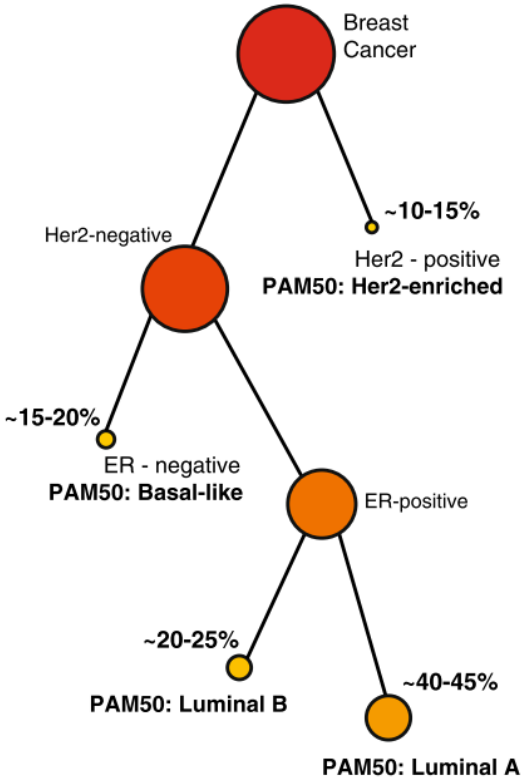

Figure 4.1: The PAM50 subtypes and commonly associated clinical phenotypes, adapted from Ciriello et al. (2013).

breast cancer is a collection of molecularly distinct diseases (Reis-Filho 2011). There have been some criticism of these approaches stating that both the intrinsic subtype and prognosis scores have only translated to incremental improvement for the patients (Weigelt et al. 2012). Part of this is due to the difficulty in relating a prognosis score or an intrinsic subtype to the response of a therapeutic treatment. Resistance to treatment can occur from many mechanisms, which are not able to be detected from gene expression technology, such as resistance originating from a small population within the tumour, a change in the expression of a single or small number of genes, or resistance possibly occurring due to a number of distinct mechanisms (Weigelt et al. 2012). For these reasons analysis of the intrinsic subtypes and different prognostic scores tell us much more about risk than possible treatment courses.

Weigelt et al. (2012) also mentions problems with the commonly used intrinsic subtypes themselves. For instance the choice of the exact subtypes present within breast cancer is problematic and varies due to the exact method used. As noted for the popular PAM50 subtypes, there is not an exact relation between the subtypes and existing clinical

measures that you would expect, such as between HER2 positive tumours and HER2-enriched subtype. Others have pointed out that the distinction between luminal A and luminal B cancer is arbitrary and better described as a continuum as it is based on the expression of proliferation related genes which are not bimodal (Weigelt et al. 2012).

4.1.3 Examining mitochondrial biogenesis in breast cancer

In this chapter, breast cancer samples will be examined in relation to mitochondrial biogenesis related biclusters that will be found using the MCbiclust methods described in Chapter 2. The resulting identified samples with altered mitochondrial expression pattern must be linked to the existing clinical features used in treating breast cancer. Since the MCbiclust method is based on gene expression data, it will be most comparable to the known intrinsic subtypes found by the PAM50 classifier.

Using publically available gene expression datasets, biclusters involving mitochondrial alterations will be sought using the MCbiclust methods. Once a suitable bicluster has been found the aim of this chapter is to investigate it in more detail using breast cancer cell lines as an experimental model.

The hope of doing this is to demonstrate this novel mitochondrial bicluster can be used in addition with the existing intrinsic subtypes. By doing so this has the potential to create a better prognosis score and find subtypes of breast cancer that may be responsive to treatments either for existing chemotherapies or to develop novel treatments targeting mitochondria and cellular metabolism (Fulda et al. 2010).

4.2 Bioinformatic analysis of a breast cancer sample dataset

4.2.1 Using a new gene set

The biclusters previously found using MCbiclust are strongly dependent on the gene set they are run on. In an attempt to find mitochondrial related biclusters, the MitoCarta gene set (Pagliarini et al. 2008) is used, and additional biclusters can be found with random gene/probe sets that may or may not be linked to the mitochondria. While the MitoCarta gene set is good for identifying mitochondrial related biclusters, it should be noted that the biclusters found do not involve all the genes in the MitoCarta gene set and also involve many other non-mitochondrial genes. Therefore there is scope for using

other mitochondrial related gene sets for finding alternative biclusters, and this shall be attempted on the breast cancer data.

One choice could be to use the mitochondrial gene ontology (GO) term which contains 1858 genes (Ashburner et al. 2000). This set includes genes with less evidence of being mitochondrial then those in MitoCarta, as such it is not clear that this gene set would produce better results. Instead of choosing a larger gene set, a better strategy would be to choose a smaller mitochondria related gene set, especially as there are many mitochondrial genes that are not strongly involved in the bicluster found.

In trying to choose this alternative mitochondria gene set, the mitochondrial related terms that have been found significant before can be examined. One set of terms that is often found to be significant is that of the mitochondrial ribosomes, often being significant too with the cytosolic ribosomes. This can be seen clearly in the bicluster identified from the MitoCarta genes in the Cancer Cell Line Encyclopedia (CCLE) data from Section 3.3.2 that can be seen in Table 4.1.

GOID	TERM	adj.p.value
GO:0042254	ribosome biogenesis	1.779E-44
GO:0005840	ribosome	2.607E-42
GO:0005739	mitochondrion	3.385E-42
GO:0005761	mitochondrial ribosome	3.911E-21
GO:0022626	cytosolic ribosome	4.590E-09

Table 4.1: Significant terms found in the CCLE MitoCarta bicluster in Section 3.3.2 related to the mitochondria and ribosome.

Indeed it is natural to assume that any alteration in the mitochondrial or cytosolic ribosomes will be involved in changes of mitochondrial biogenesis, since it is these ribosomes that are producing the mitochondrial proteins. Moreover, these ribosomes provide a general link between mitochondrial and cellular proliferation, which may be expected to exist with increased mitochondrial biogenesis. It has been noted previously in the literature that ribosomal genes are commonly correlated together (Alon et al. 1999), further making a gene set based on ribosomal genes good for the MCbiclust analysis.

On examination of the protein interactions of mitochondrial ribosomal proteins there is a gene that is a clear hub in the protein-protein interaction (PPI) network, immature colon carcinoma transcript 1 (ICT1). ICT1 is an essential mitochondrial

protein, which is a member of the large mitochondrial ribosome subunit, and has functionally shown to rescue stalled mitochondrial ribosomes (Richter et al. 2010).

ICT1 has interactions with 223 other genes, 173 of which are in MitoCarta, and include many of the mitochondrial ribosome genes, but also cytosolic ribosomes, and members of the electron transport chain (ETC). Figure 4.2 shows the PPI network centred on ICT1.

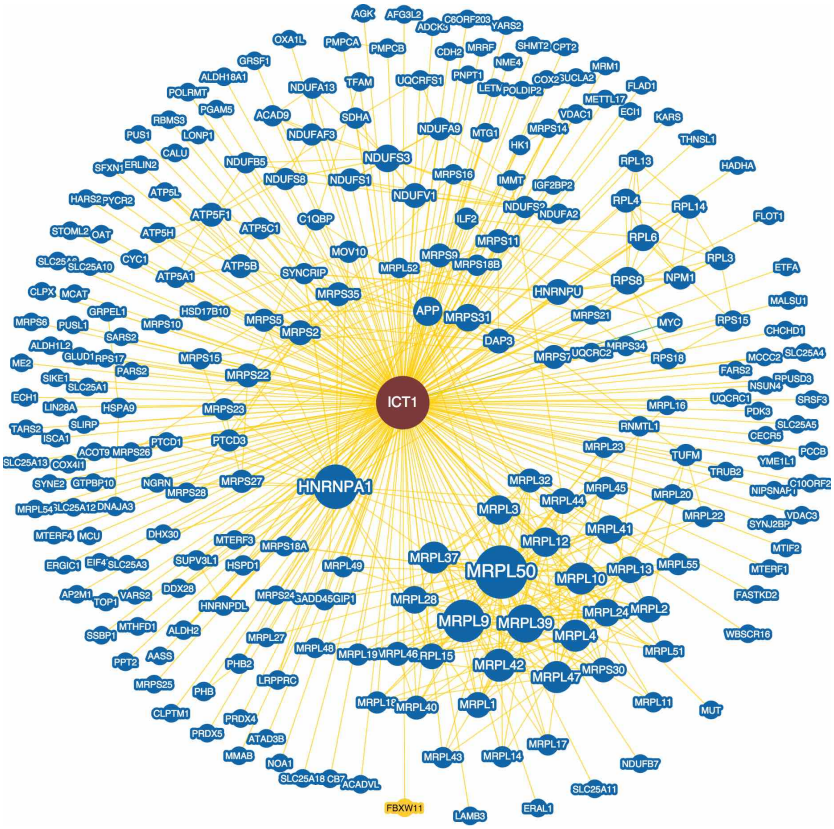

Figure 4.2: The PPI network of mitochondrial gene ICT1, greater node size represents greater connectivity and thicker edge sizes represent increased evidence supporting association. Yellow lines indicate, association is from physical evidence, while blue nodes represent that the associated gene is from the same organism and yellow nodes that it is from a different organism. Graph produced from Biogrid 3.4 (Stark et al. 2006).

However, the genes in the PPI network are still relatively few and are not guaranteed to be strongly correlated to ICT1 expression and involved in the transcriptional patterns just because of protein interactions. For this reason an ideal gene set would be to choose those genes that correlate most strongly with ICT1 across all the samples. The top 1000 ICT1 correlated genes were chosen as a gene set to run MCbiclust. This gene set contains 45 of the genes in the ICT1 PPI network and 136 genes in MitoCarta. This gene set thus contains a strong mitochondrial component, as well as genes strongly related to

the mitochondrial ribosomes that are likely to be in the same transcriptional patterns we are aiming to find.

Running a gene set enrichment analysis on this gene set using gprofiler (Reimand et al. 2007), it can be found that many mitochondrial terms are greatly significant as well as those for the ribosome. The top results of this gene set enrichment analysis are given in Table B.12 in Appendix B.

4.2.2 The data

To analyse alteration of mitochondrial function in breast cancer samples, a dataset from the Cancer Genome Atlas Network was chosen (CGAN 2012). The aims of this large study was stated to create a comprehensive molecular portrait of breast cancer, as such it includes data from 6 different platforms including the messenger RNA (mRNA) expression data of 522 primary cancer samples measured on Agilent chips, DNA methylation, copy number, micro RNA (miRNA) sequencing, whole exome sequencing to identify somatic mutations and limited proteomic data from reverse-phase protein arrays complement the expression data.

This is in addition to clinical data that included the PAM50 classification of the samples, as well as the positive or negative status of the ER, PR and HER2 receptors. One thing missing is survival data which was not available in the dataset due to the short follow up time, at the time of the publication of the study.

The biclustering algorithm, MCbiclust, from Chapter 2 was applied to this gene expression data, in the same manner that it was applied to datasets in Chapters 2 and 3. As before the aim was to find samples with altered mitochondrial function, so the algorithm was run 1000 times on the set of MitoCarta genes, 1000 times on random gene sets and 1000 times on the ICT1 related gene set discussed in Section 4.2.1.

4.2.3 Finding a mitochondrial related bicluster in a breast cancer dataset

The aim of this section is to find a mitochondrial related bicluster in the breast cancer data, which can be studied in depth.

As in Sections 2.4.2, 3.2.2 and 3.3.2 a silhouette width analysis was used to determine the number of distinct bicluster patterns for the MitoCarta, random probe sets and ICT1 related gene set runs. The results of this are given in Figure 4.3, and result in

a large number of distinct biclusters, 4 being found from the MitoCarta genes, 2 from the random probe sets and 1 from the ICT1 related gene sets. One of the MitoCarta distinct biclusters, Mito.CV4, has an negative average silhouette width, indicating that the biclusters assigned to this group would have been better clustered in one of the other 3 groups. This indicates that this group does not describe a distinct bicluster and should not be included in further analysis.

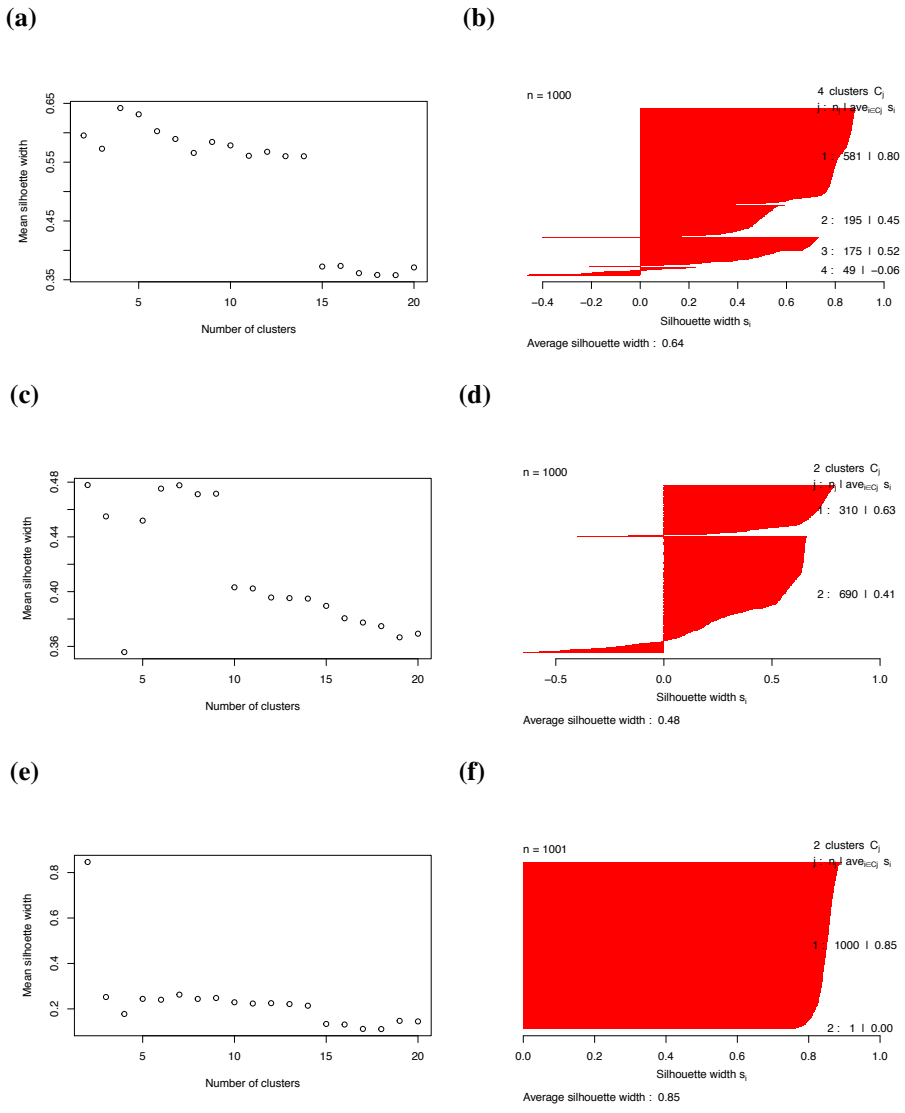

Figure 4.3: Silhouette analysis of three sets of runs in the breast cancer data, applied to the resulting correlation vectors. **(a)** and **(b)** show the silhouette analysis for the correlation vectors from the run on the MitoCarta gene set finding an optimum of four clusters. **(c)** and **(d)** show the silhouette analysis from the run on the random probe sets that finds two optimal clusters of correlation vectors. **(e)** and **(f)** show the results from the ICT1 related gene set that found there was only one optimal cluster, ignoring the random correlation vector.

All the distinct biclusters found can be compared by an examination of their correlation vectors. This can be seen in Figure 4.4 where the values of the correlation vectors for non-mitochondrial and mitochondrial probes are plotted against each other. It is immediately clear from this examination the bicluster Random.CV1 is very similar to Mito.CV3 and Random.CV2 is very similar to Mito.CV1. Thus the runs with the random probe sets have not yielded any distinct biclusters different from those found with the MitoCarta gene set. For this reason it is safe to discard the biclusters found using the random probe sets, and only focus on those found from the MitoCarta and ICT1 related gene sets.

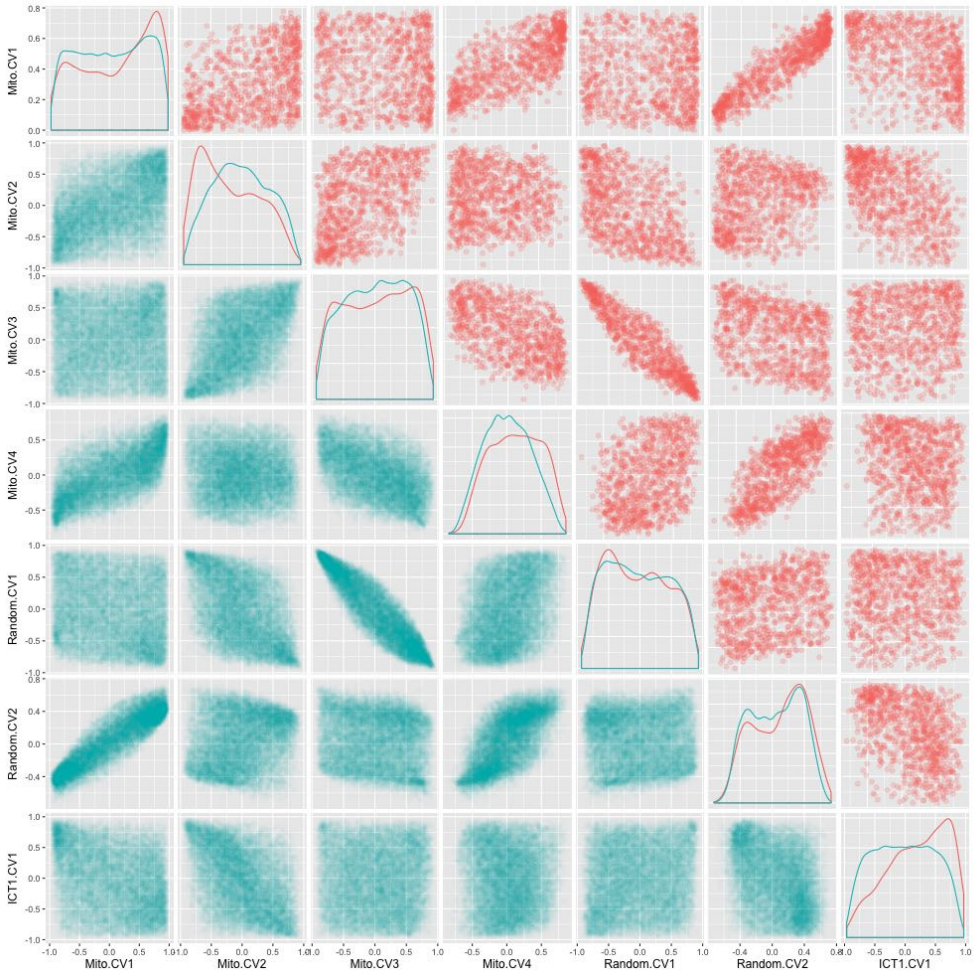

Figure 4.4: Comparison plot of the correlation vectors from the 7 biclusters found in the breast cancer data. In the scatter plots red represents mitochondrial probes and blue represents non-mitochondrial probes. Patterns Mito.CV1 is very similar to Random.CV2 and Mito.CV3 is very similar to Random.CV1.

The remaining 4 distinct biclusters can have their samples ordered by the strength of the bicluster found, using the method described in Section 2.2.4.1. The plots of

these figures can be seen in Figure 4.5, where the samples are coloured according to their PAM50 status. For biclusters Mito.CV1, Mito.CV2 and Mito.CV3, there is a clear division between basal and luminal A tumour samples. Pattern ICT1.CV1 however separates luminal A and B samples.

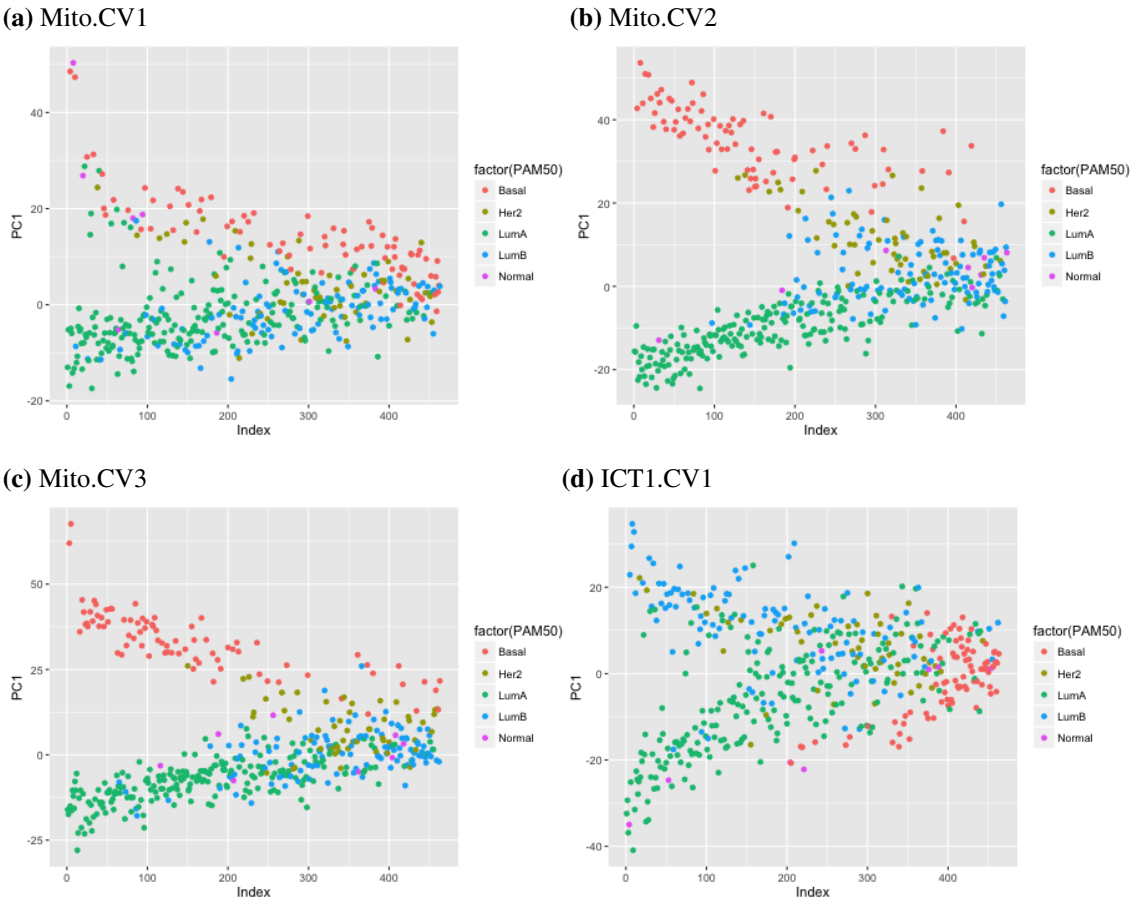

Figure 4.5: PC1 plots of 4 biclusters found in the breast cancer data plots **(a, b, c)** show the three remaining biclusters found from the MitoCarta gene set and **(d)** shows the bicluster found from the ICT1 related gene set. Samples are coloured according to their PAM50 classification.

The MCbiclust method has therefore identified four potential biclusters describing samples with expected mitochondrial differences. What is left to do is to quantify the significance of the mitochondrial changes in this bicluster with gene set enrichment analysis. This was done using Mann-Whitney test on GO terms as described in Section 2.2.5.1 on the average correlation vectors of these biclusters. The top significant gene set enrichment results can be seen in the Appendix in Tables B.13 to B.16, but below in Table 4.2 are the significance of GO terms related to mitochondrial function in all four of the biclusters.

GOID	TERM	ICT1.CV1 adj p.value	Mito.CV1 adj p.value	Mito.CV2 adj p.value	Mito.CV3 adj p.value
GO:0044429	mitochondrial part	5.569E-22	5.514E-04	4.048E-12	n.s.
GO:0005739	mitochondrion	2.695E-21	4.290E-08	7.241E-14	n.s.
GO:0005743	mitochondrial inner membrane	6.357E-17	n.s.	1.080E-09	n.s.
GO:0005740	mitochondrial envelope	9.383E-13	n.s.	1.429E-06	n.s.
GO:0005761	mitochondrial ribosome	4.955E-11	n.s.	6.311E-09	n.s.
GO:0031966	mitochondrial membrane	8.467E-11	n.s.	6.497E-06	n.s.
GO:0005759	mitochondrial matrix	5.176E-10	n.s.	3.491E-06	n.s.
GO:0044455	mitochondrial membrane part	1.409E-09	n.s.	9.435E-04	n.s.
GO:0005746	mitochondrial respiratory chain	1.114E-07	n.s.	n.s.	n.s.
GO:0005747	mitochondrial respiratory chain complex I	7.331E-07	n.s.	n.s.	n.s.
GO:0007005	mitochondrion organization	1.575E-06	n.s.	4.275E-05	n.s.
GO:0042775	mitochondrial ATP synthesis coupled electron transport	2.921E-04	n.s.	n.s.	n.s.
GO:0006120	mitochondrial electron transport, NADH to ubiquinone	5.185E-04	n.s.	n.s.	n.s.
GO:0005762	mitochondrial large ribosomal subunit	1.213E-03	n.s.	n.s.	n.s.
GO:0006839	mitochondrial transport	4.307E-03	n.s.	4.032E-02	
GO:0006626	protein targeting to mitochondrion	5.066E-03	n.s.	3.059E-02	n.s.
GO:0070585	protein localization to mitochondrion	1.181E-02	n.s.	4.291E-02	n.s.
GO:0072655	establishment of protein localization to mitochondrion	1.423E-02	n.s.	n.s.	n.s.
GO:0005763	mitochondrial small ribosomal subunit	1.613E-02	n.s.	n.s.	n.s.

Table 4.2: Significant mitochondrial related GO terms in biclusters found in the breast cancer dataset. n.s. = non significant.

Table 4.2 shows that the ICT1.CV1 correlation vector has the most significant mitochondrial related GO terms. Surprisingly the Mito.CV3 correlation vector, which has 313 significant GO terms (the top 200 are given in Table B.15), but none related to the mitochondria. Meanwhile, the Mito.CV1 correlation vector only has the generic terms

mitochondrion and mitochondrion part significant. Of the correlation vectors found using the MitoCarta gene set only Mito.CV2 has a large number of mitochondrial related GO terms significant and these are all less significant than those from the ICT1.CV1 correlation vector. Interestingly, Figure 4.4 seems to show the the non-mitochondrial probes in Mito.CV2 and Mito.CV3 are correlated, and indeed if the significant GO terms in Tables B.14 (for Mito.CV2) and B.15 (for Mito.CV3) are studied, both share many terms linked to cellular proliferation. In addition to these, Mito.CV2 has significant mitochondrial terms while Mito.CV3 has many significant terms linked to the immune system.

Further studying of the ICT1.CV1 bicluster shows the upper fork samples have increased mitochondrial expression compared to the lower fork samples. This can be seen in Table 4.3 when examining the average expression of the significant mitochondria related GO terms and shows that the difference in expression is especially great in the mitochondrial ribosome and respiratory chain.

Of the three identified suitable biclusters, ICT1.CV1 was chosen for further analysis. ICT1.CV1 as can be seen in Table 4.2 is the bicluster with the most associated significant mitochondrial changes. It is also the only bicluster that separates between luminal A and B samples in the upper and lower fork, as is seen in Figure 4.5.

Of the other three biclusters, Mito.CV3 is unsuitable due to its lack of significant mitochondrial alterations, and Mito.CV1 and Mito.CV2 have weaker associated mitochondrial changes compared with ICT1.CV1. Mito.CV1 and Mito.CV2 do however seem to represent a distinct bicluster that involves mitochondrial alterations between basal and non-basal tumour samples, and could be of interest for investigating further. However this will not be done due to the mitochondrial changes not being as significant as for ICT1.CV1 and the difference between basal and non-basal tumours being less interesting as they are widely recognised to be molecularly distinct diseases (Reis-Filho 2011). Additionally, the involvement of luminal A and B samples in ICT1.CV1 may mean that this bicluster is relevant for determining which tumours do not benefit from chemotherapy, a matter of current scientific interest (Stein et al. 2016).

GOID	TERM	Upper fork average	Lower fork average
GO:0005762	mitochondrial large ribosomal subunit	0.404	-0.249
GO:0005747	mitochondrial respiratory chain complex I	0.250	-0.138
GO:0005761	mitochondrial ribosome	0.237	-0.183
GO:0005746	mitochondrial respiratory chain	0.223	-0.127
GO:0006120	mitochondrial electron transport, NADH to ubiquinone	0.213	-0.108
GO:0042775	mitochondrial ATP synthesis coupled electron transport	0.198	-0.097
GO:0006626	protein targeting to mitochondrion	0.188	-0.094
GO:0044455	mitochondrial membrane part	0.184	-0.076
GO:0005763	mitochondrial small ribosomal subunit	0.147	-0.176
GO:0005743	mitochondrial inner membrane	0.144	-0.052
GO:0070585	protein localization to mitochondrion	0.128	-0.085
GO:0072655	establishment of protein localization to mitochondrion	0.127	-0.081
GO:0006839	mitochondrial transport	0.111	-0.043
GO:0044429	mitochondrial part	0.107	-0.022
GO:0005740	mitochondrial envelope	0.107	-0.007
GO:0031966	mitochondrial membrane	0.107	-0.005
GO:0005759	mitochondrial matrix	0.107	-0.050
GO:0007005	mitochondrion organization	0.095	-0.036
GO:0005739	mitochondrion	0.080	0.002

Table 4.3: Differences in average expression in significant mitochondria associated GO terms between the upper and lower fork samples in bicluster ICT1.CV1, the upper and lower fork samples were selected using the threshold function in MCbiclust.

4.2.4 Mutational alterations behind the bicluster

The additional data in the breast cancer dataset contains two sources that may help to explain the underlying cause of the ICT1.CV1 bicluster. This is the genetic information present in the copy number and mutational data.

The copy number data measured by CGAN (2012) on Affymetrix 6.0 single nucleotide polymorphism (SNP) arrays across 773 tumour samples, 499 of which correspond to one of the 522 primary cancer samples with measured mRNA levels. Genomic Identification of Significant Targets in Cancer 2.0 (GISTIC2.0), was used to calculate the somatic copy number alterations, in terms of deletion or amplification, for each gene (Mermel et al. 2011).

The somatic mutational data was obtained by CGAN (2012) from whole exomic sequencing of 510 tumours, identifying across the dataset mutations in 14130 unique genes. 463 of the samples in this dataset correspond to one of the 522 primary cancer samples with measured mRNA levels.

For the copy number dataset, the average copy number value for every gene was calculated for samples belonging in the upper and lower fork, as decided by the threshold biclustering algorithm described in Section 2.2.6, and also for the luminal A and B samples. Following this the copy number difference, between groups can be calculated, and regions where there is a significant difference found.

Of particular interest is the difference in copy number alterations between the upper/lower fork and luminal A/B samples. This will show for instance if there is any copy number alterations between two luminal B samples, one a member of the upper fork and one not. Similarly, this can also be done for two luminal A samples, one a member of the lower fork and one not. Figure 4.6**(a)** show the average copy number difference between upper and lower fork samples for every gene plotted against the average copy number differences between luminal A and B samples. There is a general trend that copy number alterations while occurring in similar locations are greater between the upper and lower fork samples, with a regression analysis showing that the average copy number change between luminal A and B samples is roughly 30% that between the upper and lower fork samples.

Figure 4.6**(b)** shows the average copy number difference between upper and luminal B samples plotted against that of the difference between lower and luminal A samples. From this figure it is apparent that in certain locations, upper fork samples have a much higher copy number than luminal B samples, while lower fork samples have a decrease copy number compared to luminal A samples. Thus in this way the change between upper and lower fork samples that is seen in Figure 4.6**(a)** is maximised.

To find the significant copy number alteration regions, a permutation test was used that took the sample groups and randomly reassigned them into groups of the same size. This was repeated 100 times to get a estimated probability distribution of copy number alterations expected by chance, and those regions with an adjusted p-value of less than 0.05 selected as significant.

Table 4.4 shows the regions with significant differences between the different

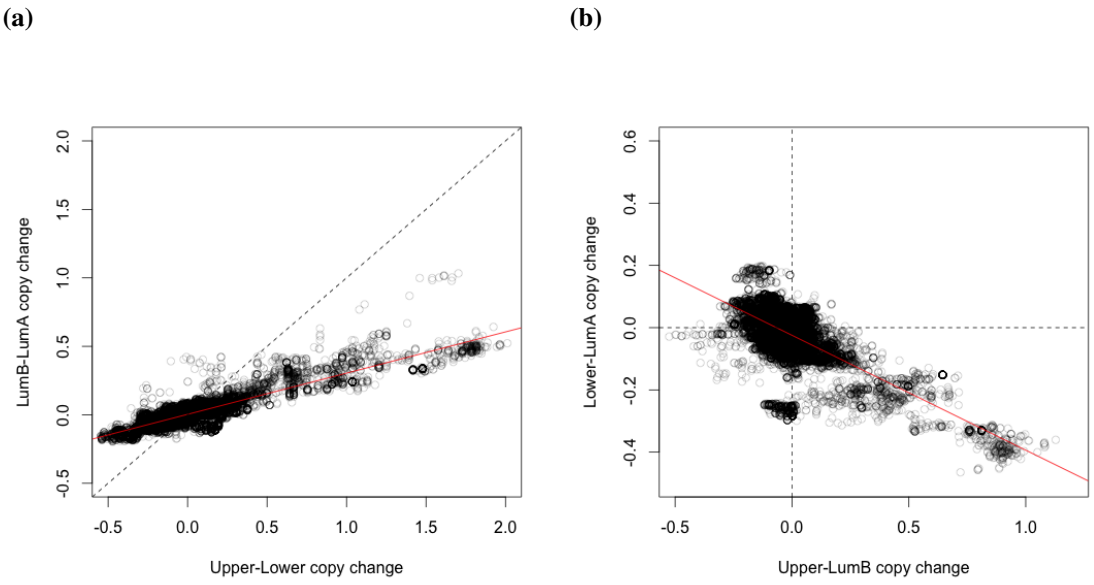

Figure 4.6: Copy number alterations between upper/lower and luminal A/B in the ICT1.CV1 bicluster, with each point representing the average copy number change of one gene over the samples. Figure **(a)** shows a scatter plot of the difference between the upper and lower samples against the difference between luminal A and B samples, with the dashed line representing $y = x$ and the red line representing the regression line with equation $y = 0.003 + 0.3 \times x$ and adjusted r-squared value of 0.7877 . Figure **(b)** shows a scatter plot of the difference between upper and luminal B against that between lower and luminal A samples, with the dashed lines representing lines $y = 0$ and $x = 0$ and the red line representing the regression line with equation $y = -0.02 - 0.369 \times x$ and adjusted r-squared value of 0.4833.

groups. Two large regions stand out, one on chromosome 8 and the other on chromosome 17. The region on chromosome 8, has a significantly lower average copy number in the lower fork samples than the luminal A, while an overlapping region has a significantly higher average copy number in the upper fork samples than the luminal B. A similar effect also seems to occur on a small region on chromosome 11. The chromosome 17 region has a significantly lower average copy number in the lower fork samples but is not significantly changed between the upper fork and luminal B samples.

For the somatic mutational data the vast majority of the mutations occur infrequently. 6398 of the 14130 found mutated genes only occur once in the dataset, and only 16 mutations occur in over 5% of the tumours. The most common mutation is in the PIK3CA gene and is present in 38.4% of the tumours.

The hypergeometric test was used to test for significant differences between the groups. Four comparisons were tested, upper-lower, upper-luminal B, lower-luminal A

Number of genes	Cytoband Location	LumA average	Lower fork average	Copy change
457	8q11.1 to 8q24.3	0.48	0.14	0.34
14	11q13.3	0.43	0.17	0.25
51	17q21.32 to 17q21.33	0.17	-0.04	0.21
4	17q22	0.14	-0.06	0.20
2	17q22	0.16	-0.03	0.18
110	17q22 to 17q24.2	0.19	-0.05	0.25
11	17q24.3 to 17q25.1	0.13	-0.07	0.20
1	17q25.1	0.13	-0.07	0.21
8	17q25.1	0.13	-0.07	0.20
16	17q25.1	0.12	-0.07	0.19
26	17q25.1	0.11	-0.07	0.18
21	17q25.2 17q25.3	0.10	-0.07	0.17
88	17q25.3	0.08	-0.07	0.16
1	20q13.2	0.39	0.08	0.31
Number of genes	Cytoband Location	LumB average	Upper fork average	Copy change
227	8q21.12 to 8q24.22	0.99	1.88	0.89
4	8q24.3	0.79	1.67	0.88
2	11q13.3	1.51	1.77	-0.26
7	11q13.3	1.44	1.82	0.38

Table 4.4: Significant regions of copy number alterations between luminal A and lower fork samples and luminal B and upper fork samples. All genes in the significant regions are significant with adjusted p-value < 0.05.

and luminal B-luminal A, with only the 16 genes that were mutated in more than 5% of the total number of tumours tested for significance.

The results of this can be seen in Table 4.5 showing that 4 genes were significantly different between the groups. The proportion of mutated samples for genes PIK3CA, MAP3K1 and TP53 were found to be significant between luminal A and luminal B samples, while mutations in CDH1 were found to be significant between Upper and Lower fork samples, with this mainly being driven by CDH1 mutations occurring much more frequently in lower fork samples than luminal A samples.

Overall the percentage difference between the frequency of the mutations between the upper and lower forks was greater than that between the luminal A and B samples for all 4 of these genes. However due to the still relative low frequency of these mutations and the few numbers of upper and lower fork samples compared to luminal A and B, only the difference in PIK3CA and CDH1 was found to be statistically significant between the upper and lower fork.

	PIK3CA	CDH1	MAP3K1	TP53
All mutations	196 (38.43%)	34 (13.14%)	67 (6.67%)	192 (37.65%)
LumA mutations	110 (52.63%)	22 (10.53%)	55 (26.32%)	24 (11.48%)
Lower mutations	21 (60%)	11 (31.43%)	12 (34.29%)	1 (2.86%)
LumB mutations	38 (18.18%)	6 (2.87%)	8 (3.83%)	38 (18.18%)
Upper mutations	4 (18.18%)	0 (0%)	1 (4.55%)	6 (27.27%)
LumA% - LumB %	34.45	7.66	22.49	-6.70
Adj p-value	**7.55e-03**	**0.496**	**1.52e-04**	**2.46e-05**
Lower% - Upper %	41.82	31.43	29.74	-24.42
Adj p-value	**0.0239**	**0.0294**	**0.0900**	**0.109**
Lower% - LumA %	7.37	20.9	7.97	-8.63
Adj p-value	**1**	**0.00262**	**1**	**0.680**
Upper% - LumB %	0	-2.87	0.718	9.09
Adj p-value	**0.699**	**1**	**1**	**1**

Table 4.5: Somatic mutations in genes PIK3CA, CDH1, MAP3K1 and TP53. Top half of the table shows number of samples with mutations in these genes, with the percentage of samples with mutated genes given in brackets. The bottom half of the table shows the difference in mutation percentage between that upper/lower fork and luminal A/B samples, and the associated p-values of these differences.

Overall the results of studying the mutational data in terms of somatic mutation frequency and copy number alterations suggest that the genomic differences between the upper and lower fork samples is greater than that between luminal A and luminal B. This in turn suggests that it is these genetic differences that are driving this bicluster.

4.3 Identification of a similar bicluster in a breast cancer cell line dataset

4.3.1 The data

Since the breast cancer tumour samples matching this bicluster are not available for further functional studies, it would be helpful to identify breast cancer derived cell lines which can be used as a model. This however presents challenges in how to obtain the cell lines that most closely resemble the type of regulation identified. Therefore before any experimental work can be undertaken, cell lines derived from breast cancer tissue must be selected, that match the bicluster identified.

For this purpose a dataset by Neve et al. (2006) was used that contains gene expression data for 51 breast cancer cell lines measured with Affymetrix GeneChip Human Genome HG-U133A. This dataset was collected to attempt to model the diverse

range of transcriptomic profiles identified in breast cancer, and the 51 cell lines were shown to mirror the expression of 145 primary breast tumour samples (Neve et al. 2006). As such this dataset should contain breast cancer cell lines that mirror the expression that has been identified in the bicluster ICT1.CV1.

This dataset only contained 51 samples so is unsuitable for use with the MCbiclust methods. Furthermore new biclusters are not being sought in this dataset, but cell lines that match the previous mitochondrial related bicluster, ICT1.CV1 identified in Section 4.2.3. To complete this purpose, a new method has to be derived.

4.3.2 Point Scoring algorithm

Since the correlation vector for the ICT1 related bicluster is known, this can be used as the basis for finding similar biclusters in other datasets. In theory, genes with positive correlation vector values should all be up-regulated together while those with negative values are down-regulated and vice-versa. A point scoring algorithm can be devised that calculates in a sample how many of the positive correlation vector genes are up-regulated together at the same time as the negative correlation vector genes are down-regulated together.

The algorithm is simple and works as follows:

1. Take two groups of genes A and B, with A all having positive correlation vector values and B all having negative correlation vector values.

2. The gene expression data is normalised by median centering for each gene, and give each sample an initial score of 0.

3. For each sample $+1$ is added to the score for every gene in A greater than 0, and every gene in B less than 0.

4. For each sample -1 is added for every gene in A less than 0 and every gene in B greater than 0.

A high positive score indicates that samples have the majority of the gene in set A upregulated while the genes in set B are downregulated. A high negative score in contrast indicates that samples have genes in set A down-regulated while genes in set B are up-regulated. P-values can be calculated using permutation tests that recalculate the point score but with randomly assigning the genes in A and B.

To demonstrate the use of this algorithm, for the breast cancer data, the point score was calculated for each sample based on the genes in the ICT1 related gene set, divided into two sets based on their correlation vector values. As can be seen in Figure 4.7, the point score values greatly match that of the first principal component.

In this case positive values represent the lower fork samples, and negative values represent the upper fork samples.

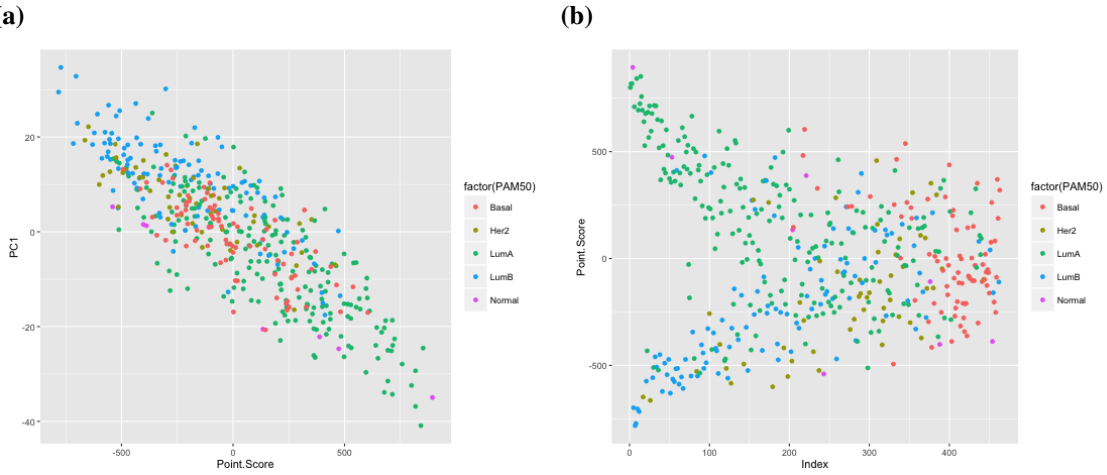

Figure 4.7: Comparison between the point score values and PC1 of the ICT1.CV1 bicluster, where the point score has been calculated from the genes in the ICT1 related gene set. **(a)** shows a scatter plot of PC1 against the point score values **(b)** shows the point score values plotted against the ranking of the samples. This produces the same fork pattern that can be seen in Figure 4.5 **(b)**. In both plots the samples are coloured according to their PAM50 classification.

4.3.3 Selecting breast cancer cell lines

The point scoring algorithm was applied on the breast cancer cell line dataset, using the genes in the ICT1 related gene set divided into two groups A and B based on the sign of their corresponding correlation vector values. The result of this can be seen in Table 4.6 with the corresponding adjusted p-values.

Many of the different cell lines were significant, but not all were easily available for experimental work. MCF7, HCC202, and MDAMB453 were chosen as representatives of the upper fork, while MDAMB436 and HS578T were chosen as representatives of the lower fork. While BT474 was selected as a possible control, belonging to neither the upper or lower fork.

Since the lower fork was found to be closely related to the luminal A subtype and the upper fork is closely related to the luminal B subtype, it is of interest to identify

CellLine	Point Score	Adj Pvalue	Sub type
SUM44PE	237	0.00E+00	Lu
HCC70	223	2.40E-09	BaA
HCC1187	217	5.03E-10	BaA
HCC1143	193	0.00E+00	BaA
SUM185PE	173	7.99E-07	Lu
MDAMB436*	169	3.71E-09	BaB
BT549	125	2.19E-03	BaB
HCC2185	125	4.27E-04	Lu
SUM52PE	119	3.30E-05	Lu
MDAMB468	115	4.39E-01	BaA
600MPE	105	2.13E-04	Lu
UACC812	105	4.21E-01	Lu
HCC1007	95	1.67E-02	Lu
ZR7530	93	3.03E-05	Lu
SUM190PT	83	9.13E-01	BaA
SUM225	75	1.00E+00	BaA
HS578T*	71	3.85E-04	BaB
HCC1937	67	1.00E+00	BaA
MDAMB415	63	2.46E-02	Lu
HCC38	57	1.00E+00	BaB
HCC1569	45	2.46E-02	BaA
HCC2157	45	9.86E-01	BaA
MDAMB231	37	1.00E+00	BaB
SUM1315MO2	35	7.85E-02	BaB
BT20	23	1.00E+00	BaA
SUM149PT	23	1.00E+00	BaB
BT474*	17	1.00E+00	Lu
MDAMB175VII	17	9.86E-01	Lu

CellLine	Point Score	Adj Pvalue	Sub type
ZR75B	-287	2.59E-31	Lu
LY2	-267	1.96E-20	Lu
T47D	-217	3.35E-11	Lu
HCC1428	-209	5.26E-13	Lu
CAMA1	-191	7.99E-07	Lu
MDAMB361	-179	6.69E-14	Lu
MDAMB453*	-175	1.17E-08	Lu
HCC202*	-165	1.34E-03	Lu
MCF7*	-157	6.55E-07	Lu
MDAMB157	-133	3.82E-07	BaB
BT483	-95	2.59E-06	Lu
MCF12A	-77	2.16E-05	BaB
MCF10A	-53	4.13E-03	BaB
HCC1500	-47	4.48E-04	BaB
SKBR3	-45	1.00E+00	Lu
MDAMB435	-43	1.00E+00	BaB
HCC1954	-37	1.00E+00	BaA
HBL100	-33	1.00E+00	BaB
SUM159PT	-31	1.00E+00	BaB
AU565	-21	1.00E+00	Lu
ZR751	-17	1.00E+00	Lu
HCC3153	-15	1.00E+00	BaA
MDAMB134VI	-7	1.00E+00	Lu

Table 4.6: Point Scores calculated for the breast cancer cell lines from Neve et al. (2006). The subtype of each cell line is based on the classifications made by Neve et al. (2006), into one of three groups Luminal, BasalA and BasalB. Significant (adjusted p-vale < 0.05) positive point score cell lines are coloured blue and significant negative point score cell lines are coloured red. Breast cancer cell lines that were available for experimental work are denoted with an asterix ($*$).

the subtype of the cell lines. Neve et al. (2006) attempted to classify them, using the same methodology as is used for the PAM50 classifications, but only identified three groups Luminal, Basal A and Basal B. These clearly are not the same standard groups found through PAM50 (Parker et al. 2009). The PAM50 classifier itself cannot be used on these samples since it is trained on breast cancer tumour data to find known breast cancer tumour subtypes.

Identifying the breast cancer intrinsic subtypes in cell lines has proved to be a more difficult than expected task. Recently Prat et al. (2013) tried to identify breast cancer

cell lines that represented all the known subtypes and surprisingly they could find no cell line that matched the luminal A subtype. Prat et al. (2013) hypothesised that this was due to most breast cancer cell lines being derived from metastatic tumours more likely to be the luminal B subtype, and that luminal A tumours in general were unsuitable for cell culture. Another hypothesis could be that the PAM methodology fails to identify luminal A cell lines. ICT1.CV1, the mitochondrial related bicluster whose lower fork is strongly related to the luminal A subtype, has here been used to identify cell lines that are seemingly similar to this luminal A subtype, at least in terms of the expression of the genes in the bicluster. It is possible that this method has identified luminal A cell lines where the PAM method has failed.

4.4 Experimental study of mitochondrial function in different breast cancer cell lines

4.4.1 Methodology

4.4.1.1 Cell culture

A laminar flow cabinet was used for all cell culture, this was so a sterile environment would be maintained. All items being placed into this cabinet were sprayed with 70% ethanol. During all cell culture a lab coat and gloves were worn at all times, the gloves being sprayed with 70% ethanol before being placed in the cabinet. Prior and after to use the cabinet was cleaned using Virkon, and after use the cabinet was closed, airflow switched off and sterilised with a UV light.

MCF7, HCC202, MDA-MB-436, Hs587t and BT474 cell lines were obtained from Barts Cancer Institute, London. Cell lines were cultured in Dulbecco's modified eagles medium (DMEM) with 10% fetal bovine Serum (FBS) and Normocin (25mg/L) in 10cm tissue culture treated sterile plates. All cell lines were cultured in a 37°C incubator set with 5% CO_2 and 95% humidity. All cell lines were passaged every 3-4 days using Trypsin, when they were between 80% and 90% confluency.

To passage a cell line, all media was removed, and then the cells were washed with phosphate buffered saline (PBS) (10ml). Then trypsin (0.25%, 2ml) was added to the dish and the cells placed in the incubator for 1-2 minutes until the cells had begun to lift from the plates. DMEM + FBS (4ml) was then added to the dish to inactivate the

trypsin and the resulting cell suspension was mixed with a pipette to ensure all cells were dislodged. The cell suspension was centrifuged at 500g for 2 minutes to form a cell pellet free of trypsin, which was resuspended in DMEM + FBS. The cell suspension was then split at a 1:2 ratio in a fresh 10cm plate or counted to plate a particular number of cells.

If the cells were to be counted 10μL of cell suspension were mixed with 10μL of trypan blue and 10μL of this was pipetted onto a haemocytometer. Using a light microscope on a 10x objective, the number of cells in each of the four corner sections of the haemocytometer was made. An average of this count was calculated and is multiplied by two to account for the dilution with trypan blue. An estimation of the number of cells per ml can then be made by multiplying this value by 10000.

4.4.1.2 NanoString

Cell lines were grown in 10cm plates and total ribonucleic acid (RNA) was extracted using the Qiagen RNeasy extraction kit, according to the manufacturer's protocols.

Hybridisation of the reporter codeset and capture probeset to the sample RNA was done using the nanostring nCounter Gene Expression Protocol, on RNA samples quantified by NanoDrop to 50ng of total RNA in a maximum of 5uL of sample, incubated in a thermocycler set to 65°C for 12 hours.

Once removed from the thermocycler the samples were proceeded immediately to post-hybridization processing with the nCounter Prep Station.

The Prep Station was set up with the hybridized samples, sample cartridge, prep plates and other components according to the nanostring nCounter Prep Station protocol. The Prep Station once set up performs wash steps to remove excess probes and non-target cellular transcripts. After washing the Target/Probe RNA complexes are eluted off and are immobilized in the cartridge for data collection.

All consumable components required for processing samples on the Prep Station are provided in the nCounter Master Kit, and after set up no further action is required by the user.

Once complete, the cartridge from the Prep Station can be analysed by the nCounter Digital Analyzer. Before analysis the reporter library file associated with the Codeset is uploaded onto the digital analyzer. Following that a cartridge definition file is created

that contains the sample information for the cartridge to be run.

The cartridge was placed within the Digital Analyzer and run according to the instructions in the nCounter Digital Analyzer protocol. The Digital analyser using a microscope objective and a charge-coupled device (CCD) camera, creates a digital image from which hundreds of thousands of target molecule counts are made. These are processed by the digital analyser and counts are tabulated into a comma separated value (CSV) format.

4.4.1.3 Western blots

A Qiagen bicinchoninic acid (BCA) protein quantification kit was used to quantify protein samples following the manufacturers instructions. Samples were then prepared with loading buffer and denatured by boiling as appropriate per antibody (for the MitoProfile cocktail antibody this was for 10 minutes at 60°C). 20μg protein per well were loaded into 4-12% BisTris NuPAGE gels at 150V in MOPS running buffer until the samples reached the bottom of the gel. Transfer buffer was used to pre-soak the blotting pads. PVDF membranes were then cut to size, activated in methanol then soaked in transfer buffer. The transfer apparatus was assembled and using a wet system at 30V for 2 hours gels were transferred onto a PVDF membrane. Ponceau-S was used to check the protein transfer and then membranes were blocked for one hour at room temperature in Tris-buffered saline (TBS)(Tris 0.5M - NaCl 1.5M)- Tween 0.1% and 5% milk. Using appropriate dilutions the primary antibodies were applied overnight at 4°C. Membranes were washed 3 times for 5 minutes each time with TBS-Tween before use of a suitable horseradish peroxidase-conjugated secondary antibody for 1 hour at room temperature in TBS-Tween and 5% milk. Then membranes were washed 3 times for 5 minutes each time using TBS-Tween and imaged on a BioRAD ChemiDoc system using BioRAD ECL. When a loading control was needed, the membranes were washed once more 3 times for 5 minutes each with TBS-Tween before the primary and secondary antibody steps were repeated using an appropriate loading control (usually beta-actin). ImageJ (`https://imagej.nih.gov/ij/`) was used to analyse the resulting images and relative intensities were normalised to the loading controls.

4.4.1.4 Oroboros

Oxygen consumption rates were measured using an Oroboros Oxygraph-2k high resolution respirometry system (Oroboros Instruments, Innsbruck, Austria). Cells were grown to confluency in 10cm plates for 48 hours prior to the assay. The cells were trypsinized, and counted so they could be diluted to 1 million cell/ml in a respiration buffer (DMEM powder (8.3g/L), sodium pyruvate (110mg/L), glucose (1000mg/L), Glutamax 100x (10ml/L, final concentration 2mM), Sodium bicarbonate (3.7g/L), FBS 10% and media adjusted to 7.4pH and filter sterilised with a 0.22 Stericup). Prior to the assay, electrode air calibration was performed with the respiration buffer, as suggested by manufacturer's protocol. 2ml of the cell suspension were added to each of the two chambers, and the O_2 flow signal allowed to stabilise to the basal respiration rate. Drugs were added to the chambers using Hamilton syringes at the following concentrations and order: oligomycin (2.5μM), carbonylcyanide-p-(trifluoromethoxy)-phenylhydrazone (FCCP) (titrated 1μl at a time from a 1mM stock, to produce maximal respiratory capacity), and antimycin A (2.5μM).

Oligomycin inhibits adenosine triphosphate (ATP) synthase and therefore blocks the main proton channel into the mitochondrial matrix, the resulting respiration rate is due to the proton leak in the inner mitochondrial membrane. FCCP uncouples the inner mitochondrial membrane allowing protons to freely pass across the membrane. This equalises the mitochondrial membrane potential but also leads to the flow of electrons in the ETC not being dependent on the number of protons in the mitochondrial matrix. This results in a maximal respiration rate where the ETC is not limited by the number of protons in the mitochondrial matrix. Antimycin A inhibits cytochrome C reductase otherwise known as Complex III in the ETC. This stops all oxygen consumption from the mitochondrial and gives us a value for non-mitochondrial respiration that can be subtracted from the basal, leak and maximal rates to give mitochondrial specific rates.

Data were then extracted and analysed using O2K cell analysis template to give oxygen consumption per unit cells. Significance between different groups was then tested by one-way analysis of variance (ANOVA).

4.4.1.5 Gas chromatography mass spectrometry (GC-MS)

Cells were grown as described in cell culture methods but with carbon-13 labelled glucose/galactose added to the media.

Before metabolite extraction, cell plates were taken to a cold room 500μL of medium from each plate was put into 1.5mL tubes, for later analysis, and frozen. The remaining media was removed and the plates placed in an ice/water bath before washing two times with 5ml of ice-cold PBS.

To extract the metabolites the following process was used: 800μL ice-cold methanol, containing an internal standard of 1mM scyllo-inositol, was added to the plates; cells were then detached from the plate by scraping with a cell scraper. This mixture was added to a 15ml tube, and the plate then washed with 400μL of methanol and 400μL of H_2O which was also added to the tube. Then 400μL of ice-cold chloroform was added to each tube. The tubes were placed in a water bath sonicator in a cold room for one hour, with 3x8 minute pulses of sonication and then centrifuged for 10 minutes at 16,000rpm at a temperature of 0°C. The supernatant was extracted and dried in a vacuum concentrator. The cell pellet was then re-extracted with 200μL of methanol and 100μL of H_2O, this was sonicated, spun and the supernatant added to previous supernatant tube and dried again in a vacuum concentrator. The remaining cell pellet was used for estimating dry weight and measuring total protein. The dried supernatant was resuspended in 50μL chloroform, 150μL methanol and 150μL H_2O and spun for 5 minutes at 0°C and 16,000rpm. The extract is then in a biphasic partition, with the upper phase containing the polar metabolites and the lower phase containing lipidic metabolites. The polar phase portions of each extract were then transferred to GC-MS vial inserts and dried in a vacuum concentrator. Separate vial inserts had 10μL of the saved cell culture medium added, with 1mM scyllo-inositol, which were also dried in a vacuum concentrator. Each vial insert then had 30μL of methanol added, containing 1μL of 5mM nor-leucine as another internal standard, followed by 30μL of methanol without nor-leucine, with the vials being dried in a vacuum concentrator after each addition.

Before running samples on the mass spectrometer, derivatiation was done to improve GC separation. 20μL methoxyamine (30mg/mL in pyridine) was added to each insert and this was vortexed briefly and then incubated at room temperature overnight,

Silylation was then done by adding 20μL of BSTFA + TCMS reagent to each inset and incubating for 1 hour at room temperature.

An Agilent 7890A GC with a 5975C triple axis detector MSD (Agilent Technologies, Santa Clara, CA) was used to analyse the samples. Metabolites were separated on an Agilent J&W 122-5532G DB-5ms capillary column (30m x 0.25mm, 0.25μm film thickness), in splitless mode. The injector and transfer line temperatures were 270 and 280°C, respectively. The flow rate of helium carrier gas was 0.7 mL/min. The oven temperature was programmed to hold at 70°C for 2 min, increased to 295°C at a 12.5°C/min ramp rate, increased from 295°C to 320°C at a 25°C/min ramp rate, and held at 320°C for 3 minutes. The mass spectrometer was operated in scan mode, after a 6 minute solvent delay with a range of $50-565$ mass/charge (m/z) and a scan-rate of 2.8 scans per second.

Metabolites were identified by matching retention times and fragmentation patterns to commercially available standards. Metabolite peaks were integrated at each isotopologue m/z using MassHunter Workstation software (Agilent Technologies). Peak areas were quantified based on peak areas of known standards using nor-leucine as an internal standard, and then metabolite levels were normalised to protein content.

Mass isotopologues were stripped of the contribution from natural abundance, based on the chemical formula of derivitised fragment quantified. Percent enrichment for an isotopologue was calculated by dividing the corrected intensity by the sum of corrected intensities of all isotopologues for that metabolite. Significance of metabolite enrichment between different samples was calculated with one-way ANOVA.

4.4.1.6 Contributions

Experimental work was done in collaboration with others, the contributions of which are described below. Michela Menegollo, a PhD student from Padova, Italy who is also working in the Szabadkai lab contributed to the experimental work by extracting the RNA used in the nanostring experiments and running all western blot experiments. The Oroboros data was collected by myself in conjunction with Cathy Qin, an undergraduate medical student at UCL whose experimental project I supervised. The GC-MS data was collected in collaboration with Dr Mariia Yuneva at the Crick Institute, who helped with the metabolite extraction, ran the samples on the mass spectrometer and assisted with

the data analysis.

4.4.2 Results

4.4.2.1 Transcriptomics with nanostring

The first task in investigating the mitochondrial functional properties of the cell lines was to confirm that the transcriptional differences discussed in Section 4.2.3. This was necessary due to the relatively high level of cell line misidentification in science (American Type Culture Collection Standards Development Organization Workgroup 2010). By confirming that the cell lines match the expected regulation, we can be sure that they are a true representation of the cell lines from the data collected by Neve et al. (2006) used in Section 4.3.3.

Besides confirming the transcriptional differences, there is the opportunity to gain more precise measurements than those available from microarrays. Microarrays are inherently noisy and have a limited dynamical range and provide a measurement that cannot be used to find the precise count of each transcript, or measure transcripts with low copy numbers. For this reason a different method of measuring transcriptomics was used.

RNA sequencing (RNA-seq) while a possible method was deemed not cost effective, while methods such as quantitative polymerase chain reaction (q-PCR) while highly accurate is not high-throughput and impractical to measure a large number of genes across many samples. Instead it was decided to measure mRNA transcripts with Nanostring nCounter analysis system (Malkov et al. 2009) that has the accuracy of q-PCR but the potential for high throughput measurements of hundreds of genes.

Nanostring chips only measure a select number of genes, in this case 172, so in order to proceed with the transcriptomics, a 172 sized gene set had to be chosen to measure. To choose the genes in the gene set several criteria were used. This gene set needed to include genes from which the bicluster could be confirmed and other transcripts that may be useful in determining other features of the sample such as those involved in the transcription network, additionally nanostring required all genes to have GenBankIDs.

Table 4.7 gives a brief overview of the main groups of genes included in the nanostring gene set, along with a brief description of each one. Table C.1 in Appendix C

gives a full overview of all the genes in the nanostring dataset.

Gene group	Description	Number of genes
Transcription factor network	Chosen with reference to literature, see Hock (2009)	32
mtDNA	The required GenBankIDs were from Jourdain et al. (2013).	10
p53-induced genes	Chosen from Sen et al. (2011), p53 genes were of particular interest for work on a separate project not discussed in this thesis.	25
MitoCarta	Total number of genes linked to the mitochondria.	61
Mitochondrial genes linked to bicluster	Chosen due to the size of the log fold change between the upper and lower fork. 15 predicted upregulated in the upper fork and 15 predicted downregulated in the upper fork .	30
Non-mitochondrial genes linked to bicluster	Chosen due to the size of the log fold change between the upper and lower fork. 14 predicted upregulated in the upper fork and 15 predicted downregulated in the upper fork.	29
Cytosolic ribosome	Chose genes that encode cytosolic ribosome proteins.	16
Mitochondrial ribosome	Chose genes that encode mitochondrial ribosome proteins	19
ETC	Genes that are members of the electron transport chain.	20
Control	Genes chosen for their lack of correlation to genes in the bicluster present at differing amounts.	4

Table 4.7: Groups of genes selected for the nanostring gene set. Note there is some overlap in these groups, e.g. all 10 of the mtDNA genes are in the ETC.

From these measured mRNA transcripts a scoring system had to be derived to judge whether the sample best matched the upper or lower fork group. A similar scoring system to the point score system used in Section 4.3.2 was used, but limited to genes measured by the nanostring probes. This scoring system was based on the regulation of 59 genes measured by the nanostring, chosen as 29 are up-regulated in the upper fork and 30 downregulated in the lower fork. The 29 gene up-regulated in the upper fork gene set will be referred to as gene set Up, and the 30 gene down-regulated gene set will be referred to as gene set Down.

After normalising the counts to the median of each gene, the score is calculated with four values

1. $\mathrm{G1}_{pos} = |which(\mathrm{Up} > 0)|$

2. $\mathrm{G1}_{neg} = |which(\mathrm{Up} < 0)|$

3. $\mathrm{G2}_{pos} = |which(\mathrm{Down} < 0)|$

4. $\mathrm{G2}_{neg} = |which(\mathrm{Down} > 0)|$

The score can then be calculated as follows:

$$Score = \frac{\mathrm{G1}_{pos} - \mathrm{G1}_{neg} - \mathrm{G2}_{pos} + \mathrm{G2}_{neg}}{59} \tag{4.2}$$

With 59 being the total number of genes measured by nanostring for the means of determining the classification of the sample.

The workings of this method can be demonstrated on the original breast cancer microarray data (CGAN 2012). In a similar way to Section 4.3.2 with the scoring system used to find the breast cancer cell lines, this nanostring scoring system when applied on the breast cancer dataset, recreates the fork plot and the score values are strongly correlated to that of the first principal component as can be seen in Figure 4.8.

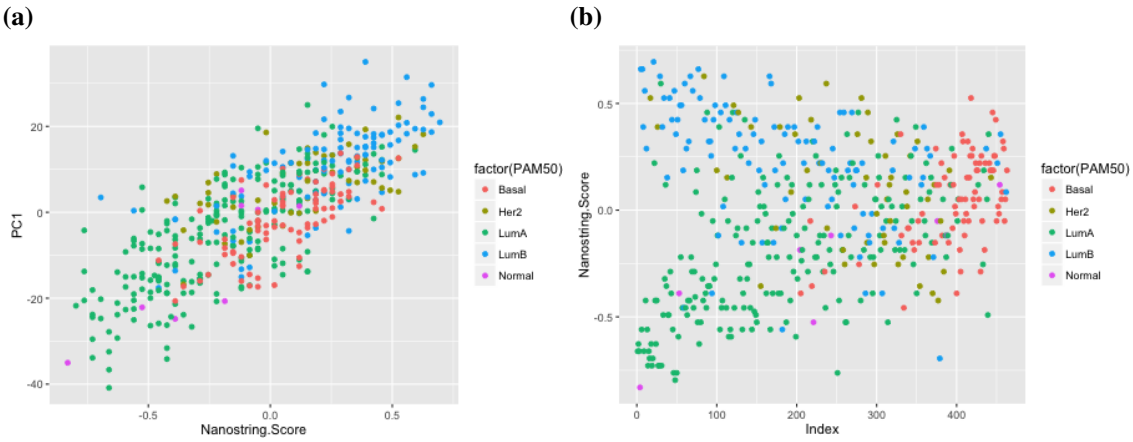

Figure 4.8: Comparison between the nanostring score values and PC1 the ICT1.CV1 bicluster. **(a)** shows a scatter plot of PC1 against the nanostring score values **(b)** shows the nanostring score values plotted against the ranking of the samples. This produces the same fork pattern that can be seen in Figure 4.5**(b)**. In both plots the samples are coloured according to their PAM50 classification.

Additionally significance can be calculated using a permutation test in which the genes in gene set Up and Down are randomly reassigned and the score recalculated.

This is repeated 10000 times to get an approximate distribution of the scores which is then used to calculate the p-value.

Cell lines MCF7, HCC202 representing the upper fork and MDA436 and Hs587t representing the lower fork had RNA extracted. Transcripts were measured using nanostring in triplicate in the manner described in Section 4.4.1. The nanostring data before analysis was normalised by subtracting the average of the negative control probes as background then normalising to the average count number of the control genes. Table 4.8 shows the nanostring score calculated from the nanostring data. This table shows that all cell lines have significant scores are truly representatives of their respective forks.

Cell Line	Fork	Replicate	Nanostring Score	Adj p-value
HCC202	Upper	1	0.49	9.566E-04
HCC202	Upper	2	0.46	1.548E-03
HCC202	Upper	3	0.36	2.054E-02
Hs578t	Lower	1	-0.73	2.339E-07
Hs578t	Lower	2	-0.59	4.253E-05
Hs578t	Lower	3	-0.69	1.245E-06
MCF7	Upper	1	0.69	1.418E-06
MCF7	Upper	2	0.49	9.516E-04
MCF7	Upper	3	0.63	8.119E-06
MDA436	Lower	1	-0.22	1.339E-01
MDA436	Lower	2	-0.22	1.339E-01
MDA436	Lower	3	-0.46	2.433E-03

Table 4.8: Nanostring scores for breast cancer cell lines

4.4.2.2 Western Blots

The cancer cell lines HCC202, MCF7, MDA453, MDA436, Hs587t and BT474 were grown and the levels of mitochondrial proteins were measured using western blots. The focus was on measuring members of the ETC to assess if there were any major differences in the proteomics of this key mitochondrial pathway.

This was achieved using the MitoProfile antibody cocktail that measures one protein from each complex of the ETC. For normalisation purposes three additional proteins were measured β-tubulin a housekeeping gene, GRP-75 a mitochondrial heat shock protein and GAPDH a protein involved in glycolysis. Thus the protein levels of the ETC could be normalised to the mitochondria, glycolysis as well as a β-tubulin general housekeeping gene.

Cell lines HCC202, MCF7 and MDA453 representing the upper fork and cell lines MDA436 and Hs587t representing the lower fork and cell line BT474 which was included as a control were all measured. A representative blot from this work is given in Figure 4.9.

Figure 4.10 shows the summary of all the results after being quantified and tested for significance. It was found that Complex I and IV are upregulated in the upper fork cell lines compared with the lower fork cell lines when normalised to the general state of the mitochondria with GRP-75. This confirms the results from the gene set analysis of the ICT.CV1 bicluster which showed the expression of complex I and other members of the respiratory chain were significantly up-regulated in upper fork samples, as can be seen in Table 4.3.

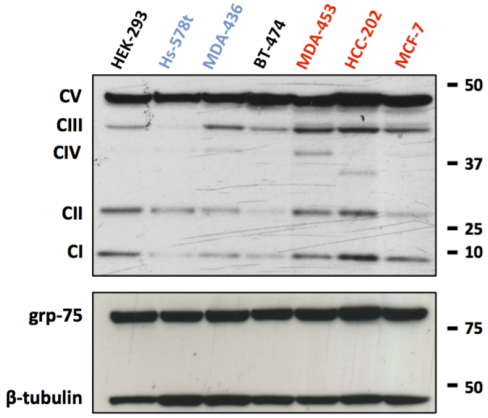

Figure 4.9: Representative western blot of breast cancer cell lines MCF7, HCC202, MDA-453, MDA-436, Hs578t and BT474. Cell lines were measured after being grown as described in the cell culture methods in Section 4.4.1.1. Upper fork cell lines are coloured red, while lower fork cell lines are coloured blue and control cell lines are coloured black. Note that HEK-293 is not a breast cancer cell line, but derived from human embryonic kidney cells and was included in the blot as an alternative control cell line from a different tissue of origin. Figure and blot were produced by Michela Menegollo.

4.4.2.3 Oxygen Consumption

The respiratory state of the cell lines were tested to determine whether there is a functional difference between the upper and lower fork cell lines. Mitochondria require oxygen to produce ATP, so any differences between the oxygen consumption will indicate functional differences in the workings of the ETC.

To do this the cell lines were grown and measured under different conditions on the

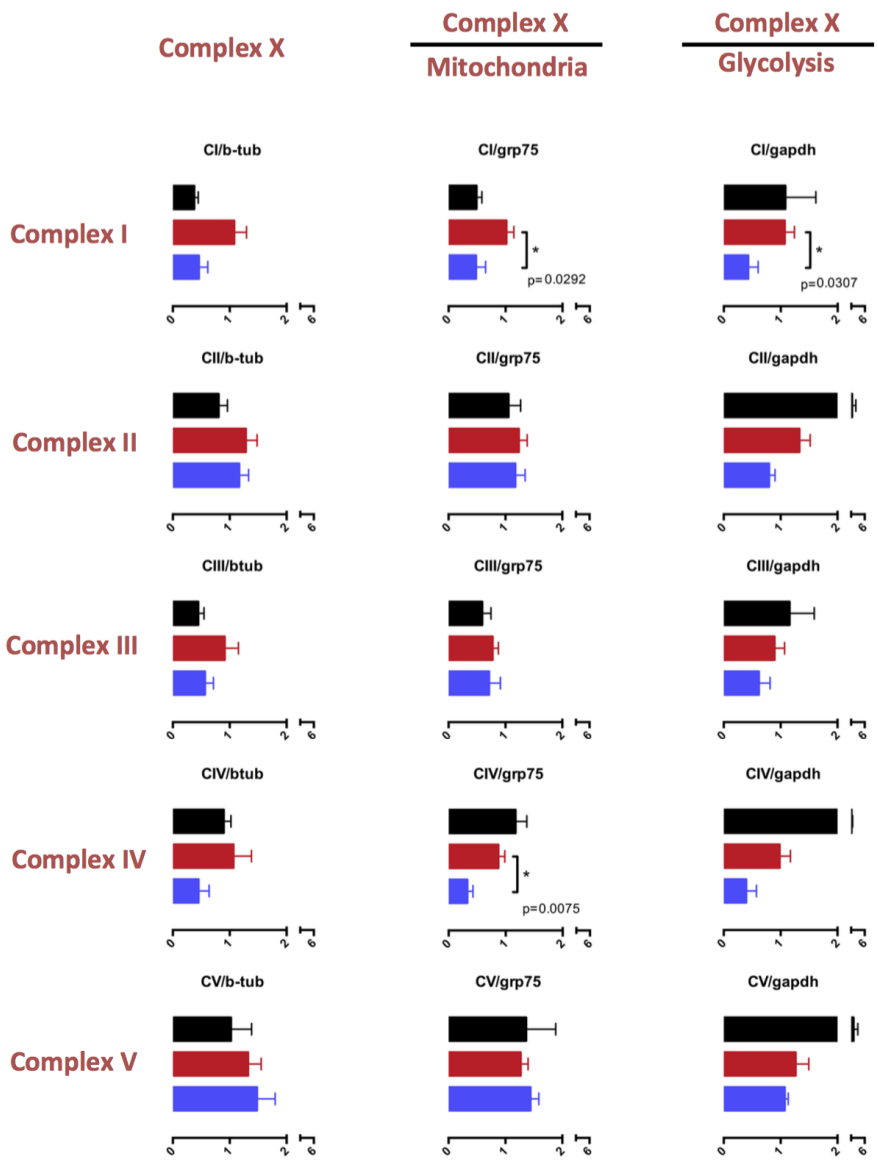

Figure 4.10: Summary of the western blots analysing protein levels of different ETC complexes. Red represents the average of the upper fork cell lines, blue the average of the lower fork cell lines, and black that of BT474, a control cell line. When normalised to β-tubulin there are no significant differences, however when normalised to GRP-75 a mitochondrial heat shock protein, there are significant differences in the protein levels for complex I and IV, and when normalised to GAPDH a protein involved in glycolysis only complex I is significant, figure produced by Gyorgy Szabadkai.

Oroboros. Three states were measured first a basal rate of oxygen consumption, then the leak state where ATP synthase is blocked and oxygen consumption comes from the small amount of electron flow driven by the protons that can leak across the inner membrane. After this the maximal state is measured by uncoupling the mitochondrial membrane. Uncoupling refers to the state when protons can easily enter the mitochondrial matrix,

equalising the membrane potential and allowing electron flow in the ETC to not be constrained by the proton gradient across the inner mitochondrial membrane.

Figure 4.11 shows the final results of the respirometry experiments showing that the upper fork breast cancer cell lines had significantly higher respiration than the lower fork cell lines. Thereby confirming the transcriptomic and proteomic differences affecting the mitochondrial ETC have an effect on its functional role.

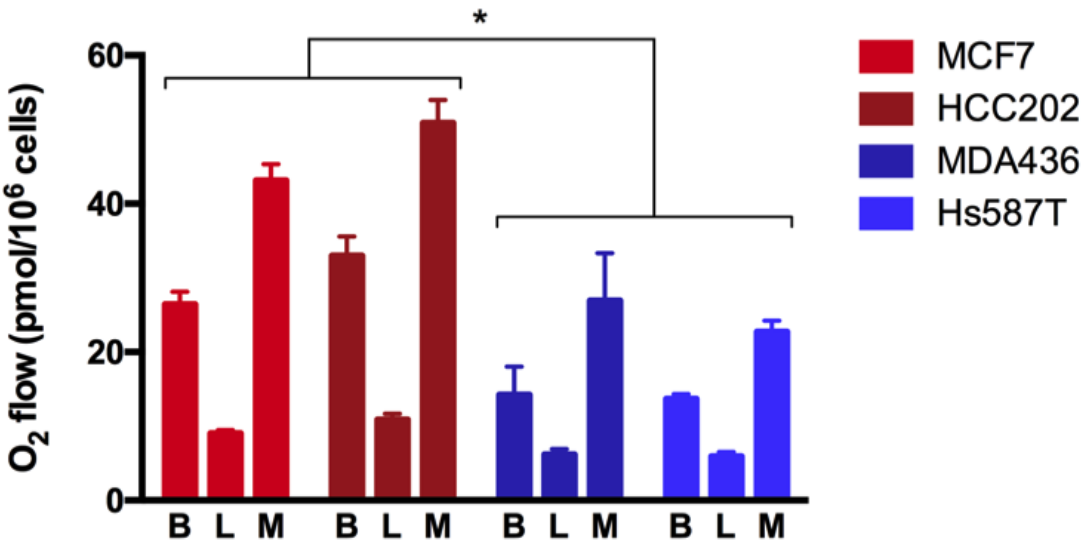

Figure 4.11: Differing oxygen consumption rates in the cancer cell lines, B = basal rate, L = leak rate and M = maximal rate. The difference between the upper and lower fork cell lines was found to be significant with a p-value < 0.05. Figure produced by Gyorgy Szabadkai.

4.4.2.4 Metabolism

The metabolic fluxes through central carbon metabolism of the cell state was studied. Cell lines HCC202, MCF7 and MDA453 representing the upper fork and cell lines MDA436 and Hs587t representing the lower fork were grown in a medium containing labelled carbon-13 glucose or carbon-13 glutamine and then the derived metabolites were measured using gas chromatography mass spectrometry. This was done to give more insight into the metabolomic differences between the upper and lower fork cell lines besides the known mitochondrial alterations, particularly in regards to how glucose and glutamine are utilised in the tricarboxylic acid (TCA) cycle. The main results from this analysis are given in Figures 4.12 and 4.13.

The right side of Figure 4.12 shows how labelled glucose enters the TCA cycle through Acetyl-CoA. This labels two carbon atoms in Acetyl-CoA and to all the follow-

ing intermediates, further rounds of the cycle can also produce $+3$ or $+4$ carbon labelled intermediates. The right side of Figure 4.13 similarly shows how labelled glutamine is metabolised through α-ketoglutarate.

To understand the efficiency of glucose and glutamine utilisation in the TCA cycle, the fraction of labelled metabolites can be examined. In particular the reduction of non-labelled ($+0$) metabolites can be examined, representing the average total incorporation of labelled carbons from a particular substrate. Figures 4.12 and 4.13 show the reduction of non-labelled metabolites and the fractional incorporation of labelled carbon in a specific manner (from $+1$ to $+n$, n =the total number of carbons in a specific metabolite), as an average for the lower and upper fork cell lines. For glucose, shown in Figure 4.12, there is a greater reduction of non-labelled (+0) metabolites in the upper fork compared to lower fork cell lines. For glutamine, shown in Figure 4.13, the opposite is seen as there is a greater reduction of non-labelled (+0) in the lower fork compared to upper fork cell lines. In both cases these reductions were found to be significant with p-values < 0.05.

Therefore from these results we can conclude that the upper fork cell lines are more dependent on glucose for their metabolism, while the lower fork cell lines are more dependent on glutamine. This indicates that lower fork samples are producing more energy via glutaminolysis, a process that has been associated to many types of cancer (Medina 2001, Yuneva 2008).

4.5 Conclusion

In this chapter the MCbiclust biclustering method was applied to breast cancer tumour samples. In accordance to the results of previous chapters this led to finding biclusters whose samples had significant different regulation of the mitochondria between them. Out of the biclusters found, the one with the most significant mitochondrial changes was chosen for further investigation.

Within this bicluster, ICT.CV1, two groups of samples were found, one called the upper fork that had significantly up-regulated mitochondrial genes compared with the other group, called the lower fork. These groups seem to be comprised of subsets of the luminal A and B subtypes of breast cancer as found by the PAM50 method. In this case, the upper fork samples were a subset of luminal B and the lower fork samples were a

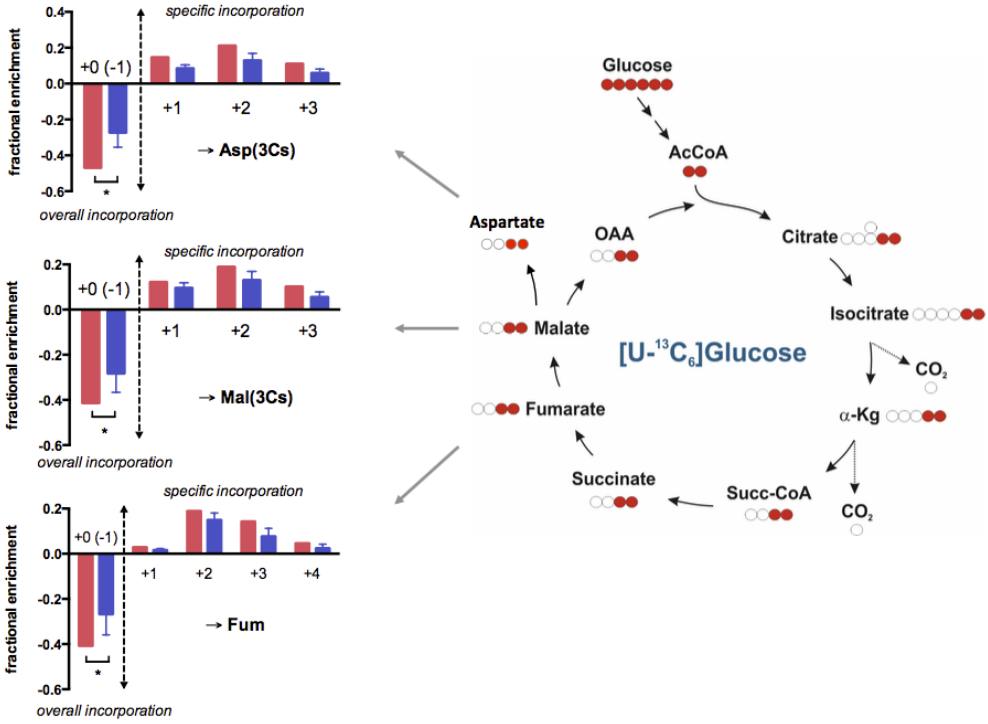

Figure 4.12: Results of mass spectrometry of cancer cell lines from glucose labelling, showing on the right how labelled glucose enters the TCA cycle, and on the left the utilisation of metabolites aspartate, malate, and fumerate. All show greater utilisation of the carbon labelled glucose in the upper fork cell lines (in red) versus the lower fork cell lines (in blue), this can be seen in the differences of the fractional enrichment for metabolites with +1 or more labelled carbons. The fractional enrichment of the non-labelled +0 metabolites has had 1 subtracted from it before plotting so that the fork with the greater reduction (the upper fork cell lines) has the greatest negative score. Significant differences are labelled with an asterix and denote p-value < 0.05. Figure produced by Gyorgy Szabadkai.

subset of luminal A.

While there were clear and large overlap between luminal A and lower fork samples as well as luminal B and upper fork samples, this relationship was not exact. There were for example a small number of luminal B samples in the lower fork and luminal A samples in the upper fork as well as luminal A/B samples that were not in either the upper and lower fork. This shows that this method is not simply replicating the PAM50 classifications, and is possibly giving a better classification of cancer tumours.

Using additional genetic data from the breast cancer dataset as available from CGAN (2012), the mutational differences between the upper and lower fork were found to be significantly greater than that between luminal A and B samples for both copy

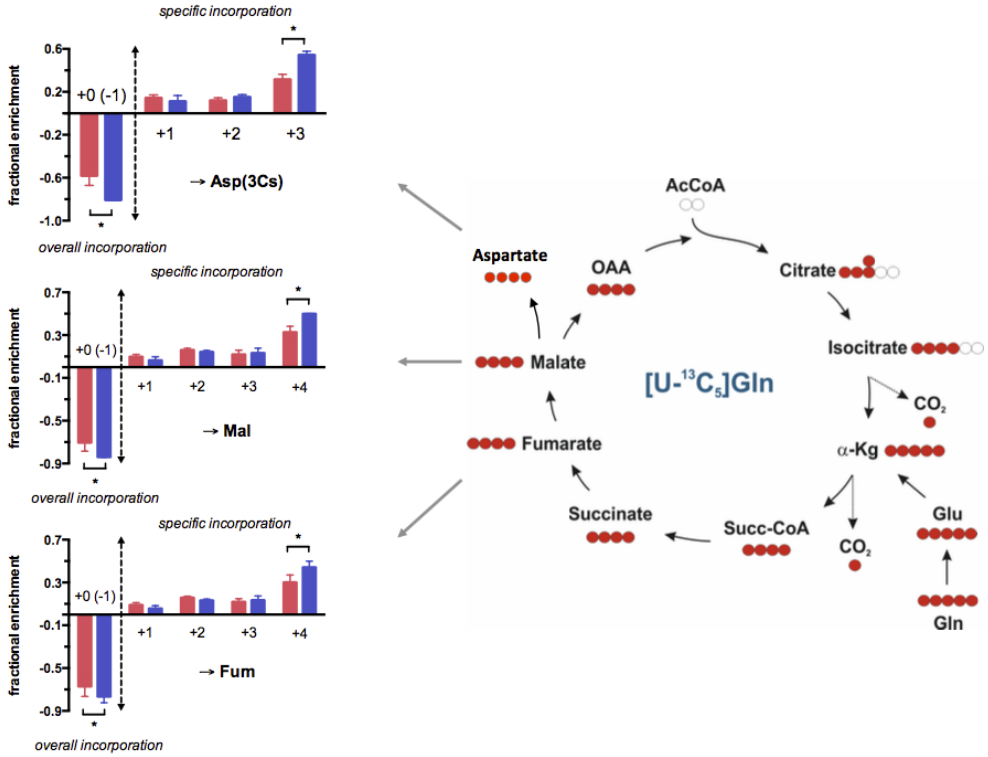

Figure 4.13: Results of mass spectrometry of cancer cell lines from glutamine labelling, showing on the right how labelled glutamine enters the TCA cycle, and on the left the utilisation of metabolites aspartate, malate, and fumerate. All show greater utilisation of the carbon labelled glutamine in the lower fork cell lines (in blue) versus the upper fork cell lines (in red), this can be seen in the differences of the fractional enrichment for metabolites with +1 or more labelled carbons. The fractional enrichment of the non-labelled +0 metabolites has had 1 subtracted from it before plotting so that the fork with the greater reduction (the lower fork cell lines) has the greatest negative score. Significant differences are labelled with an asterix and denote p-value < 0.05. Figure produced by Gyorgy Szabadkai.

number alterations and somatic mutations, as discussed in Section 4.2.4.

After this analysis was completed it was decided to attempt to experimentally test samples representative of this bicluster. Since breast cancer tumour samples were not available, cancer cell line representatives of this bicluster were identified with a novel algorithm.

These cell lines were then obtained for experimental study. The first step was to confirm the transcriptomic changes between the upper and lower fork samples with nanostring, then it was shown that these transcriptomic changes corresponded with proteomic changes in the mitochondria, particularly in terms of the proteins of the ETC, Complex I and IV. Then this proteomic change was associated with a functional change

between the cell lines by examining the rate of oxygen consumpton, finding that upper fork cell lines consume oxygen at a higher rate. Finally the metabolomics of the upper fork and lower fork cell lines were examined, revealing that the upper fork cells were more dependent on glucose in the TCA cycle while the lower fork cell lines were more dependent on glutamine.

There are many directions in which this work can continue. For example a more in depth look could be taken of the functional properties of the cell lines, such as by examining their cell growth rates, mitochondrial membrane potential and metabolic state. This is work that is currently being undertaken by other members of the Szabadkai lab.

One important experiment to undertake would be to find whether the upper or lower fork samples are more susceptible to chemotherapy with mitochondrial targeting drugs. Another direction would be to use the nanostring chip scoring system in Section 4.4.2.1 to develop a method for classifying samples that match the bicluster. Finally it could be tested whether incorporating knowledge of this bicluster improves breast cancer prognosis scores.

What is perhaps more important than the specific results coming from study of this bicluster, is the creation of a workflow pipeline, of identifying a bicluster of interest using the MCbiclust methods, selecting cell lines that are representative of the bicluster and finally experimental studies on these cell lines to gain greater understanding of the regulation behind the bicluster. This generalised workflow can be applied to any bicluster found in any type of cancer with a large enough number of suitable cancer cell lines and is not limited to studying mitochondrial biogenesis.

The bioinformatic methods developed in this work have succeeded as aimed in identifying mitochondrial based biclusters in the gene expression data within disease biology. A further aim however was to use these methods to learn about the regulation of mitochondrial biogenesis. Two breast cancer types with differences in mitochondrial regulation have been shown to exist what is causing them is more difficult to find, and must be the subject of future work. One thing that these results have shown is that mitochondria are not regulated completely independently, and mitochondrial biogenesis frequently as part of a much wider biological program such as cellular proliferation, reaction to the immune response or response to the cold.

Chapter 5

Conclusions

The aim of this thesis was to develop methods to investigate the role of mitochondrial biogenesis in disease.

As discussed in detail in the Introduction in Chapter 1, mitochondrial biogenesis is a very complex process involving the coordination of the nuclear genome with hundreds of copies of the mitochondrial genome scattered across the cell in the creation of over 1000 proteins. Mitochondrial biogenesis exist as both a continuous underlying process occuring in order to replenish mitochondria during standard mitochondrial turnover, and as a dynamic process that can increase mitochondrial number in response to environmental conditions. The mitochondrial proteome varies greatly between different tissues, and this too is indicative of the varying nature of the regulation of mitochondrial biogenesis.

Clearly due to its varying nature and our lack of a comprehensive understanding of the system regulating mitochondrial biogenesis new tools are needed. There is however greater urgency behind this due to the wide role mitochondria play in disease, and the involvement of deregulation of mitochondrial biogenesis within these conditions. Mitochondrial defects have long been known to occur in cancer, neuro-degeneration, heart disease, diabetes and even ageing. The creation of novel tools to investigate mitochondrial biogenesis thus will not only greatly increase our understanding of mitochondria, but potentially reveal new targets and methods to treat these diseases.

The approach taken in this thesis to investigate mitochondrial biogenesis is with bioinformatics, specifically by investigating a transcriptomic signature of mitochondrial biogenesis. Using large gene expression datasets, focusing on those genes known to be involved in the mitochondria a method to achieve this was created in Chapter 2.

The resulting method Massively Correlating Biclustering (MCbiclust), takes a gene set of interest, in this case a mitochondrial related gene set. With this gene set, samples in the dataset are found in which the average strength of the correlation of the genes in the gene set are maximised. Further steps of the method involve ranking the samples by how well they preserve this correlation and scoring every gene by the strength of its correlation with the average expression of a group of genes that strongly correlate with each other over the selected samples.

The end result of this method results in a ranking of samples and genes, from which a precise bicluster can be thresholded, and the bicluster can be further analysed, for instance using principal component analysis to divide the samples of the bicluster into different forks and gene set enrichment analysis to find the significant GO terms associated with the bicluster found.

This method is described in detail in Chapter 2 and what is more it is shown to outperform alternative biclustering methods in finding these large scale biclusters that resemble signs of mitochondrial biogenesis. This method is also found to be more universal than a tool for investigating mitochondrial biogenesis when it is applied to a bacterial *E. coli* dataset and found a bicluster representing the stalling of DNA replication following treatment with an antibiotic norfloxacin.

This suitability of the method on bacterial data was another indication that it was ideal for investigating a similar sized system, that of mitochondrial biogenesis in disease. This investigation was first approached in Chapter 3 in which MCbiclust was applied on a hypertrophic cardiomyopathy dataset and a cancer cell line dataset.

Hypertrophic cardiomyopathy (HCM) represents a thickening of the heart muscles, is often undiagnosed and is one of the leading causes of sudden death in the young.

The MCbiclust method was applied to a RNA-Seq dataset of 146 samples, and found a striking bicluster related to mitochondrial function that divided healthy control samples into one fork and HCM samples into the other fork. This was a strong indicator of a significant mitochondrial difference that is present in some control samples but never in a disease samples. This bicluster was related to a down-regulation of mitochondrial genes corresponding to an up-regulation of cell proliferation genes in the healthy control samples, the absence of this regulation in the HCM samples suggests a possible mechanism by which HCM can occur.

Other mitochondrial biclusters were found in the HCM data involving only the disease samples, these while involving different regulation of mitochondria did not also involve these cell proliferation related genes, and absence of additional mutational or any other clinical data meant that no further investigation of the meaning of these biclusters could be undertaken.

The MCbiclust method was then applied to microarray data from the Cancer Cell Line Encyclopedia (CCLE). Two different unique biclusters were found, only one which was strongly related to mitochondrial function. This bicluster mainly seemed to be tissue driven, representing differences between haematopoietic and lymphoid derived cell lines and carcinoma derived cell lines. As with the HCM bicluster, along with mitochondrial terms being significant, so were general cellular proliferation terms.

With the additional data in the CCLE dataset it was possible to study whether there was any significant mutational or pharmacological differences between the samples representative of each fork. In both cases significant regions of the copy number alterations were found and pharmacological compounds which have significantly different effects.

The main issue with this analysis is that the differences appeared to be primarily tissue driven. Differences between cancer cell lines derived from different tissue are known to be very large and as such finding differences between them is not so surprising. While this demonstrated the ability of MCbiclust to find mitochondrial based biclusters in cancer data, it was decided that further investigation in the alterations of mitochondrial biogenesis in cancer should be studied in only one cancer type at a time.

Chapter 4 was therefore aimed to study mitochondrial alterations in breast cancer. This work identified a bicluster significantly related to mitochondrial function seemingly related to the luminal A and luminal B subtypes found with PAM50. The samples in this bicluster however had greater mutational differences than those between luminal A and luminal B.

To understand the precise mitochondrial differences, cancer cell lines that were representative of the bicluster were selected. These cell lines had their mitochondrial differences experimentally verified using nanostring technology to measure mRNA levels. In collaboration with other groups more functional differences were shown by examining the proteomics, metabolomics and oxygen consumption levels.

The limitations of this work should be briefly discussed. There are two fundamental

issues with the MCbiclust algorithm. The first is that is when examining a data set it is not known how many significant biclusters exist within it. Due to the combinatorially large number of possibilities, no method could check them all, as such there will always be a level of uncertainty about how many biclusters exist within a dataset, though this can in some ways be taken into consideration by running the algorithm many times with different random seeds and on different gene sets. There is certainly a bias in the algorithm to find the largest possible bicluster while not finding smaller biclusters.

The second issue for MCbiclust is of one of performance, MCbiclust was not written for speed and calculating large correlation matrices, a task that is needed to be done thousands of times is very computationally expensive. As the R package currently exists, it is functional especially when used in conjunction with high throughput computing resources but there is certainly scope for improving its performance.

The other main limitation is the ability to understand the results of MCbiclust itself. There is a very simple and obvious disconnect to the patterns that are identified in these biclusters and the mechanisms that are causing them. In many data sets there is a reliance on additional clinical data, and if this is lacking interpreting the biclusters becomes very difficult, as was the case in Chapter 3 when examining HCM. With patient samples in the absence of large amounts of clinical data, experimental models are ideally needed. Finding an experimental model that matches a known bicluster however is a long process in itself, as was seen in Chapter 4.

This work has ended with a novel bioinformatic method to investigate mitochondrial biogenesis fully established. Chapter 4 presents a work pipeline for finding a bicluster of interest to selecting a relevant model and running experiments that could be repeated in many different systems. Importantly the work had shown the potential to improve treatment for disease. In the case of breast cancer there is a possibility of creating a nanostring based assay to classify samples into this group and by doing so possibly improving the determination of prognosis and deciding therapies. In the case of hypertrophic cardiomyopathy the bicluster has suggested a possible means of dysregulation that leads to the disease.

It is important to mention that the method MCbiclust developed has more general applications than to mitochondrial biogenesis in disease, and seems particularly suitable to bacterial datasets as was shown in the *E. coli* work in Chapter 2. However in the

investigation of mitochondrial biogenesis it is especially relevant.

It is feasible using this method and a dataset containing enough samples under enough conditions to build an encyclopedia of the many modes of mitochondrial biogenesis and the co-regulation that exists with other non-mitochondrial pathways. Upon doing so the different modes of mitochondrial biogenesis once found can be related to the state of the transcription factor network underlying it, gaining us understanding of the workings of that network. If this is achieved pathological modes of mitochondrial biogenesis will be easily identified and understood and hopefully along with that insight, treated.

Bibliography

Abdi, Hervé & Williams, L. J. (2010), 'Principal component analysis', *Wiley Interdisciplinary Reviews: Computational Statistics* **2**(4), 433–459.

Aguilar-Ruiz, J. S. (2005), 'Shifting and scaling patterns from gene expression data', *Bioinformatics* **21**(20), 3840–3845.

Ahlqvist, K. J., Hämäläinen, R. H., Yatsuga, S., Uutela, M., Terzioglu, M., Götz, A., Forsström, S., Salven, P., Angers-Loustau, A., Kopra, O. H. et al. (2012), 'Somatic progenitor cell vulnerability to mitochondrial DNA mutagenesis underlies progeroid phenotypes in polg mutator mice', *Cell metabolism* **15**(1), 100–109.

Alaynick, W. A., Kondo, R. P., Xie, W., He, W., Dufour, C. R., Downes, M., Jonker, J. W., Giles, W., Naviaux, R. K., Giguere, V. et al. (2007), 'ERRγ directs and maintains the transition to oxidative metabolism in the postnatal heart', *Cell metabolism* **6**(1), 13–24.

Allen, J. F. (1993), 'Control of gene expression by redox potential and the requirement for chloroplast and mitochondrial genomes', *Journal of Theoretical Biology* **165**(4), 609–631.

Alon, U., Barkai, N., Notterman, D. A., Gish, K., Ybarra, S., Mack, D. & Levine, A. J. (1999), 'Broad patterns of gene expression revealed by clustering analysis of tumor and normal colon tissues probed by oligonucleotide arrays', *Proceedings of the National Academy of Sciences* **96**(12), 6745–6750.

Ambrus, A. M., Islam, A. B., Holmes, K. B., Moon, N. S., Lopez-Bigas, N., Benevolenskaya, E. V. & Frolov, M. V. (2013), 'Loss of dE2F compromises mitochondrial function', *Developmental cell* **27**(4), 438–451.

American Type Culture Collection Standards Development Organization Workgroup (2010), 'Cell line misidentification: the beginning of the end', *Nature Reviews Cancer* **10**(6).

Anders, Simon & Huber, W. (2010), 'Differential expression analysis for sequence count data', *Genome biol* **11**(10), R106.

Andersson, S. G., Zomorodipour, A., Andersson, J. O., Sicheritz-Pontén, T., Alsmark, U. C. M., Podowski, R. M., Näslund, A. K., Eriksson, A.-S., Winkler, H. H. & Kurland, C. G. (1998), 'The genome sequence of Rickettsia prowazekii and the origin of mitochondria', *Nature* **396**(6707), 133–140.

Andersson, Ulf & Scarpulla, R. C. (2001), 'PGC-1-related coactivator, a novel, serum-inducible coactivator of nuclear respiratory factor 1-dependent transcription in mammalian cells', *Molecular and cellular biology* **21**(11), 3738–3749.

Andres, A. M., Stotland, A., Queliconi, B. B. & Gottlieb, R. A. (2015), 'A time to reap, a time to sow: mitophagy and biogenesis in cardiac pathophysiology', *Journal of molecular and cellular cardiology* **78**, 62–72.

Arany, Z., Lebrasseur, N., Morris, C., Smith, E., Yang, W., Ma, Y., Chin, S. & Spiegelman, B. M. (2007), 'The transcriptional coactivator PGC-1β drives the formation of oxidative type iix fibers in skeletal muscle', *Cell metabolism* **5**(1), 35–46.

Arsenijevic, D., Onuma, H., Pecqueur, C., Raimbault, S., Manning, B. S., Miroux, B., Couplan, E., Alves-Guerra, M.-C., Goubern, M., Surwit, R. et al. (2000), 'Disruption of the uncoupling protein-2 gene in mice reveals a role in immunity and reactive oxygen species production', *Nature genetics* **26**(4), 435–439.

Aschrafi, A., Schwechter, A. D., Mameza, M. G., Natera-Naranjo, O., Gioio, A. E. & Kaplan, B. B. (2008), 'MicroRNA-338 regulates local cytochrome c oxidase IV mRNA levels and oxidative phosphorylation in the axons of sympathetic neurons', *The Journal of Neuroscience* **28**(47), 12581–12590.

Ashburner, M., Ball, C. A., Blake, J. A., Botstein, D., Butler, H., Cherry, J. M., Davis, A. P., Dolinski, K., Dwight, S. S., Eppig, J. T. et al. (2000), 'Gene ontology: tool for the unification of biology', *Nature genetics* **25**(1), 25–29.

Baar, K., Song, Z., Semenkovich, C. F., Jones, T. E., Han, D.-H., Nolte, L. A., Ojuka, E. O., Chen, M. & Holloszy, J. O. (2003), 'Skeletal muscle overexpression of nuclear respiratory factor 1 increases glucose transport capacity', *The FASEB Journal* **17**(12), 1666–1673.

Baar, K., Wende, A. R., Jones, T. E., Marison, M., Nolte, L. A., Chen, M., Kelly, D. P. & Holloszy, J. O. (2002), 'Adaptations of skeletal muscle to exercise: rapid increase in the transcriptional coactivator PGC-1', *The FASEB Journal* **16**(14), 1879–1886.

Baltzer, C., Tiefenböck, S. K. & Frei, C. (2010), 'Mitochondria in response to nutrients and nutrient-sensitive pathways', *Mitochondrion* **10**(6), 589–597.

Bardella, C., Pollard, P. J. & Tomlinson, I. (2011), 'SDH mutations in cancer', *Biochimica et Biophysica Acta (BBA)-Bioenergetics* **1807**(11), 1432–1443.

Barrès, R., Osler, M. E., Yan, J., Rune, A., Fritz, T., Caidahl, K., Krook, A. & Zierath, J. R. (2009), 'Non-cpg methylation of the pgc-1α promoter through dnmt3b controls mitochondrial density', *Cell metabolism* **10**(3), 189–198.

Barretina, J., Caponigro, G., Stransky, N., Venkatesan, K., Margolin, A. A., Kim, S., Wilson, C. J., Lehár, J., Kryukov, G. V., Sonkin, D. et al. (2012), 'The cancer cell line encyclopedia enables predictive modelling of anticancer drug sensitivity', *Nature* **483**(7391), 603–607.

Barrey, E., Saint-Auret, G., Bonnamy, B., Damas, D., Boyer, O. & Gidrol, X. (2011), 'Pre-microRNA and mature microRNA in human mitochondria', *PloS one* **6**(5), e20220.

Bastin, J., Aubey, F., Rotig, A., Munnich, A. & Djouadi, F. (2008), 'Activation of peroxisome proliferator-activated receptor pathway stimulates the mitochondrial respiratory chain and can correct deficiencies in patients cells lacking its components', *The Journal of Clinical Endocrinology & Metabolism* **93**(4), 1433–1441.

Benevolenskaya, Elizaveta V & Frolov, M. V. (2015), 'Emerging links between E2F control and mitochondrial function', *Cancer research* **75**(4), 619–623.

Bergmann, S., Ihmels, J. & Barkai, N. (2003), 'Iterative signature algorithm for the analysis of large-scale gene expression data', *Physical review E* **67**(3), 031902.

Blanchet, E., Annicotte, J.-S., Lagarrigue, S., Aguilar, V., Clapé, C., Chavey, C., Fritz, V., Casas, F., Apparailly, F., Auwerx, J. et al. (2011), 'E2F transcription factor-1 regulates oxidative metabolism', *Nature cell biology* **13**(9), 1146–1152.

Bogacka, I., Xie, H., Bray, G. A. & Smith, S. R. (2005), 'Pioglitazone induces mitochondrial biogenesis in human subcutaneous adipose tissue in vivo', *Diabetes* **54**(5), 1392–1399.

Bolstad, B., Collin, F., Simpson, K., Irizarry, R. & Speed, T. (2004), 'Experimental design and low-level analysis of microarray data', *International review of neurobiology* **60**, 25–58.

Bookout, A. L., Jeong, Y., Downes, M., Ruth, T. Y., Evans, R. M. & Mangelsdorf, D. J. (2006), 'Anatomical profiling of nuclear receptor expression reveals a hierarchical transcriptional network', *Cell* **126**(4), 789–799.

Bozdağ, D., Parvin, J. D. & Catalyurek, U. V. (2009), A biclustering method to discover co-regulated genes using diverse gene expression datasets, *in* 'Bioinformatics and Computational Biology', Springer, pp. 151–163.

Brand, Martin D & Nicholls, D. G. (2011), 'Assessing mitochondrial dysfunction in cells', *Biochemical Journal* **435**(2), 297–312.

Bratic, A., Larsson, N.-G. et al. (2013), 'The role of mitochondria in aging', *The Journal of clinical investigation* **123**(123 (3)), 951–957.

Calvo, S. E., Clauser, K. R. & Mootha, V. K. (2015), 'MitoCarta2.0: an updated inventory of mammalian mitochondrial proteins', *Nucleic acids research* p. gkv1003.

Calvo, S., Jain, M., Xie, X., Sheth, S. A., Chang, B., Goldberger, O. A., Spinazzola, A., Zeviani, M., Carr, S. A. & Mootha, V. K. (2006), 'Systematic identification of human mitochondrial disease genes through integrative genomics', *Nature genetics* **38**(5), 576–582.

Cam, H., Balciunaite, E., Blais, A., Spektor, A., Scarpulla, R. C., Young, R., Kluger, Y. & Dynlacht, B. D. (2004), 'A common set of gene regulatory networks links metabolism and growth inhibition', *Molecular cell* **16**(3), 399–411.

Catic, A., Suh, C. Y., Hill, C. T., Daheron, L., Henkel, T., Orford, K. W., Dombkowski, D. M., Liu, T., Liu, X. S. & Scadden, D. T. (2013), 'Genome-wide map of nuclear protein degradation shows NCoR1 turnover as a key to mitochondrial gene regulation', *Cell* **155**(6), 1380–1395.

CGAN (2012), 'Comprehensive molecular portraits of human breast tumours', *Nature* **490**(7418), 61–70.

Chan, J. Y., Kwong, M., Lu, R., Chang, J., Wang, B., Yen, T. B. & Kan, Y. W. (1998), 'Targeted disruption of the ubiquitous CNC-bZIP transcription factor, nrf-1, results in anemia and embryonic lethality in mice', *The EMBO Journal* **17**(6), 1779–1787.

Chan, S. Y., Zhang, Y.-Y., Hemann, C., Mahoney, C. E., Zweier, J. L. & Loscalzo, J. (2009), 'MicroRNA-210 controls mitochondrial metabolism during hypoxia by repressing the iron-sulfur cluster assembly proteins ISCU1/2', *Cell metabolism* **10**(4), 273–284.

Chang, T.-C., Yu, D., Lee, Y.-S., Wentzel, E. A., Arking, D. E., West, K. M., Dang, C. V., Thomas-Tikhonenko, A. & Mendell, J. T. (2008), 'Widespread microRNA repression by Myc contributes to tumorigenesis', *Nature genetics* **40**(1), 43–50.

Cheng, Yizong & Church, G. M. (2000), Biclustering of expression data., *in* 'Ismb', Vol. 8, pp. 93–103.

Chipuk, J., Bouchier-Hayes, L. & Green, D. (2006), 'Mitochondrial outer membrane permeabilization during apoptosis: the innocent bystander scenario', *Cell Death & Differentiation* **13**(8), 1396–1402.

Ciriello, G., Sinha, R., Hoadley, K. A., Jacobsen, A. S., Reva, B., Perou, C. M., Sander, C. & Schultz, N. (2013), 'The molecular diversity of Luminal A breast tumors', *Breast cancer research and treatment* **141**(3), 409–420.

Civitarese, A. E., Carling, S., Heilbronn, L. K., Hulver, M. H., Ukropcova, B., Deutsch, W. A., Smith, S. R. & Ravussin, E. (2007), 'Calorie restriction increases muscle mitochondrial biogenesis in healthy humans', *PLoS med* **4**(3), e76.

Crick, F. . o. (1970), 'Central dogma of molecular biology', *Nature* **227**(5258), 561–563.

Csárdi, G., Kutalik, Z. & Bergmann, S. (2010), 'Modular analysis of gene expression data with R', *Bioinformatics* **26**(10), 1376–1377.

Cunningham, J. T., Rodgers, J. T., Arlow, D. H., Vazquez, F., Mootha, V. K. & Puigserver, P. (2007), 'mTOR controls mitochondrial oxidative function through a YY1–PGC-1&agr; transcriptional complex', *nature* **450**(7170), 736–740.

Dang, C. V. (2012), 'MYC on the path to cancer', *Cell* **149**(1), 22–35.

Dennis Jr, G., Sherman, B. T., Hosack, D. A., Yang, J., Gao, W., Lane, H. C., Lempicki, R. A. et al. (2003), 'DAVID: database for annotation, visualization, and integrated discovery', *Genome biol* **4**(5), P3.

Dillies, M.-A., Rau, A., Aubert, J., Hennequet-Antier, C., Jeanmougin, M., Servant, N., Keime, C., Marot, G., Castel, D., Estelle, J. et al. (2013), 'A comprehensive evaluation of normalization methods for illumina high-throughput RNA sequencing data analysis', *Briefings in bioinformatics* **14**(6), 671–683.

Divakaruni, A. S., Rogers, G. W. & Murphy, A. N. (2014), 'Measuring mitochondrial function in permeabilized cells using the seahorse XF analyzer or a clark-type oxygen electrode', *Current Protocols in Toxicology* pp. 25–2.

Dominy, J. E., Lee, Y., Gerhart-Hines, Z. & Puigserver, P. (2010), 'Nutrient-dependent regulation of PGC-1α's acetylation state and metabolic function through the enzymatic activities of Sirt1/GCN5', *Biochimica et Biophysica Acta (BBA)-Proteins and Proteomics* **1804**(8), 1676–1683.

Dowsett, M., Sestak, I., Lopez-Knowles, E., Sidhu, K., Dunbier, A. K., Cowens, J. W., Ferree, S., Storhoff, J., Schaper, C. & Cuzick, J. (2013), 'Comparison of PAM50 risk of recurrence score with oncotype dx and ihc4 for predicting risk of distant recurrence after endocrine therapy', *Journal of Clinical Oncology* pp. JCO–2012.

Duchen, Michael R & Szabadkai, G. (2010), 'Roles of mitochondria in human disease', *Essays Biochem* **47**, 115–137.

Dufour, C. R., Wilson, B. J., Huss, J. M., Kelly, D. P., Alaynick, W. A., Downes, M., Evans, R. M., Blanchette, M. & Giguere, V. (2007), 'Genome-wide orchestration of cardiac functions by the orphan nuclear receptors ERRα and γ', *Cell metabolism* **5**(5), 345–356.

Early Breast Cancer Trialists Collaborative Group (2005), 'Effects of chemotherapy and hormonal therapy for early breast cancer on recurrence and 15-year survival: an overview of the randomised trials', *The Lancet* **365**(9472), 1687–1717.

Eisen, M. B., Spellman, P. T., Brown, P. O. & Botstein, D. (1998), 'Cluster analysis and display of genome-wide expression patterns', *Proceedings of the National Academy of Sciences* **95**(25), 14863–14868.

Emanuelsson, O., Brunak, S., von Heijne, G. & Nielsen, H. (2007), 'Locating proteins in the cell using TargetP, SignalP and related tools', *Nature protocols* **2**(4), 953–971.

Epstein, C. B., Waddle, J. A., Hale, W., Davé, V., Thornton, J., Macatee, T. L., Garner, H. R. & Butow, R. A. (2001), 'Genome-wide responses to mitochondrial dysfunction', *Molecular biology of the cell* **12**(2), 297–308.

Evans, R. M., Barish, G. D. & Wang, Y.-X. (2004), 'PPARs and the complex journey to obesity', *Nature medicine* **10**(4), 355–361.

Exner, N., Lutz, A. K., Haass, C. & Winklhofer, K. F. (2012), 'Mitochondrial dysfunction in Parkinson's disease: molecular mechanisms and pathophysiological consequences', *The EMBO journal* **31**(14), 3038–3062.

Faith, J. J., Driscoll, M. E., Fusaro, V. A., Cosgrove, E. J., Hayete, B., Juhn, F. S., Schneider, S. J. & Gardner, T. S. (2008), 'Many microbe microarrays database: uniformly normalized affymetrix compendia with structured experimental metadata', *Nucleic acids research* **36**(suppl 1), D866–D870.

Fassone, Elisa & Rahman, S. (2012), 'Complex I deficiency: clinical features, biochemistry and molecular genetics', *Journal of medical genetics* **49**(9), 578–590.

Feinberg, A. P. (2008), 'Epigenetics at the epicenter of modern medicine', *Jama* **299**(11), 1345–1350.

Feinberg, Andrew P & Tycko, B. (2004), 'The history of cancer epigenetics', *Nature Reviews Cancer* **4**(2), 143–153.

Fisher, R. A. (1922), 'On the interpretation of $\chi 2$ from contingency tables, and the calculation of p', *Journal of the Royal Statistical Society* pp. 87–94.

Fletcher, Martin J & Sanadi, D. (1961), 'Turnover of rat-liver mitochondria', *Biochimica et biophysica acta* **51**(2), 356–360.

Foulkes, W. D., Flanders, T. Y., Pollock, P. M. & Hayward, N. K. (1997), 'The CDKN2A (p16) gene and human cancer.', *Molecular Medicine* **3**(1), 5.

Fulda, S., Galluzzi, L. & Kroemer, G. (2010), 'Targeting mitochondria for cancer therapy', *Nature reviews Drug discovery* **9**(6), 447–464.

Gakh, O., Cavadini, P. & Isaya, G. (2002), 'Mitochondrial processing peptidases', *Biochimica et Biophysica Acta (BBA)-Molecular Cell Research* **1592**(1), 63–77.

Gallo, C. A., Carballido, J. A. & Ponzoni, I. (2009), Bihea: A hybrid evolutionary approach for microarray biclustering, *in* 'Advances in Bioinformatics and Computational Biology', Springer, pp. 36–47.

Gama-Castro, S., Salgado, H., Peralta-Gil, M., Santos-Zavaleta, A., Muñiz-Rascado, L., Solano-Lira, H., Jimenez-Jacinto, V., Weiss, V., García-Sotelo, J. S., López-Fuentes, A. et al. (2011), 'RegulonDB version 7.0: transcriptional regulation of escherichia coli k-12 integrated within genetic sensory response units (gensor units)', *Nucleic acids research* **39**(suppl 1), D98–D105.

Gao, P., Tchernyshyov, I., Chang, T.-C., Lee, Y.-S., Kita, K., Ochi, T., Zeller, K. I., De Marzo, A. M., Van Eyk, J. E., Mendell, J. T. et al. (2009), 'c-Myc suppression of miR-23a/b enhances mitochondrial glutaminase expression and glutamine metabolism', *Nature* **458**(7239), 762–765.

García-Prat, L., Martínez-Vicente, M., Perdiguero, E., Ortet, L., Rodríguez-Ubreva, J., Rebollo, E., Ruiz-Bonilla, V., Gutarra, S., Ballestar, E., Serrano, A. L. et al. (2016), 'Autophagy maintains stemness by preventing senescence', *Nature* **529**(7584), 37–42.

Garzon, R., Calin, G. A. & Croce, C. M. (2009), 'MicroRNAs in cancer', *Annual review of medicine* **60**, 167–179.

Gasch, Audrey P & Eisen, M. B. (2002), 'Exploring the conditional coregulation of yeast gene expression through fuzzy k-means clustering', *Genome Biol* **3**(11), 1–22.

Gerdes, F., Tatsuta, T. & Langer, T. (2012), 'Mitochondrial aaa proteasestowards a molecular understanding of membrane-bound proteolytic machines', *Biochimica Et Biophysica Acta (BBA)-Molecular Cell Research* **1823**(1), 49–55.

Gerhart-Hines, Z., Rodgers, J. T., Bare, O., Lerin, C., Kim, S.-H., Mostoslavsky, R., Alt, F. W., Wu, Z. & Puigserver, P. (2007), 'Metabolic control of muscle mitochondrial function and fatty acid oxidation through SIRT1/PGC-1α', *The EMBO journal* **26**(7), 1913–1923.

Giguère, V., Yang, N., Segui, P. & Evans, R. M. (1988), 'Identification of a new class of steroid hormone receptors'.

Giordano, S. H., Buzdar, A. U. & Hortobagyi, G. N. (2002), 'Breast cancer in men', *Annals of internal medicine* **137**(8), 678–687.

Gnaiger, E. (2007), 'Mitochondrial pathways and respiratory control', *Textbook on Mitochondrial Physiology, edited by E Gnaiger Innsbruck, Austria: OROBOROS MiPNet* pp. 1–95.

Gogvadze, V., Orrenius, S. & Zhivotovsky, B. (2008), 'Mitochondria in cancer cells: what is so special about them?', *Trends in cell biology* **18**(4), 165–173.

Griffiths-Jones, S., Grocock, R. J., Van Dongen, S., Bateman, A. & Enright, A. J. (2006), 'miRBase: microRNA sequences, targets and gene nomenclature', *Nucleic acids research* **34**(suppl 1), D140–D144.

Gugneja, Sajiv Scarpulla, R. C. (1997), 'Serine phosphorylation within a concise amino-terminal domain in nuclear respiratory factor 1 enhances DNA binding', *Journal of Biological Chemistry* **272**(30), 18732–18739.

Hanahan, Douglas & Weinberg, R. A. (2000), 'The hallmarks of cancer', *cell* **100**(1), 57–70.

Hanahan, Douglas & Weinberg, R. A. (2011), 'Hallmarks of cancer: the next generation', *cell* **144**(5), 646–674.

Hancock, C. R., Han, D.-H., Higashida, K., Kim, S. H. & Holloszy, J. O. (2011), 'Does calorie restriction induce mitochondrial biogenesis? a reevaluation', *The FASEB Journal* **25**(2), 785–791.

Handschin, C. (2009), 'The biology of PGC-1α and its therapeutic potential', *Trends in pharmacological sciences* **30**(6), 322–329.

Hara, E., Smith, R., Parry, D., Tahara, H., Stone, S. & Peters, G. (1996), 'Regulation of p16CDKN2 expression and its implications for cell immortalization and senescence.', *Molecular and Cellular Biology* **16**(3), 859–867.

Harman, D. (1955), 'Aging: a theory based on free radical and radiation chemistry'.

Hartigan, J. A. (1972), 'Direct clustering of a data matrix', *Journal of the american statistical association* **67**(337), 123–129.

Haybittle, J., Blamey, R., Elston, C., Johnson, J., Doyle, P., Campbell, F., Nicholson, R. & Griffiths, K. (1982), 'A prognostic index in primary breast cancer.', *British journal of cancer* **45**(3), 361.

Haynes, Brian C & Brent, M. R. (2009), 'Benchmarking regulatory network reconstruction with GRENDEL', *Bioinformatics* **25**(6), 801–807.

Hebl, V. B., Bos, J., Oberg, A. L., Sun, Z., Maleszewski, J. J., Ogut, O., Bishu, K., dos Remedios, C. G., Ommen, S., Schaff, H. V. et al. (2012), 'Transcriptome profiling of surgical myectomy tissue from patients with hypertrophic cardiomyopathy reveals marked overexpression of ACE2', *Circulation* **126**(21 Supplement), A11099.

Hekimi, S., Lapointe, J. & Wen, Y. (2011), 'Taking a good look at free radicals in the aging process', *Trends in cell biology* **21**(10), 569–576.

Herschkowitz, J. I., Simin, K., Weigman, V. J., Mikaelian, I., Usary, J., Hu, Z., Rasmussen, K. E., Jones, L. P., Assefnia, S., Chandrasekharan, S. et al. (2007), 'Identification of conserved gene expression features between murine mammary carcinoma models and human breast tumors', *Genome biology* **8**(5), R76.

Herzig, S., Long, F., Jhala, U. S., Hedrick, S., Quinn, R., Bauer, A., Rudolph, D., Schutz, G., Yoon, C., Puigserver, P. et al. (2001), 'CREB regulates hepatic gluconeogenesis through the coactivator PGC-1', *Nature* **413**(6852), 179–183.

Hirschey, M. D., DeBerardinis, R. J., Diehl, A. M. E., Drew, J. E., Frezza, C., Green, M. F., Jones, L. W., Ko, Y. H., Le, A., Lea, M. A. et al. (2015), Dysregulated metabolism contributes to oncogenesis, *in* 'Seminars in cancer biology', Vol. 35, Elsevier, pp. S129–S150.

Hochreiter, S., Bodenhofer, U., Heusel, M., Mayr, A., Mitterecker, A., Kasim, A., Khamiakova, T., Van Sanden, S., Lin, D., Talloen, W. et al. (2010), 'FABIA: factor analysis for bicluster acquisition', *Bioinformatics* **26**(12), 1520–1527.

Hock, M Benjamin & Kralli, A. (2009), 'Transcriptional control of mitochondrial biogenesis and function', *Annual review of physiology* **71**, 177–203.

Hoitzing, H., Johnston, I. G. & Jones, N. S. (2015), 'What is the function of mitochondrial networks? a theoretical assessment of hypotheses and proposal for future research', *BioEssays* **37**(6), 687–700.

Holmgren, D., Wåhlander, H., Eriksson, B., Oldfors, A., Holme, E. & Tulinius, M. (2003), 'Cardiomyopathy in children with mitochondrial disease clinical course and cardiological findings', *European heart journal* **24**(3), 280–288.

Hondares, E., Mora, O., Yubero, P., de la Concepción, M. R., Iglesias, R., Giralt, M. & Villarroya, F. (2006), 'Thiazolidinediones and rexinoids induce peroxisome proliferator-activated receptor-coactivator (PGC)-1α gene transcription: an autoregulatory loop controls PGC-1α expression in adipocytes via peroxisome proliferator-activated receptor-γ coactivation', *Endocrinology* **147**(6), 2829–2838.

Horton, T. M., Petros, J. A., Heddi, A., Shoffner, J., Kaufman, A. E., Graham, S. D., Gramlich, T. & Wallace, D. C. (1996), 'Novel mitochondrial DNA deletion found in a renal cell carcinoma', *Genes, Chromosomes and Cancer* **15**(2), 95–101.

Huq, M. M., Gupta, P., Tsai, N.-P., White, R., Parker, M. G. & Wei, L.-N. (2006), 'Suppression of receptor interacting protein 140 repressive activity by protein arginine methylation', *The EMBO journal* **25**(21), 5094–5104.

Huss, J. M., Garbacz, W. G. & Xie, W. (2015), 'Constitutive activities of estrogen-related receptors: transcriptional regulation of metabolism by the ERR pathways in health and disease', *Biochimica et Biophysica Acta (BBA)-Molecular Basis of Disease* **1852**(9), 1912–1927.

Irizarry, R. A., Hobbs, B., Collin, F., Beazer-Barclay, Y. D., Antonellis, K. J., Scherf, U., Speed, T. P. et al. (2003), 'Exploration, normalization, and summaries of high density oligonucleotide array probe level data', *Biostatistics* **4**(2), 249–264.

Ishikawa, K., Takenaga, K., Akimoto, M., Koshikawa, N., Yamaguchi, A., Imanishi, H., Nakada, K., Honma, Y. & Hayashi, J.-I. (2008), 'ROS-generating mitochondrial DNA mutations can regulate tumor cell metastasis', *Science* **320**(5876), 661–664.

Issemann, Isabelle & Green, S. (1990), 'Activation of a member of the steroid hormone receptor superfamily by peroxisome proliferators.', *Nature* **347**(6294), 645–650.

Ivanova, N., Dobrin, R., Lu, R., Kotenko, I., Levorse, J., DeCoste, C., Schafer, X., Lun, Y. & Lemischka, I. R. (2006), 'Dissecting self-renewal in stem cells with RNA interference', *Nature* **442**(7102), 533–538.

Jäger, S., Handschin, C., Pierre, J. S. & Spiegelman, B. M. (2007), 'AMP-activated protein kinase (AMPK) action in skeletal muscle via direct phosphorylation of PGC-1α', *Proceedings of the National Academy of Sciences* **104**(29), 12017–12022.

Johnson, L. V., Walsh, M. L. & Chen, L. B. (1980), 'Localization of mitochondria in living cells with rhodamine 123', *Proceedings of the National Academy of Sciences* **77**(2), 990–994.

Jones, A. W., Yao, Z., Vicencio, J. M., Karkucinska-Wieckowska, A. & Szabadkai, G. (2012), 'PGC-1 family coactivators and cell fate: Roles in cancer, neurodegeneration, cardiovascular disease and retrograde mitochondria–nucleus signalling', *Mitochondrion* **12**(1), 86–99.

Jones, Peter A & Laird, P. W. (1999), 'Cancer-epigenetics comes of age', *Nature genetics* **21**(2), 163–167.

Jourdain, A. A., Koppen, M., Wydro, M., Rodley, C. D., Lightowlers, R. N., Chrzanowska-Lightowlers, Z. M. & Martinou, J.-C. (2013), 'GRSF1 regulates RNA processing in mitochondrial RNA granules', *Cell metabolism* **17**(3), 399–410.

Kaiser, Sebastian & Leisch, F. (2008), 'A toolbox for bicluster analysis in r'.

Kallen, J., Schlaeppi, J.-M., Bitsch, F., Filipuzzi, I., Schilb, A., Riou, V., Graham, A., Strauss, A., Geiser, M. & Fournier, B. (2004), 'Evidence for ligand-independent transcriptional activation of the human estrogen-related receptor α (ERRα) crystal structure of ERRα ligand binding domain in complex with peroxisome proliferator-activated receptor coactivator-1α', *Journal of Biological Chemistry* **279**(47), 49330–49337.

Kalyana-Sundaram, S., Kumar-Sinha, C., Shankar, S., Robinson, D. R., Wu, Y.-M., Cao, X., Asangani, I. A., Kothari, V., Prensner, J. R., Lonigro, R. J. et al. (2012), 'Expressed pseudogenes in the transcriptional landscape of human cancers', *Cell* **149**(7), 1622–1634.

Kanehisa, Minoru & Goto, S. (2000), 'KEGG: kyoto encyclopedia of genes and genomes', *Nucleic acids research* **28**(1), 27–30.

Karras, J. R., Paisie, C. A. & Huebner, K. (2014), 'Replicative stress and the FHIT gene: roles in tumor suppression, genome stability and prevention of carcinogenesis', *Cancers* **6**(2), 1208–1219.

Kersten, S., Seydoux, J., Peters, J. M., Gonzalez, F. J., Desvergne, B. & Wahli, W. (1999), 'Peroxisome proliferator–activated receptor α mediates the adaptive response to fasting', *Journal of Clinical Investigation* **103**(11), 1489.

Kim, I., Rodriguez-Enriquez, S. & Lemasters, J. J. (2007), 'Selective degradation of mitochondria by mitophagy', *Archives of biochemistry and biophysics* **462**(2), 245–253.

Kim, J., Lee, J. & Iyer, V. R. (2008), 'Global identification of Myc target genes reveals its direct role in mitochondrial biogenesis and its E-box usage in vivo', *PloS one* **3**(3), e1798.

Kim, T.-Y., Wang, D., Kim, A. K., Lau, E., Lin, A. J., Liem, D. A., Zhang, J., Zong, N. C., Lam, M. P. & Ping, P. (2012), 'Metabolic labeling reveals proteome dynamics of mouse mitochondria', *Molecular & Cellular Proteomics* **11**(12), 1586–1594.

Kissová, I., Deffieu, M., Manon, S. & Camougrand, N. (2004), 'Uth1p is involved in the autophagic degradation of mitochondria', *Journal of Biological Chemistry* **279**(37), 39068–39074.

Kroemer, Guido & Pouyssegur, J. (2008), 'Tumor cell metabolism: cancer's Achilles' heel', *Cancer cell* **13**(6), 472–482.

Kuhn, H. W. (1955), 'The hungarian method for the assignment problem', *Naval research logistics quarterly* **2**(1-2), 83–97.

Kundu, M., Lindsten, T., Yang, C.-Y., Wu, J., Zhao, F., Zhang, J., Selak, M. A., Ney, P. A. & Thompson, C. B. (2008), 'Ulk1 plays a critical role in the autophagic clearance of mitochondria and ribosomes during reticulocyte maturation', *Blood* **112**(4), 1493–1502.

Kuznetsov, A. V., Hermann, M., Saks, V., Hengster, P. & Margreiter, R. (2009), 'The cell-type specificity of mitochondrial dynamics', *The international journal of biochemistry & cell biology* **41**(10), 1928–1939.

Lai, L., Leone, T. C., Zechner, C., Schaeffer, P. J., Kelly, S. M., Flanagan, D. P., Medeiros, D. M., Kovacs, A. & Kelly, D. P. (2008), 'Transcriptional coactivators PGC-1α and PGC-lβ control overlapping programs required for perinatal maturation of the heart', *Genes & development* **22**(14), 1948–1961.

Lane, N. (2005), *Power, sex, suicide: mitochondria and the meaning of life*, OUP Oxford.

Lanza, I. R., Zabielski, P., Klaus, K. A., Morse, D. M., Heppelmann, C. J., Bergen, H. R., Dasari, S., Walrand, S., Short, K. R., Johnson, M. L. et al. (2012), 'Chronic caloric restriction preserves mitochondrial function in senescence without increasing mitochondrial biogenesis', *Cell metabolism* **16**(6), 777–788.

Larsson, N.-G., Wang, J., Wilhelmsson, H., Oldfors, A., Rustin, P., Lewandoski, M., Barsh, G. S. & Clayton, D. A. (1998), 'Mitochondrial transcription factor A is necessary for mtDNA maintance and embryogenesis in mice', *Nature genetics* **18**(3), 231–236.

Lazzeroni, L., Owen, A. et al. (2002), 'Plaid models for gene expression data', *Statistica sinica* **12**(1), 61–86.

Lee, B. C., Lee, H.-j. & Chung, J.-H. (2006), 'Peroxisome proliferator-activated receptor-γ2 pro12ala polymorphism is associated with reduced risk for ischemic stroke with type 2 diabetes', *Neuroscience letters* **410**(2), 141–145.

Lee, C.-K., Klopp, R. G., Weindruch, R. & Prolla, T. A. (1999), 'Gene expression profile of aging and its retardation by caloric restriction', *Science* **285**(5432), 1390–1393.

Lee, H.-C., Yin, P.-H., Chi, C.-W. & Wei, Y.-H. (2002), 'Increase in mitochondrial mass in human fibroblasts under oxidative stress and during replicative cell senescence', *Journal of biomedical science* **9**(6), 517–526.

Lee, S., Kim, S., Sun, X., Lee, J.-H. & Cho, H. (2007), 'Cell cycle-dependent mitochondrial biogenesis and dynamics in mammalian cells', *Biochemical and biophysical research communications* **357**(1), 111–117.

Lemasters, J. J. (2005), 'Selective mitochondrial autophagy, or mitophagy, as a targeted defense against oxidative stress, mitochondrial dysfunction, and aging', *Rejuvenation research* **8**(1), 3–5.

Leonardsson, G., Steel, J. H., Christian, M., Pocock, V., Milligan, S., Bell, J., So, P.-W., Medina-Gomez, G., Vidal-Puig, A., White, R. et al. (2004), 'Nuclear receptor

corepressor RIP140 regulates fat accumulation', *Proceedings of the National Academy of Sciences of the United States of America* **101**(22), 8437–8442.

Li, F., Wang, Y., Zeller, K. I., Potter, J. J., Wonsey, D. R., O'Donnell, K. A., Kim, J.-w., Yustein, J. T., Lee, L. A. & Dang, C. V. (2005), 'Myc stimulates nuclearly encoded mitochondrial genes and mitochondrial biogenesis', *Molecular and cellular biology* **25**(14), 6225–6234.

Li, G., Ma, Q., Tang, H., Paterson, A. H. & Xu, Y. (2009), 'QUBIC: a qualitative biclustering algorithm for analyses of gene expression data', *Nucleic acids research* p. gkp491.

Li, J., Donath, S., Li, Y., Qin, D., Prabhakar, B. S. & Li, P. (2010), 'miR-30 regulates mitochondrial fission through targeting p53 and the dynamin-related protein-1 pathway', *PLoS Genet* **6**(1), e1000795.

Li, P., Jiao, J., Gao, G. & Prabhakar, B. S. (2012), 'Control of mitochondrial activity by miRNAs', *Journal of cellular biochemistry* **113**(4), 1104–1110.

Li, X., Nair, A., Wang, S. & Wang, L. (2015), Quality control of RNA-Seq experiments, *in* 'RNA Bioinformatics', Springer, pp. 137–146.

Liang, Huiyun & Ward, W. F. (2006), 'PGC-1α: a key regulator of energy metabolism', *Advances in physiology education* **30**(4), 145–151.

Lin, J., Puigserver, P., Donovan, J., Tarr, P. & Spiegelman, B. M. (2002), 'Peroxisome proliferator-activated receptor γ coactivator 1β (PGC-1β), a novel PGC-1-related transcription coactivator associated with host cell factor', *Journal of Biological Chemistry* **277**(3), 1645–1648.

Lin, J., Wu, P.-H., Tarr, P. T., Lindenberg, K. S., St-Pierre, J., Zhang, C.-y., Mootha, V. K., Jäger, S., Vianna, C. R., Reznick, R. M. et al. (2004), 'Defects in adaptive energy metabolism with CNS-linked hyperactivity in PGC-1α null mice', *Cell* **119**(1), 121–135.

Liu, Xiaowen & Wang, L. (2007), 'Computing the maximum similarity bi-clusters of gene expression data', *Bioinformatics* **23**(1), 50–56.

Lopez, M. F., Kristal, B. S., Chernokalskaya, E., Lazarev, A., Shestopalov, A. I., Bogdanova, A. & Robinson, M. (2000), 'High-throughput profiling of the mitochondrial proteome using affinity fractionation and automation', *Electrophoresis* **21**(16), 3427–3440.

López-Otín, C., Blasco, M. A., Partridge, L., Serrano, M. & Kroemer, G. (2013), 'The hallmarks of aging', *Cell* **153**(6), 1194–1217.

Lu, H., Li, G., Liu, L., Feng, L., Wang, X. & Jin, H. (2013), 'Regulation and function of mitophagy in development and cancer', *Autophagy* **9**(11), 1720–1736.

Luo, J., Sladek, R., Bader, J.-A., Matthyssen, A., Rossant, J. & Giguère, V. (1997), 'Placental abnormalities in mouse embryos lacking the orphan nuclear receptor ERR-β', *Nature* **388**(6644), 778–782.

Luo, W., Friedman, M. S., Shedden, K., Hankenson, K. D. & Woolf, P. J. (2009), 'GAGE: generally applicable gene set enrichment for pathway analysis', *BMC bioinformatics* **10**(1), 161.

Lynn, E. G., Stevens, M. V., Wong, R. P., Carabenciov, D., Jacobson, J., Murphy, E. & Sack, M. N. (2010), 'Transient upregulation of PGC-1α diminishes cardiac ischemia tolerance via upregulation of ANT1', *Journal of molecular and cellular cardiology* **49**(4), 693–698.

Maciejewski, H. (2013), 'Gene set analysis methods: statistical models and methodological differences', *Briefings in bioinformatics* p. bbt002.

Madeira, Sara C & Oliveira, A. L. (2004), 'Biclustering algorithms for biological data analysis: a survey', *IEEE/ACM Transactions on Computational Biology and Bioinformatics (TCBB)* **1**(1), 24–45.

Maglioni, S., Schiavi, A., Runci, A., Shaik, A. & Ventura, N. (2014), 'Mitochondrial stress extends lifespan in c. elegans through neuronal hormesis', *Experimental gerontology* **56**, 89–98.

Maier, R., Zimmer, R. & Küffner, R. (2013), 'A turing test for artificial expression data', *Bioinformatics* **29**(20), 2603–2609.

Malkov, V. A., Serikawa, K. A., Balantac, N., Watters, J., Geiss, G., Mashadi-Hossein, A. & Fare, T. (2009), 'Multiplexed measurements of gene signatures in different analytes using the nanostring nCounter assay system', *BMC research notes* **2**(1), 80.

Mandemakers, W., Morais, V. A. & De Strooper, B. (2007), 'A cell biological perspective on mitochondrial dysfunction in Parkinson disease and other neurodegenerative diseases', *Journal of cell science* **120**(10), 1707–1716.

Mann, Henry B & Whitney, D. R. (1947), 'On a test of whether one of two random variables is stochastically larger than the other', *The annals of mathematical statistics* pp. 50–60.

Marioni, J. C., Mason, C. E., Mane, S. M., Stephens, M. & Gilad, Y. (2008), 'RNA-seq: an assessment of technical reproducibility and comparison with gene expression arrays', *Genome research* **18**(9), 1509–1517.

Maron, B. J. (2003), 'Sudden death in young athletes', *New England Journal of Medicine* **349**(11), 1064–1075.

Maron, B. J., Gardin, J. M., Flack, J. M., Gidding, S. S., Kurosaki, T. T. & Bild, D. E. (1995), 'Prevalence of hypertrophic cardiomyopathy in a general population of young adults echocardiographic analysis of 4111 subjects in the CARDIA study', *Circulation* **92**(4), 785–789.

Maron, B. J., Maron, M. S. & Semsarian, C. (2012), 'Genetics of hypertrophic cardiomyopathy after 20 years: clinical perspectives', *Journal of the American College of Cardiology* **60**(8), 705–715.

Maron, Barry J & Braunwald, E. (2012), 'Evolution of hypertrophic cardiomyopathy to a contemporary treatable disease', *Circulation* **126**(13), 1640–1644.

Maron, Barry J & Maron, M. S. (2015), 'The 20 advances that have defined contemporary hypertrophic cardiomyopathy', *Trends in cardiovascular medicine* **25**(1), 54–64.

Martínez-Reyes, I., Diebold, L. P., Kong, H., Schieber, M., Huang, H., Hensley, C. T., Mehta, M. M., Wang, T., Santos, J. H., Woychik, R. et al. (2015), 'TCA cycle and

mitochondrial membrane potential are necessary for diverse biological functions', *Molecular cell* .

Maruszak, A., Safranow, K., Branicki, W., Gaweda-Walerych, K., Pośpiech, E., Gabryelewicz, T., Canter, J. A., Barcikowska, M. & Żekanowski, C. (2011), 'The impact of mitochondrial and nuclear DNA variants on late-onset Alzheimer's disease risk', *Journal of Alzheimer's Disease* **27**(1), 197.

Masters, J. R. (2000), 'Human cancer cell lines: fact and fantasy', *Nature reviews Molecular cell biology* **1**(3), 233–236.

Matys, V., Fricke, E., Geffers, R., Gößling, E., Haubrock, M., Hehl, R., Hornischer, K., Karas, D., Kel, A. E., Kel-Margoulis, O. V. et al. (2003), 'TRANSFAC®: transcriptional regulation, from patterns to profiles', *Nucleic acids research* **31**(1), 374–378.

McKenzie, M., Liolitsa, D., Akinshina, N., Campanella, M., Sisodiya, S., Hargreaves, I., Nirmalananthan, N., Sweeney, M. G., Abou-Sleiman, P. M., Wood, N. W. et al. (2007), 'Mitochondrial ND5 gene variation associated with encephalomyopathy and mitochondrial ATP consumption', *Journal of Biological Chemistry* **282**(51), 36845–36852.

McKiernan, S. H., Tuen, V. C., Baldwin, K., Wanagat, J., Djamali, A. & Aiken, J. M. (2007), 'Adult-onset calorie restriction delays the accumulation of mitochondrial enzyme abnormalities in aging rat kidney tubular epithelial cells', *American Journal of Physiology-Renal Physiology* **292**(6), F1751–F1760.

Medeiros, D. M. (2008), 'Assessing mitochondria biogenesis', *Methods* **46**(4), 288–294.

Medina, M. A. (2001), 'Glutamine and cancer', *The Journal of nutrition* **131**(9), 2539S–2542S.

Mela, L., Bacalzo, L. & Miller, L. (1971), 'Defective oxidative metabolism of rat liver mitochondria in hemorrhagic and endotoxin shock', *American Journal of Physiology–Legacy Content* **220**(2), 571–577.

Menzies, Robert A & Gold, P. H. (1971), 'The turnover of mitochondria in a variety of

tissues of young adult and aged rats', *Journal of Biological Chemistry* **246**(8), 2425–2429.

Mermel, C. H., Schumacher, S. E., Hill, B., Meyerson, M. L., Beroukhim, R., Getz, G. et al. (2011), 'GISTIC2. 0 facilitates sensitive and confident localization of the targets of focal somatic copy-number alteration in human cancers', *Genome Biol* **12**(4), R41.

Mitchell, P. (1961), 'Coupling of phosphorylation to electron and hydrogen transfer by a chemi-osmotic type of mechanism', *Nature* **191**(4784), 144–148.

Miyaki, M., Iijima, T., Konishi, M., Sakai, K., Ishii, A., Yasuno, M., Hishima, T., Koike, M., Shitara, N., Iwama, T. et al. (1999), 'Higher frequency of Smad4 gene mutation in human colorectal cancer with distant metastasis.', *Oncogene* **18**(20), 3098–3103.

Mochizuki, Satsuki & Okada, Y. (2007), 'ADAMs in cancer cell proliferation and progression', *Cancer science* **98**(5), 621–628.

Mohammed, H., Russell, I. A., Stark, R., Rueda, O. M., Hickey, T. E., Tarulli, G. A., Serandour, A. A., Birrell, S. N., Bruna, A., Saadi, A. et al. (2015), 'Progesterone receptor modulates ERα action in breast cancer.', *Nature* **526**(7571), 144.

Mook, S., Van't Veer, L. J., Rutgers, E. J., Piccart-Gebhart, M. J. & Cardoso, F. (2007), 'Individualization of therapy using mammaprint® ì: From development to the MINDACT trial', *Cancer Genomics-Proteomics* **4**(3), 147–155.

Mootha, V. K., Handschin, C., Arlow, D., Xie, X., Pierre, J. S., Sihag, S., Yang, W., Altshuler, D., Puigserver, P., Patterson, N. et al. (2004), 'Errα and gabpa/b specify PGC-1α-dependent oxidative phosphorylation gene expression that is altered in diabetic muscle', *Proceedings of the National Academy of Sciences of the United States of America* **101**(17), 6570–6575.

Nagrath, D., Caneba, C., Karedath, T. & Bellance, N. (2011), 'Metabolomics for mitochondrial and cancer studies', *Biochimica et Biophysica Acta (BBA)-Bioenergetics* **1807**(6), 650–663.

Narendra, D. P., Jin, S. M., Tanaka, A., Suen, D.-F., Gautier, C. A., Shen, J., Cookson, M. R., Youle, R. J. et al. (2010), 'PINK1 is selectively stabilized on impaired mitochondria to activate parkin', *PLoS biology* **8**(1), 142.

Naya, F. J., Black, B. L., Wu, H., Bassel-Duby, R., Richardson, J. A., Hill, J. A. & Olson, E. N. (2002), 'Mitochondrial deficiency and cardiac sudden death in mice lacking the MEF2A transcription factor', *Nature medicine* **8**(11), 1303–1309.

Neve, R. M., Chin, K., Fridlyand, J., Yeh, J., Baehner, F. L., Fevr, T., Clark, L., Bayani, N., Coppe, J.-P., Tong, F. et al. (2006), 'A collection of breast cancer cell lines for the study of functionally distinct cancer subtypes', *Cancer cell* **10**(6), 515–527.

Nielsen, T. O., Parker, J. S., Leung, S., Voduc, D., Ebbert, M., Vickery, T., Davies, S. R., Snider, J., Stijleman, I. J., Reed, J. et al. (2010), 'A comparison of PAM50 intrinsic subtyping with immunohistochemistry and clinical prognostic factors in tamoxifen-treated estrogen receptor–positive breast cancer', *Clinical Cancer Research* **16**(21), 5222–5232.

Nielsen, T., Wallden, B., Schaper, C., Ferree, S., Liu, S., Gao, D., Barry, G., Dowidar, N., Maysuria, M. & Storhoff, J. (2014), 'Analytical validation of the PAM50-based prosigna breast cancer prognostic gene signature assay and ncounter analysis system using formalin-fixed paraffin-embedded breast tumor specimens', *BMC cancer* **14**(1), 1.

Nisoli, E., Tonello, C., Cardile, A., Cozzi, V., Bracale, R., Tedesco, L., Falcone, S., Valerio, A., Cantoni, O., Clementi, E. et al. (2005), 'Calorie restriction promotes mitochondrial biogenesis by inducing the expression of eNOS', *Science* **310**(5746), 314–317.

Odegaard, J. I., Ricardo-Gonzalez, R. R., Goforth, M. H., Morel, C. R., Subramanian, V., Mukundan, L., Eagle, A. R., Vats, D., Brombacher, F., Ferrante, A. W. et al. (2007), 'Macrophage-specific PPAR&ggr; controls alternative activation and improves insulin resistance', *Nature* **447**(7148), 1116–1120.

O'Donnell, K. A., Wentzel, E. A., Zeller, K. I., Dang, C. V. & Mendell, J. T. (2005), 'c-Myc-regulated microRNAs modulate E2F1 expression', *nature* **435**(7043), 839–843.

Ojuka, E. O., Jones, T. E., Han, D.-H., Chen, M. & Holloszy, J. O. (2003), 'Raising Ca2+ in L6 myotubes mimics effects of exercise on mitochondrial biogenesis in muscle', *The FASEB Journal* **17**(6), 675–681.

Okoniewski, Michał J & Miller, C. J. (2006), 'Hybridization interactions between probesets in short oligo microarrays lead to spurious correlations', *BMC bioinformatics* **7**(1), 276.

O'Malley, B. (1990), 'Minireview: The steroid receptor superfamily: More excitement predicted for the future', *Molecular Endocrinology* **4**(3), 363–369.

Pagliarini, D. J., Calvo, S. E., Chang, B., Sheth, S. A., Vafai, S. B., Ong, S.-E., Walford, G. A., Sugiana, C., Boneh, A., Chen, W. K. et al. (2008), 'A mitochondrial protein compendium elucidates complex i disease biology', *Cell* **134**(1), 112–123.

Palikaras, K., Lionaki, E. & Tavernarakis, N. (2015), 'Coordination of mitophagy and mitochondrial biogenesis during ageing in C. elegans', *Nature* .

Parikh, V. S., MoRGAN, M. M., Scott, R., Clements, L. S. & Butow, R. A. (1987), 'The mitochondrial genotype can influence nuclear gene expression in yeast', *Science* **235**(4788), 576–580.

Parisi, Melissa A & Clayton, D. A. (1991), 'Similarity of human mitochondrial transcription factor 1 to high mobility group proteins', *Science* **252**(5008), 965–969.

Parker, J. S., Mullins, M., Cheang, M. C., Leung, S., Voduc, D., Vickery, T., Davies, S., Fauron, C., He, X., Hu, Z. et al. (2009), 'Supervised risk predictor of breast cancer based on intrinsic subtypes', *Journal of clinical oncology* **27**(8), 1160–1167.

Patti, Mary-Elizabeth & Corvera, S. (2010), 'The role of mitochondria in the pathogenesis of type 2 diabetes', *Endocrine Reviews* **31**(3), 364–395.

Pearson, K. (1901), 'On lines and planes of closest fit to systems of points in space', *The London, Edinburgh, and Dublin Philosophical Magazine and Journal of Science* **2**(11), 559–572.

Pendergrass, W., Wolf, N. & Poot, M. (2004), 'Efficacy of MitoTracker Green and CMXRosamine to measure changes in mitochondrial membrane potentials in living cells and tissues', *Cytometry Part A* **61**(2), 162–169.

Pérez-Schindler, J., Summermatter, S., Salatino, S., Zorzato, F., Beer, M., Balwierz, P. J., van Nimwegen, E., Feige, J. N., Auwerx, J. & Handschin, C. (2012), 'The corepressor NCoR1 antagonizes PGC-1α and estrogen-related receptor α in the regulation of skeletal muscle function and oxidative metabolism', *Molecular and cellular biology* **32**(24), 4913–4924.

Perou, C. M., Sørlie, T., Eisen, M. B., van de Rijn, M., Jeffrey, S. S., Rees, C. A., Pollack, J. R., Ross, D. T., Johnsen, H., Akslen, L. A. et al. (2000), 'Molecular portraits of human breast tumours', *Nature* **406**(6797), 747–752.

Petros, J. A., Baumann, A. K., Ruiz-Pesini, E., Amin, M. B., Sun, C. Q., Hall, J., Lim, S., Issa, M. M., Flanders, W. D., Hosseini, S. H. et al. (2005), 'mtDNA mutations increase tumorigenicity in prostate cancer', *Proceedings of the National Academy of Sciences of the United States of America* **102**(3), 719–724.

Piantadosi, Claude A & Suliman, H. B. (2012), 'Transcriptional control of mitochondrial biogenesis and its interface with inflammatory processes', *Biochimica et Biophysica Acta (BBA)-General Subjects* **1820**(4), 532–541.

Pilegaard, H., Saltin, B. & Neufer, P. D. (2003), 'Exercise induces transient transcriptional activation of the PGC-1α gene in human skeletal muscle', *The Journal of physiology* **546**(3), 851–858.

Pontes, B., Giráldez, R. & Aguilar-Ruiz, J. S. (2015a), 'Biclustering on expression data: A review', *Journal of biomedical informatics* **57**, 163–180.

Pontes, B., Girldez, R. & Aguilar-Ruiz, J. S. (2015b), 'Quality measures for gene expression biclusters', *PloS one* **10**(3), e0115497.

Powelka, A. M., Seth, A., Virbasius, J. V., Kiskinis, E., Nicoloro, S. M., Guilherme, A., Tang, X., Straubhaar, J., Cherniack, A. D., Parker, M. G. et al. (2006), 'Suppression of oxidative metabolism and mitochondrial biogenesis by the transcriptional corepressor RIP140 in mouse adipocytes', *The Journal of clinical investigation* **116**(1), 125.

Poyton, Robert O & McEwen, J. E. (1996), 'Crosstalk between nuclear and mitochondrial genomes', *Annual review of biochemistry* **65**(1), 563–607.

Prat, A., Karginova, O., Parker, J. S., Fan, C., He, X., Bixby, L., Harrell, J. C., Roman, E., Adamo, B., Troester, M. et al. (2013), 'Characterization of cell lines derived from breast cancers and normal mammary tissues for the study of the intrinsic molecular subtypes', *Breast cancer research and treatment* **142**(2), 237–255.

Prat, Aleix & Perou, C. M. (2011), 'Deconstructing the molecular portraits of breast cancer', *Molecular oncology* **5**(1), 5–23.

Prelić, A., Bleuler, S., Zimmermann, P., Wille, A., Bühlmann, P., Gruissem, W., Hennig, L., Thiele, L. & Zitzler, E. (2006), 'A systematic comparison and evaluation of biclustering methods for gene expression data', *Bioinformatics* **22**(9), 1122–1129.

Puigserver, P., Wu, Z., Park, C. W., Graves, R., Wright, M. & Spiegelman, B. M. (1998), 'A cold-inducible coactivator of nuclear receptors linked to adaptive thermogenesis', *Cell* **92**(6), 829–839.

Quirós, P. M., Langer, T. & López-Otín, C. (2015), 'New roles for mitochondrial proteases in health, ageing and disease', *Nature Reviews Molecular Cell Biology* .

Ramachandran, B., Yu, G. & Gulick, T. (2008), 'Nuclear respiratory factor 1 controls myocyte enhancer factor 2A transcription to provide a mechanism for coordinate expression of respiratory chain subunits', *Journal of Biological Chemistry* **283**(18), 11935–11946.

Rasbach, K. A., Green, P. T. & Schnellmann, R. G. (2008), 'Oxidants and Ca+ 2 induce PGC-1α degradation through calpain', *Archives of biochemistry and biophysics* **478**(2), 130–135.

Ravdin, P. M., Siminoff, L. A., Davis, G. J., Mercer, M. B., Hewlett, J., Gerson, N. & Parker, H. L. (2001), 'Computer program to assist in making decisions about adjuvant therapy for women with early breast cancer', *Journal of Clinical Oncology* **19**(4), 980–991.

Rehm, H. L., Berg, J. S., Brooks, L. D., Bustamante, C. D., Evans, J. P., Landrum, M. J., Ledbetter, D. H., Maglott, D. R., Martin, C. L., Nussbaum, R. L. et al. (2015), 'ClinGenthe clinical genome resource', *New England Journal of Medicine* .

Reimand, J., Kull, M., Peterson, H., Hansen, J. & Vilo, J. (2007), 'g:Profilera web-based toolset for functional profiling of gene lists from large-scale experiments', *Nucleic acids research* **35**(suppl 2), W193–W200.

Reis-Filho, Jorge S & Pusztai, L. (2011), 'Gene expression profiling in breast cancer: classification, prognostication, and prediction', *The Lancet* **378**(9805), 1812–1823.

Ricci, C., Pastukh, V., Leonard, J., Turrens, J., Wilson, G., Schaffer, D. & Schaffer, S. W. (2008), 'Mitochondrial dna damage triggers mitochondrial-superoxide generation and apoptosis', *American Journal of Physiology-Cell Physiology* **294**(2), C413–C422.

Richter, R., Rorbach, J., Pajak, A., Smith, P. M., Wessels, H. J., Huynen, M. A., Smeitink, J. A., Lightowlers, R. N. & Chrzanowska-Lightowlers, Z. M. (2010), 'A functional peptidyl-trna hydrolase, ICT1, has been recruited into the human mitochondrial ribosome', *The EMBO Journal* **29**(6), 1116–1125.

Rooney, J. P., Ryde, I. T., Sanders, L. H., Howlett, E. H., Colton, M. D., Germ, K. E., Mayer, G. D., Greenamyre, J. T. & Meyer, J. N. (2015), 'PCR based determination of mitochondrial DNA copy number in multiple species', *Mitochondrial Regulation: Methods and Protocols* pp. 23–38.

Rosca, M. G., Tandler, B. & Hoppel, C. L. (2013), 'Mitochondria in cardiac hypertrophy and heart failure', *Journal of molecular and cellular cardiology* **55**, 31–41.

Rosmarin, A. G., Resendes, K. K., Yang, Z., McMillan, J. N. & Fleming, S. L. (2004), 'GA-binding protein transcription factor: a review of GABP as an integrator of intracellular signaling and protein–protein interactions', *Blood Cells, Molecules, and Diseases* **32**(1), 143–154.

Ross, D. T., Scherf, U., Eisen, M. B., Perou, C. M., Rees, C., Spellman, P., Iyer, V., Jeffrey, S. S., Van de Rijn, M., Waltham, M. et al. (2000), 'Systematic variation in gene expression patterns in human cancer cell lines', *Nature genetics* **24**(3), 227–235.

Rossignol, R., Faustin, B., Rocher, C., Malgat, M., Mazat, J.-P. & Letellier, T. (2003), 'Mitochondrial threshold effects', *Biochemical Journal* **370**(3), 751–762.

Rousseeuw, P. J. (1987), 'Silhouettes: a graphical aid to the interpretation and validation of cluster analysis', *Journal of computational and applied mathematics* **20**, 53–65.

Rousset, S., Emre, Y., Join-Lambert, O., Hurtaud, C., Ricquier, D. & Cassard-Doulcier, A.-M. (2006), 'The uncoupling protein 2 modulates the cytokine balance in innate immunity', *Cytokine* **35**(3), 135–142.

Russell, L. K., Mansfield, C. M., Lehman, J. J., Kovacs, A., Courtois, M., Saffitz, J. E., Medeiros, D. M., Valencik, M. L., McDonald, J. A. & Kelly, D. P. (2004), 'Cardiac-specific induction of the transcriptional coactivator peroxisome proliferator-activated receptor γ coactivator-1α promotes mitochondrial biogenesis and reversible cardiomyopathy in a developmental stage-dependent manner', *Circulation research* **94**(4), 525–533.

Sakamaki, T., Casimiro, M. C., Ju, X., Quong, A. A., Katiyar, S., Liu, M., Jiao, X., Li, A., Zhang, X., Lu, Y. et al. (2006), 'Cyclin D1 determines mitochondrial function in vivo', *Molecular and cellular biology* **26**(14), 5449–5469.

Sato, Miyuki & Sato, K. (2011), 'Degradation of paternal mitochondria by fertilization-triggered autophagy in C. elegans embryos', *Science* **334**(6059), 1141–1144.

Satoh, Masaya & Kuroiwa, T. (1991), 'Organization of multiple nucleoids and DNA molecules in mitochondria of a human cell', *Experimental cell research* **196**(1), 137–140.

Scaduto, Russell C & Grotyohann, L. W. (1999), 'Measurement of mitochondrial membrane potential using fluorescent rhodamine derivatives', *Biophysical journal* **76**(1), 469–477.

Scarpulla, R. C. (2008), 'Transcriptional paradigms in mammalian mitochondrial biogenesis and function', *Physiological reviews* **88**(2), 611–638.

Scarpulla, R. C., Vega, R. B. & Kelly, D. P. (2012), 'Transcriptional integration of mitochondrial biogenesis', *Trends in Endocrinology & Metabolism* **23**(9), 459–466.

Schaffter, T., Marbach, D. & Floreano, D. (2011), 'GeneNetWeaver: in silico benchmark generation and performance profiling of network inference methods', *Bioinformatics* **27**(16), 2263–2270.

Schena, M., Shalon, D., Davis, R. W. & Brown, P. O. (1995), 'Quantitative monitoring of gene expression patterns with a complementary DNA microarray', *Science* **270**(5235), 467–470.

Schreiber, S. N., Emter, R., Hock, M. B., Knutti, D., Cardenas, J., Podvinec, M., Oakeley, E. J. & Kralli, A. (2004), 'The estrogen-related receptor α (ERRα) functions in PPARγ coactivator 1α (PGC-1α)-induced mitochondrial biogenesis', *Proceedings of the National Academy of Sciences of the United States of America* **101**(17), 6472–6477.

Schuler, M., Ali, F., Chambon, C., Duteil, D., Bornert, J.-M., Tardivel, A., Desvergne, B., Wahli, W., Chambon, P. & Metzger, D. (2006), 'PGC1α expression is controlled in skeletal muscles by PPARβ, whose ablation results in fiber-type switching, obesity, and type 2 diabetes', *Cell metabolism* **4**(5), 407–414.

Schulze-Osthoff, K., Bakker, A., Vanhaesebroeck, B., Beyaert, R., Jacob, W. A. & Fiers, W. (1992), 'Cytotoxic activity of tumor necrosis factor is mediated by early damage of mitochondrial functions. evidence for the involvement of mitochondrial radical generation.', *Journal of Biological Chemistry* **267**(8), 5317–5323.

Schweers, R. L., Zhang, J., Randall, M. S., Loyd, M. R., Li, W., Dorsey, F. C., Kundu, M., Opferman, J. T., Cleveland, J. L., Miller, J. L. et al. (2007), 'NIX is required for programmed mitochondrial clearance during reticulocyte maturation', *Proceedings of the National Academy of Sciences* **104**(49), 19500–19505.

Semsarian, C., Ingles, J., Maron, M. S. & Maron, B. J. (2015), 'New perspectives on the prevalence of hypertrophic cardiomyopathy', *Journal of the American College of Cardiology* **65**(12), 1249–1254.

Sen, N., Satija, Y. K. & Das, S. (2011), 'PGC-1α, a key modulator of p53, promotes cell survival upon metabolic stress', *Molecular cell* **44**(4), 621–634.

Shaywitz, Adam J & Greenberg, M. E. (1999), 'CREB: a stimulus-induced transcription factor activated by a diverse array of extracellular signals', *Annual review of biochemistry* **68**(1), 821–861.

Shibata, D., Reale, M. A., Lavin, P., Silverman, M., Fearon, E. R., Steele Jr, G., Jessup, J. M., Loda, M. & Summerhayes, I. C. (1996), 'The DCC protein and prognosis in colorectal cancer', *New England Journal of Medicine* **335**(23), 1727–1732.

Shimada, K., Crother, T. R., Karlin, J., Dagvadorj, J., Chiba, N., Chen, S., Ramanujan, V. K., Wolf, A. J., Vergnes, L., Ojcius, D. M. et al. (2012), 'Oxidized mitochondrial dna activates the nlrp3 inflammasome during apoptosis', *Immunity* **36**(3), 401–414.

Shin, J.-H., Ko, H. S., Kang, H., Lee, Y., Lee, Y.-I., Pletinkova, O., Troconso, J. C., Dawson, V. L. & Dawson, T. M. (2011), 'PARIS (ZNF746) repression of PGC-1α contributes to neurodegeneration in Parkinson's disease', *Cell* **144**(5), 689–702.

Siegel, R. L., Miller, K. D. & Jemal, A. (2015), 'Cancer statistics, 2016', *CA: A cancer journal for clinicians* .

Siegel, R., Naishadham, D. & Jemal, A. (2012), 'Cancer statistics, 2012', *CA: a cancer journal for clinicians* **62**(1), 10–29.

Siprashvili, Z., Sozzi, G., Barnes, L. D., McCue, P., Robinson, A. K., Eryomin, V., Sard, L., Tagliabue, E., Greco, A., Fusetti, L. et al. (1997), 'Replacement of fhit in cancer cells suppresses tumorigenicity', *Proceedings of the National Academy of Sciences* **94**(25), 13771–13776.

Skloot, Rebecca & Turpin, B. (2010), *The immortal life of Henrietta Lacks*, Crown Publishers New York:.

Slager, J., Kjos, M., Attaiech, L. & Veening, J.-W. (2014), 'Antibiotic-induced replication stress triggers bacterial competence by increasing gene dosage near the origin', *Cell* **157**(2), 395–406.

Smigrodzki, Rafal M & Khan, S. M. (2005), 'Mitochondrial microheteroplasmy and a theory of aging and age-related disease', *Rejuvenation research* **8**(3), 172–198.

Smiraglia, D., Kulawiec, M., Bistulfi, G. L., Ghoshal, S. & Singh, K. K. (2008), 'A novel role for mitochondria in regulating epigenetic modifications in the nucleus', *Cancer biology & therapy* **7**(8), 1182–1190.

Smith, A. C., Blackshaw, J. A. & Robinson, A. J. (2011), 'MitoMiner: a data warehouse for mitochondrial proteomics data', *Nucleic acids research* p. gkr1101.

Smith, Anthony C & Robinson, A. J. (2009), 'MitoMiner, an integrated database for the storage and analysis of mitochondrial proteomics data', *Molecular & Cellular Proteomics* **8**(6), 1324–1337.

Smits, P., Saada, A., Wortmann, S. B., Heister, A. J., Brink, M., Pfundt, R., Miller, C., Haas, D., Hantschmann, R., Rodenburg, R. J. et al. (2011), 'Mutation in mitochondrial ribosomal protein MRPS22 leads to cornelia de lange-like phenotype, brain abnormalities and hypertrophic cardiomyopathy', *European Journal of Human Genetics* **19**(4), 394–399.

Smyth, G. K. (2005), Limma: linear models for microarray data, *in* 'Bioinformatics and computational biology solutions using R and Bioconductor', Springer, pp. 397–420.

Sonoda, J., Laganière, J., Mehl, I. R., Barish, G. D., Chong, L.-W., Li, X., Scheffler, I. E., Mock, D. C., Bataille, A. R., Robert, F. et al. (2007a), 'Nuclear receptor ERRα and coactivator PGC-1β are effectors of IFN-γ-induced host defense', *Genes & development* **21**(15), 1909–1920.

Sonoda, J., Mehl, I. R., Chong, L.-W., Nofsinger, R. R. & Evans, R. M. (2007b), 'PGC-1β controls mitochondrial metabolism to modulate circadian activity, adaptive thermogenesis, and hepatic steatosis', *Proceedings of the National Academy of Sciences* **104**(12), 5223–5228.

Sørlie, T., Perou, C. M., Tibshirani, R., Aas, T., Geisler, S., Johnsen, H., Hastie, T., Eisen, M. B., van de Rijn, M., Jeffrey, S. S. et al. (2001), 'Gene expression patterns of breast carcinomas distinguish tumor subclasses with clinical implications', *Proceedings of the National Academy of Sciences* **98**(19), 10869–10874.

St-Pierre, J., Drori, S., Uldry, M., Silvaggi, J. M., Rhee, J., Jäger, S., Handschin, C.,

Zheng, K., Lin, J., Yang, W. et al. (2006), 'Suppression of reactive oxygen species and neurodegeneration by the PGC-1 transcriptional coactivators', *Cell* **127**(2), 397–408.

Stark, C., Breitkreutz, B.-J., Reguly, T., Boucher, L., Breitkreutz, A. & Tyers, M. (2006), 'BioGRID: a general repository for interaction datasets', *Nucleic acids research* **34**(suppl 1), D535–D539.

Stein, R. C., Dunn, J. A., Bartlett, J. M., Campbell, A. F., Marshall, A., Hall, P., Rooshenas, L., Morgan, A., Poole, C., Pinder, S. E. et al. (2016), 'OPTIMA prelim: a randomised feasibility study of personalised care in the treatment of women with early breast cancer'.

Stein, RA & McDonnell, D. (2006), 'Estrogen-related receptor α as a therapeutic target in cancer', *Endocrine-related cancer* **13**(Supplement 1), S25–S32.

Subramanian, A., Tamayo, P., Mootha, V. K., Mukherjee, S., Ebert, B. L., Gillette, M. A., Paulovich, A., Pomeroy, S. L., Golub, T. R., Lander, E. S. et al. (2005), 'Gene set enrichment analysis: a knowledge-based approach for interpreting genome-wide expression profiles', *Proceedings of the National Academy of Sciences of the United States of America* **102**(43), 15545–15550.

Szabadkai, György & Duchen, M. R. (2008), 'Mitochondria: the hub of cellular Ca2+ signaling', *Physiology* **23**(2), 84–94.

Taherzadeh-Fard, E., Saft, C., Akkad, D. A., Wieczorek, S., Haghikia, A., Chan, A., Epplen, J. T. & Arning, L. (2011), 'PGC-1alpha downstream transcription factors NRF-1 and TFAM are genetic modifiers of Huntington disease', *Mol Neurodegener* **6**(1), 32.

Takayama, T., Miyanishi, K., Hayashi, T., Sato, Y. & Niitsu, Y. (2006), 'Colorectal cancer: genetics of development and metastasis', *Journal of gastroenterology* **41**(3), 185–192.

Tal, R., Winter, G., Ecker, N., Klionsky, D. J. & Abeliovich, H. (2007), 'Aup1p, a yeast mitochondrial protein phosphatase homolog, is required for efficient stationary phase mitophagy and cell survival', *Journal of Biological Chemistry* **282**(8), 5617–5624.

Tanay, A., Sharan, R. & Shamir, R. (2002), 'Discovering statistically significant biclusters in gene expression data', *Bioinformatics* **18**(suppl 1), S136–S144.

Terada, Shin &Tabata, I. (2004), 'Effects of acute bouts of running and swimming exercise on PGC-1α protein expression in rat epitrochlearis and soleus muscle', *American Journal of Physiology-Endocrinology and Metabolism* **286**(2), E208–E216.

Terman, A., Kurz, T., Navratil, M., Arriaga, E. A. & Brunk, U. T. (2010), 'Mitochondrial turnover and aging of long-lived postmitotic cells: the mitochondrial–lysosomal axis theory of aging', *Antioxidants & redox signaling* **12**(4), 503–535.

Teyssier, C., Ma, H., Emter, R., Kralli, A. & Stallcup, M. R. (2005), 'Activation of nuclear receptor coactivator PGC-1α by arginine methylation', *Genes & development* **19**(12), 1466–1473.

The Histology Guide University of Leeds (2016), `http://www.histology.leeds.ac.uk/cell/cell_organelles.php`. Accessed: 2016-03-15.

Tibshirani, R., Hastie, T., Narasimhan, B. & Chu, G. (2002), 'Diagnosis of multiple cancer types by shrunken centroids of gene expression', *Proceedings of the National Academy of Sciences* **99**(10), 6567–6572.

Tjaden, B., Saxena, R. M., Stolyar, S., Haynor, D. R., Kolker, E. & Rosenow, C. (2002), 'Transcriptome analysis of escherichia coli using high-density oligonucleotide probe arrays', *Nucleic acids research* **30**(17), 3732–3738.

Torre, L. A., Bray, F., Siegel, R. L., Ferlay, J., Lortet-Tieulent, J. & Jemal, A. (2015), 'Global cancer statistics, 2012', *CA: a cancer journal for clinicians* **65**(2), 87–108.

Towbin, H., Staehelin, T. & Gordon, J. (1979), 'Electrophoretic transfer of proteins from polyacrylamide gels to nitrocellulose sheets: procedure and some applications', *Proceedings of the National Academy of Sciences* **76**(9), 4350–4354.

Trausch-Azar, J., Leone, T. C., Kelly, D. P. & Schwartz, A. L. (2010), 'Ubiquitin proteasome-dependent degradation of the transcriptional coactivator PGC-1α via the n-terminal pathway', *Journal of Biological Chemistry* **285**(51), 40192–40200.

Trifunovic, A., Wredenberg, A., Falkenberg, M., Spelbrink, J. N., Rovio, A. T., Bruder, C. E., Bohlooly-Y, M., Gidlöf, S., Oldfors, A., Wibom, R. et al. (2004), 'Premature ageing in mice expressing defective mitochondrial DNA polymerase', *Nature* **429**(6990), 417–423.

Turner, H., Bailey, T. & Krzanowski, W. (2005), 'Improved biclustering of microarray data demonstrated through systematic performance tests', *Computational statistics & data analysis* **48**(2), 235–254.

Twig, G., Elorza, A., Molina, A. J., Mohamed, H., Wikstrom, J. D., Walzer, G., Stiles, L., Haigh, S. E., Katz, S., Las, G. et al. (2008), 'Fission and selective fusion govern mitochondrial segregation and elimination by autophagy', *The EMBO journal* **27**(2), 433–446.

Uldry, M., Yang, W., St-Pierre, J., Lin, J., Seale, P. & Spiegelman, B. M. (2006), 'Complementary action of the PGC-1 coactivators in mitochondrial biogenesis and brown fat differentiation', *Cell metabolism* **3**(5), 333–341.

Valle, I., Álvarez-Barrientos, A., Arza, E., Lamas, S. & Monsalve, M. (2005), 'PGC-1α regulates the mitochondrial antioxidant defense system in vascular endothelial cells', *Cardiovascular research* **66**(3), 562–573.

Van den Bulcke, T., Van Leemput, K., Naudts, B., van Remortel, P., Ma, H., Verschoren, A., De Moor, B. & Marchal, K. (2006), 'SynTReN: a generator of synthetic gene expression data for design and analysis of structure learning algorithms', *BMC bioinformatics* **7**(1), 43.

Vander Heiden, M. G., Cantley, L. C. & Thompson, C. B. (2009), 'Understanding the warburg effect: the metabolic requirements of cell proliferation', *science* **324**(5930), 1029–1033.

Vandin, F., Upfal, E. & Raphael, B. J. (2011), 'Algorithms for detecting significantly mutated pathways in cancer', *Journal of Computational Biology* **18**(3), 507–522.

VanGuilder, H. D., Vrana, K. E. & Freeman, W. M. (2008), 'Twenty-five years of quantitative PCR for gene expression analysis', *Biotechniques* **44**(5), 619.

Vasudevan, S. (2012), 'Posttranscriptional upregulation by microRNAs', *Wiley Interdisciplinary Reviews: RNA* **3**(3), 311–330.

Vercauteren, K., Gleyzer, N. & Scarpulla, R. C. (2009), 'Short hairpin RNA-mediated silencing of PRC (PGC-1-related coactivator) results in a severe respiratory chain deficiency associated with the proliferation of aberrant mitochondria', *Journal of Biological Chemistry* **284**(4), 2307–2319.

Vercauteren, K., Pasko, R. A., Gleyzer, N., Marino, V. M. & Scarpulla, R. C. (2006), 'PGC-1-related coactivator: immediate early expression and characterization of a CREB/NRF-1 binding domain associated with cytochrome c promoter occupancy and respiratory growth', *Molecular and cellular biology* **26**(20), 7409–7419.

Villena, J. A., Hock, M. B., Chang, W. Y., Barcas, J. E., Giguère, V. & Kralli, A. (2007), 'Orphan nuclear receptor estrogen-related receptor α is essential for adaptive thermogenesis', *Proceedings of the National Academy of Sciences* **104**(4), 1418–1423.

Virbasius, C.-m. A., Virbasius, J. V. & Scarpulla, R. C. (1993*a*), 'NRF-1, an activator involved in nuclear-mitochondrial interactions, utilizes a new DNA-binding domain conserved in a family of developmental regulators.', *Genes & development* **7**(12a), 2431–2445.

Virbasius, J. V., Virbasius, C.-m. A. & Scarpulla, R. C. (1993*b*), 'Identity of GABP with NRF-2, a multisubunit activator of cytochrome oxidase expression, reveals a cellular role for an ETS domain activator of viral promoters.', *Genes & development* **7**(3), 380–392.

Wallace, D. C. (2012), 'Mitochondria and cancer', *Nature Reviews Cancer* **12**(10), 685–698.

Wang, C., Li, Z., Lu, Y., Du, R., Katiyar, S., Yang, J., Fu, M., Leader, J. E., Quong, A., Novikoff, P. M. et al. (2006), 'Cyclin D1 repression of nuclear respiratory factor 1 integrates nuclear DNA synthesis and mitochondrial function', *Proceedings of the National Academy of Sciences* **103**(31), 11567–11572.

Wang, S., Fu, C., Wang, H., Shi, Y., Xu, X., Chen, J., Song, X., Sun, K., Wang, J., Fan, X. et al. (2007), 'Polymorphisms of the peroxisome proliferator-activated receptor-γ

coactivator-1α gene are associated with hypertrophic cardiomyopathy and not with hypertension hypertrophy', *Clinical Chemical Laboratory Medicine* **45**(8), 962–967.

Wang, Z., Gerstein, M. & Snyder, M. (2009), 'RNA-Seq: a revolutionary tool for transcriptomics', *Nature Reviews Genetics* **10**(1), 57–63.

Warburg, O. (1956), 'On the origin of cancer cells', *Science* **123**(3191), 309–314.

Weigelt, B., Pusztai, L., Ashworth, A. & Reis-Filho, J. S. (2012), 'Challenges translating breast cancer gene signatures into the clinic', *Nature reviews Clinical oncology* **9**(1), 58–64.

White, R., Morganstein, D., Christian, M., Seth, A., Herzog, B. & Parker, M. G. (2008), 'Role of RIP140 in metabolic tissues: connections to disease', *FEBS letters* **582**(1), 39–45.

Willson, T. M., Brown, P. J., Sternbach, D. D. & Henke, B. R. (2000), 'The PPARs: from orphan receptors to drug discovery', *Journal of medicinal chemistry* **43**(4), 527–550.

Wise, D. R., DeBerardinis, R. J., Mancuso, A., Sayed, N., Zhang, X.-Y., Pfeiffer, H. K., Nissim, I., Daikhin, E., Yudkoff, M., McMahon, S. B. et al. (2008), 'Myc regulates a transcriptional program that stimulates mitochondrial glutaminolysis and leads to glutamine addiction', *Proceedings of the National Academy of Sciences* **105**(48), 18782–18787.

Wold, S., Esbensen, K. & Geladi, P. (1987), 'Principal component analysis', *Chemometrics and intelligent laboratory systems* **2**(1), 37–52.

Wolfgang, C. D., Essand, M., Vincent, J. J., Lee, B. & Pastan, I. (2000), 'TARP: a nuclear protein expressed in prostate and breast cancer cells derived from an alternate reading frame of the t cell receptor γ chain locus', *Proceedings of the National Academy of Sciences* **97**(17), 9437–9442.

Wright, D. C., Han, D.-H., Garcia-Roves, P. M., Geiger, P. C., Jones, T. E. & Holloszy, J. O. (2007), 'Exercise-induced mitochondrial biogenesis begins before the increase in muscle PGC-1α expression', *Journal of Biological Chemistry* **282**(1), 194–199.

Wu, Z., Puigserver, P., Andersson, U., Zhang, C., Adelmant, G., Mootha, V., Troy, A., Cinti, S., Lowell, B., Scarpulla, R. C. et al. (1999), 'Mechanisms controlling mitochondrial biogenesis and respiration through the thermogenic coactivator PGC-1', *Cell* **98**(1), 115–124.

Yang, J., Wang, H., Wang, W. & Yu, P. (2003), Enhanced biclustering on expression data, *in* 'Bioinformatics and Bioengineering, 2003. Proceedings. Third IEEE Symposium on', IEEE, pp. 321–327.

Yang, J., Wang, H., Wang, W. & Yu, P. S. (2005), 'An improved biclustering method for analyzing gene expression profiles', *International Journal on Artificial Intelligence Tools* **14**(05), 771–789.

Yang, Z.-F., Mott, S. & Rosmarin, A. G. (2007), 'The Ets transcription factor GABP is required for cell-cycle progression', *Nature cell biology* **9**(3), 339–346.

Yang, Zhifen & Klionsky, D. J. (2010), 'Eaten alive: a history of macroautophagy', *Nature cell biology* **12**(9), 814–822.

Yeo, H. C., Beh, T. T., Quek, J., Koh, G., Chan, K. & Lee, D.-Y. (2011), 'Integrated transcriptome and binding sites analysis implicates E2F in the regulation of self-renewal in human pluripotent stem cells', *PloS one* **6**(11), e27231–e27231.

Youle, Richard J & Narendra, D. P. (2011), 'Mechanisms of mitophagy', *Nature reviews Molecular cell biology* **12**(1), 9–14.

Youle, Richard J & Van Der Bliek, A. M. (2012), 'Mitochondrial fission, fusion, and stress', *Science* **337**(6098), 1062–1065.

Yu-Wai-Man, P., Griffiths, P. G., Hudson, G. & Chinnery, P. F. (2009), 'Inherited mitochondrial optic neuropathies', *Journal of medical genetics* **46**(3), 145–158.

Yuneva, M. (2008), 'Finding an achilles heel of cancer: the role of glucose and glutamine metabolism in the survival of transformed cells', *Cell Cycle* **7**(14), 2083–2089.

Zardavas, D., Irrthum, A., Swanton, C. & Piccart, M. (2015), 'Clinical management of breast cancer heterogeneity', *Nature reviews Clinical oncology* **12**(7), 381–394.

Zhang, X., Zuo, X., Yang, B., Li, Z., Xue, Y., Zhou, Y., Huang, J., Zhao, X., Zhou, J., Yan, Y. et al. (2014), 'MicroRNA directly enhances mitochondrial translation during muscle differentiation', *Cell* **158**(3), 607–619.

Zhang, Y., Goldman, S., Baerga, R., Zhao, Y., Komatsu, M. & Jin, S. (2009), 'Adipose-specific deletion of autophagy-related gene 7 (atg7) in mice reveals a role in adipogenesis', *Proceedings of the National Academy of Sciences* **106**(47), 19860–19865.

Appendix A

MCbiclust - an R package for massively correlated biclustering

A.1 About

Massively Correlating Biclustering (MCbiclust) is a R package for running massively correlating biclustering analysis on gene expression data in the manner described in Chapter 2. All results in this work produced using the MCbiclust method were done in R using this package which was created in the course of my PhD. The code to run the package with a tutorial to explain its use is currently available on github: `https://github.com/rbentham/MCbiclust`

A.2 Installation

Four steps need to be followed to install MCbiclust:

1. Create a folder called MCbiclust containing all the files on the github.

2. On terminal/command line, go to the directory containing the MCbiclust folder.

3. Run command R CMD build MCbiclust on the terminal/command line. This builds the file MCbi- clust_1.0.0.tar.gz

4. While running R the package can now be installed from source

```
install.packages(path.to.file, repos = NULL, type="source")
```

Where “path.to.file” on windows will be replaced by the path to the file e.g. for windows *C:*

MCbiclust_1.0.0.tar.gz or on linux or mac */Users/bobbybentham/MCbiclust_1.0.0.tar.gz*

The package can now be loaded, with others that are necessary for the analysis as follows:

```
library(MCbiclust)
library(gplots)
library(ggplot2)
```

A.3 Example workflow

For this example analysis, the aim is to find biclusters related to mitochondrial function in the cancer cell line encyclopedia. For this two datasets are needed, both of which are available on the MCbiclust package. The first in *CCLE_data* that contains the gene expression values found in the Cancer Cell Line Encyclopedia (CCLE) data set, the second, *Mitochondrial_genes*, is a list of mitochondrial genes that can be found from MitoCarta1.0.

```
data(CCLE_data)
data(Mitochondrial_genes)
```

It is a simple procedure to create a new matrix *CCLE.mito* only containing the mitochondrial genes. While there are 1023 known mitochondrial genes, not all of these are measured in *CCLE_data*.

```
mito.loc <- which(as.character(CCLE_data[,2]) %in%
   Mitochondrial_genes)
CCLE.mito <- CCLE_data[mito.loc,-c(1,2)]
row.names(CCLE.mito) <- CCLE_data[mito.loc,2]
```

The first step in using MCbiclust is to find a subset of samples that have the most highly correlating genes in the chosen gene expression matrix. This is done by, calculating the associated correlation matrix and then calculating the absolute mean of the correlations, as a correlation score.

This is achieved with function *FindSeed()*, the argument gem stands for gene expression matrix, seed.size indicates the size of the subset of samples that is sought.

iterations indicates how many iterations of the algorithm to carry out before stopping, in general the higher the iterations the more optimal the solution in terms of maximising the strength of the correlation.

For reproducibility set.seed has been used to set Rs pseudo-random number generator. It should also be noted that the for gem the data matrix can not contain all the genes, since *FindSeed()* involves the calculation of correlation matrices which are not computationally efficient to compute if they involve greater than ≈1000 genes.

```
set.seed(102)
CCLE.seed <- FindSeed(gem = CCLE.mito,
                  seed.size = 10,
                  iterations = 10000)
```

The results of FindSeed can also be visualised by examining the associated correlation matrix, and viewing the result as a heatmap.

```
CCLE.mito.cor <- cor(t(CCLE.mito[,CCLE.seed]))
heatmap.2(CCLE.mito.cor,trace = "none")
```

heatmap.2 is a function from the gplots R package. As can be clearly seen from the heat map, not all the mitochondrial genes are equally strongly correlated to each other. There is a function in MCbiclust which automatically selects those genes that are most strongly associated with the pattern. This function is *HclustGenesHiCor()* and it works by using hierarchical clustering to select the genes into n different groups, and then discarding any of these groups that fails to have a correlation score greater than the correlation score from all the genes together.

```
CCLE.hicor.genes <- HclustGenesHiCor(CCLE.mito,CCLE.seed,cuts = 8)
CCLE.mito.cor2 <-
    cor(t(CCLE.mito[as.numeric(CCLE.hicor.genes),CCLE.seed]))
CCLE.heat <- heatmap.2(CCLE.mito.cor2,trace = "none")
```

Figure A.1 shows the outputs of *heatmap.2()* of the correlation matrix before and after the selection of the highly correlated mitochondrial genes.

Non-mitochondrial genes are likely also involved in this pattern and it is important to identify them. All genes can be measured by how they match to this pattern in two steps. The first step is to summarise this pattern. This is done by finding a subset of genes

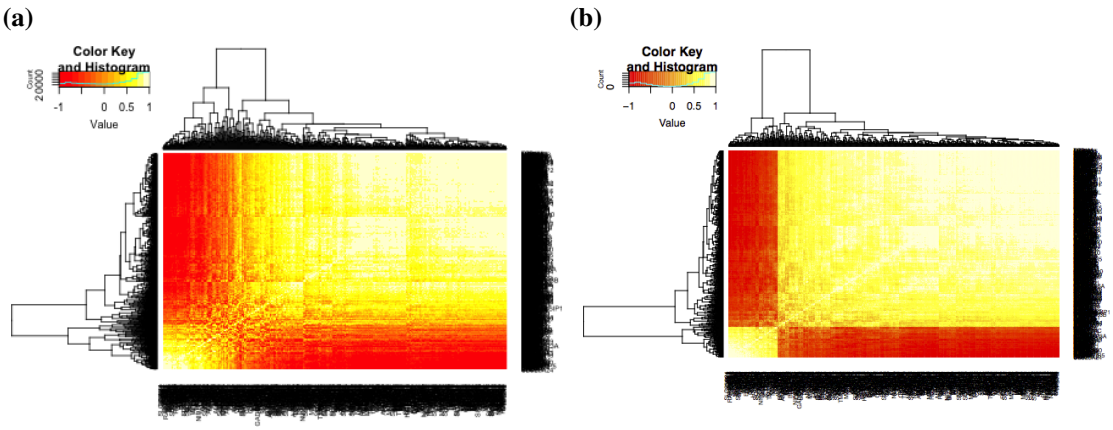

Figure A.1: Heatmap of correlation matrix before and after selection of genes.

which all strongly correlate with each other, and calculating their average expression value. The function *GeneVecFun()* achieves this step. Similarly to *HclustGenesHiCor()* the genes are clustered into groups using hierarchical clustering, but the best group is judged by the correlation score multiplied by the square root of the number of genes. This is done to bias against selecting a group of very small genes. The second function *CalcCorVector()* calculates the correlation vector by calculating the correlation of the average expression value found in the first step to every gene measured in the data set. This value is called the correlation vector.

```
CCLE.gene.vec <- GeneVecFun(CCLE.mito, CCLE.seed, 10) CCLE.cor.vec
    <- CalcCorVector(gene.vec = CCLE.gene.vec,
gem = CCLE_data[,-c(1,2)][,CCLE.seed])
```

Using the calculated correlation vector, it is a relatively simple task to perform gene set enrichment. This can be done on any platform (e.g. DAVID, gprofiler, etc.) but MCbiclust comes with an inbuilt function for calculating gene ontology (GO) enrichment values using the Mann-Whitney non-parametric test.

```
GSE.MW <- GOEnrichmentAnalysis(gene.names =
    as.character(CCLE_data[,2]), gene.values = CCLE.cor.vec,
                        sig.rate = 0.05)
```

Already all the genes in the data set have had the correlation calculated to the pattern found. One more task that can be readily done is to order the samples according to the strength of correlation. Function *FindSeed()* found the initial *n* samples that had a

very strong correlation with the gene set of interest, the $n+1$ sample is to be selected as that sample which best maintains the correlation strength, this process can be simply repeated until all or the desired number of samples are ordered.

SampleSort() is the function in MCbiclust that completes this procedure, it has 4 main inputs, the first is the gene expression matrix with all the samples and the gene set of interest. seed is the initial subsample found with FindSeed. For increasing what can be a very slow computation, the code can be run on multiple cores, with the number of cores selected from the argument num.cores and instead of sorting the entire length, only the first sort.length samples need to be ordered.

```
CCLE.samp.sort <-
    SampleSort(CCLE.mito[as.numeric(CCLE.hicor.genes),], seed =
    CCLE.seed,num.cores = 3,
                      sort.length = 100)
```

Once the samples have been sorted it is possible to summarise the correlation pattern found using principal component analysis (PCA).

The first principal component (PC1) captures the highest variance within the data, so if PCA is run on the found bicluster with very strong correlations between the genes, PC1 will be a variable that summarises this correlation. *PC1VecFun()* is a function that calculates the PC1 values for all sorted samples. It takes three inputs:

1. *top.gem*: the gene expression matrix with only the most highly correlated genes but with all the sample data.

2. *seed.sort*: is the sorting of the data samples found with function *SampleSort()*.

3. *n*: the number of samples used for initially calculating the weighting of PC1. If set to 10, the first 10 samples are used to calculate the weighting of PC1 and then the value of PC1 is calculated for all samples in the ordering.

```
top.mat <- CCLE.mito[as.numeric(CCLE.hicor.genes),]
pc1.vec <- PC1VecFun(top.gem = top.mat, seed.sort = CCLE.samp.sort,
   n = 10)
```

Once the samples have been ordered and PC1 and the average gene sets calculated it is a simple procedure to produce plots of these against the ordered samples. This is

done here using the *ggplot2* package.

```
CCLE.df <- data.frame(CCLE.name =
    colnames(CCLE_data)[-c(1,2)][CCLE.samp.sort],
           PC1 = pc1.vec,
           Order = seq(length = length(pc1.vec)))

ggplot(CCLE.df, aes(Order,PC1)) + geom_point() + ylab("PC1")
```

The output for this code is shown in Figure A.2.

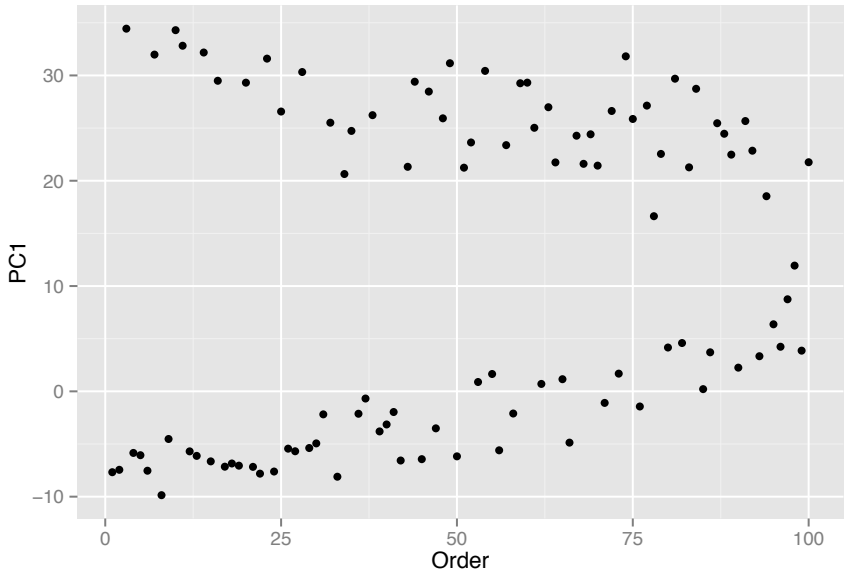

Figure A.2: PC1 of the first 100 samples in a bicluster found in the CCLE data.

The R package contains other functions involved in the MCbiclust analysis such as for setting up and dealing with multiple runs. For further and more detailed information on the use of MCbiclust, there is a tutorial on the github site.

Appendix B

Gene set enrichment result tables

Table B.1: Gene set enrichment results of average correlation vector for biclustering pattern $E1$ found in *E. coli* analysis in Section 2.4.3, showing 175 significant terms with adjusted p value < 0.05.

GOID	TERM	Number of genes	Genes in genelist	p value	Average correlation vector
GO:0044237	cellular metabolic process	1606	1599	1.534E-101	0.357
GO:0009058	biosynthetic process	967	962	2.068E-101	0.447
GO:0008152	metabolic process	1781	1775	2.919E-97	0.333
GO:0009987	cellular process	1891	1884	1.310E-88	0.308
GO:0006807	nitrogen compound metabolic process	1041	1038	1.531E-74	0.373
GO:0006725	cellular aromatic compound metabolic process	751	748	1.598E-68	0.417
GO:0006139	nucleobase-containing compound metabolic process	724	721	1.789E-66	0.419
GO:0009059	macromolecule biosynthetic process	515	510	4.706E-63	0.463
GO:0019538	protein metabolic process	323	318	6.877E-43	0.483
GO:0006412	translation	146	140	5.152E-39	0.673
GO:0006796	phosphate-containing compound metabolic process	445	444	4.044E-38	0.398
GO:0006793	phosphorus metabolic process	462	461	9.151E-37	0.383
GO:0019438	aromatic compound biosynthetic process	407	407	4.102E-33	0.380
GO:0016070	RNA metabolic process	364	365	1.580E-32	0.409
Intergenic	Intergenic	3083	3083	6.670E-29	-0.168
GO:0065007	biological regulation	466	466	9.386E-28	0.332
GO:0008610	lipid biosynthetic process	128	129	1.004E-27	0.609
GO:0055086	nucleobase-containing small molecule metabolic process	260	259	1.004E-27	0.437
GO:0009117	nucleotide metabolic process	232	231	4.589E-25	0.436
GO:0050896	response to stimulus	503	502	1.452E-23	0.296
GO:0006629	lipid metabolic process	155	156	1.828E-23	0.513
GO:0019752	carboxylic acid metabolic process	364	364	1.127E-20	0.313
GO:0051186	cofactor metabolic process	147	147	3.588E-20	0.503
GO:0009165	nucleotide biosynthetic process	111	111	4.126E-19	0.549
GO:0009116	nucleoside metabolic process	159	158	7.772E-19	0.467
GO:0006950	response to stress	323	322	1.019E-18	0.338
GO:0006399	tRNA metabolic process	63	64	3.695E-18	0.741
GO:0006396	RNA processing	66	67	4.407E-18	0.729
GO:0051188	cofactor biosynthetic process	113	113	4.982E-18	0.551
NonIntergenic	NonIntergenic	4376	4376	8.284E-18	0.090
GO:0016051	carbohydrate biosynthetic process	107	108	1.087E-17	0.532
GO:0006520	cellular amino acid metabolic process	251	251	1.342E-17	0.353
GO:0006259	DNA metabolic process	149	146	1.498E-16	0.464
GO:0009163	nucleoside biosynthetic process	53	53	3.990E-16	0.747
GO:0042455	ribonucleoside biosynthetic process	51	51	4.494E-16	0.757
GO:0006163	purine nucleotide metabolic process	145	144	8.263E-16	0.444
GO:0034470	ncRNA processing	59	60	1.987E-15	0.716
GO:0010468	regulation of gene expression	296	296	4.191E-15	0.306
GO:0000271	polysaccharide biosynthetic process	86	87	7.742E-15	0.539
GO:0043412	macromolecule modification	147	147	1.408E-14	0.423
GO:0044262	cellular carbohydrate metabolic process	149	150	1.563E-14	0.406

GOID	TERM	Number of genes	Genes in genelist	p value	Average correlation vector
GO:0008653	lipopolysaccharide metabolic process	64	65	2.450E-14	0.613
GO:0009103	lipopolysaccharide biosynthetic process	64	65	2.450E-14	0.613
GO:0009056	catabolic process	393	392	4.429E-14	0.255
GO:0005975	carbohydrate metabolic process	306	307	2.111E-13	0.269
GO:0006164	purine nucleotide biosynthetic process	48	48	3.266E-13	0.700
GO:0044248	cellular catabolic process	248	247	8.536E-13	0.307
GO:0009152	purine ribonucleotide biosynthetic process	46	46	1.387E-12	0.697
GO:0009451	RNA modification	54	54	2.157E-12	0.680
GO:0007049	cell cycle	57	57	2.564E-12	0.662
GO:0048519	negative regulation of biological process	94	94	6.814E-12	0.501
GO:0006644	phospholipid metabolic process	52	52	9.108E-12	0.674
GO:0051301	cell division	53	53	3.279E-11	0.655
GO:0010608	posttranscriptional regulation of gene expression	48	48	6.068E-11	0.662
GO:0008654	phospholipid biosynthetic process	48	48	7.703E-11	0.670
GO:0051171	regulation of nitrogen compound metabolic process	261	261	1.570E-10	0.273
GO:0006351	transcription, DNA-templated	255	255	2.176E-10	0.274
GO:0008652	cellular amino acid biosynthetic process	169	169	3.171E-10	0.335
GO:0019439	aromatic compound catabolic process	141	140	4.758E-10	0.377
GO:0034655	nucleobase-containing compound catabolic process	135	134	7.567E-10	0.380
GO:0042254	ribosome biogenesis	33	33	1.952E-09	0.748
GO:0032774	RNA biosynthetic process	202	202	2.518E-09	0.294
GO:0006417	regulation of translation	39	39	4.513E-09	0.682
GO:0033554	cellular response to stress	201	201	6.268E-09	0.303
GO:0015949	nucleobase-containing small molecule interconversion	36	36	7.690E-09	0.715
GO:0051252	regulation of RNA metabolic process	248	248	1.034E-08	0.256
GO:0009312	oligosaccharide biosynthetic process	37	37	1.397E-08	0.661
GO:0008360	regulation of cell shape	33	33	2.599E-08	0.696
GO:0006418	tRNA aminoacylation for protein translation	25	25	2.649E-08	0.807
GO:0008033	tRNA processing	36	37	2.908E-08	0.685
GO:0043039	tRNA aminoacylation	26	26	3.631E-08	0.787
GO:2001141	regulation of RNA biosynthetic process	245	245	4.303E-08	0.249
GO:0000910	cytokinesis	38	38	4.428E-08	0.674
GO:0015992	proton transport	44	44	5.604E-08	0.583
GO:0006355	regulation of transcription, DNA-templated	244	244	6.261E-08	0.246
GO:0009244	lipopolysaccharide core region biosynthetic process	22	22	7.676E-08	0.833
GO:0016310	phosphorylation	151	151	8.269E-08	0.311
GO:0006974	cellular response to DNA damage stimulus	159	159	8.927E-08	0.323
GO:0009628	response to abiotic stimulus	83	82	1.978E-07	0.442
GO:0006261	DNA-dependent DNA replication	39	39	2.009E-07	0.619
GO:0032259	methylation	50	50	2.250E-07	0.532
GO:0000270	peptidoglycan metabolic process	39	39	3.249E-07	0.620
GO:0006260	DNA replication	49	49	4.460E-07	0.535
GO:0009311	oligosaccharide metabolic process	47	47	4.641E-07	0.526
GO:0055114	oxidation-reduction process	331	331	5.225E-07	0.190
GO:0006364	rRNA processing	24	24	1.273E-06	0.763
GO:0010629	negative regulation of gene expression	58	58	1.631E-06	0.493
GO:0009266	response to temperature stimulus	42	42	1.874E-06	0.598
GO:0016072	rRNA metabolic process	25	25	1.951E-06	0.738
GO:0006633	fatty acid biosynthetic process	38	38	2.365E-06	0.552
NanR	NanR	1229	1232	2.413E-06	0.092
GO:0006006	glucose metabolic process	49	49	2.460E-06	0.501
GO:0044036	cell wall macromolecule metabolic process	33	33	2.589E-06	0.620
GO:0006119	oxidative phosphorylation	27	27	3.489E-06	0.659
GO:0044038	cell wall macromolecule biosynthetic process	30	30	3.543E-06	0.648
GO:0009273	peptidoglycan-based cell wall biogenesis	30	30	4.150E-06	0.647
GO:0006400	tRNA modification	28	28	5.011E-06	0.684
GO:0045892	negative regulation of transcription, DNA-templated	54	54	5.799E-06	0.492
GO:0046677	response to antibiotic	64	63	7.661E-06	0.418
GO:0019646	aerobic electron transport chain	22	22	8.821E-06	0.746
GO:0009252	peptidoglycan biosynthetic process	29	29	1.108E-05	0.638
GO:0006281	DNA repair	61	61	1.669E-05	0.446
GO:0006096	glycolysis	21	21	2.046E-05	0.770
GO:0001510	RNA methylation	24	24	2.255E-05	0.691
GO:0006007	glucose catabolic process	32	32	2.500E-05	0.578
GO:0009243	O antigen biosynthetic process	13	14	2.709E-05	0.824

GOID	TERM	Number of genes	Genes in genelist	p value	Average correlation vector
GO:0042221	response to chemical	168	167	3.069E-05	0.229
GO:0009166	nucleotide catabolic process	103	102	4.148E-05	0.318
GO:0009164	nucleoside catabolic process	103	102	5.016E-05	0.313
GO:0006152	purine nucleoside catabolic process	99	98	8.512E-05	0.314
GO:0006508	proteolysis	58	59	1.014E-04	0.429
GO:0009991	response to extracellular stimulus	48	48	1.132E-04	0.476
GO:0046034	ATP metabolic process	87	87	1.357E-04	0.320
GO:0046474	glycerophospholipid biosynthetic process	21	21	1.474E-04	0.705
GO:0006744	ubiquinone biosynthetic process	16	16	1.489E-04	0.766
GO:0071555	cell wall organization	23	23	1.562E-04	0.668
GO:0042454	ribonucleoside catabolic process	101	100	1.626E-04	0.302
GO:0009226	nucleotide-sugar biosynthetic process	19	19	1.822E-04	0.636
GO:0017148	negative regulation of translation	19	19	1.924E-04	0.697
GO:0009408	response to heat	25	25	2.000E-04	0.677
GO:0015031	protein transport	50	50	2.248E-04	0.414
GO:0009156	ribonucleoside monophosphate biosynthetic process	35	35	2.345E-04	0.527
GO:0009143	nucleoside triphosphate catabolic process	97	96	2.409E-04	0.303
GO:0009636	response to toxic substance	75	74	2.868E-04	0.325
GO:0009225	nucleotide-sugar metabolic process	23	23	3.486E-04	0.553
GO:0046365	monosaccharide catabolic process	64	64	4.978E-04	0.362
GO:0090305	nucleic acid phosphodiester bond hydrolysis	44	45	5.538E-04	0.445
GO:0006760	folic acid-containing compound metabolic process	21	21	7.530E-04	0.656
GO:0006886	intracellular protein transport	14	14	9.699E-04	0.729
GO:0006413	translational initiation	12	12	1.045E-03	0.802
GO:0006464	cellular protein modification process	79	79	1.045E-03	0.296
GO:0034220	ion transmembrane transport	95	95	1.186E-03	0.260
GO:0046654	tetrahydrofolate biosynthetic process	19	19	1.296E-03	0.673
GO:0042558	pteridine-containing compound metabolic process	22	22	1.432E-03	0.615
GO:0032506	cytokinetic process	16	16	1.528E-03	0.737
GO:0009432	SOS response	20	20	1.600E-03	0.706
GO:0009396	folic acid-containing compound biosynthetic process	20	20	1.789E-03	0.644
GO:0043241	protein complex disassembly	23	23	2.130E-03	0.577
GO:0006401	RNA catabolic process	15	15	2.156E-03	0.760
GO:0006310	DNA recombination	41	38	2.190E-03	0.465
GO:0043094	cellular metabolic compound salvage	15	15	2.223E-03	0.724
GO:0009060	aerobic respiration	57	57	2.449E-03	0.377
GO:0009246	enterobacterial common antigen biosynthetic process	11	12	2.449E-03	0.784
GO:0005996	monosaccharide metabolic process	98	98	3.003E-03	0.262
GO:0033014	tetrapyrrole biosynthetic process	20	20	3.188E-03	0.613
GO:0006779	porphyrin-containing compound biosynthetic process	18	18	4.315E-03	0.627
GO:0070475	rRNA base methylation	12	12	5.535E-03	0.772
GO:0031167	rRNA methylation	14	14	5.568E-03	0.714
GO:0019318	hexose metabolic process	79	79	5.768E-03	0.276
GO:0006812	cation transport	129	129	6.002E-03	0.207
Fis	Fis	515	520	7.273E-03	0.102
GO:0006811	ion transport	242	242	7.882E-03	0.145
GO:0006654	phosphatidic acid biosynthetic process	13	13	8.684E-03	0.727
GO:0000917	barrier septum assembly	13	13	9.061E-03	0.734
GO:0006221	pyrimidine nucleotide biosynthetic process	20	20	9.800E-03	0.598
GO:0006631	fatty acid metabolic process	57	57	1.040E-02	0.310
GO:0009168	purine ribonucleoside monophosphate biosynthetic process	22	22	1.040E-02	0.543
GO:0015990	electron transport coupled proton transport	23	23	1.040E-02	0.521
GO:0007059	chromosome segregation	12	12	1.146E-02	0.726
GO:0042773	ATP synthesis coupled electron transport	15	15	1.289E-02	0.665
GO:0006457	protein folding	31	31	1.373E-02	0.483
GO:0045454	cell redox homeostasis	15	15	1.377E-02	0.643
GO:0006353	DNA-templated transcription, termination	18	18	1.614E-02	0.584
GO:0016052	carbohydrate catabolic process	147	147	1.653E-02	0.188
GO:0006184	GTP catabolic process	20	19	1.785E-02	0.547
GO:0007155	cell adhesion	21	21	2.083E-02	-0.566
GO:0022610	biological adhesion	21	21	2.083E-02	-0.566
GO:0006783	heme biosynthetic process	12	12	2.285E-02	0.700
MarA	MarA	81	81	2.505E-02	0.259
GO:0031555	transcriptional attenuation	14	14	2.524E-02	0.658
GO:0009257	10-formyltetrahydrofolate biosynthetic process	11	11	2.602E-02	0.735

GOID	TERM	Number of genes	Genes in genelist	p value	Average correlation vector
Cra	Cra	52	53	3.519E-02	0.328
GO:0006810	transport	546	547	3.574E-02	0.077
GO:0042168	heme metabolic process	11	11	4.150E-02	0.693
GO:0045333	cellular respiration	109	109	4.456E-02	0.219

Table B.2: Gene set enrichment results of average correlation vector for biclustering pattern $E2$ found in *E. coli* analysis in Section 2.4.3, showing 25 significant terms with adjusted p value < 0.05.

GOID	TERM	Number of genes	Genes in genelist	p value	Average correlation vector
Intergenic	Intergenic	3083	3083	1.603E-28	-0.109
NonIntergenic	NonIntergenic	4376	4376	1.518E-17	0.132
Sigma 70	Sigma 70	1262	1267	3.446E-14	0.176
Sigma 38	Sigma 38	1048	1053	2.508E-12	0.178
NanR	NanR	1229	1232	1.589E-07	0.147
Sigma 24	Sigma 24	393	395	1.666E-07	0.211
GO:0009432	SOS response	20	20	2.764E-05	-0.645
GO:0001539	ciliary or bacterial-type flagellar motility	21	21	1.138E-04	0.649
Fis	Fis	515	520	1.971E-04	0.162
GO:0006928	cellular component movement	31	31	2.741E-04	0.525
IclR	IclR	523	526	2.741E-04	0.164
GO:0009061	anaerobic respiration	76	76	5.137E-04	0.372
GO:0006935	chemotaxis	21	21	5.685E-04	0.652
GO:0042330	taxis	21	21	5.685E-04	0.652
GO:0045333	cellular respiration	109	109	7.049E-04	0.314
GO:0042126	nitrate metabolic process	19	19	1.587E-03	0.595
GO:0042128	nitrate assimilation	19	19	1.587E-03	0.595
GO:0048870	cell motility	24	24	1.687E-03	0.550
GO:0055114	oxidation-reduction process	331	331	3.403E-03	0.182
GO:0019752	carboxylic acid metabolic process	364	364	4.308E-03	0.176
NarL	NarL	180	183	7.068E-03	0.216
Sigma 32	Sigma 32	323	325	2.265E-02	0.165
GO:0008652	cellular amino acid biosynthetic process	169	169	2.613E-02	0.220
GO:0000105	histidine biosynthetic process	12	12	3.900E-02	0.695
GO:0009246	enterobacterial common antigen biosynthetic process	11	12	4.271E-02	-0.668

Table B.3: Gene set enrichment results of average correlation vector for biclustering pattern $E3$ found in *E. coli* analysis in Section 2.4.3, showing 196 significant terms with adjusted p value < 0.05.

GOID	TERM	Number of genes	Genes in genelist	p value	Average correlation vector
Intergenic	Intergenic	3083	3083	2.355E-299	-0.422
NonIntergenic	NonIntergenic	4376	4376	1.076E-187	0.622
GO:0009987	cellular process	1891	1884	1.488E-138	0.713
GO:0008152	metabolic process	1781	1775	6.671E-136	0.718
GO:0044237	cellular metabolic process	1606	1599	7.931E-125	0.720
GO:0006807	nitrogen compound metabolic process	1041	1038	2.040E-103	0.748
Sigma 70	Sigma 70	1262	1267	3.553E-84	0.634
GO:0009058	biosynthetic process	967	962	1.830E-81	0.721
GO:0006725	cellular aromatic compound metabolic process	751	748	8.023E-77	0.752
GO:0006139	nucleobase-containing compound metabolic process	724	721	3.425E-74	0.748
Sigma 38	Sigma 38	1048	1053	6.636E-74	0.638
NanR	NanR	1229	1232	4.557E-73	0.630
GO:0006796	phosphate-containing compound metabolic process	445	444	4.510E-47	0.744
GO:0006793	phosphorus metabolic process	462	461	6.877E-47	0.736
GO:0009059	macromolecule biosynthetic process	515	510	1.085E-40	0.703
GO:0019438	aromatic compound biosynthetic process	407	407	2.090E-37	0.731
GO:0050896	response to stimulus	503	502	2.101E-37	0.705
GO:0006810	transport	546	547	1.223E-36	0.666
GO:0009056	catabolic process	393	392	5.703E-35	0.723
GO:0019752	carboxylic acid metabolic process	364	364	2.641E-33	0.722

GOID	TERM	Number of genes	Genes in genelist	p value	Average correlation vector
GO:0065007	biological regulation	466	466	5.597E-33	0.691
GO:0055086	nucleobase-containing small molecule metabolic process	260	259	1.368E-32	0.786
GO:0016070	RNA metabolic process	364	365	3.484E-32	0.706
Fis	Fis	515	520	3.831E-32	0.629
IclR	IclR	523	526	7.372E-29	0.606
GO:0044248	cellular catabolic process	248	247	1.131E-28	0.763
GO:0009117	nucleotide metabolic process	232	231	1.958E-28	0.782
Sigma 24	Sigma 24	393	395	4.353E-27	0.613
GO:0019538	protein metabolic process	323	318	3.487E-26	0.730
Sigma 32	Sigma 32	323	325	5.505E-24	0.639
GO:0006950	response to stress	323	322	1.925E-22	0.700
GO:0009116	nucleoside metabolic process	159	158	3.166E-22	0.810
GO:0055114	oxidation-reduction process	331	331	3.305E-21	0.698
Dan	Dan	270	271	4.200E-21	0.670
GO:0006163	purine nucleotide metabolic process	145	144	6.395E-21	0.823
GO:0010468	regulation of gene expression	296	296	3.675E-20	0.676
GO:0005975	carbohydrate metabolic process	306	307	7.545E-20	0.671
GO:0006520	cellular amino acid metabolic process	251	251	1.546E-19	0.705
GO:0006629	lipid metabolic process	155	156	2.850E-18	0.744
GO:0051171	regulation of nitrogen compound metabolic process	261	261	4.819E-18	0.675
GO:0006259	DNA metabolic process	149	146	5.088E-18	0.770
GO:0051186	cofactor metabolic process	147	147	2.094E-17	0.778
GO:0006351	transcription, DNA-templated	255	255	3.798E-17	0.675
GO:0034655	nucleobase-containing compound catabolic process	135	134	8.923E-17	0.779
GO:0019439	aromatic compound catabolic process	141	140	1.773E-16	0.776
GO:0051188	cofactor biosynthetic process	113	113	3.088E-16	0.819
GO:0008610	lipid biosynthetic process	128	129	3.508E-16	0.744
GO:2001141	regulation of RNA biosynthetic process	245	245	3.604E-16	0.668
GO:0043412	macromolecule modification	147	147	3.891E-16	0.766
GO:0051252	regulation of RNA metabolic process	248	248	4.314E-16	0.664
GO:0006355	regulation of transcription, DNA-templated	244	244	6.069E-16	0.667
GO:0033554	cellular response to stress	201	201	1.909E-14	0.707
GO:0009165	nucleotide biosynthetic process	111	111	2.314E-14	0.819
GO:0009164	nucleoside catabolic process	103	102	2.872E-14	0.804
GO:0006152	purine nucleoside catabolic process	99	98	6.220E-14	0.805
GO:0006811	ion transport	242	242	7.101E-14	0.653
GO:0009143	nucleoside triphosphate catabolic process	97	96	7.850E-14	0.803
GO:0009166	nucleotide catabolic process	103	102	9.210E-14	0.791
GO:0042454	ribonucleoside catabolic process	101	100	1.059E-13	0.802
GO:0032774	RNA biosynthetic process	202	202	3.378E-13	0.675
GO:0006396	RNA processing	66	67	2.682E-12	0.844
GO:0046034	ATP metabolic process	87	87	3.332E-12	0.813
NarL	NarL	180	183	5.020E-12	0.660
NarP	NarP	121	123	7.697E-12	0.669
GO:0006974	cellular response to DNA damage stimulus	159	159	8.242E-12	0.704
GO:0006200	ATP catabolic process	78	78	1.421E-11	0.810
GO:0008652	cellular amino acid biosynthetic process	169	169	1.777E-11	0.658
GO:0006399	tRNA metabolic process	63	64	1.982E-11	0.826
GO:0042221	response to chemical	168	167	4.385E-11	0.671
GO:0034470	ncRNA processing	59	60	1.031E-10	0.838
GO:0055085	transmembrane transport	191	191	1.831E-10	0.640
MqsA	MqsA	156	157	1.976E-10	0.635
GO:0016310	phosphorylation	151	151	2.219E-10	0.699
GO:0044262	cellular carbohydrate metabolic process	149	150	1.008E-09	0.646
CRP	CRP	243	247	1.226E-09	0.593
GO:0009451	RNA modification	54	54	2.731E-09	0.823
GO:0016051	carbohydrate biosynthetic process	107	108	3.069E-09	0.708
GO:0006812	cation transport	129	129	3.605E-09	0.700
GO:0048519	negative regulation of biological process	94	94	8.481E-09	0.740
GO:0008033	tRNA processing	36	37	8.829E-09	0.875
CpxR	CpxR	83	83	9.030E-09	0.766
GO:0008653	lipopolysaccharide metabolic process	64	65	1.487E-08	0.744
GO:0009103	lipopolysaccharide biosynthetic process	64	65	1.487E-08	0.744
Sigma 28	Sigma 28	105	105	1.781E-08	0.729
GO:0006281	DNA repair	61	61	3.519E-08	0.808

GOID	TERM	Number of genes	Genes in genelist	p value	Average correlation vector
GO:0000271	polysaccharide biosynthetic process	86	87	4.580E-08	0.687
GO:0006508	proteolysis	58	59	1.168E-07	0.788
OmpR	OmpR	109	110	1.736E-07	0.606
MarA	MarA	81	81	2.014E-07	0.722
GO:0006412	translation	146	140	3.275E-07	0.675
GO:0090305	nucleic acid phosphodiester bond hydrolysis	44	45	3.317E-07	0.851
HNS	HNS	140	141	4.527E-07	0.618
GO:0015031	protein transport	50	50	5.743E-07	0.780
ArcA	ArcA	173	175	9.078E-07	0.557
GO:0006400	tRNA modification	28	28	9.087E-07	0.882
GO:0007049	cell cycle	57	57	9.970E-07	0.788
GO:0009163	nucleoside biosynthetic process	53	53	1.016E-06	0.822
GO:0016052	carbohydrate catabolic process	147	147	2.403E-06	0.645
GO:0006644	phospholipid metabolic process	52	52	2.485E-06	0.733
Fur	Fur	143	145	2.614E-06	0.612
GO:0009636	response to toxic substance	75	74	2.867E-06	0.728
GO:0042455	ribonucleoside biosynthetic process	51	51	3.853E-06	0.819
GO:0008654	phospholipid biosynthetic process	48	48	4.478E-06	0.739
GO:0051301	cell division	53	53	5.975E-06	0.810
GO:0006164	purine nucleotide biosynthetic process	48	48	6.153E-06	0.860
GO:0006464	cellular protein modification process	79	79	7.999E-06	0.743
GO:0006310	DNA recombination	41	38	9.754E-06	0.757
GO:0006790	sulfur compound metabolic process	66	66	1.142E-05	0.745
GO:0046677	response to antibiotic	64	63	1.155E-05	0.723
NagC	NagC	111	112	1.296E-05	0.605
GO:0048518	positive regulation of biological process	59	59	1.494E-05	0.733
AsnC	AsnC	125	127	1.668E-05	0.533
GO:0032259	methylation	50	50	1.907E-05	0.762
GO:0006260	DNA replication	49	49	2.006E-05	0.745
Rob	Rob	75	75	2.137E-05	0.656
ExuR	ExuR	62	62	2.673E-05	0.689
GO:0009605	response to external stimulus	69	69	3.199E-05	0.818
GO:0006865	amino acid transport	70	70	3.415E-05	0.673
IHF	IHF	117	117	3.532E-05	0.607
GO:0009152	purine ribonucleotide biosynthetic process	46	46	4.026E-05	0.857
PhoB	PhoB	56	56	4.056E-05	0.695
GO:0006261	DNA-dependent DNA replication	39	39	4.427E-05	0.771
GO:0007165	signal transduction	74	74	4.807E-05	0.690
GO:0005996	monosaccharide metabolic process	98	98	4.891E-05	0.644
GO:0006631	fatty acid metabolic process	57	57	5.479E-05	0.735
GO:0030001	metal ion transport	59	59	1.401E-04	0.695
BaeR	BaeR	32	32	1.966E-04	0.810
GO:0045892	negative regulation of transcription, DNA-templated	54	54	2.394E-04	0.736
SoxS	SoxS	71	71	2.637E-04	0.627
GO:0022900	electron transport chain	83	83	2.726E-04	0.663
GO:0046942	carboxylic acid transport	86	86	2.887E-04	0.604
GO:0010629	negative regulation of gene expression	58	58	3.003E-04	0.708
GO:0009991	response to extracellular stimulus	48	48	3.611E-04	0.850
GO:0009628	response to abiotic stimulus	83	82	4.810E-04	0.710
Lrp	Lrp	100	100	4.980E-04	0.629
GO:0015949	nucleobase-containing small molecule interconversion	36	36	5.120E-04	0.829
GO:0042493	response to drug	49	49	6.174E-04	0.681
GO:0042254	ribosome biogenesis	33	33	6.682E-04	0.781
XylR	XylR	53	53	6.877E-04	0.672
GO:0045333	cellular respiration	109	109	7.087E-04	0.652
ArgR	ArgR	113	117	8.284E-04	0.558
Cra	Cra	52	53	1.494E-03	0.730
GO:0000270	peptidoglycan metabolic process	39	39	1.517E-03	0.809
GO:0000160	phosphorelay signal transduction system	62	62	1.929E-03	0.655
PhoP	PhoP	105	106	2.029E-03	0.578
ModE	ModE	31	31	2.381E-03	0.759
GO:0000910	cytokinesis	38	38	2.412E-03	0.769
GO:0019318	hexose metabolic process	79	79	2.412E-03	0.623
GO:0001510	RNA methylation	24	24	2.422E-03	0.812
GO:0034220	ion transmembrane transport	95	95	2.575E-03	0.621

GOID	TERM	Number of genes	Genes in genelist	p value	Average correlation vector
GO:0046474	glycerophospholipid biosynthetic process	21	21	2.575E-03	0.814
GO:0015833	peptide transport	32	32	2.639E-03	0.761
GO:0006006	glucose metabolic process	49	49	3.441E-03	0.780
GO:0009312	oligosaccharide biosynthetic process	37	37	4.176E-03	0.702
AgaR	AgaR	110	111	4.702E-03	0.514
GO:0009311	oligosaccharide metabolic process	47	47	4.839E-03	0.650
MetJ	MetJ	66	67	5.313E-03	0.587
GO:0006457	protein folding	31	31	6.344E-03	0.860
GO:0009156	ribonucleoside monophosphate biosynthetic process	35	35	6.504E-03	0.784
GO:0008360	regulation of cell shape	33	33	7.266E-03	0.800
GO:0006461	protein complex assembly	40	40	7.335E-03	0.682
FNR	FNR	92	92	7.593E-03	0.602
UlaR	UlaR	48	49	8.421E-03	0.587
NhaR	NhaR	39	40	1.002E-02	0.699
AraC	AraC	31	31	1.006E-02	0.803
GO:0007059	chromosome segregation	12	12	1.074E-02	0.910
GO:0043094	cellular metabolic compound salvage	15	15	1.079E-02	0.840
GO:0009061	anaerobic respiration	76	76	1.152E-02	0.637
GO:0006777	Mo-molybdopterin cofactor biosynthetic process	12	12	1.247E-02	0.851
DcuR	DcuR	42	43	1.356E-02	0.682
GO:0006633	fatty acid biosynthetic process	38	38	1.394E-02	0.695
GO:0009226	nucleotide-sugar biosynthetic process	19	19	1.516E-02	0.847
Nac	Nac	73	73	1.565E-02	0.487
GO:0009244	lipopolysaccharide core region biosynthetic process	22	22	1.659E-02	0.765
GO:0009273	peptidoglycan-based cell wall biogenesis	30	30	1.730E-02	0.794
GO:0044036	cell wall macromolecule metabolic process	33	33	1.759E-02	0.783
GO:0035556	intracellular signal transduction	45	45	1.845E-02	0.657
GO:0006744	ubiquinone biosynthetic process	16	16	1.957E-02	0.846
GO:0015698	inorganic anion transport	26	26	1.999E-02	0.765
GO:0006364	rRNA processing	24	24	2.045E-02	0.790
GO:0044038	cell wall macromolecule biosynthetic process	30	30	2.045E-02	0.794
PurR	PurR	51	51	2.045E-02	0.667
HipB	HipB	19	19	2.409E-02	0.819
GO:0010608	posttranscriptional regulation of gene expression	48	48	2.436E-02	0.705
GO:0042594	response to starvation	23	23	2.436E-02	0.873
GO:0006869	lipid transport	13	13	2.478E-02	0.899
GO:0007155	cell adhesion	21	21	2.639E-02	0.858
GO:0022610	biological adhesion	21	21	2.639E-02	0.858
GO:0009073	aromatic amino acid family biosynthetic process	24	24	3.227E-02	0.833
LexA	LexA	70	70	3.234E-02	0.627
GO:0046365	monosaccharide catabolic process	64	64	3.290E-02	0.641
GO:0016072	rRNA metabolic process	25	25	3.674E-02	0.757
CytR	CytR	40	40	3.691E-02	0.702
GO:0009168	purine ribonucleoside monophosphate biosynthetic process	22	22	3.799E-02	0.858
GO:0009252	peptidoglycan biosynthetic process	29	29	3.933E-02	0.790
GO:0009225	nucleotide-sugar metabolic process	23	23	4.710E-02	0.731

Table B.4: Gene set enrichment results of average correlation vector for biclustering pattern Mito.1 found in HCM analysis in Section 3.2.3.1, showing top 200 of 998 significant terms with adjusted p value < 0.05.

GOID	TERM	Number of genes	Genes in genelist	p value	Average correlation vector
GO:0002376	immune system process	3353	2069	2.732E-55	-0.159
GO:0006950	response to stress	4845	3064	2.589E-53	-0.125
GO:0044822	poly(A) RNA binding	1170	981	1.224E-52	-0.243
GO:0003723	RNA binding	1808	1303	3.869E-47	-0.195
GO:0031981	nuclear lumen	2785	1891	1.263E-45	-0.151
GO:0006952	defense response	1956	1337	2.033E-44	-0.178
GO:0044403	symbiosis, encompassing mutualism through parasitism	847	732	6.180E-42	-0.247
GO:0044419	interspecies interaction between organisms	847	732	6.180E-42	-0.247
GO:0051704	multi-organism process	2482	1902	2.540E-41	-0.143
GO:0006955	immune response	1821	1241	3.027E-41	-0.181
GO:0044428	nuclear part	3483	2230	1.044E-40	-0.130

GOID	TERM	Number of genes	Genes in genelist	p value	Average correlation vector
GO:0016032	viral process	770	669	4.063E-40	-0.253
GO:0050896	response to stimulus	13313	7013	6.567E-40	-0.061
GO:0044764	multi-organism cellular process	790	678	9.590E-40	-0.250
GO:0051716	cellular response to stimulus	10013	5706	6.741E-39	-0.068
GO:0007165	signal transduction	7988	4789	9.466E-38	-0.074
GO:0006613	cotranslational protein targeting to membrane	111	108	4.959E-36	-0.647
GO:0045047	protein targeting to ER	117	109	1.564E-35	-0.641
GO:0006614	SRP-dependent cotranslational protein targeting to membrane	109	106	3.958E-35	-0.646
GO:0005515	protein binding	12021	7591	4.086E-35	-0.056
GO:0005829	cytosol	3022	2475	6.585E-35	-0.114
GO:0016071	mRNA metabolic process	885	535	8.858E-35	-0.264
GO:0070972	protein localization to endoplasmic reticulum	135	127	1.119E-34	-0.583
GO:0071840	cellular component organization or biogenesis	7363	4521	1.403E-34	-0.077
GO:0072599	establishment of protein localization to endoplasmic reticulum	118	110	2.787E-34	-0.627
GO:0048518	positive regulation of biological process	6634	3876	3.634E-34	-0.083
GO:0045333	cellular respiration	221	148	1.127E-33	0.549
GO:0042254	ribosome biogenesis	188	139	1.254E-33	-0.537
GO:0044429	mitochondrial part	1081	711	1.331E-33	0.275
GO:0009605	response to external stimulus	2532	1822	1.632E-33	-0.128
GO:0007154	cell communication	9101	5346	4.062E-33	-0.063
GO:0023052	signaling	8975	5274	5.159E-33	-0.064
GO:0044700	single organism signaling	8975	5274	5.159E-33	-0.064
GO:0002684	positive regulation of immune system process	930	642	1.124E-32	-0.231
GO:0005925	focal adhesion	374	347	5.469E-32	-0.328
GO:0022613	ribonucleoprotein complex biogenesis	339	229	1.146E-31	-0.397
GO:0065007	biological regulation	18926	9296	2.427E-31	-0.043
GO:0001775	cell activation	1101	824	2.903E-31	-0.203
GO:0019538	protein metabolic process	7013	4216	6.101E-31	-0.076
GO:0005924	cell-substrate adherens junction	380	352	6.256E-31	-0.320
GO:0030055	cell-substrate junction	388	355	7.225E-31	-0.318
GO:0000184	nuclear-transcribed mRNA catabolic process, nonsense-mediated decay	141	113	1.107E-30	-0.580
GO:0002682	regulation of immune system process	1544	1054	4.798E-30	-0.167
GO:0050789	regulation of biological process	17691	8861	6.885E-30	-0.043
GO:0044267	cellular protein metabolic process	5601	3442	8.997E-30	-0.084
GO:0048583	regulation of response to stimulus	4468	2819	9.778E-30	-0.093
GO:0048522	positive regulation of cellular process	5622	3479	1.539E-29	-0.082
GO:0016043	cellular component organization	7202	4443	2.985E-29	-0.069
GO:0043170	macromolecule metabolic process	14207	7230	3.323E-29	-0.050
GO:0006413	translational initiation	238	162	6.110E-29	-0.469
GO:0045087	innate immune response	1006	782	1.247E-28	-0.189
GO:0005654	nucleoplasm	1793	1283	1.269E-28	-0.141
GO:0044260	cellular macromolecule metabolic process	12514	6427	1.443E-28	-0.054
GO:0035556	intracellular signal transduction	2879	2013	1.584E-28	-0.110
GO:0050794	regulation of cellular process	16220	8406	1.638E-28	-0.042
GO:0051179	localization	7894	4588	3.776E-28	-0.066
GO:0009611	response to wounding	1117	903	5.909E-28	-0.179
GO:0010467	gene expression	7890	4323	6.117E-28	-0.068
GO:0006954	inflammatory response	649	538	9.008E-28	-0.235
GO:0005912	adherens junction	457	409	1.552E-27	-0.277
GO:0048584	positive regulation of response to stimulus	2005	1395	3.734E-27	-0.136
GO:0080134	regulation of response to stress	1172	896	5.132E-27	-0.174
GO:0016070	RNA metabolic process	6737	3662	6.233E-27	-0.072
GO:0070161	anchoring junction	478	425	7.520E-27	-0.266
GO:0031988	membrane-bounded vesicle	3783	3068	9.860E-27	-0.085
GO:0005730	nucleolus	728	600	1.001E-26	-0.224
GO:0022904	respiratory electron transport chain	146	96	1.443E-26	0.608
GO:0070887	cellular response to chemical stimulus	3061	2099	1.489E-26	-0.106
GO:0007166	cell surface receptor signaling pathway	4618	3015	2.696E-26	-0.078
GO:0005634	nucleus	8112	5475	2.998E-26	-0.056
GO:0050776	regulation of immune response	1013	709	4.591E-26	-0.195
GO:0005739	mitochondrion	2109	1334	4.690E-26	0.189
GO:0022900	electron transport chain	149	98	1.078E-25	0.594

GOID	TERM	Number of genes	Genes in genelist	p value	Average correlation vector
GO:0005759	mitochondrial matrix	365	300	1.706E-25	0.360
GO:0051246	regulation of protein metabolic process	2545	1843	2.401E-25	-0.112
GO:0006612	protein targeting to membrane	183	162	2.428E-25	-0.439
GO:0050778	positive regulation of immune response	652	456	2.950E-25	-0.245
GO:0031982	vesicle	3913	3152	3.266E-25	-0.080
GO:0045184	establishment of protein localization	1692	1390	3.598E-25	-0.132
GO:0006415	translational termination	97	93	5.052E-25	-0.581
GO:0043230	extracellular organelle	2671	2451	5.828E-25	-0.095
GO:0065010	extracellular membrane-bounded organelle	2671	2451	5.828E-25	-0.095
GO:0070062	extracellular vesicular exosome	2669	2451	5.828E-25	-0.095
GO:0048519	negative regulation of biological process	5363	3407	7.104E-25	-0.074
GO:0000956	nuclear-transcribed mRNA catabolic process	233	174	7.188E-25	-0.415
GO:0016020	membrane	13317	7440	8.856E-25	-0.042
GO:0002253	activation of immune response	541	381	1.241E-24	-0.267
GO:0090304	nucleic acid metabolic process	7863	4108	1.854E-24	-0.063
GO:0009607	response to biotic stimulus	877	654	2.765E-24	-0.192
GO:0015031	protein transport	1553	1294	2.785E-24	-0.135
GO:0016477	cell migration	1277	960	3.146E-24	-0.159
GO:0012505	endomembrane system	4489	2929	3.751E-24	-0.083
GO:0022626	cytosolic ribosome	109	93	8.003E-24	-0.562
GO:0002757	immune response-activating signal transduction	449	333	9.364E-24	-0.285
GO:0044763	single-organism cellular process	22442	10387	9.628E-24	-0.032
GO:0071702	organic substance transport	2770	2059	1.096E-23	-0.100
GO:0043933	macromolecular complex subunit organization	1860	1441	2.003E-23	-0.119
GO:0033036	macromolecule localization	2639	1987	2.057E-23	-0.103
GO:0006401	RNA catabolic process	282	210	2.593E-23	-0.368
GO:0006396	RNA processing	993	566	3.000E-23	-0.205
GO:0071310	cellular response to organic substance	2362	1669	3.153E-23	-0.112
GO:0009987	cellular process	29906	12505	4.387E-23	-0.027
GO:1901363	heterocyclic compound binding	7008	5015	5.200E-23	-0.054
GO:0044421	extracellular region part	3939	3270	6.389E-23	-0.076
GO:0043207	response to external biotic stimulus	839	628	7.306E-23	-0.191
GO:0051707	response to other organism	839	628	7.306E-23	-0.191
GO:0097159	organic cyclic compound binding	7093	5080	1.010E-22	-0.053
GO:0006402	mRNA catabolic process	248	184	1.468E-22	-0.387
GO:0010033	response to organic substance	3172	2215	1.626E-22	-0.092
GO:0005576	extracellular region	5375	3838	1.795E-22	-0.066
GO:0044699	single-organism process	26973	11482	2.048E-22	-0.027
GO:0008283	cell proliferation	2136	1638	2.766E-22	-0.110
GO:0048523	negative regulation of cellular process	4754	3100	3.339E-22	-0.073
GO:0016482	cytoplasmic transport	1000	792	3.430E-22	-0.170
GO:0012501	programmed cell death	2391	1590	4.327E-22	-0.111
GO:0005488	binding	21458	11123	4.920E-22	-0.029
GO:0030529	ribonucleoprotein complex	744	541	6.265E-22	-0.210
GO:0051641	cellular localization	3221	2269	6.522E-22	-0.091
GO:0008104	protein localization	2180	1719	7.879E-22	-0.107
GO:0001816	cytokine production	708	511	1.272E-21	-0.214
GO:0003676	nucleic acid binding	4689	3304	1.432E-21	-0.069
GO:0009059	macromolecule biosynthetic process	7259	4077	1.519E-21	-0.058
GO:0006364	rRNA processing	125	96	1.579E-21	-0.526
GO:0051649	establishment of localization in cell	2769	1997	1.764E-21	-0.097
GO:0048870	cell motility	1374	1025	2.695E-21	-0.142
GO:0051674	localization of cell	1375	1025	2.695E-21	-0.142
GO:0070469	respiratory chain	114	63	3.000E-21	0.680
GO:0006915	apoptotic process	2351	1574	3.674E-21	-0.109
GO:0031347	regulation of defense response	640	499	4.633E-21	-0.211
GO:0005743	mitochondrial inner membrane	488	310	4.792E-21	0.327
GO:0042221	response to chemical	5076	3439	5.036E-21	-0.064
GO:0040011	locomotion	1887	1350	5.522E-21	-0.119
GO:0061024	membrane organization	927	747	5.710E-21	-0.173
GO:0044085	cellular component biogenesis	2373	1791	6.406E-21	-0.099
GO:0051234	establishment of localization	6434	3788	8.750E-21	-0.061
GO:0034645	cellular macromolecule biosynthetic process	7021	3950	1.332E-20	-0.057
GO:0002764	immune response-regulating signaling pathway	566	431	1.492E-20	-0.227
GO:0019083	viral transcription	162	153	1.534E-20	-0.402

GOID	TERM	Number of genes	Genes in genelist	p value	Average correlation vector
GO:0071822	protein complex subunit organization	1617	1294	1.739E-20	-0.118
GO:0033365	protein localization to organelle	706	582	1.902E-20	-0.193
GO:0016072	rRNA metabolic process	134	100	2.541E-20	-0.500
GO:0044446	intracellular organelle part	9239	5803	2.700E-20	-0.046
GO:0019080	viral gene expression	172	163	2.736E-20	-0.387
GO:0010941	regulation of cell death	1719	1259	5.054E-20	-0.123
GO:0006810	transport	6295	3708	5.102E-20	-0.061
GO:0019058	viral life cycle	354	298	5.323E-20	-0.275
GO:0002252	immune effector process	751	550	6.049E-20	-0.193
GO:0015980	energy derivation by oxidation of organic compounds	436	320	6.583E-20	0.301
GO:0006139	nucleobase-containing compound metabolic process	9873	5355	7.031E-20	-0.047
GO:0050790	regulation of catalytic activity	2611	1869	8.566E-20	-0.095
GO:0045321	leukocyte activation	812	606	9.241E-20	-0.190
GO:0008219	cell death	2665	1798	1.011E-19	-0.096
GO:0016265	death	2669	1802	1.259E-19	-0.096
GO:0044455	mitochondrial membrane part	212	125	1.320E-19	0.474
GO:0043067	regulation of programmed cell death	1643	1212	1.763E-19	-0.124
GO:0042981	regulation of apoptotic process	1625	1203	1.767E-19	-0.125
GO:0044033	multi-organism metabolic process	184	172	1.910E-19	-0.367
GO:0006091	generation of precursor metabolites and energy	565	403	1.934E-19	0.270
GO:0044802	single-organism membrane organization	754	615	2.145E-19	-0.186
GO:0032268	regulation of cellular protein metabolic process	1891	1440	2.227E-19	-0.112
GO:0072594	establishment of protein localization to organelle	532	448	3.061E-19	-0.218
GO:0043228	non-membrane-bounded organelle	4369	3035	3.128E-19	-0.068
GO:0043232	intracellular non-membrane-bounded organelle	4369	3035	3.128E-19	-0.068
GO:0090150	establishment of protein localization to membrane	321	282	3.164E-19	-0.286
GO:0070727	cellular macromolecule localization	1374	1079	3.274E-19	-0.132
GO:0006886	intracellular protein transport	873	730	3.646E-19	-0.165
GO:0008150	biological_process	36763	14056	4.302E-19	-0.019
GO:0043227	membrane-bounded organelle	16165	9780	4.887E-19	-0.029
GO:0005746	mitochondrial respiratory chain	106	58	8.323E-19	0.672
GO:0034613	cellular protein localization	1368	1074	1.025E-18	-0.130
GO:0044238	primary metabolic process	17640	8883	1.836E-18	-0.030
GO:0032502	developmental process	7760	4740	2.197E-18	-0.046
GO:0005575	cellular_component	32553	14710	3.934E-18	-0.017
GO:0043412	macromolecule modification	4389	2817	4.151E-18	-0.067
GO:0044422	organelle part	9563	5972	4.194E-18	-0.042
GO:0050900	leukocyte migration	362	290	4.312E-18	-0.270
GO:0003674	molecular_function	31584	13703	4.660E-18	-0.019
GO:0044765	single-organism transport	5155	3161	6.052E-18	-0.063
GO:0044767	single-organism developmental process	7612	4697	6.927E-18	-0.046
GO:0044249	cellular biosynthetic process	8617	4824	9.232E-18	-0.045
GO:0034660	ncRNA metabolic process	400	277	1.257E-17	-0.269
GO:0071704	organic substance metabolic process	18496	9145	1.359E-17	-0.028
GO:0005623	cell	25739	13112	1.370E-17	-0.019
GO:0044464	cell part	25736	13111	1.465E-17	-0.019
GO:1901360	organic cyclic compound metabolic process	10552	5713	1.606E-17	-0.040
GO:0009966	regulation of signal transduction	3216	2166	2.033E-17	-0.080
GO:0034470	ncRNA processing	259	194	2.611E-17	-0.326
GO:0046483	heterocycle metabolic process	10158	5508	2.670E-17	-0.042
GO:0072657	protein localization to membrane	412	361	2.889E-17	-0.239
GO:0042060	wound healing	781	640	2.908E-17	-0.171
GO:0006725	cellular aromatic compound metabolic process	10189	5523	3.670E-17	-0.041
GO:0005886	plasma membrane	6168	4188	4.212E-17	-0.046
GO:0065009	regulation of molecular function	3194	2257	5.600E-17	-0.078
GO:0006414	translational elongation	127	119	6.430E-17	-0.424
GO:0019222	regulation of metabolic process	8809	5390	6.510E-17	-0.041
GO:0046907	intracellular transport	1822	1339	7.966E-17	-0.109
GO:0032991	macromolecular complex	5558	3936	8.411E-17	-0.052
GO:0080090	regulation of primary metabolic process	7699	4866	1.028E-16	-0.043
GO:0009617	response to bacterium	461	373	1.033E-16	-0.214
GO:1902531	regulation of intracellular signal transduction	1855	1318	1.043E-16	-0.108

Table B.5: Gene set enrichment results of average correlation vector for biclustering pattern Random.1 found in HCM analysis in Section 3.2.3.1, showing top 200 of 482 significant terms with adjusted p value < 0.05.

GOID	TERM	Number of genes	Genes in genelist	p value	Average correlation vector
GO:0005488	binding	21458	11123	1.311E-44	-0.006
GO:0044238	primary metabolic process	17640	8883	1.574E-41	-0.000
GO:0071704	organic substance metabolic process	18496	9145	6.198E-41	-0.002
GO:0044424	intracellular part	20932	11034	1.515E-40	-0.010
GO:0005622	intracellular	21143	11127	2.045E-40	-0.010
GO:0008150	biological_process	36763	14056	6.415E-40	-0.019
GO:0008152	metabolic process	20321	9851	7.152E-40	-0.006
GO:0043170	macromolecule metabolic process	14207	7230	1.586E-39	0.007
GO:0043227	membrane-bounded organelle	16165	9780	1.959E-39	-0.007
GO:0003674	molecular_function	31584	13703	2.579E-39	-0.018
GO:0043231	intracellular membrane-bounded organelle	14352	8707	5.103E-39	-0.003
GO:0005575	cellular_component	32553	14710	5.991E-39	-0.021
GO:0043226	organelle	18456	10534	4.665E-38	-0.011
GO:0009987	cellular process	29906	12505	5.618E-38	-0.017
GO:0044260	cellular macromolecule metabolic process	12514	6427	6.056E-38	0.010
GO:0044237	cellular metabolic process	17519	8675	2.878E-37	-0.004
GO:0065007	biological regulation	18926	9296	1.282E-36	-0.010
GO:0043229	intracellular organelle	16594	9609	1.386E-36	-0.009
GO:0050789	regulation of biological process	17691	8861	1.023E-35	-0.009
GO:0044464	cell part	25736	13111	1.917E-35	-0.020
GO:0005623	cell	25739	13112	2.179E-35	-0.021
GO:0050794	regulation of cellular process	16220	8406	1.148E-34	-0.008
GO:0005634	nucleus	8112	5475	3.724E-34	0.012
GO:0005515	protein binding	12021	7591	2.287E-33	-0.004
GO:0044699	single-organism process	26973	11482	5.000E-31	-0.023
GO:0080090	regulation of primary metabolic process	7699	4866	8.161E-31	0.010
GO:0031323	regulation of cellular metabolic process	7614	4816	2.436E-30	0.010
GO:0019222	regulation of metabolic process	8809	5390	4.916E-30	0.005
GO:0044763	single-organism cellular process	22442	10387	5.145E-30	-0.021
GO:0097159	organic cyclic compound binding	7093	5080	1.269E-29	0.009
GO:1901363	heterocyclic compound binding	7008	5015	1.688E-29	0.009
GO:1901360	organic cyclic compound metabolic process	10552	5713	4.536E-29	0.002
GO:0005737	cytoplasm	14272	8513	5.552E-29	-0.015
GO:0050896	response to stimulus	13313	7013	5.924E-29	-0.010
GO:0006139	nucleobase-containing compound metabolic process	9873	5355	9.623E-29	0.005
GO:0060255	regulation of macromolecule metabolic process	7210	4549	1.796E-28	0.011
GO:0006725	cellular aromatic compound metabolic process	10189	5523	2.547E-28	0.003
GO:0046483	heterocycle metabolic process	10158	5508	5.504E-28	0.002
GO:0034641	cellular nitrogen compound metabolic process	10485	5721	1.784E-27	-0.000
GO:0010467	gene expression	7890	4323	6.132E-27	0.013
GO:0051171	regulation of nitrogen compound metabolic process	5711	3790	2.861E-26	0.015
GO:0006807	nitrogen compound metabolic process	11158	6065	3.204E-26	-0.005
GO:0019219	regulation of nucleobase-containing compound metabolic process	5589	3700	3.930E-26	0.016
GO:0051716	cellular response to stimulus	10013	5706	4.465E-26	-0.006
GO:0090304	nucleic acid metabolic process	7863	4108	5.539E-26	0.014
GO:0019538	protein metabolic process	7013	4216	1.147E-25	0.010
GO:0044249	cellular biosynthetic process	8617	4824	1.238E-25	0.004
GO:0034645	cellular macromolecule biosynthetic process	7021	3950	1.401E-25	0.014
GO:0009058	biosynthetic process	8929	4988	1.812E-25	0.002
GO:0023052	signaling	8975	5274	2.569E-25	-0.005
GO:0044700	single organism signaling	8975	5274	2.569E-25	-0.005
GO:0007165	signal transduction	7988	4789	3.407E-25	-0.001
GO:1901576	organic substance biosynthetic process	8804	4917	4.099E-25	0.002
GO:0007154	cell communication	9101	5346	8.466E-25	-0.006
GO:0048518	positive regulation of biological process	6634	3876	8.601E-25	0.009
GO:0016070	RNA metabolic process	6737	3662	8.937E-25	0.017
GO:0009059	macromolecule biosynthetic process	7259	4077	1.051E-24	0.011
GO:0031326	regulation of cellular biosynthetic process	5114	3435	1.312E-24	0.017
GO:2000112	regulation of cellular macromolecule biosynthetic process	4707	3197	3.183E-24	0.020

GOID	TERM	Number of genes	Genes in genelist	p value	Average correlation vector
GO:0010468	regulation of gene expression	5356	3538	4.189E-24	0.015
GO:0010556	regulation of macromolecule biosynthetic process	4909	3295	8.574E-24	0.018
GO:0009889	regulation of biosynthetic process	5182	3475	1.185E-23	0.014
GO:0043167	ion binding	6315	5308	4.722E-23	-0.008
GO:0006351	transcription, DNA-templated	5382	3011	7.766E-23	0.021
GO:0051252	regulation of RNA metabolic process	4486	3022	9.377E-23	0.020
GO:0048583	regulation of response to stimulus	4468	2819	3.922E-22	0.018
GO:2001141	regulation of RNA biosynthetic process	4359	2961	4.626E-22	0.020
GO:0044267	cellular protein metabolic process	5601	3442	4.734E-22	0.013
GO:0048522	positive regulation of cellular process	5622	3479	5.469E-22	0.008
GO:0006464	cellular protein modification process	4196	2712	1.062E-21	0.024
GO:0036211	protein modification process	4196	2712	1.062E-21	0.024
GO:0006355	regulation of transcription, DNA-templated	4286	2929	1.937E-21	0.019
GO:0003676	nucleic acid binding	4689	3304	3.078E-21	0.015
GO:0048519	negative regulation of biological process	5363	3407	3.241E-21	0.007
GO:0043412	macromolecule modification	4389	2817	5.690E-21	0.020
GO:0044444	cytoplasmic part	10781	6379	1.385E-20	-0.018
GO:0032774	RNA biosynthetic process	5516	3117	1.609E-20	0.015
GO:0006950	response to stress	4845	3064	1.918E-20	0.011
GO:0035556	intracellular signal transduction	2879	2013	2.153E-20	0.033
GO:0016020	membrane	13317	7440	3.177E-20	-0.024
GO:0003824	catalytic activity	7631	4714	5.099E-20	-0.007
GO:1901362	organic cyclic compound biosynthetic process	6314	3592	1.109E-19	0.006
GO:0044767	single-organism developmental process	7612	4697	1.589E-19	-0.011
GO:0032502	developmental process	7760	4740	1.804E-19	-0.012
GO:0034654	nucleobase-containing compound biosynthetic process	6012	3419	7.420E-19	0.006
GO:0019438	aromatic compound biosynthetic process	6127	3486	8.910E-19	0.005
GO:0010646	regulation of cell communication	3631	2433	1.023E-18	0.016
GO:0032501	multicellular organismal process	9979	5997	1.516E-18	-0.022
GO:0048523	negative regulation of cellular process	4754	3100	1.660E-18	0.006
GO:0018130	heterocycle biosynthetic process	6129	3479	1.684E-18	0.005
GO:0044422	organelle part	9563	5972	2.344E-18	-0.018
GO:0044271	cellular nitrogen compound biosynthetic process	6227	3537	2.367E-18	0.004
GO:0048856	anatomical structure development	6783	4231	2.516E-18	-0.010
GO:0044707	single-multicellular organism process	9631	5814	2.625E-18	-0.022
GO:0023051	regulation of signaling	3620	2427	3.831E-18	0.015
GO:0009966	regulation of signal transduction	3216	2166	5.526E-18	0.020
GO:0006793	phosphorus metabolic process	5280	3277	1.040E-17	-0.002
GO:0007275	multicellular organismal development	6429	4159	1.594E-17	-0.011
GO:0044446	intracellular organelle part	9239	5803	1.861E-17	-0.018
GO:0006796	phosphate-containing compound metabolic process	5210	3234	2.095E-17	-0.002
GO:0048731	system development	5637	3658	2.197E-17	-0.006
GO:0006366	transcription from RNA polymerase II promoter	2334	1538	2.939E-17	0.043
GO:0007166	cell surface receptor signaling pathway	4618	3015	1.600E-16	0.000
GO:0010033	response to organic substance	3172	2215	2.280E-16	0.016
GO:0009893	positive regulation of metabolic process	3236	2243	4.510E-16	0.019
GO:0031325	positive regulation of cellular metabolic process	3037	2124	4.754E-16	0.020
GO:0044710	single-organism metabolic process	8623	4887	1.644E-15	-0.019
GO:0006357	regulation of transcription from RNA polymerase II promoter	1964	1412	2.668E-15	0.041
GO:0036094	small molecule binding	2659	2295	8.995E-15	0.011
GO:0048584	positive regulation of response to stimulus	2005	1395	9.373E-15	0.035
GO:0070887	cellular response to chemical stimulus	3061	2099	1.055E-14	0.014
GO:0042221	response to chemical	5076	3439	1.305E-14	-0.010
GO:0044428	nuclear part	3483	2230	1.886E-14	0.017
GO:0071840	cellular component organization or biogenesis	7363	4521	2.312E-14	-0.019
GO:0046872	metal ion binding	4089	3566	2.579E-14	-0.011
GO:0043169	cation binding	4173	3631	2.686E-14	-0.011
GO:0000166	nucleotide binding	2357	2045	3.676E-14	0.015
GO:1901265	nucleoside phosphate binding	2358	2046	4.356E-14	0.014
GO:0010604	positive regulation of macromolecule metabolic process	2853	2029	4.900E-14	0.018
GO:0051239	regulation of multicellular organismal process	2892	2002	1.435E-13	0.009
GO:0043168	anion binding	2673	2317	2.301E-13	0.004
GO:0008219	cell death	2665	1798	2.733E-13	0.019
GO:0016265	death	2669	1802	2.743E-13	0.019

GOID	TERM	Number of genes	Genes in genelist	p value	Average correlation vector
GO:0012505	endomembrane system	4489	2929	3.021E-13	-0.006
GO:0016043	cellular component organization	7202	4443	4.092E-13	-0.022
GO:0003723	RNA binding	1808	1303	6.196E-13	0.048
GO:0002376	immune system process	3353	2069	6.477E-13	0.011
GO:0016740	transferase activity	2851	1785	6.817E-13	0.019
GO:0051246	regulation of protein metabolic process	2545	1843	7.801E-13	0.017
GO:0031981	nuclear lumen	2785	1891	9.205E-13	0.022
GO:0051179	localization	7894	4588	1.022E-12	-0.023
GO:0048869	cellular developmental process	4670	3176	1.070E-12	-0.012
GO:0071310	cellular response to organic substance	2362	1669	1.648E-12	0.019
GO:1902531	regulation of intracellular signal transduction	1855	1318	1.944E-12	0.029
GO:0003677	DNA binding	2781	2094	3.135E-12	0.010
GO:0065008	regulation of biological quality	4124	2811	3.387E-12	-0.008
GO:0030154	cell differentiation	4368	3015	3.705E-12	-0.011
GO:0032549	ribonucleoside binding	1839	1636	3.791E-12	0.019
GO:0097367	carbohydrate derivative binding	2250	1978	3.944E-12	0.008
GO:0001882	nucleoside binding	1849	1644	4.498E-12	0.019
GO:0065009	regulation of molecular function	3194	2257	4.773E-12	0.000
GO:0032553	ribonucleotide binding	1893	1677	4.929E-12	0.017
GO:0032550	purine ribonucleoside binding	1835	1632	6.396E-12	0.018
GO:0001883	purine nucleoside binding	1838	1634	7.271E-12	0.018
GO:0010647	positive regulation of cell communication	1360	1060	8.056E-12	0.040
GO:0017076	purine nucleotide binding	1897	1683	8.088E-12	0.016
GO:0009605	response to external stimulus	2532	1822	1.203E-11	0.008
GO:0035639	purine ribonucleoside triphosphate binding	1804	1625	1.289E-11	0.017
GO:0032555	purine ribonucleotide binding	1877	1663	1.569E-11	0.016
GO:0051234	establishment of localization	6434	3788	1.671E-11	-0.020
GO:0009891	positive regulation of biosynthetic process	1857	1372	2.688E-11	0.027
GO:0031974	membrane-enclosed lumen	3621	2576	2.851E-11	-0.001
GO:0031328	positive regulation of cellular biosynthetic process	1821	1353	2.852E-11	0.027
GO:0045944	positive regulation of transcription from RNA polymerase II promoter	963	808	3.216E-11	0.064
GO:0043233	organelle lumen	3548	2523	3.631E-11	-0.000
GO:0023056	positive regulation of signaling	1355	1054	4.402E-11	0.036
GO:0006810	transport	6295	3708	4.915E-11	-0.021
GO:0009967	positive regulation of signal transduction	1285	1000	6.669E-11	0.039
GO:0070013	intracellular organelle lumen	3486	2465	7.601E-11	0.000
GO:0033554	cellular response to stress	1930	1291	8.166E-11	0.030
GO:0010557	positive regulation of macromolecule biosynthetic process	1702	1262	8.727E-11	0.031
GO:0044425	membrane part	7949	5467	2.031E-10	-0.036
GO:0032268	regulation of cellular protein metabolic process	1891	1440	2.187E-10	0.021
GO:1902680	positive regulation of RNA biosynthetic process	1482	1118	2.306E-10	0.037
GO:0016310	phosphorylation	2583	1690	3.591E-10	0.006
GO:0005886	plasma membrane	6168	4188	3.927E-10	-0.028
GO:0006952	defense response	1956	1337	4.522E-10	0.020
GO:0045893	positive regulation of transcription, DNA-templated	1426	1086	4.534E-10	0.037
GO:0051254	positive regulation of RNA metabolic process	1517	1134	4.717E-10	0.034
GO:0048513	organ development	3828	2703	4.809E-10	-0.014
GO:0008283	cell proliferation	2136	1638	7.039E-10	0.005
GO:0051173	positive regulation of nitrogen compound metabolic process	1757	1304	8.228E-10	0.025
GO:0030554	adenyl nucleotide binding	1525	1369	8.450E-10	0.019
GO:0005524	ATP binding	1462	1319	8.747E-10	0.022
GO:0071944	cell periphery	6341	4273	1.005E-09	-0.030
GO:0005829	cytosol	3022	2475	1.121E-09	-0.007
GO:0044822	poly(A) RNA binding	1170	981	1.187E-09	0.050
GO:0032559	adenyl ribonucleotide binding	1507	1351	1.222E-09	0.019
GO:0044765	single-organism transport	5155	3161	1.224E-09	-0.019
GO:0009056	catabolic process	3733	2602	1.276E-09	-0.011
GO:0045935	positive regulation of nucleobase-containing compound metabolic process	1714	1277	1.368E-09	0.025
GO:0010628	positive regulation of gene expression	1547	1187	1.907E-09	0.029
GO:0012501	programmed cell death	2391	1590	1.971E-09	0.008
GO:0044248	cellular catabolic process	3220	2257	2.077E-09	-0.005
GO:0006468	protein phosphorylation	1903	1288	2.849E-09	0.019
GO:0009892	negative regulation of metabolic process	2224	1621	2.977E-09	0.009

GOID	TERM	Number of genes	Genes in genelist	p value	Average correlation vector
GO:1901575	organic substance catabolic process	3412	2396	4.435E-09	-0.009
GO:0006915	apoptotic process	2351	1574	4.510E-09	0.007
GO:0016021	integral component of membrane	5650	4543	4.859E-09	-0.035
GO:0051174	regulation of phosphorus metabolic process	2363	1633	6.978E-09	0.002
GO:0005654	nucleoplasm	1793	1283	8.645E-09	0.026
GO:0070647	protein modification by small protein conjugation or removal	1004	701	9.147E-09	0.066
GO:0007399	nervous system development	2516	1837	9.230E-09	-0.006
GO:0051128	regulation of cellular component organization	2022	1496	1.007E-08	0.007
GO:0044093	positive regulation of molecular function	1953	1431	1.367E-08	0.006
GO:0019220	regulation of phosphate metabolic process	2347	1621	1.368E-08	0.001
GO:0031224	intrinsic component of membrane	5833	4652	1.472E-08	-0.036
GO:0006955	immune response	1821	1241	1.526E-08	0.019
GO:2000026	regulation of multicellular organismal development	1647	1255	1.656E-08	0.014
GO:0032879	regulation of localization	2401	1750	2.565E-08	-0.004

Table B.6: Gene set enrichment results of average correlation vector for biclustering pattern Mitonc.1 found in HCM analysis in Section 3.2.3.1, showing the top 200 of 213 significant terms with adjusted p value < 0.05.

GOID	TERM	Number of genes	Genes in genelist	p value	Average correlation vector
GO:0005488	binding	21458	11123	4.709E-23	-0.006
GO:0043170	macromolecule metabolic process	14207	7230	5.490E-22	0.006
GO:0044260	cellular macromolecule metabolic process	12514	6427	2.449E-21	0.010
GO:0005575	cellular_component	32553	14710	3.484E-20	-0.016
GO:0008150	biological_process	36763	14056	7.320E-20	-0.016
GO:0003674	molecular_function	31584	13703	7.356E-20	-0.015
GO:0005622	intracellular	21143	11127	8.737E-20	-0.009
GO:0044424	intracellular part	20932	11034	1.055E-19	-0.008
GO:0071704	organic substance metabolic process	18496	9145	7.544E-19	-0.005
GO:0044238	primary metabolic process	17640	8883	8.686E-19	-0.004
GO:0005634	nucleus	8112	5475	1.118E-18	0.010
GO:0043231	intracellular membrane-bounded organelle	14352	8707	1.842E-18	-0.004
GO:0065007	biological regulation	18926	9296	4.199E-18	-0.010
GO:0043229	intracellular organelle	16594	9609	6.503E-18	-0.007
GO:0008152	metabolic process	20321	9851	1.053E-17	-0.008
GO:0050789	regulation of biological process	17691	8861	1.638E-17	-0.010
GO:0043226	organelle	18456	10534	2.645E-17	-0.011
GO:0009987	cellular process	29906	12505	6.498E-17	-0.017
GO:0050794	regulation of cellular process	16220	8406	6.865E-17	-0.010
GO:0043227	membrane-bounded organelle	16165	9780	8.133E-17	-0.009
GO:1901363	heterocyclic compound binding	7008	5015	2.211E-16	0.009
GO:0097159	organic cyclic compound binding	7093	5080	3.041E-16	0.008
GO:0044464	cell part	25736	13111	3.182E-16	-0.018
GO:0005623	cell	25739	13112	3.232E-16	-0.018
GO:0044237	cellular metabolic process	17519	8675	7.100E-16	-0.008
GO:0043167	ion binding	6315	5308	1.768E-15	0.001
GO:0090304	nucleic acid metabolic process	7863	4108	7.218E-15	0.013
GO:2000112	regulation of cellular macromolecule biosynthetic process	4707	3197	2.543E-14	0.019
GO:0034645	cellular macromolecule biosynthetic process	7021	3950	3.881E-14	0.012
GO:0060255	regulation of macromolecule metabolic process	7210	4549	4.235E-14	0.006
GO:0010556	regulation of macromolecule biosynthetic process	4909	3295	9.158E-14	0.016
GO:0006351	transcription, DNA-templated	5382	3011	1.041E-13	0.020
GO:0005515	protein binding	12021	7591	1.406E-13	-0.009
GO:0010468	regulation of gene expression	5356	3538	1.507E-13	0.014
GO:0009059	macromolecule biosynthetic process	7259	4077	1.641E-13	0.010
GO:0031323	regulation of cellular metabolic process	7614	4816	2.573E-13	0.002
GO:0010467	gene expression	7890	4323	3.168E-13	0.008
GO:0016070	RNA metabolic process	6737	3662	3.545E-13	0.013
GO:2001141	regulation of RNA biosynthetic process	4359	2961	3.792E-13	0.018
GO:0019222	regulation of metabolic process	8809	5390	3.909E-13	-0.002
GO:0051252	regulation of RNA metabolic process	4486	3022	4.162E-13	0.018
GO:0080090	regulation of primary metabolic process	7699	4866	4.290E-13	0.001

GOID	TERM	Number of genes	Genes in genelist	p value	Average correlation vector
GO:0031326	regulation of cellular biosynthetic process	5114	3435	4.494E-13	0.013
GO:1901360	organic cyclic compound metabolic process	10552	5713	4.540E-13	-0.002
GO:0006355	regulation of transcription, DNA-templated	4286	2929	8.443E-13	0.018
GO:0019219	regulation of nucleobase-containing compound metabolic process	5589	3700	1.049E-12	0.009
GO:0044699	single-organism process	26973	11482	1.220E-12	-0.022
GO:0051171	regulation of nitrogen compound metabolic process	5711	3790	1.514E-12	0.008
GO:0006725	cellular aromatic compound metabolic process	10189	5523	1.515E-12	-0.002
GO:0009889	regulation of biosynthetic process	5182	3475	1.585E-12	0.011
GO:0006139	nucleobase-containing compound metabolic process	9873	5355	2.526E-12	-0.001
GO:0046483	heterocycle metabolic process	10158	5508	4.077E-12	-0.003
GO:0034641	cellular nitrogen compound metabolic process	10485	5721	1.034E-11	-0.005
GO:0009058	biosynthetic process	8929	4988	1.157E-11	-0.001
GO:0044763	single-organism cellular process	22442	10387	1.228E-11	-0.022
GO:0044249	cellular biosynthetic process	8617	4824	1.412E-11	-0.000
GO:1901576	organic substance biosynthetic process	8804	4917	1.882E-11	-0.001
GO:0003676	nucleic acid binding	4689	3304	1.929E-11	0.013
GO:0023052	signaling	8975	5274	2.478E-11	-0.010
GO:0044700	single organism signaling	8975	5274	2.478E-11	-0.010
GO:0006464	cellular protein modification process	4196	2712	3.095E-11	0.018
GO:0036211	protein modification process	4196	2712	3.095E-11	0.018
GO:0005737	cytoplasm	14272	8513	3.891E-11	-0.015
GO:0050896	response to stimulus	13313	7013	4.624E-11	-0.017
GO:0006807	nitrogen compound metabolic process	11158	6065	4.870E-11	-0.008
GO:0032774	RNA biosynthetic process	5516	3117	5.157E-11	0.012
GO:0007154	cell communication	9101	5346	6.677E-11	-0.011
GO:0043412	macromolecule modification	4389	2817	1.920E-10	0.014
GO:0043169	cation binding	4173	3631	3.618E-10	-0.000
GO:0051716	cellular response to stimulus	10013	5706	6.050E-10	-0.014
GO:0019538	protein metabolic process	7013	4216	6.403E-10	-0.000
GO:0046872	metal ion binding	4089	3566	7.092E-10	-0.000
GO:0007165	signal transduction	7988	4789	8.409E-10	-0.011
GO:1901362	organic cyclic compound biosynthetic process	6314	3592	1.721E-09	0.003
GO:0044767	single-organism developmental process	7612	4697	3.851E-09	-0.011
GO:0032502	developmental process	7760	4740	6.132E-09	-0.012
GO:0019438	aromatic compound biosynthetic process	6127	3486	6.904E-09	0.003
GO:0048856	anatomical structure development	6783	4231	7.169E-09	-0.009
GO:0034654	nucleobase-containing compound biosynthetic process	6012	3419	1.028E-08	0.003
GO:0044267	cellular protein metabolic process	5601	3442	1.075E-08	0.004
GO:0003677	DNA binding	2781	2094	1.160E-08	0.017
GO:0035556	intracellular signal transduction	2879	2013	1.313E-08	0.017
GO:0018130	heterocycle biosynthetic process	6129	3479	1.901E-08	0.001
GO:0044271	cellular nitrogen compound biosynthetic process	6227	3537	2.003E-08	0.001
GO:0048731	system development	5637	3658	2.079E-08	-0.007
GO:0007275	multicellular organismal development	6429	4159	2.207E-08	-0.011
GO:0003824	catalytic activity	7631	4714	2.290E-08	-0.009
GO:0006366	transcription from RNA polymerase II promoter	2334	1538	3.058E-08	0.029
GO:0032501	multicellular organismal process	9979	5997	3.259E-08	-0.021
GO:0044707	single-multicellular organism process	9631	5814	1.889E-07	-0.022
GO:0006357	regulation of transcription from RNA polymerase II promoter	1964	1412	2.012E-07	0.028
GO:0043168	anion binding	2673	2317	2.672E-07	0.006
GO:0032549	ribonucleoside binding	1839	1636	3.318E-07	0.019
GO:0001882	nucleoside binding	1849	1644	3.713E-07	0.019
GO:0000166	nucleotide binding	2357	2045	4.900E-07	0.012
GO:0016020	membrane	13317	7440	4.961E-07	-0.026
GO:0036094	small molecule binding	2659	2295	5.054E-07	0.008
GO:0032550	purine ribonucleoside binding	1835	1632	5.216E-07	0.019
GO:0001883	purine nucleoside binding	1838	1634	5.640E-07	0.018
GO:1901265	nucleoside phosphate binding	2358	2046	6.310E-07	0.012
GO:0032553	ribonucleotide binding	1893	1677	7.043E-07	0.017
GO:0017076	purine nucleotide binding	1897	1683	7.676E-07	0.016
GO:0010646	regulation of cell communication	3631	2433	7.723E-07	0.001
GO:0048519	negative regulation of biological process	5363	3407	1.058E-06	-0.007
GO:0032555	purine ribonucleotide binding	1877	1663	1.194E-06	0.016

GOID	TERM	Number of genes	Genes in genelist	p value	Average correlation vector
GO:0035639	purine ribonucleoside triphosphate binding	1804	1625	1.366E-06	0.017
GO:0071840	cellular component organization or biogenesis	7363	4521	1.430E-06	-0.012
GO:0097367	carbohydrate derivative binding	2250	1978	1.540E-06	0.008
GO:0048583	regulation of response to stimulus	4468	2819	1.625E-06	-0.005
GO:0023051	regulation of signaling	3620	2427	2.424E-06	-0.001
GO:0048523	negative regulation of cellular process	4754	3100	2.641E-06	-0.006
GO:0048518	positive regulation of biological process	6634	3876	2.714E-06	-0.011
GO:0009966	regulation of signal transduction	3216	2166	3.802E-06	0.003
GO:0044444	cytoplasmic part	10781	6379	4.022E-06	-0.020
GO:0007399	nervous system development	2516	1837	5.189E-06	0.005
GO:0016740	transferase activity	2851	1785	6.840E-06	0.014
GO:0016043	cellular component organization	7202	4443	9.278E-06	-0.015
GO:0048522	positive regulation of cellular process	5622	3479	1.003E-05	-0.010
GO:0030554	adenyl nucleotide binding	1525	1369	1.043E-05	0.020
GO:0045944	positive regulation of transcription from RNA polymerase II promoter	963	808	1.073E-05	0.046
GO:0005524	ATP binding	1462	1319	1.255E-05	0.021
GO:0032559	adenyl ribonucleotide binding	1507	1351	1.284E-05	0.020
GO:0044422	organelle part	9563	5972	1.503E-05	-0.019
GO:0012505	endomembrane system	4489	2929	1.620E-05	-0.007
GO:0044428	nuclear part	3483	2230	6.498E-05	0.008
GO:0007166	cell surface receptor signaling pathway	4618	3015	8.056E-05	-0.015
GO:0031981	nuclear lumen	2785	1891	8.796E-05	0.014
GO:0044446	intracellular organelle part	9239	5803	1.013E-04	-0.020
GO:0031325	positive regulation of cellular metabolic process	3037	2124	1.043E-04	0.001
GO:0048869	cellular developmental process	4670	3176	1.209E-04	-0.015
GO:0009893	positive regulation of metabolic process	3236	2243	1.887E-04	-0.002
GO:0033554	cellular response to stress	1930	1291	2.246E-04	0.018
GO:1902531	regulation of intracellular signal transduction	1855	1318	2.385E-04	0.011
GO:0030154	cell differentiation	4368	3015	2.675E-04	-0.015
GO:0006793	phosphorus metabolic process	5280	3277	3.637E-04	-0.015
GO:0003723	RNA binding	1808	1303	3.637E-04	0.027
GO:0016787	hydrolase activity	3107	2077	3.853E-04	-0.004
GO:0005794	Golgi apparatus	1552	1138	4.635E-04	0.020
GO:0016265	death	2669	1802	5.162E-04	0.002
GO:0006796	phosphate-containing compound metabolic process	5210	3234	5.446E-04	-0.015
GO:0045893	positive regulation of transcription, DNA-templated	1426	1086	5.598E-04	0.022
GO:0008219	cell death	2665	1798	5.654E-04	0.002
GO:1902680	positive regulation of RNA biosynthetic process	1482	1118	6.275E-04	0.020
GO:0010604	positive regulation of macromolecule metabolic process	2853	2029	6.318E-04	-0.000
GO:0003735	structural constituent of ribosome	160	144	6.594E-04	-0.260
GO:0010557	positive regulation of macromolecule biosynthetic process	1702	1262	8.995E-04	0.015
GO:0051179	localization	7894	4588	1.333E-03	-0.024
GO:0048468	cell development	2228	1682	1.462E-03	-0.003
GO:0070647	protein modification by small protein conjugation or removal	1004	701	1.731E-03	0.046
GO:0005783	endoplasmic reticulum	1847	1261	1.816E-03	0.009
GO:0006950	response to stress	4845	3064	1.879E-03	-0.018
GO:0044710	single-organism metabolic process	8623	4887	1.899E-03	-0.024
GO:0044822	poly(A) RNA binding	1170	981	2.284E-03	0.035
GO:0051254	positive regulation of RNA metabolic process	1517	1134	2.539E-03	0.016
GO:0010647	positive regulation of cell communication	1360	1060	2.606E-03	0.012
GO:0009891	positive regulation of biosynthetic process	1857	1372	2.785E-03	0.007
GO:0010628	positive regulation of gene expression	1547	1187	2.968E-03	0.013
GO:0042221	response to chemical	5076	3439	2.983E-03	-0.024
GO:0043228	non-membrane-bounded organelle	4369	3035	3.200E-03	-0.014
GO:0043232	intracellular non-membrane-bounded organelle	4369	3035	3.200E-03	-0.014
GO:0031328	positive regulation of cellular biosynthetic process	1821	1353	3.321E-03	0.007
GO:0005886	plasma membrane	6168	4188	3.641E-03	-0.030
GO:0051234	establishment of localization	6434	3788	4.307E-03	-0.021
GO:0071944	cell periphery	6341	4273	4.561E-03	-0.030
GO:0004674	protein serine/threonine kinase activity	590	404	4.569E-03	0.066
GO:0005730	nucleolus	728	600	5.231E-03	0.052
GO:0006810	transport	6295	3708	6.128E-03	-0.021
GO:0048513	organ development	3828	2703	6.786E-03	-0.019

GOID	TERM	Number of genes	Genes in genelist	p value	Average correlation vector
GO:0044431	Golgi apparatus part	904	696	7.882E-03	0.032
GO:0022008	neurogenesis	1639	1238	8.048E-03	0.002
GO:0051128	regulation of cellular component organization	2022	1496	8.852E-03	0.002
GO:0030182	neuron differentiation	1394	1072	9.085E-03	0.008
GO:0001071	nucleic acid binding transcription factor activity	1335	958	9.142E-03	0.015
GO:0005654	nucleoplasm	1793	1283	9.725E-03	0.015
GO:0010033	response to organic substance	3172	2215	9.972E-03	-0.014
GO:0009967	positive regulation of signal transduction	1285	1000	1.107E-02	0.010
GO:0003700	sequence-specific DNA binding transcription factor activity	1331	957	1.116E-02	0.014
GO:0023056	positive regulation of signaling	1355	1054	1.179E-02	0.007
GO:0048584	positive regulation of response to stimulus	2005	1395	1.199E-02	-0.002
GO:0065008	regulation of biological quality	4124	2811	1.205E-02	-0.019
GO:0045333	cellular respiration	221	148	1.212E-02	-0.250
GO:0051239	regulation of multicellular organismal process	2892	2002	1.236E-02	-0.014
GO:0048699	generation of neurons	1536	1167	1.246E-02	0.004
GO:0044391	ribosomal subunit	153	130	1.343E-02	-0.241
GO:0006468	protein phosphorylation	1903	1288	1.369E-02	0.003
GO:0022904	respiratory electron transport chain	146	96	1.483E-02	-0.300
GO:0032446	protein modification by small protein conjugation	895	624	1.535E-02	0.042
GO:0070887	cellular response to chemical stimulus	3061	2099	1.572E-02	-0.013
GO:0051173	positive regulation of nitrogen compound metabolic process	1757	1304	1.795E-02	0.005
GO:0006614	SRP-dependent cotranslational protein targeting to membrane	109	106	1.831E-02	-0.262
GO:0004129	cytochrome-c oxidase activity	26	22	1.847E-02	-0.571
GO:0015002	heme-copper terminal oxidase activity	26	22	1.847E-02	-0.571
GO:0016676	oxidoreductase activity, acting on a heme group of donors, oxygen as acceptor	26	22	1.847E-02	-0.571
GO:0072599	establishment of protein localization to endoplasmic reticulum	118	110	2.059E-02	-0.256
GO:0022900	electron transport chain	149	98	2.059E-02	-0.294
GO:0070013	intracellular organelle lumen	3486	2465	2.133E-02	-0.007
GO:0051246	regulation of protein metabolic process	2545	1843	2.146E-02	-0.007
GO:0043233	organelle lumen	3548	2523	2.163E-02	-0.008
GO:0044425	membrane part	7949	5467	2.320E-02	-0.036
GO:0022626	cytosolic ribosome	109	93	2.396E-02	-0.275

Table B.7: Gene set enrichment results of average correlation vector for biclustering pattern Mitonc.2 found in HCM analysis in Section 3.2.3.1, showing the 25 significant terms with adjusted p value < 0.05.

GOID	TERM	Number of genes	Genes in genelist	p value	Average correlation vector
GO:0044710	single-organism metabolic process	8623	4887	2.006E-06	-0.030
GO:0005515	protein binding	12021	7591	3.050E-05	-0.020
GO:0008152	metabolic process	20321	9851	4.484E-04	-0.014
GO:0006914	autophagy	212	140	5.242E-04	-0.200
GO:0070013	intracellular organelle lumen	3486	2465	5.248E-04	-0.041
GO:0005737	cytoplasm	14272	8513	7.773E-04	-0.016
GO:0043233	organelle lumen	3548	2523	1.018E-03	-0.039
GO:0071704	organic substance metabolic process	18496	9145	1.316E-03	-0.014
GO:0003824	catalytic activity	7631	4714	1.459E-03	-0.024
GO:0044422	organelle part	9563	5972	1.474E-03	-0.021
GO:0031974	membrane-enclosed lumen	3621	2576	1.500E-03	-0.038
GO:0044237	cellular metabolic process	17519	8675	2.664E-03	-0.014
GO:0044446	intracellular organelle part	9239	5803	3.550E-03	-0.020
GO:0044444	cytoplasmic part	10781	6379	3.698E-03	-0.019
GO:0044238	primary metabolic process	17640	8883	4.221E-03	-0.013
GO:0044822	poly(A) RNA binding	1170	981	1.076E-02	-0.065
GO:0009894	regulation of catabolic process	1130	809	2.313E-02	-0.060
GO:0048011	neurotrophin TRK receptor signaling pathway	281	270	2.881E-02	-0.115
GO:1901360	organic cyclic compound metabolic process	10552	5713	3.040E-02	-0.016
GO:0038179	neurotrophin signaling pathway	290	272	3.202E-02	-0.114
GO:0043227	membrane-bounded organelle	16165	9780	3.785E-02	-0.010
GO:0009056	catabolic process	3733	2602	3.827E-02	-0.030

GOID	TERM	Number of genes	Genes in genelist	p value	Average correlation vector
GO:0005488	binding	21458	11123	4.208E-02	-0.008
GO:0005773	vacuole	606	466	4.271E-02	-0.082
GO:0044712	single-organism catabolic process	2384	1719	4.789E-02	-0.038

Table B.8: Gene set enrichment results of average correlation vector for biclustering pattern Mitonc.3 found in HCM analysis in Section 3.2.3.1, showing the 124 significant terms with adjusted p value < 0.05.

GOID	TERM	Number of genes	Genes in genelist	p value	Average correlation vector
GO:0005739	mitochondrion	2109	1334	7.077E-32	0.141
GO:0044429	mitochondrial part	1081	711	4.360E-23	0.169
GO:0005759	mitochondrial matrix	365	300	4.700E-18	0.241
GO:0030198	extracellular matrix organization	422	357	3.513E-09	-0.207
GO:0043062	extracellular structure organization	424	358	3.877E-09	-0.207
GO:0003779	actin binding	402	350	7.029E-09	-0.206
GO:0005740	mitochondrial envelope	743	482	1.514E-08	0.129
GO:0055114	oxidation-reduction process	1187	905	6.836E-08	0.084
GO:0006935	chemotaxis	799	606	1.089E-07	-0.150
GO:0042330	taxis	799	606	1.089E-07	-0.150
GO:0031012	extracellular matrix	558	390	1.541E-07	-0.187
GO:0009653	anatomical structure morphogenesis	3188	2160	1.649E-07	-0.094
GO:0031967	organelle envelope	1166	778	1.746E-07	0.090
GO:0006955	immune response	1821	1241	2.454E-07	-0.111
GO:0031966	mitochondrial membrane	689	451	2.649E-07	0.124
GO:0006928	cellular component movement	2080	1488	3.695E-07	-0.105
GO:0048037	cofactor binding	274	236	3.811E-07	0.178
GO:0031975	envelope	1172	782	5.317E-07	0.088
GO:0040011	locomotion	1887	1350	7.393E-07	-0.107
GO:0022610	biological adhesion	1342	999	1.006E-06	-0.122
GO:0007155	cell adhesion	1334	995	1.116E-06	-0.122
GO:0050662	coenzyme binding	191	168	1.131E-06	0.212
GO:0019752	carboxylic acid metabolic process	1430	905	1.748E-06	0.074
GO:0016054	organic acid catabolic process	304	196	1.806E-06	0.184
GO:0046395	carboxylic acid catabolic process	304	196	1.806E-06	0.184
GO:0002376	immune system process	3353	2069	1.861E-06	-0.089
GO:0005743	mitochondrial inner membrane	488	310	2.972E-06	0.149
GO:0044282	small molecule catabolic process	371	255	4.350E-06	0.156
GO:0000904	cell morphogenesis involved in differentiation	954	757	4.857E-06	-0.130
GO:0006952	defense response	1956	1337	6.233E-06	-0.102
GO:0000902	cell morphogenesis	1341	1025	6.544E-06	-0.115
GO:0009611	response to wounding	1117	903	6.575E-06	-0.123
GO:0032989	cellular component morphogenesis	1428	1093	7.239E-06	-0.112
GO:0009605	response to external stimulus	2532	1822	1.135E-05	-0.091
GO:0042060	wound healing	781	640	1.267E-05	-0.138
GO:0015629	actin cytoskeleton	462	365	1.603E-05	-0.172
GO:0045333	cellular respiration	221	148	3.650E-05	0.208
GO:0019866	organelle inner membrane	531	345	3.863E-05	0.127
GO:0030036	actin cytoskeleton organization	599	451	3.992E-05	-0.155
GO:0005615	extracellular space	1277	1103	4.095E-05	-0.110
GO:0043436	oxoacid metabolic process	1574	1012	4.874E-05	0.061
GO:0009060	aerobic respiration	60	46	5.733E-05	0.384
GO:0005578	proteinaceous extracellular matrix	365	320	6.081E-05	-0.178
GO:0007599	hemostasis	622	515	6.450E-05	-0.145
GO:0006082	organic acid metabolic process	1593	1026	7.265E-05	0.059
GO:0042641	actomyosin	63	58	9.342E-05	-0.380
GO:0016491	oxidoreductase activity	984	607	1.111E-04	0.086
GO:0007596	blood coagulation	615	510	1.122E-04	-0.144
GO:0030029	actin filament-based process	677	501	1.253E-04	-0.143
GO:1990204	oxidoreductase complex	123	76	1.493E-04	0.285
GO:0005518	collagen binding	65	60	1.507E-04	-0.359
GO:0032963	collagen metabolic process	124	105	1.743E-04	-0.280
GO:0002682	regulation of immune system process	1544	1054	2.054E-04	-0.104
GO:0016477	cell migration	1277	960	2.293E-04	-0.108

GOID	TERM	Number of genes	Genes in genelist	p value	Average correlation vector
GO:0044259	multicellular organismal macromolecule metabolic process	130	111	2.987E-04	-0.268
GO:0050817	coagulation	619	513	3.034E-04	-0.140
GO:0031589	cell-substrate adhesion	315	257	3.478E-04	-0.181
GO:0005925	focal adhesion	374	347	3.659E-04	-0.156
GO:0048870	cell motility	1374	1025	3.753E-04	-0.104
GO:0051674	localization of cell	1375	1025	3.753E-04	-0.104
GO:0005576	extracellular region	5375	3838	5.204E-04	-0.067
GO:0032432	actin filament bundle	54	52	6.212E-04	-0.377
GO:0007409	axonogenesis	611	512	8.611E-04	-0.135
GO:0022617	extracellular matrix disassembly	131	119	9.037E-04	-0.255
GO:0005924	cell-substrate adherens junction	380	352	9.473E-04	-0.151
GO:0005777	peroxisome	184	112	1.001E-03	0.208
GO:0042579	microbody	184	112	1.001E-03	0.208
GO:0050878	regulation of body fluid levels	765	630	1.051E-03	-0.124
GO:0009063	cellular amino acid catabolic process	172	108	1.204E-03	0.209
GO:0001725	stress fiber	52	50	1.253E-03	-0.374
GO:0007005	mitochondrion organization	400	257	1.374E-03	0.126
GO:0061564	axon development	635	530	1.388E-03	-0.131
GO:0045087	innate immune response	1006	782	1.558E-03	-0.109
GO:0006631	fatty acid metabolic process	442	305	1.667E-03	0.114
GO:0030055	cell-substrate junction	388	355	1.793E-03	-0.147
GO:0007166	cell surface receptor signaling pathway	4618	3015	2.152E-03	-0.071
GO:0006954	inflammatory response	649	538	2.262E-03	-0.128
GO:0019395	fatty acid oxidation	112	78	2.520E-03	0.240
GO:0050776	regulation of immune response	1013	709	2.520E-03	-0.113
GO:0048646	anatomical structure formation involved in morphogenesis	1187	911	2.986E-03	-0.104
GO:0003824	catalytic activity	7631	4714	3.228E-03	0.013
GO:0044421	extracellular region part	3939	3270	3.315E-03	-0.066
GO:0009062	fatty acid catabolic process	105	70	3.375E-03	0.252
GO:0002684	positive regulation of immune system process	930	642	3.996E-03	-0.114
GO:0048583	regulation of response to stimulus	4468	2819	4.085E-03	-0.071
GO:0001944	vasculature development	711	543	4.412E-03	-0.125
GO:0051186	cofactor metabolic process	375	245	4.991E-03	0.123
GO:0050793	regulation of developmental process	2231	1631	5.567E-03	-0.085
GO:0034440	lipid oxidation	114	80	6.687E-03	0.227
GO:0043405	regulation of MAP kinase activity	285	253	7.317E-03	-0.167
GO:0001568	blood vessel development	665	515	7.350E-03	-0.125
GO:0045595	regulation of cell differentiation	1560	1177	7.690E-03	-0.094
GO:0007411	axon guidance	415	357	7.977E-03	-0.146
GO:0097485	neuron projection guidance	415	357	7.977E-03	-0.146
GO:0001775	cell activation	1101	824	8.595E-03	-0.103
GO:0006732	coenzyme metabolic process	289	188	9.268E-03	0.142
GO:0051239	regulation of multicellular organismal process	2892	2002	1.023E-02	-0.077
GO:0044243	multicellular organismal catabolic process	89	78	1.082E-02	-0.280
GO:0030574	collagen catabolic process	83	72	1.261E-02	-0.290
GO:0008092	cytoskeletal protein binding	862	679	1.332E-02	-0.111
GO:0044455	mitochondrial membrane part	212	125	1.362E-02	0.182
GO:0030258	lipid modification	204	149	1.415E-02	0.156
GO:0022904	respiratory electron transport chain	146	96	1.529E-02	0.211
GO:0005516	calmodulin binding	177	163	1.561E-02	-0.198
GO:0006099	tricarboxylic acid cycle	41	29	1.664E-02	0.401
GO:0048812	neuron projection morphogenesis	717	588	1.692E-02	-0.117
GO:0019783	small conjugating protein-specific protease activity	85	70	1.730E-02	0.244
GO:0072329	monocarboxylic acid catabolic process	127	86	1.796E-02	0.209
GO:0015980	energy derivation by oxidation of organic compounds	436	320	1.972E-02	0.102
GO:0048667	cell morphogenesis involved in neuron differentiation	700	579	2.053E-02	-0.116
GO:0022900	electron transport chain	149	98	2.248E-02	0.204
GO:0030199	collagen fibril organization	44	39	2.759E-02	-0.382
GO:0022411	cellular component disassembly	469	428	3.288E-02	-0.126
GO:0006091	generation of precursor metabolites and energy	565	403	3.412E-02	0.087
GO:0042773	ATP synthesis coupled electron transport	55	47	3.426E-02	0.303
GO:0042775	mitochondrial ATP synthesis coupled electron transport	55	47	3.426E-02	0.303
GO:0048468	cell development	2228	1682	3.662E-02	-0.079
GO:0009083	branched-chain amino acid catabolic process	34	19	4.213E-02	0.480
GO:0044438	microbody part	107	76	4.225E-02	0.222

GOID	TERM	Number of genes	Genes in genelist	p value	Average correlation vector
GO:0044439	peroxisomal part	107	76	4.225E-02	0.222
GO:0010812	negative regulation of cell-substrate adhesion	44	37	4.459E-02	-0.363
GO:0004872	receptor activity	1940	1421	4.819E-02	-0.082
GO:0034097	response to cytokine	752	572	4.841E-02	-0.110
GO:0016790	thiolester hydrolase activity	79	58	4.918E-02	0.247

Table B.9: Gene set enrichment results of average correlation vector for biclustering pattern Mito.CV1 found in CCLE analysis in Section 3.3.3.2, showing the top 200 of 1219 significant terms with adjusted p value < 0.05.

GOID	TERM	Number of genes	Genes in genelist	p value	Average correlation vector
GO:0005739	mitochondrion	2109	1334	7.077E-32	0.141
GO:0044429	mitochondrial part	1081	711	4.360E-23	0.169
GO:0005759	mitochondrial matrix	365	300	4.700E-18	0.241
GO:0030198	extracellular matrix organization	422	357	3.513E-09	-0.207
GO:0043062	extracellular structure organization	424	358	3.877E-09	-0.207
GO:0003779	actin binding	402	350	7.029E-09	-0.206
GO:0005740	mitochondrial envelope	743	482	1.514E-08	0.129
GO:0055114	oxidation-reduction process	1187	905	6.836E-08	0.084
GO:0006935	chemotaxis	799	606	1.089E-07	-0.150
GO:0042330	taxis	799	606	1.089E-07	-0.150
GO:0031012	extracellular matrix	558	390	1.541E-07	-0.187
GO:0009653	anatomical structure morphogenesis	3188	2160	1.649E-07	-0.094
GO:0031967	organelle envelope	1166	778	1.746E-07	0.090
GO:0006955	immune response	1821	1241	2.454E-07	-0.111
GO:0031966	mitochondrial membrane	689	451	2.649E-07	0.124
GO:0006928	cellular component movement	2080	1488	3.695E-07	-0.105
GO:0048037	cofactor binding	274	236	3.811E-07	0.178
GO:0031975	envelope	1172	782	5.317E-07	0.088
GO:0040011	locomotion	1887	1350	7.393E-07	-0.107
GO:0022610	biological adhesion	1342	999	1.006E-06	-0.122
GO:0007155	cell adhesion	1334	995	1.116E-06	-0.122
GO:0050662	coenzyme binding	191	168	1.131E-06	0.212
GO:0019752	carboxylic acid metabolic process	1430	905	1.748E-06	0.074
GO:0016054	organic acid catabolic process	304	196	1.806E-06	0.184
GO:0046395	carboxylic acid catabolic process	304	196	1.806E-06	0.184
GO:0002376	immune system process	3353	2069	1.861E-06	-0.089
GO:0005743	mitochondrial inner membrane	488	310	2.972E-06	0.149
GO:0044282	small molecule catabolic process	371	255	4.350E-06	0.156
GO:0000904	cell morphogenesis involved in differentiation	954	757	4.857E-06	-0.130
GO:0006952	defense response	1956	1337	6.233E-06	-0.102
GO:0000902	cell morphogenesis	1341	1025	6.544E-06	-0.115
GO:0009611	response to wounding	1117	903	6.575E-06	-0.123
GO:0032989	cellular component morphogenesis	1428	1093	7.239E-06	-0.112
GO:0009605	response to external stimulus	2532	1822	1.135E-05	-0.091
GO:0042060	wound healing	781	640	1.267E-05	-0.138
GO:0015629	actin cytoskeleton	462	365	1.603E-05	-0.172
GO:0045333	cellular respiration	221	148	3.650E-05	0.208
GO:0019866	organelle inner membrane	531	345	3.863E-05	0.127
GO:0030036	actin cytoskeleton organization	599	451	3.992E-05	-0.155
GO:0005615	extracellular space	1277	1103	4.095E-05	-0.110
GO:0043436	oxoacid metabolic process	1574	1012	4.874E-05	0.061
GO:0009060	aerobic respiration	60	46	5.733E-05	0.384
GO:0005578	proteinaceous extracellular matrix	365	320	6.081E-05	-0.178
GO:0007599	hemostasis	622	515	6.450E-05	-0.145
GO:0006082	organic acid metabolic process	1593	1026	7.265E-05	0.059
GO:0042641	actomyosin	63	58	9.342E-05	-0.380
GO:0016491	oxidoreductase activity	984	607	1.111E-04	0.086
GO:0007596	blood coagulation	615	510	1.122E-04	-0.144
GO:0030029	actin filament-based process	677	501	1.253E-04	-0.143
GO:1990204	oxidoreductase complex	123	76	1.493E-04	0.285
GO:0005518	collagen binding	65	60	1.507E-04	-0.359
GO:0032963	collagen metabolic process	124	105	1.743E-04	-0.280

GOID	TERM	Number of genes	Genes in genelist	p value	Average correlation vector
GO:0002682	regulation of immune system process	1544	1054	2.054E-04	-0.104
GO:0016477	cell migration	1277	960	2.293E-04	-0.108
GO:0044259	multicellular organismal macromolecule metabolic process	130	111	2.987E-04	-0.268
GO:0050817	coagulation	619	513	3.034E-04	-0.140
GO:0031589	cell-substrate adhesion	315	257	3.478E-04	-0.181
GO:0005925	focal adhesion	374	347	3.659E-04	-0.156
GO:0048870	cell motility	1374	1025	3.753E-04	-0.104
GO:0051674	localization of cell	1375	1025	3.753E-04	-0.104
GO:0005576	extracellular region	5375	3838	5.204E-04	-0.067
GO:0032432	actin filament bundle	54	52	6.212E-04	-0.377
GO:0007409	axonogenesis	611	512	8.611E-04	-0.135
GO:0022617	extracellular matrix disassembly	131	119	9.037E-04	-0.255
GO:0005924	cell-substrate adherens junction	380	352	9.473E-04	-0.151
GO:0005777	peroxisome	184	112	1.001E-03	0.208
GO:0042579	microbody	184	112	1.001E-03	0.208
GO:0050878	regulation of body fluid levels	765	630	1.051E-03	-0.124
GO:0009063	cellular amino acid catabolic process	172	108	1.204E-03	0.209
GO:0001725	stress fiber	52	50	1.253E-03	-0.374
GO:0007005	mitochondrion organization	400	257	1.374E-03	0.126
GO:0061564	axon development	635	530	1.388E-03	-0.131
GO:0045087	innate immune response	1006	782	1.558E-03	-0.109
GO:0006631	fatty acid metabolic process	442	305	1.667E-03	0.114
GO:0030055	cell-substrate junction	388	355	1.793E-03	-0.147
GO:0007166	cell surface receptor signaling pathway	4618	3015	2.152E-03	-0.071
GO:0006954	inflammatory response	649	538	2.262E-03	-0.128
GO:0019395	fatty acid oxidation	112	78	2.520E-03	0.240
GO:0050776	regulation of immune response	1013	709	2.520E-03	-0.113
GO:0048646	anatomical structure formation involved in morphogenesis	1187	911	2.986E-03	-0.104
GO:0003824	catalytic activity	7631	4714	3.228E-03	0.013
GO:0044421	extracellular region part	3939	3270	3.315E-03	-0.066
GO:0009062	fatty acid catabolic process	105	70	3.375E-03	0.252
GO:0002684	positive regulation of immune system process	930	642	3.996E-03	-0.114
GO:0048583	regulation of response to stimulus	4468	2819	4.085E-03	-0.071
GO:0001944	vasculature development	711	543	4.412E-03	-0.125
GO:0051186	cofactor metabolic process	375	245	4.991E-03	0.123
GO:0050793	regulation of developmental process	2231	1631	5.567E-03	-0.085
GO:0034440	lipid oxidation	114	80	6.687E-03	0.227
GO:0043405	regulation of MAP kinase activity	285	253	7.317E-03	-0.167
GO:0001568	blood vessel development	665	515	7.350E-03	-0.125
GO:0045595	regulation of cell differentiation	1560	1177	7.690E-03	-0.094
GO:0007411	axon guidance	415	357	7.977E-03	-0.146
GO:0097485	neuron projection guidance	415	357	7.977E-03	-0.146
GO:0001775	cell activation	1101	824	8.595E-03	-0.103
GO:0006732	coenzyme metabolic process	289	188	9.268E-03	0.142
GO:0051239	regulation of multicellular organismal process	2892	2002	1.023E-02	-0.077
GO:0044243	multicellular organismal catabolic process	89	78	1.082E-02	-0.280
GO:0030574	collagen catabolic process	83	72	1.261E-02	-0.290
GO:0008092	cytoskeletal protein binding	862	679	1.332E-02	-0.111
GO:0044455	mitochondrial membrane part	212	125	1.362E-02	0.182
GO:0030258	lipid modification	204	149	1.415E-02	0.156
GO:0022904	respiratory electron transport chain	146	96	1.529E-02	0.211
GO:0005516	calmodulin binding	177	163	1.561E-02	-0.198
GO:0006099	tricarboxylic acid cycle	41	29	1.664E-02	0.401
GO:0048812	neuron projection morphogenesis	717	588	1.692E-02	-0.117
GO:0019783	small conjugating protein-specific protease activity	85	70	1.730E-02	0.244
GO:0072329	monocarboxylic acid catabolic process	127	86	1.796E-02	0.209
GO:0015980	energy derivation by oxidation of organic compounds	436	320	1.972E-02	0.102
GO:0048667	cell morphogenesis involved in neuron differentiation	700	579	2.053E-02	-0.116
GO:0022900	electron transport chain	149	98	2.248E-02	0.204
GO:0030199	collagen fibril organization	44	39	2.759E-02	-0.382
GO:0022411	cellular component disassembly	469	428	3.288E-02	-0.126
GO:0006091	generation of precursor metabolites and energy	565	403	3.412E-02	0.087
GO:0042773	ATP synthesis coupled electron transport	55	47	3.426E-02	0.303
GO:0042775	mitochondrial ATP synthesis coupled electron transport	55	47	3.426E-02	0.303
GO:0048468	cell development	2228	1682	3.662E-02	-0.079

GOID	TERM	Number of genes	Genes in genelist	p value	Average correlation vector
GO:0009083	branched-chain amino acid catabolic process	34	19	4.213E-02	0.480
GO:0044438	microbody part	107	76	4.225E-02	0.222
GO:0044439	peroxisomal part	107	76	4.225E-02	0.222
GO:0010812	negative regulation of cell-substrate adhesion	44	37	4.459E-02	-0.363
GO:0004872	receptor activity	1940	1421	4.819E-02	-0.082
GO:0034097	response to cytokine	752	572	4.841E-02	-0.110
GO:0016790	thiolester hydrolase activity	79	58	4.918E-02	0.247

Table B.10: Gene set enrichment results of average correlation vector for biclustering pattern Random.CV1 found in CCLE analysis in Section 3.3.3.2, showing the top 200 of 1061 significant terms with adjusted p value < 0.05.

GOID	TERM	Number of genes	Genes in genelist	p value	Average correlation vector
GO:0003676	nucleic acid binding	4689	3350	2.586E-91	-0.133
GO:0090304	nucleic acid metabolic process	7863	4176	3.400E-77	-0.103
GO:0005576	extracellular region	5375	3798	8.376E-77	0.214
GO:0005634	nucleus	8112	5630	1.348E-72	-0.081
GO:0044421	extracellular region part	3939	3230	4.597E-69	0.217
GO:0003677	DNA binding	2781	2080	2.747E-67	-0.149
GO:0005654	nucleoplasm	1793	1352	7.682E-66	-0.183
GO:0031981	nuclear lumen	2785	1990	2.335E-65	-0.143
GO:0044428	nuclear part	3483	2343	6.489E-63	-0.125
GO:0016070	RNA metabolic process	6737	3690	1.874E-61	-0.095
GO:0006952	defense response	1956	1314	2.036E-55	0.270
GO:0005615	extracellular space	1277	1085	3.828E-54	0.290
GO:0006139	nucleobase-containing compound metabolic process	9873	5452	5.174E-54	-0.063
GO:0043230	extracellular organelle	2671	2413	1.369E-52	0.216
GO:0065010	extracellular membrane-bounded organelle	2671	2413	1.369E-52	0.216
GO:0070062	extracellular vesicular exosome	2669	2413	1.369E-52	0.216
GO:0051276	chromosome organization	1127	741	1.776E-52	-0.232
GO:1901363	heterocyclic compound binding	7008	5069	2.535E-52	-0.065
GO:0046483	heterocycle metabolic process	10158	5608	5.391E-49	-0.057
GO:0097159	organic cyclic compound binding	7093	5136	8.291E-49	-0.060
GO:0006725	cellular aromatic compound metabolic process	10189	5618	1.582E-48	-0.056
GO:0006955	immune response	1821	1235	3.003E-48	0.262
GO:0071944	cell periphery	6341	3965	9.122E-47	0.179
GO:0031982	vesicle	3913	3116	1.369E-46	0.191
GO:0005886	plasma membrane	6168	3876	2.998E-46	0.180
GO:0032774	RNA biosynthetic process	5516	3094	4.327E-46	-0.087
GO:0031224	intrinsic component of membrane	5833	4422	4.973E-46	0.174
GO:0044451	nucleoplasm part	717	589	6.541E-46	-0.241
GO:0044425	membrane part	7949	5245	6.728E-46	0.166
GO:0031988	membrane-bounded vesicle	3783	3029	6.980E-46	0.192
GO:0016021	integral component of membrane	5650	4318	2.911E-44	0.173
GO:0006351	transcription, DNA-templated	5382	3031	1.070E-43	-0.085
GO:0051252	regulation of RNA metabolic process	4486	3046	2.535E-43	-0.084
GO:0044459	plasma membrane part	2761	2039	3.088E-43	0.215
GO:0034641	cellular nitrogen compound metabolic process	10485	5809	4.265E-43	-0.049
GO:2000112	regulation of cellular macromolecule biosynthetic process	4707	3201	2.300E-42	-0.080
GO:0034654	nucleobase-containing compound biosynthetic process	6012	3404	3.820E-42	-0.075
GO:0010467	gene expression	7890	4342	5.898E-42	-0.061
GO:0019438	aromatic compound biosynthetic process	6127	3474	5.702E-41	-0.072
GO:0003723	RNA binding	1808	1346	6.125E-41	-0.132
GO:0018130	heterocycle biosynthetic process	6129	3468	1.287E-40	-0.072
GO:1901360	organic cyclic compound metabolic process	10552	5810	1.397E-40	-0.046
GO:0002376	immune system process	3353	2071	1.443E-40	0.206
GO:2001141	regulation of RNA biosynthetic process	4359	2971	4.417E-40	-0.081
GO:0006954	inflammatory response	649	529	9.354E-40	0.338
GO:0006355	regulation of transcription, DNA-templated	4286	2936	6.760E-39	-0.080
GO:0010556	regulation of macromolecule biosynthetic process	4909	3301	1.110E-38	-0.072
GO:0044271	cellular nitrogen compound biosynthetic process	6227	3521	1.862E-38	-0.068
GO:0006397	mRNA processing	610	383	2.044E-38	-0.282
GO:0006325	chromatin organization	853	558	2.265E-38	-0.229

GOID	TERM	Number of genes	Genes in genelist	p value	Average correlation vector
GO:0006396	RNA processing	993	629	7.450E-38	-0.204
GO:0034645	cellular macromolecule biosynthetic process	7021	3948	8.405E-38	-0.061
GO:0008380	RNA splicing	525	313	1.369E-37	-0.312
GO:0016071	mRNA metabolic process	885	537	3.668E-37	-0.222
GO:0016568	chromatin modification	661	495	6.727E-37	-0.240
GO:0005694	chromosome	905	668	7.767E-37	-0.200
GO:0031326	regulation of cellular biosynthetic process	5114	3445	1.007E-36	-0.067
GO:0031226	intrinsic component of plasma membrane	1430	1244	1.695E-36	0.239
GO:1901362	organic cyclic compound biosynthetic process	6314	3582	2.399E-36	-0.064
GO:0000278	mitotic cell cycle	1169	838	3.330E-36	-0.168
GO:0044822	poly(A) RNA binding	1170	1019	1.047E-35	-0.146
GO:0006259	DNA metabolic process	1393	841	1.459E-35	-0.168
GO:0005887	integral component of plasma membrane	1359	1199	7.192E-35	0.238
GO:0043207	response to external biotic stimulus	839	606	1.129E-34	0.303
GO:0051707	response to other organism	839	606	1.129E-34	0.303
GO:0009605	response to external stimulus	2532	1801	1.405E-34	0.205
GO:0009889	regulation of biosynthetic process	5182	3483	4.059E-34	-0.062
GO:0044260	cellular macromolecule metabolic process	12514	6531	4.486E-34	-0.034
GO:0009059	macromolecule biosynthetic process	7259	4074	6.901E-34	-0.054
GO:0010468	regulation of gene expression	5356	3560	1.198E-33	-0.061
GO:0019219	regulation of nucleobase-containing compound metabolic process	5589	3760	1.583E-33	-0.057
GO:0009607	response to biotic stimulus	877	635	1.680E-33	0.293
GO:0007049	cell cycle	2122	1445	2.440E-33	-0.111
GO:0006807	nitrogen compound metabolic process	11158	6162	1.196E-32	-0.034
GO:0022402	cell cycle process	1520	1076	1.046E-31	-0.131
GO:1903047	mitotic cell cycle process	966	728	1.186E-31	-0.169
GO:0002682	regulation of immune system process	1544	1051	2.697E-31	0.238
GO:0070013	intracellular organelle lumen	3486	2557	3.505E-31	-0.068
GO:0006281	DNA repair	578	378	3.530E-31	-0.254
GO:0051171	regulation of nitrogen compound metabolic process	5711	3845	1.508E-30	-0.052
GO:0000375	RNA splicing, via transesterification reactions	358	214	1.782E-30	-0.347
GO:0044427	chromosomal part	783	577	1.992E-30	-0.195
GO:0009611	response to wounding	1117	890	5.677E-30	0.251
GO:0004872	receptor activity	1940	1117	6.129E-30	0.233
GO:0000377	RNA splicing, via transesterification reactions with bulged adenosine as nucleophile	349	209	6.728E-30	-0.349
GO:0000398	mRNA splicing, via spliceosome	349	209	6.728E-30	-0.349
GO:0009986	cell surface	703	605	3.137E-29	0.288
GO:0002252	immune effector process	751	539	1.368E-28	0.293
GO:0098589	membrane region	1607	1312	1.436E-28	0.215
GO:0002684	positive regulation of immune system process	930	639	4.430E-28	0.275
GO:0001816	cytokine production	708	509	6.881E-28	0.298
GO:0043233	organelle lumen	3548	2610	1.171E-27	-0.061
GO:0031974	membrane-enclosed lumen	3621	2666	2.884E-27	-0.059
GO:0098542	defense response to other organism	438	329	1.841E-26	0.347
GO:1903034	regulation of response to wounding	393	325	2.258E-26	0.356
GO:0045087	innate immune response	1006	768	3.003E-26	0.249
GO:0009617	response to bacterium	461	358	3.867E-26	0.338
GO:0030198	extracellular matrix organization	422	356	9.629E-26	0.341
GO:0043062	extracellular structure organization	424	357	2.068E-25	0.339
GO:0038023	signaling receptor activity	1651	917	2.731E-25	0.237
GO:0031347	regulation of defense response	640	489	4.230E-25	0.293
GO:0001817	regulation of cytokine production	630	452	6.830E-25	0.300
GO:0004871	signal transducer activity	1971	1205	6.832E-25	0.212
GO:0060089	molecular transducer activity	1971	1205	6.832E-25	0.212
GO:0044770	cell cycle phase transition	530	443	1.836E-24	-0.198
GO:0001775	cell activation	1101	819	2.015E-24	0.240
GO:0042221	response to chemical	5076	3106	2.219E-24	0.155
GO:0015630	microtubule cytoskeleton	1219	860	3.312E-24	-0.126
GO:0016020	membrane	13317	7238	4.326E-24	0.128
GO:0044772	mitotic cell cycle phase transition	518	434	7.779E-24	-0.197
GO:0004888	transmembrane signaling receptor activity	1508	817	8.924E-24	0.243
GO:0032101	regulation of response to external stimulus	686	547	1.543E-23	0.274
GO:0006996	organelle organization	3692	2468	1.918E-23	-0.056

GOID	TERM	Number of genes	Genes in genelist	p value	Average correlation vector
GO:0044249	cellular biosynthetic process	8617	4844	1.721E-22	-0.028
GO:0030529	ribonucleoprotein complex	744	528	3.930E-22	-0.160
GO:0048584	positive regulation of response to stimulus	2005	1395	5.038E-22	0.191
GO:0005813	centrosome	435	374	5.513E-22	-0.205
GO:0050776	regulation of immune response	1013	703	3.270E-21	0.241
GO:0070887	cellular response to chemical stimulus	3061	2054	6.905E-21	0.166
GO:1901576	organic substance biosynthetic process	8804	4937	1.591E-20	-0.024
GO:0022610	biological adhesion	1342	987	3.722E-20	0.211
GO:1990234	transferase complex	618	514	6.334E-20	-0.157
GO:0005681	spliceosomal complex	164	135	7.516E-20	-0.356
GO:0007155	cell adhesion	1334	982	7.941E-20	0.210
GO:0006974	cellular response to DNA damage stimulus	982	643	1.690E-19	-0.138
GO:0005783	endoplasmic reticulum	1847	1297	1.841E-19	0.189
GO:0009058	biosynthetic process	8929	5007	2.818E-19	-0.022
GO:0006950	response to stress	4845	3075	3.665E-19	0.143
GO:0044432	endoplasmic reticulum part	1158	912	5.614E-19	0.212
GO:0005815	microtubule organizing center	586	489	7.047E-19	-0.158
GO:0016569	covalent chromatin modification	447	341	7.824E-19	-0.203
GO:0051240	positive regulation of multicellular organismal process	724	565	1.287E-18	0.252
GO:0016570	histone modification	439	336	1.552E-18	-0.203
GO:0050727	regulation of inflammatory response	264	226	1.720E-18	0.361
GO:0016604	nuclear body	339	300	1.827E-18	-0.217
GO:0007165	signal transduction	7988	4490	2.144E-18	0.131
GO:0007017	microtubule-based process	631	464	2.642E-18	-0.161
GO:0000226	microtubule cytoskeleton organization	393	309	4.032E-18	-0.207
GO:0080134	regulation of response to stress	1172	899	4.698E-18	0.207
GO:1902494	catalytic complex	927	750	5.044E-18	-0.112
GO:0032991	macromolecular complex	5558	3965	5.663E-18	-0.024
GO:0002697	regulation of immune effector process	302	247	8.161E-18	0.337
GO:0003682	chromatin binding	422	385	9.164E-18	-0.187
GO:0034097	response to cytokine	752	557	1.050E-17	0.243
GO:0050865	regulation of cell activation	492	392	1.275E-17	0.283
GO:0000323	lytic vacuole	533	425	3.674E-17	0.268
GO:0005764	lysosome	533	425	3.674E-17	0.268
GO:0010033	response to organic substance	3172	2199	3.838E-17	0.154
GO:0070161	anchoring junction	478	414	4.912E-17	0.276
GO:1902533	positive regulation of intracellular signal transduction	820	659	5.633E-17	0.226
GO:0071824	protein-DNA complex subunit organization	165	132	6.133E-17	-0.349
GO:0012505	endomembrane system	4489	3002	7.334E-17	0.140
GO:0007166	cell surface receptor signaling pathway	4618	2712	9.610E-17	0.146
GO:0043231	intracellular membrane-bounded organelle	14352	8936	1.285E-16	-0.002
GO:0098552	side of membrane	311	279	1.347E-16	0.319
GO:0031012	extracellular matrix	558	388	1.561E-16	0.281
GO:0005125	cytokine activity	226	188	2.059E-16	0.369
GO:0045321	leukocyte activation	812	606	2.456E-16	0.233
GO:0048583	regulation of response to stimulus	4468	2843	4.898E-16	0.141
GO:0043229	intracellular organelle	16594	9839	5.355E-16	0.000
GO:0005102	receptor binding	1689	1199	5.508E-16	0.183
GO:0031323	regulation of cellular metabolic process	7614	4869	6.578E-16	-0.017
GO:1902589	single-organism organelle organization	2350	1660	1.221E-15	-0.056
GO:0000228	nuclear chromosome	390	330	1.328E-15	-0.191
GO:0050778	positive regulation of immune response	652	454	1.348E-15	0.255
GO:0043228	non-membrane-bounded organelle	4369	3101	2.085E-15	-0.027
GO:0043232	intracellular non-membrane-bounded organelle	4369	3101	2.085E-15	-0.027
GO:0032993	protein-DNA complex	334	244	2.240E-15	-0.225
GO:0000775	chromosome, centromeric region	214	153	2.948E-15	-0.295
GO:0051241	negative regulation of multicellular organismal process	416	355	3.077E-15	0.279
GO:0002237	response to molecule of bacterial origin	265	233	3.108E-15	0.328
GO:0005912	adherens junction	457	397	3.234E-15	0.270
GO:0042393	histone binding	139	123	3.276E-15	-0.339
GO:0002694	regulation of leukocyte activation	460	363	3.762E-15	0.276
GO:0016477	cell migration	1277	962	4.067E-15	0.192
GO:0005126	cytokine receptor binding	285	207	5.074E-15	0.344
GO:0042060	wound healing	781	632	5.124E-15	0.224
GO:0050896	response to stimulus	13313	6725	7.172E-15	0.114

GOID	TERM	Number of genes	Genes in genelist	p value	Average correlation vector
GO:0052547	regulation of peptidase activity	447	337	1.023E-14	0.280
GO:0042742	defense response to bacterium	193	146	1.142E-14	0.396
GO:0000280	nuclear division	606	474	1.260E-14	-0.138
GO:0006261	DNA-dependent DNA replication	161	121	1.324E-14	-0.328
GO:0005773	vacuole	606	476	1.459E-14	0.243
GO:0071345	cellular response to cytokine stimulus	631	464	1.515E-14	0.243
GO:0006310	DNA recombination	273	202	2.180E-14	-0.244
GO:0005819	spindle	287	242	2.327E-14	-0.214
GO:0050900	leukocyte migration	362	288	2.587E-14	0.296
GO:0044839	cell cycle G2/M phase transition	180	163	2.654E-14	-0.274
GO:0009897	external side of plasma membrane	224	205	3.090E-14	0.340
GO:0048870	cell motility	1374	1029	3.702E-14	0.185
GO:0051674	localization of cell	1375	1029	3.702E-14	0.185
GO:0016607	nuclear speck	176	168	3.946E-14	-0.265
GO:0009888	tissue development	2160	1550	4.102E-14	0.164
GO:0000086	G2/M transition of mitotic cell cycle	178	162	4.245E-14	-0.273
GO:0030055	cell-substrate junction	388	341	4.941E-14	0.279
GO:0043170	macromolecule metabolic process	14207	7340	5.292E-14	-0.002
GO:0052548	regulation of endopeptidase activity	422	320	5.296E-14	0.280
GO:0098588	bounding membrane of organelle	2558	1891	5.427E-14	0.153
GO:0019221	cytokine-mediated signaling pathway	475	359	5.961E-14	0.265
GO:0006260	DNA replication	388	290	6.136E-14	-0.189

Table B.11: Gene set enrichment results of average correlation vector for biclustering pattern Random.CV2 found in CCLE analysis in Section 3.3.3.2, showing the top 200 of 1186 significant terms with adjusted p value < 0.05.

GOID	TERM	Number of genes	Genes in genelist	p value	Average correlation vector
GO:0006396	RNA processing	993	629	2.736E-101	0.677
GO:0003723	RNA binding	1808	1346	1.029E-86	0.510
GO:0031981	nuclear lumen	2785	1990	4.893E-78	0.460
GO:0044428	nuclear part	3483	2343	4.125E-74	0.436
GO:0012505	endomembrane system	4489	3002	2.136E-73	0.018
GO:0044822	poly(A) RNA binding	1170	1019	2.236E-72	0.513
GO:0098588	bounding membrane of organelle	2558	1891	3.131E-71	-0.021
GO:0030529	ribonucleoprotein complex	744	528	7.328E-70	0.633
GO:0016071	mRNA metabolic process	885	537	8.385E-67	0.632
GO:0005654	nucleoplasm	1793	1352	2.545E-66	0.489
GO:0009653	anatomical structure morphogenesis	3188	2184	4.611E-62	0.010
GO:0006397	mRNA processing	610	383	2.102E-59	0.672
GO:0022613	ribonucleoprotein complex biogenesis	339	250	2.049E-56	0.746
GO:0008380	RNA splicing	525	313	1.027E-54	0.700
GO:0005794	Golgi apparatus	1552	1173	1.452E-54	-0.067
GO:0070013	intracellular organelle lumen	3486	2557	1.810E-53	0.394
GO:0031982	vesicle	3913	3116	2.202E-53	0.060
GO:0003676	nucleic acid binding	4689	3350	1.082E-51	0.393
GO:0031974	membrane-enclosed lumen	3621	2666	4.990E-51	0.388
GO:0031988	membrane-bounded vesicle	3783	3029	7.218E-51	0.061
GO:0034660	ncRNA metabolic process	400	299	2.431E-50	0.676
GO:0043233	organelle lumen	3548	2610	4.818E-50	0.387
GO:0005783	endoplasmic reticulum	1847	1297	8.794E-49	-0.021
GO:0044421	extracellular region part	3939	3230	2.804E-48	0.077
GO:0000375	RNA splicing, via transesterification reactions	358	214	2.907E-48	0.755
GO:0000377	RNA splicing, via transesterification reactions with bulged adenosine as nucleophile	349	209	9.253E-48	0.760
GO:0000398	mRNA splicing, via spliceosome	349	209	9.253E-48	0.760
GO:0034470	ncRNA processing	259	212	2.037E-47	0.741
GO:0005912	adherens junction	457	397	4.136E-46	-0.282
GO:0070161	anchoring junction	478	414	5.306E-46	-0.268
GO:0043230	extracellular organelle	2671	2413	1.750E-45	0.048
GO:0065010	extracellular membrane-bounded organelle	2671	2413	1.750E-45	0.048
GO:0070062	extracellular vesicular exosome	2669	2413	1.750E-45	0.048
GO:0009888	tissue development	2160	1550	1.156E-44	0.026

GOID	TERM	Number of genes	Genes in genelist	p value	Average correlation vector
GO:0005576	extracellular region	5375	3798	8.353E-44	0.106
GO:0044431	Golgi apparatus part	904	713	1.585E-43	-0.097
GO:0044432	endoplasmic reticulum part	1158	912	5.730E-43	-0.050
GO:0098589	membrane region	1607	1312	1.947E-42	0.009
GO:0005925	focal adhesion	374	333	3.549E-41	-0.316
GO:0005924	cell-substrate adherens junction	380	338	4.963E-41	-0.310
GO:0030055	cell-substrate junction	388	341	6.150E-41	-0.305
GO:0072358	cardiovascular system development	1116	818	1.184E-40	-0.061
GO:0072359	circulatory system development	1116	818	1.184E-40	-0.061
GO:0006928	cellular component movement	2080	1497	8.602E-40	0.022
GO:0030198	extracellular matrix organization	422	356	1.914E-39	-0.239
GO:0044451	nucleoplasm part	717	589	2.093E-39	0.530
GO:0043062	extracellular structure organization	424	357	2.793E-39	-0.237
GO:0006259	DNA metabolic process	1393	841	1.418E-38	0.480
GO:0000139	Golgi membrane	624	535	2.562E-38	-0.130
GO:0040011	locomotion	1887	1358	2.393E-37	0.017
GO:0000902	cell morphogenesis	1341	1054	3.490E-37	-0.023
GO:0042254	ribosome biogenesis	188	146	7.699E-37	0.764
GO:0032989	cellular component morphogenesis	1428	1121	1.077E-36	-0.013
GO:0044425	membrane part	7949	5245	1.920E-36	0.143
GO:0030054	cell junction	1167	980	8.074E-36	-0.025
GO:0048731	system development	5637	3653	1.064E-34	0.114
GO:0005681	spliceosomal complex	164	135	1.708E-34	0.784
GO:0016192	vesicle-mediated transport	1419	1037	1.768E-34	-0.013
GO:0031090	organelle membrane	3375	2427	2.279E-34	0.069
GO:0016477	cell migration	1277	962	3.163E-34	-0.017
GO:0009966	regulation of signal transduction	3216	2194	6.245E-34	0.067
GO:0030030	cell projection organization	1349	1040	1.469E-33	-0.002
GO:0005694	chromosome	905	668	1.482E-33	0.490
GO:0001944	vasculature development	711	543	2.272E-33	-0.106
GO:0051276	chromosome organization	1127	741	8.585E-33	0.498
GO:0022610	biological adhesion	1342	987	4.257E-32	0.011
GO:0007155	cell adhesion	1334	982	7.356E-32	0.011
GO:0048856	anatomical structure development	6783	4258	8.134E-32	0.126
GO:0090304	nucleic acid metabolic process	7863	4176	9.095E-32	0.353
GO:0000904	cell morphogenesis involved in differentiation	954	767	1.344E-31	-0.043
GO:0005789	endoplasmic reticulum membrane	948	761	1.454E-31	-0.030
GO:0023051	regulation of signaling	3620	2458	3.502E-31	0.086
GO:0048646	anatomical structure formation involved in morphogenesis	1187	925	4.486E-31	-0.004
GO:0010646	regulation of cell communication	3631	2464	5.333E-31	0.087
GO:0048870	cell motility	1374	1029	7.590E-31	0.005
GO:0051674	localization of cell	1375	1029	7.590E-31	0.005
GO:0042175	nuclear outer membrane-endoplasmic reticulum membrane network	971	776	9.223E-31	-0.024
GO:0060429	epithelium development	1252	962	2.233E-30	0.020
GO:0048858	cell projection morphogenesis	913	737	2.346E-30	-0.035
GO:0032502	developmental process	7760	4766	3.216E-30	0.135
GO:0006281	DNA repair	578	378	3.401E-30	0.545
GO:0001568	blood vessel development	665	513	4.518E-30	-0.097
GO:0022603	regulation of anatomical structure morphogenesis	843	697	7.400E-30	-0.042
GO:0007399	nervous system development	2516	1842	7.996E-30	0.074
GO:0007275	multicellular organismal development	6429	4162	1.899E-29	0.132
GO:0044767	single-organism developmental process	7612	4719	1.927E-29	0.136
GO:2000145	regulation of cell motility	608	501	2.294E-29	-0.100
GO:0016020	membrane	13317	7238	2.381E-29	0.156
GO:0005840	ribosome	251	149	3.883E-29	0.723
GO:0007154	cell communication	9101	5048	6.223E-29	0.147
GO:0023052	signaling	8975	4978	9.935E-29	0.146
GO:0044700	single organism signaling	8975	4978	9.935E-29	0.146
GO:0022008	neurogenesis	1639	1245	9.968E-29	0.043
GO:0032990	cell part morphogenesis	933	756	1.028E-28	-0.025
GO:0051179	localization	7894	4603	1.870E-28	0.135
GO:0005730	nucleolus	728	644	3.123E-28	0.454
GO:0006364	rRNA processing	125	106	3.225E-28	0.769
GO:0007165	signal transduction	7988	4490	3.754E-28	0.139

GOID	TERM	Number of genes	Genes in genelist	p value	Average correlation vector
GO:0009887	organ morphogenesis	1011	818	4.789E-28	-0.001
GO:0040012	regulation of locomotion	685	553	5.724E-28	-0.073
GO:0016072	rRNA metabolic process	134	111	6.422E-28	0.757
GO:0031224	intrinsic component of membrane	5833	4422	6.989E-28	0.156
GO:0030334	regulation of cell migration	576	478	9.076E-28	-0.100
GO:0016021	integral component of membrane	5650	4318	9.417E-28	0.155
GO:0051270	regulation of cellular component movement	691	567	7.752E-27	-0.064
GO:0031410	cytoplasmic vesicle	1290	988	1.373E-26	0.022
GO:0044427	chromosomal part	783	577	2.154E-26	0.477
GO:0048583	regulation of response to stimulus	4468	2843	2.683E-26	0.108
GO:0048699	generation of neurons	1536	1174	2.787E-26	0.047
GO:0007167	enzyme linked receptor protein signaling pathway	1306	935	3.134E-26	0.006
GO:0048468	cell development	2228	1700	3.996E-26	0.075
GO:0071944	cell periphery	6341	3965	1.683E-25	0.150
GO:0031012	extracellular matrix	558	388	3.578E-25	-0.105
GO:0001501	skeletal system development	515	424	3.855E-25	-0.099
GO:0048869	cellular developmental process	4670	3189	4.254E-25	0.122
GO:0048514	blood vessel morphogenesis	583	448	5.136E-25	-0.091
GO:0031175	neuron projection development	943	756	7.766E-25	-0.005
GO:0048729	tissue morphogenesis	606	510	9.554E-25	-0.052
GO:0030182	neuron differentiation	1394	1078	9.933E-25	0.048
GO:0048812	neuron projection morphogenesis	717	590	1.013E-24	-0.042
GO:0003735	structural constituent of ribosome	160	97	2.857E-24	0.778
GO:0061564	axon development	635	531	8.577E-24	-0.049
GO:0008104	protein localization	2180	1688	8.701E-24	0.070
GO:0005886	plasma membrane	6168	3876	1.235E-23	0.153
GO:0050793	regulation of developmental process	2231	1648	1.531E-23	0.079
GO:0048667	cell morphogenesis involved in neuron differentiation	700	582	1.635E-23	-0.036
GO:2000026	regulation of multicellular organismal development	1647	1256	1.708E-23	0.060
GO:0042995	cell projection	1718	1367	3.670E-23	0.077
GO:0006310	DNA recombination	273	202	3.855E-23	0.642
GO:0005773	vacuole	606	476	7.406E-23	-0.082
GO:0035556	intracellular signal transduction	2879	2032	1.103E-22	0.097
GO:0048666	neuron development	1092	872	1.117E-22	0.029
GO:0007409	axonogenesis	611	513	1.424E-22	-0.048
GO:0042221	response to chemical	5076	3106	1.789E-22	0.133
GO:0048513	organ development	3828	2685	2.166E-22	0.123
GO:0051239	regulation of multicellular organismal process	2892	2012	2.633E-22	0.104
GO:0030154	cell differentiation	4368	3012	3.017E-22	0.127
GO:0044707	single-multicellular organism process	9631	5534	4.419E-22	0.166
GO:0016023	cytoplasmic membrane-bounded vesicle	1184	908	6.986E-22	0.033
GO:0005615	extracellular space	1277	1085	1.409E-21	0.078
GO:0044437	vacuolar part	374	315	1.544E-21	-0.154
GO:0022618	ribonucleoprotein complex assembly	173	121	1.803E-21	0.720
GO:0070887	cellular response to chemical stimulus	3061	2054	3.843E-21	0.108
GO:1902531	regulation of intracellular signal transduction	1855	1356	5.247E-21	0.070
GO:0071826	ribonucleoprotein complex subunit organization	180	128	6.280E-21	0.698
GO:0002009	morphogenesis of an epithelium	476	405	8.542E-21	-0.062
GO:0007507	heart development	533	420	1.425E-20	-0.057
GO:0032501	multicellular organismal process	9979	5713	1.595E-20	0.170
GO:0009100	glycoprotein metabolic process	495	366	2.127E-20	-0.084
GO:0072001	renal system development	330	263	2.317E-20	-0.133
GO:0016604	nuclear body	339	300	3.636E-20	0.520
GO:0044391	ribosomal subunit	153	84	4.234E-20	0.781
GO:0006261	DNA-dependent DNA replication	161	121	4.636E-20	0.679
GO:0006401	RNA catabolic process	282	169	4.732E-20	0.631
GO:0001525	angiogenesis	464	367	5.082E-20	-0.091
GO:0071310	cellular response to organic substance	2362	1650	6.035E-20	0.092
GO:0035295	tube development	675	566	6.377E-20	-0.011
GO:0030029	actin filament-based process	677	508	6.400E-20	-0.036
GO:0010033	response to organic substance	3172	2199	9.571E-20	0.113
GO:0071013	catalytic step 2 spliceosome	80	75	1.008E-19	0.808
GO:0006260	DNA replication	388	290	1.401E-19	0.510
GO:0001655	urogenital system development	373	300	1.929E-19	-0.102
GO:0005578	proteinaceous extracellular matrix	365	316	2.273E-19	-0.091

GOID	TERM	Number of genes	Genes in genelist	p value	Average correlation vector
GO:0000323	lytic vacuole	533	425	4.422E-19	-0.078
GO:0005764	lysosome	533	425	4.422E-19	-0.078
GO:0033036	macromolecule localization	2639	1976	4.498E-19	0.095
GO:0016070	RNA metabolic process	6737	3690	5.286E-19	0.335
GO:0030036	actin cytoskeleton organization	599	457	6.984E-19	-0.050
GO:0061061	muscle structure development	629	479	7.464E-19	-0.028
GO:1901363	heterocyclic compound binding	7008	5069	7.506E-19	0.324
GO:0045184	establishment of protein localization	1692	1342	8.596E-19	0.069
GO:0005634	nucleus	8112	5630	1.200E-18	0.314
GO:0015031	protein transport	1553	1242	2.700E-18	0.065
GO:0044444	cytoplasmic part	10781	6514	2.868E-18	0.151
GO:0001822	kidney development	309	248	3.429E-18	-0.119
GO:0097159	organic cyclic compound binding	7093	5136	3.549E-18	0.323
GO:0006974	cellular response to DNA damage stimulus	982	643	6.602E-18	0.421
GO:0048193	Golgi vesicle transport	241	198	7.141E-18	-0.184
GO:0010647	positive regulation of cell communication	1360	1065	7.398E-18	0.058
GO:0023057	negative regulation of signaling	1127	867	8.309E-18	0.029
GO:0034330	cell junction organization	262	217	9.561E-18	-0.147
GO:0005768	endosome	818	600	9.986E-18	-0.006
GO:0010648	negative regulation of cell communication	1129	869	1.150E-17	0.030
GO:0009611	response to wounding	1117	890	1.222E-17	0.058
GO:0048598	embryonic morphogenesis	650	536	1.258E-17	0.003
GO:0023056	positive regulation of signaling	1355	1060	1.329E-17	0.059
GO:0006810	transport	6295	3693	1.406E-17	0.151
GO:0070848	response to growth factor	843	648	1.529E-17	0.014
GO:0031589	cell-substrate adhesion	315	260	1.745E-17	-0.133
GO:0044765	single-organism transport	5155	3114	1.775E-17	0.148
GO:0007411	axon guidance	415	353	1.930E-17	-0.069
GO:0097485	neuron projection guidance	415	353	1.930E-17	-0.069
GO:0050673	epithelial cell proliferation	325	283	2.342E-17	-0.089
GO:0071363	cellular response to growth factor stimulus	822	632	2.576E-17	0.011
GO:0000228	nuclear chromosome	390	330	2.823E-17	0.506
GO:0051234	establishment of localization	6434	3778	3.016E-17	0.152
GO:0009968	negative regulation of signal transduction	1081	826	3.047E-17	0.025
GO:0032879	regulation of localization	2401	1757	4.952E-17	0.113
GO:0031252	cell leading edge	336	292	6.938E-17	-0.126
GO:0000278	mitotic cell cycle	1169	838	7.755E-17	0.389

Table B.12: Top 200 of 651 significant terms for ICT1 related gene set from Section 4.2.1 calculated by gprofiler

TERM ID	TERM	Term size	Overlap size	p value
GO:0044446	intracellular organelle part	7885	545	1.090E-39
GO:0044422	organelle part	8104	550	1.180E-37
TF:M00803_1	Factor: E2F; motif: GGCGSG; match class: 1	14302	699	7.990E-35
GO:0031974	membrane-enclosed lumen	4250	351	5.570E-34
TF:M00716_1	Factor: ZF5; motif: GSGCGCGR; match class: 1	16480	760	2.450E-33
TF:M00803_0	Factor: E2F; motif: GGCGSG; match class: 0	17619	787	1.950E-31
GO:0070013	intracellular organelle lumen	4140	337	1.000E-30
GO:0044424	intracellular part	13685	751	4.730E-30
GO:0043233	organelle lumen	4194	338	5.930E-30
GO:0043229	intracellular organelle	11855	684	2.580E-29
GO:0043231	intracellular membrane-bounded organelle	10791	636	9.680E-27
GO:0005622	intracellular	14067	755	8.220E-26
GO:0043227	membrane-bounded organelle	11947	678	1.780E-25
GO:0043226	organelle	12901	713	2.960E-25
GO:0000786	nucleosome	106	41	9.780E-25
GO:0044815	DNA packaging complex	112	41	1.270E-23
TF:M00716_0	Factor: ZF5; motif: GSGCGCGR; match class: 0	19516	819	5.540E-23
GO:0006996	organelle organization	3711	293	6.290E-23
GO:0044429	mitochondrial part	967	122	7.600E-23
GO:0032991	macromolecular complex	4503	335	9.550E-23
GO:0043228	non-membrane-bounded organelle	3828	298	2.000E-22

TERM ID	TERM	Term size	Overlap size	p value
GO:0043232	intracellular non-membrane-bounded organelle	3828	298	2.000E-22
GO:0005743	mitochondrial inner membrane	496	82	5.510E-22
GO:0031981	nuclear lumen	3435	275	6.130E-22
REAC:2299718	Condensation of Prophase Chromosomes	72	34	3.110E-21
REAC:5334118	DNA methylation	63	32	3.660E-21
GO:0044428	nuclear part	3773	290	1.130E-20
GO:0071840	cellular component organization or biogenesis	6327	420	1.420E-20
REAC:73728	RNA Polymerase I Promoter Opening	61	31	1.840E-20
GO:0006414	translational elongation	219	52	2.090E-20
GO:0019866	organelle inner membrane	551	83	1.600E-19
TF:M04687_1	Factor: BRCA1; motif: TMTCGCGAG; match class: 1	19299	807	2.030E-19
GO:0006415	translational termination	179	46	2.480E-19
TF:M04710_1	Factor: CHD2; motif: TCTCGCGAG; match class: 1	19229	805	2.590E-19
GO:0005739	mitochondrion	1699	165	3.050E-19
REAC:912446	Meiotic recombination	86	35	3.170E-19
REAC:5625886	Activated PKN1 stimulates transcription of AR (androgen receptor) regulated genes KLK2 and KLK3	66	31	3.870E-19
REAC:427359	SIRT1 negatively regulates rRNA Expression	66	31	3.870E-19
REAC:212300	PRC2 methylates histones and DNA	71	32	4.140E-19
GO:0005740	mitochondrial envelope	720	96	5.010E-19
TF:M01240_1	Factor: BEN; motif: CAGCGRNV; match class: 1	19940	822	5.350E-19
TF:M04703_1	Factor: c-ets-1; motif: TCTCGCGAG; match class: 1	19373	808	5.530E-19
TF:M02065_1	Factor: ER81; motif: RCCGGAARYN; match class: 1	12310	590	5.910E-19
REAC:73777	RNA Polymerase I Chain Elongation	88	35	7.910E-19
REAC:3214815	HDACs deacetylate histones	94	36	9.550E-19
GO:0032993	protein-DNA complex	169	44	1.210E-18
GO:0016043	cellular component organization	6199	407	1.730E-18
TF:M04760_1	Factor: GR; motif: TCTCGCGAG; match class: 1	18786	791	3.310E-18
REAC:427413	NoRC negatively regulates rRNA expression	104	37	5.190E-18
TF:M07250_0	Factor: E2F1; motif: NNNSSCGCSAANN; match class: 0	15286	686	8.940E-18
TF:M02065_0	Factor: ER81; motif: RCCGGAARYN; match class: 0	18422	780	9.590E-18
TF:M00025_0	Factor: Elk-1; motif: NNNNCCGGAARTNN; match class: 0	16217	715	1.130E-17
REAC:5250941	Negative epigenetic regulation of rRNA expression	107	37	1.610E-17
GO:0031966	mitochondrial membrane	679	90	1.750E-17
GO:0071822	protein complex subunit organization	1879	172	1.820E-17
GO:0043933	macromolecular complex subunit organization	2636	217	2.140E-17
GO:0005840	ribosome	235	50	2.730E-17
TF:M00196_0	Factor: Sp1; motif: NGGGGGCGGGGYN; match class: 0	15939	704	6.920E-17
REAC:5625740	RHO GTPases activate PKNs	93	34	7.270E-17
REAC:977225	Amyloid fiber formation	99	35	7.480E-17
KEGG:05322	Systemic lupus erythematosus	132	39	9.410E-17
GO:0000790	nuclear chromatin	291	55	1.090E-16
TF:M00695_0	Factor: ETF; motif: GVGGMGG; match class: 0	12819	600	1.150E-16
GO:0006413	translational initiation	273	53	1.510E-16
REAC:5250913	Positive epigenetic regulation of rRNA expression	89	33	1.510E-16
REAC:5250924	B-WICH complex positively regulates rRNA expression	89	33	1.510E-16
REAC:2559582	Senescence-Associated Secretory Phenotype (SASP)	108	36	2.130E-16
GO:0070125	mitochondrial translational elongation	84	30	2.350E-16
REAC:212165	Epigenetic regulation of gene expression	136	40	3.660E-16
TF:M01660_1	Factor: GABPalpha; motif: CTTCCK; match class: 1	9803	489	4.170E-16
GO:0044238	primary metabolic process	10482	591	5.050E-16
TF:M00025_1	Factor: Elk-1; motif: NNNNCCGGAARTNN; match class: 1	9525	478	5.740E-16
TF:M00333_0	Factor: ZF5; motif: NRNGNGCGCGCWN; match class: 0	16969	733	6.020E-16
GO:0044260	cellular macromolecule metabolic process	8596	509	6.970E-16
GO:0071704	organic substance metabolic process	10808	604	7.450E-16
GO:0008152	metabolic process	12055	654	1.090E-15
GO:0005737	cytoplasm	10606	595	1.110E-15
REAC:73854	RNA Polymerase I Promoter Clearance	107	35	1.330E-15
TF:M01660_0	Factor: GABPalpha; motif: CTTCCK; match class: 0	16709	724	1.380E-15
REAC:201722	Formation of the beta-catenin:TCF transactivating complex	89	32	1.550E-15
REAC:2559580	Oxidative Stress Induced Senescence	121	37	1.820E-15
GO:0032543	mitochondrial translation	118	34	1.970E-15
GO:0000785	chromatin	442	67	2.050E-15

TERM ID	TERM	Term size	Overlap size	p value
GO:0044237	cellular metabolic process	10390	585	2.060E-15
REAC:73864	RNA Polymerase I Transcription	109	35	2.610E-15
GO:0000228	nuclear chromosome	494	71	3.580E-15
REAC:1500620	Meiosis	117	36	4.170E-15
REAC:5578749	Transcriptional regulation by small RNAs	104	34	4.180E-15
GO:0034641	cellular nitrogen compound metabolic process	6616	415	4.490E-15
GO:0044391	ribosomal subunit	162	39	5.530E-15
TF:M04760_0	Factor: GR; motif: TCTCGCGAG; match class: 0	20652	831	1.020E-14
REAC:5619507	Activation of HOX genes during differentiation	121	36	1.420E-14
REAC:5617472	Activation of anterior HOX genes in hindbrain development during early embryogenesis	121	36	1.420E-14
GO:0044454	nuclear chromosome part	460	67	1.740E-14
GO:0003735	structural constituent of ribosome	223	45	2.140E-14
GO:0043624	cellular protein complex disassembly	285	51	2.960E-14
REAC:2559583	Cellular Senescence	191	45	3.080E-14
GO:0070124	mitochondrial translational initiation	84	28	3.310E-14
GO:0000788	nuclear nucleosome	43	21	3.430E-14
GO:0006807	nitrogen compound metabolic process	6922	426	3.730E-14
GO:0003723	RNA binding	1598	146	3.780E-14
GO:0043170	macromolecule metabolic process	9286	533	3.820E-14
REAC:5389840	Mitochondrial translation elongation	86	30	4.730E-14
KEGG:05034	Alcoholism	180	42	5.500E-14
TF:M02052_0	Factor: EHF; motif: CSCGGAARTN; match class: 0	15733	688	6.270E-14
GO:0070126	mitochondrial translational termination	86	28	6.710E-14
TF:M02071_0	Factor: ETV7; motif: NCCGGAANNN; match class: 0	15243	672	6.760E-14
TF:M02070_1	Factor: TEL1; motif: CNCGGAANNN; match class: 1	9180	457	6.820E-14
TF:M00986_0	Factor: Churchill; motif: CGGGNN; match class: 0	18592	775	6.840E-14
GO:0044822	poly(A) RNA binding	1179	118	1.030E-13
REAC:68886	M Phase	302	57	1.050E-13
TF:M07395_0	Factor: Sp1; motif: NGGGGCGGGGN; match class: 0	14838	658	1.050E-13
REAC:171306	Packaging Of Telomere Ends	50	23	1.400E-13
GO:0007005	mitochondrion organization	765	89	1.450E-13
GO:0043241	protein complex disassembly	309	52	2.150E-13
TF:M07056_1	Factor: Pitx2; motif: WNTAAWCCCA; match class: 1	11975	558	2.470E-13
TF:M02114_1	Factor: pitx2; motif: NNTAAWCCCA; match class: 1	11975	558	2.470E-13
TF:M07052_0	Factor: NRF-1; motif: GCGCMTGCGCN; match class: 0	2876	190	3.460E-13
GO:0031967	organelle envelope	1109	112	3.820E-13
REAC:69278	Cell Cycle, Mitotic	482	74	3.830E-13
REAC:5368287	Mitochondrial translation	92	30	3.990E-13
TF:M02102_0	Factor: NRF-1; motif: YGCGCMTGCGC; match class: 0	4374	258	4.280E-13
TF:M02070_0	Factor: TEL1; motif: CNCGGAANNN; match class: 0	16235	701	5.020E-13
GO:0031975	envelope	1115	112	5.650E-13
REAC:201681	TCF dependent signaling in response to WNT	231	48	5.740E-13
GO:1990904	ribonucleoprotein complex	717	84	7.790E-13
GO:0030529	intracellular ribonucleoprotein complex	717	84	7.790E-13
GO:0006412	translation	677	81	8.220E-13
GO:1901363	heterocyclic compound binding	5944	374	9.440E-13
GO:0043043	peptide biosynthetic process	706	83	9.680E-13
GO:0032984	macromolecular complex disassembly	320	52	9.820E-13
GO:0006334	nucleosome assembly	144	34	1.610E-12
REAC:2559586	DNA Damage/Telomere Stress Induced Senescence	78	27	2.070E-12
TF:M04687_0	Factor: BRCA1; motif: TMTCGCGAG; match class: 0	21180	839	2.090E-12
TF:M02089_0	Factor: E2F-3; motif: GGCGGGN; match class: 0	16847	718	2.420E-12
REAC:211000	Gene Silencing by RNA	133	35	2.630E-12
GO:0010467	gene expression	5430	347	2.980E-12
REAC:5368286	Mitochondrial translation initiation	86	28	3.870E-12
REAC:5419276	Mitochondrial translation termination	86	28	3.870E-12
GO:0044427	chromosomal part	751	85	3.970E-12
GO:0044267	cellular protein metabolic process	5157	333	4.070E-12
REAC:195258	RHO GTPase Effectors	290	53	5.200E-12
GO:0044444	cytoplasmic part	8003	467	6.570E-12
TF:M07063_0	Factor: Sp1; motif: GGGGCGGGGC; match class: 0	14183	629	8.020E-12
TF:M07250_1	Factor: E2F1; motif: NNNSSCGCSAANN; match class: 1	9775	471	8.670E-12
GO:0097159	organic cyclic compound binding	6027	374	9.600E-12

TERM ID	TERM	Term size	Overlap size	p value
REAC:504046	RNA Polymerase I, RNA Polymerase III, and Mitochondrial Transcription	146	36	9.660E-12
REAC:68875	Mitotic Prophase	139	35	1.130E-11
TF:M04703_0	Factor: c-ets-1; motif: TCTCGCGAG; match class: 0	21372	842	1.180E-11
GO:0065004	protein-DNA complex assembly	193	38	1.840E-11
GO:0005654	nucleoplasm	2802	208	1.990E-11
TF:M00196_1	Factor: Sp1; motif: NGGGGGCGGGGYN; match class: 1	11615	537	2.360E-11
GO:0045814	negative regulation of gene expression, epigenetic	166	35	2.460E-11
GO:0005634	nucleus	6842	411	2.510E-11
GO:0044464	cell part	16166	791	2.580E-11
GO:0005759	mitochondrial matrix	405	57	2.580E-11
TF:M00931_0	Factor: Sp1; motif: GGGGCGGGGC; match class: 0	14606	641	3.110E-11
REAC:3214847	HATs acetylate histones	144	35	3.580E-11
REAC:392499	Metabolism of proteins	1065	118	4.230E-11
TF:M02067_0	Factor: ER71; motif: ACCGGAARYN; match class: 0	9257	448	5.400E-11
REAC:3214858	RMTs methylate histone arginines	75	25	5.850E-11
GO:0034728	nucleosome organization	171	35	6.350E-11
KEGG:03010	Ribosome	132	32	6.440E-11
GO:0031497	chromatin assembly	162	34	6.870E-11
GO:0003676	nucleic acid binding	4026	271	7.330E-11
TF:M03807_0	Factor: SP2; motif: GNNGGGGGCGGGGSN; match class: 0	12009	549	7.670E-11
GO:0005623	cell	16203	791	7.810E-11
REAC:1640170	Cell Cycle	579	78	8.870E-11
REAC:774815	Nucleosome assembly	71	24	1.280E-10
REAC:606279	Deposition of new CENPA-containing nucleosomes at the centromere	71	24	1.280E-10
TF:M03969_0	Factor: ELF5; motif: ANSMGGAAGTN; match class: 0	6745	348	1.280E-10
GO:0043604	amide biosynthetic process	784	84	1.350E-10
TF:M04710_0	Factor: CHD2; motif: TCTCGCGAG; match class: 0	21162	835	1.690E-10
TF:M00333_1	Factor: ZF5; motif: NRNGNGCGCGCWN; match class: 1	13100	586	1.880E-10
GO:0006333	chromatin assembly or disassembly	187	36	1.960E-10
GO:0005694	chromosome	848	88	2.050E-10
TF:M00428_0	Factor: E2F-1; motif: NKTSSCGC; match class: 0	8854	430	2.110E-10
REAC:157579	Telomere Maintenance	79	25	2.250E-10
GO:0006518	peptide metabolic process	835	87	2.280E-10
GO:0071824	protein-DNA complex subunit organization	220	39	2.930E-10
TF:M00932_0	Factor: Sp1; motif: NNGGGGCGGGGNN; match class: 0	14944	648	3.830E-10
TF:M07039_0	Factor: ETF; motif: CCCCGCCCCYN; match class: 0	14296	626	3.960E-10
GO:0043234	protein complex	3793	256	4.290E-10
GO:0006342	chromatin silencing	118	28	5.290E-10
REAC:1221632	Meiotic synapsis	76	24	6.960E-10
REAC:74160	Gene Expression	1411	140	7.180E-10
TF:M03924_0	Factor: YY1; motif: NNCGCCATTNN; match class: 0	7604	379	7.220E-10
GO:0000313	organellar ribosome	73	22	1.060E-09
GO:0005761	mitochondrial ribosome	73	22	1.060E-09
REAC:194315	Signaling by Rho GTPases	403	60	1.070E-09
TF:M07056_0	Factor: Pitx2; motif: WNTAAWCCCA; match class: 0	16403	694	1.310E-09
TF:M02114_0	Factor: pitx2; motif: NNTAAWCCCA; match class: 0	16403	694	1.310E-09
GO:0034622	cellular macromolecular complex assembly	923	91	1.460E-09
GO:0019538	protein metabolic process	5770	352	1.850E-09
TF:M02052_1	Factor: EHF; motif: CSCGGAARTN; match class: 1	8304	404	2.420E-09
TF:M02066_0	Factor: PEA3; motif: RCCGGAAGYN; match class: 0	5617	296	3.080E-09
REAC:69620	Cell Cycle Checkpoints	184	37	3.390E-09
REAC:195721	Signaling by Wnt	330	52	3.970E-09
GO:0043603	cellular amide metabolic process	1004	95	4.810E-09
TF:M02089_1	Factor: E2F-3; motif: GGCGGGN; match class: 1	12682	565	4.860E-09

Table B.13: Gene set enrichment results of average correlation vector for biclustering pattern Mito.CV1 found in breast cancer analysis in Section 4.2.3, showing the 120 significant terms with adjusted p value < 0.05.

GOID	TERM	Number of genes	Genes in genelist	p value	Average correlation vector
GO:0098588	bounding membrane of organelle	2558	1770	5.991E-12	0.154
GO:0044444	cytoplasmic part	10781	6195	7.827E-12	0.109
GO:0044257	cellular protein catabolic process	614	451	1.868E-11	0.249
GO:0051603	proteolysis involved in cellular protein catabolic process	592	435	3.934E-11	0.250
GO:0031090	organelle membrane	3375	2291	5.007E-11	0.138
GO:0030163	protein catabolic process	762	560	1.303E-10	0.223
GO:0019941	modification-dependent protein catabolic process	542	400	6.791E-10	0.249
GO:0012505	endomembrane system	4489	2813	1.818E-09	0.126
GO:0006511	ubiquitin-dependent protein catabolic process	531	394	2.024E-09	0.246
GO:0043632	modification-dependent macromolecule catabolic process	546	404	3.683E-09	0.242
GO:0070647	protein modification by small protein conjugation or removal	1004	678	4.421E-09	0.197
GO:0005768	endosome	818	567	6.512E-09	0.212
GO:0005739	mitochondrion	2109	1317	4.290E-08	0.150
GO:0005773	vacuole	606	455	1.133E-07	0.221
GO:0032446	protein modification by small protein conjugation	895	603	1.411E-07	0.195
GO:0043230	extracellular organelle	2671	2381	1.735E-07	0.123
GO:0065010	extracellular membrane-bounded organelle	2671	2381	1.735E-07	0.123
GO:0070062	extracellular vesicular exosome	2669	2381	1.735E-07	0.123
GO:0003824	catalytic activity	7631	4533	2.062E-07	0.104
GO:0016567	protein ubiquitination	817	567	2.370E-07	0.197
GO:0000323	lytic vacuole	533	410	2.973E-07	0.227
GO:0005764	lysosome	533	410	2.973E-07	0.227
GO:0048193	Golgi vesicle transport	241	189	6.386E-07	0.304
GO:0031982	vesicle	3913	3061	8.228E-07	0.113
GO:0031988	membrane-bounded vesicle	3783	2976	1.529E-06	0.113
GO:0044248	cellular catabolic process	3220	2183	1.653E-06	0.122
GO:0044267	cellular protein metabolic process	5601	3337	2.952E-06	0.108
GO:0006508	proteolysis	1615	1166	5.042E-06	0.147
GO:0044440	endosomal part	403	302	5.697E-06	0.239
GO:1902494	catalytic complex	927	695	1.109E-05	0.168
GO:0045184	establishment of protein localization	1692	1344	1.282E-05	0.137
GO:0005794	Golgi apparatus	1552	1103	1.640E-05	0.145
GO:0009056	catabolic process	3733	2523	1.959E-05	0.113
GO:0015031	protein transport	1553	1252	2.227E-05	0.139
GO:0005737	cytoplasm	14272	8228	3.492E-05	0.086
GO:0010498	proteasomal protein catabolic process	322	262	3.709E-05	0.240
GO:0004930	G-protein coupled receptor activity	987	646	7.246E-05	-0.079
GO:0010008	endosome membrane	394	294	8.631E-05	0.227
GO:0000786	nucleosome	67	54	9.704E-05	-0.393
GO:1990104	DNA bending complex	67	54	9.704E-05	-0.393
GO:0044815	DNA packaging complex	75	59	1.111E-04	-0.373
GO:0007264	small GTPase mediated signal transduction	567	453	1.152E-04	0.194
GO:0019001	guanyl nucleotide binding	409	334	1.273E-04	0.217
GO:0043565	sequence-specific DNA binding	829	661	1.339E-04	-0.079
GO:0005525	GTP binding	370	315	1.476E-04	0.220
GO:1901575	organic substance catabolic process	3412	2316	1.684E-04	0.111
GO:0032561	guanyl ribonucleotide binding	408	333	1.794E-04	0.215
GO:0008104	protein localization	2180	1666	2.433E-04	0.121
GO:0019003	GDP binding	48	47	3.496E-04	0.477
GO:0016787	hydrolase activity	3107	1999	4.395E-04	0.114
GO:0044437	vacuolar part	374	301	4.613E-04	0.217
GO:0016874	ligase activity	468	362	5.432E-04	0.199
GO:0044429	mitochondrial part	1081	707	5.514E-04	0.155
GO:0000209	protein polyubiquitination	199	178	5.902E-04	0.262
GO:0043161	proteasome-mediated ubiquitin-dependent protein catabolic process	296	243	6.971E-04	0.230
GO:0003008	system process	2235	1570	7.992E-04	-0.031
GO:1990234	transferase complex	618	465	8.593E-04	0.177
GO:0006892	post-Golgi vesicle-mediated transport	99	86	9.056E-04	0.360

GOID	TERM	Number of genes	Genes in genelist	p value	Average correlation vector
GO:0044431	Golgi apparatus part	904	664	1.091E-03	0.157
GO:0000139	Golgi membrane	624	493	1.533E-03	0.173
GO:0019538	protein metabolic process	7013	4073	1.552E-03	0.093
GO:0045335	phagocytic vesicle	98	71	1.585E-03	0.386
GO:0006505	GPI anchor metabolic process	51	30	1.909E-03	0.549
GO:0006464	cellular protein modification process	4196	2626	1.972E-03	0.102
GO:0036211	protein modification process	4196	2626	1.972E-03	0.102
GO:0007186	G-protein coupled receptor signaling pathway	1476	978	2.245E-03	-0.045
GO:0005777	peroxisome	184	107	2.383E-03	0.311
GO:0042579	microbody	184	107	2.383E-03	0.311
GO:0033036	macromolecule localization	2639	1933	3.108E-03	0.110
GO:1902582	single-organism intracellular transport	1497	1104	3.537E-03	0.128
GO:0045892	negative regulation of transcription, DNA-templated	1116	833	3.739E-03	-0.056
GO:0000977	RNA polymerase II regulatory region sequence-specific DNA binding	301	264	3.830E-03	-0.128
GO:0044710	single-organism metabolic process	8623	4735	4.344E-03	0.089
GO:0006506	GPI anchor biosynthetic process	47	28	4.542E-03	0.548
GO:0030659	cytoplasmic vesicle membrane	426	354	4.580E-03	0.191
GO:0001012	RNA polymerase II regulatory region DNA binding	304	267	4.617E-03	-0.125
GO:0051340	regulation of ligase activity	115	104	4.721E-03	0.309
GO:0009083	branched-chain amino acid catabolic process	34	19	4.940E-03	0.657
GO:0006323	DNA packaging	164	116	5.143E-03	-0.217
GO:0051348	negative regulation of transferase activity	306	264	5.244E-03	0.214
GO:0009057	macromolecule catabolic process	1291	929	6.086E-03	0.132
GO:0043412	macromolecule modification	4389	2727	6.312E-03	0.099
GO:0000151	ubiquitin ligase complex	198	155	6.608E-03	0.255
GO:0000981	sequence-specific DNA binding RNA polymerase II transcription factor activity	495	358	6.865E-03	-0.100
GO:0019882	antigen processing and presentation	258	215	7.266E-03	0.230
GO:0060271	cilium morphogenesis	187	130	7.453E-03	0.280
GO:0048002	antigen processing and presentation of peptide antigen	213	176	8.050E-03	0.247
GO:0012506	vesicle membrane	444	367	8.728E-03	0.185
GO:0044281	small molecule metabolic process	4814	2936	8.982E-03	0.097
GO:0031424	keratinization	49	43	9.515E-03	-0.369
GO:0051352	negative regulation of ligase activity	76	74	9.515E-03	0.349
GO:0051444	negative regulation of ubiquitin-protein transferase activity	76	74	9.515E-03	0.349
GO:0061024	membrane organization	927	729	9.528E-03	0.144
GO:0006661	phosphatidylinositol biosynthetic process	126	87	9.761E-03	0.321
GO:0007600	sensory perception	997	720	1.051E-02	-0.054
GO:0009081	branched-chain amino acid metabolic process	40	23	1.060E-02	0.588
GO:0043167	ion binding	6315	5058	1.117E-02	0.086
GO:0050877	neurological system process	1400	1033	1.168E-02	-0.038
GO:0005774	vacuolar membrane	299	235	1.418E-02	0.216
GO:1902679	negative regulation of RNA biosynthetic process	1142	850	1.496E-02	-0.049
GO:0002474	antigen processing and presentation of peptide antigen via MHC class I	112	96	1.624E-02	0.309
GO:0044265	cellular macromolecule catabolic process	1040	740	1.624E-02	0.138
GO:0002478	antigen processing and presentation of exogenous peptide antigen	176	161	1.760E-02	0.249
GO:0019884	antigen processing and presentation of exogenous antigen	178	163	1.785E-02	0.247
GO:0031396	regulation of protein ubiquitination	227	194	1.816E-02	0.227
GO:0005179	hormone activity	132	107	2.143E-02	-0.205
GO:0051436	negative regulation of ubiquitin-protein ligase activity involved in mitotic cell cycle	68	67	2.589E-02	0.352
GO:0044712	single-organism catabolic process	2384	1667	2.674E-02	0.110
GO:0051253	negative regulation of RNA metabolic process	1174	872	3.028E-02	-0.045
GO:0016197	endosomal transport	217	157	3.081E-02	0.244
GO:0051351	positive regulation of ligase activity	96	88	3.098E-02	0.310
GO:0000122	negative regulation of transcription from RNA polymerase II promoter	668	570	3.193E-02	-0.065
GO:0004888	transmembrane signaling receptor activity	1508	1000	3.233E-02	-0.034
GO:0006501	C-terminal protein lipidation	27	27	3.282E-02	0.517
GO:0071103	DNA conformation change	246	167	3.399E-02	-0.157
GO:0046907	intracellular transport	1822	1305	3.485E-02	0.115
GO:0051438	regulation of ubiquitin-protein transferase activity	110	99	3.522E-02	0.293

GOID	TERM	Number of genes	Genes in genelist	p value	Average correlation vector
GO:0000976	transcription regulatory region sequence-specific DNA binding	366	311	3.565E-02	-0.100
GO:0006664	glycolipid metabolic process	137	93	3.599E-02	0.304
GO:0044782	cilium organization	165	117	4.631E-02	0.272

Table B.14: Gene set enrichment results of average correlation vector for biclustering pattern Mito.CV2 found in breast cancer analysis in Section 4.2.3, showing the top 200 of 443 significant terms with adjusted p value < 0.05.

GOID	TERM	Number of genes	Genes in genelist	p value	Average correlation vector
GO:0003723	RNA binding	1808	1270	9.219E-32	-0.186
GO:0044428	nuclear part	3483	2183	5.253E-31	-0.150
GO:0000278	mitotic cell cycle	1169	781	1.476E-29	-0.229
GO:0031981	nuclear lumen	2785	1856	7.638E-29	-0.156
GO:0044822	poly(A) RNA binding	1170	964	8.930E-27	-0.195
GO:1903047	mitotic cell cycle process	966	674	1.021E-24	-0.226
GO:0034660	ncRNA metabolic process	400	274	7.249E-24	-0.324
GO:0070013	intracellular organelle lumen	3486	2415	1.579E-22	-0.128
GO:0031974	membrane-enclosed lumen	3621	2527	1.103E-21	-0.124
GO:0006259	DNA metabolic process	1393	778	2.784E-20	-0.193
GO:0043233	organelle lumen	3548	2472	6.835E-20	-0.121
GO:0005654	nucleoplasm	1793	1266	1.511E-19	-0.155
GO:0022402	cell cycle process	1520	1000	4.644E-18	-0.169
GO:0006396	RNA processing	993	548	5.761E-18	-0.210
GO:0006399	tRNA metabolic process	193	119	9.289E-18	-0.419
GO:0031012	extracellular matrix	558	386	1.045E-17	0.207
GO:0009653	anatomical structure morphogenesis	3188	2109	1.624E-17	0.079
GO:0044772	mitotic cell cycle phase transition	518	416	2.259E-17	-0.240
GO:0044770	cell cycle phase transition	530	427	1.017E-16	-0.234
GO:0030529	ribonucleoprotein complex	744	529	1.443E-15	-0.205
GO:0007049	cell cycle	2122	1355	4.754E-15	-0.140
GO:0034470	ncRNA processing	259	193	1.539E-14	-0.309
GO:0005578	proteinaceous extracellular matrix	365	316	1.561E-14	0.209
GO:0005739	mitochondrion	2109	1317	7.241E-14	-0.135
GO:0005730	nucleolus	728	585	3.128E-13	-0.184
GO:0005694	chromosome	905	627	3.599E-13	-0.179
GO:0008033	tRNA processing	106	77	3.918E-12	-0.440
GO:0044429	mitochondrial part	1081	707	4.048E-12	-0.165
GO:0000902	cell morphogenesis	1341	1011	6.741E-12	0.098
GO:0000793	condensed chromosome	200	149	9.314E-12	-0.336
GO:0072358	cardiovascular system development	1116	797	1.116E-11	0.110
GO:0072359	circulatory system development	1116	797	1.116E-11	0.110
GO:0007059	chromosome segregation	197	141	1.330E-11	-0.343
GO:0022613	ribonucleoprotein complex biogenesis	339	227	1.530E-11	-0.263
GO:0007167	enzyme linked receptor protein signaling pathway	1306	921	2.227E-11	0.102
GO:0000075	cell cycle checkpoint	275	224	2.597E-11	-0.271
GO:0022610	biological adhesion	1342	951	3.070E-11	0.099
GO:0006281	DNA repair	578	354	3.483E-11	-0.216
GO:0007155	cell adhesion	1334	947	3.831E-11	0.099
GO:0000082	G1/S transition of mitotic cell cycle	256	217	7.817E-11	-0.268
GO:0032989	cellular component morphogenesis	1428	1074	8.841E-11	0.090
GO:0032993	protein-DNA complex	334	239	1.140E-10	-0.256
GO:0048285	organelle fission	644	447	1.484E-10	-0.198
GO:0010646	regulation of cell communication	3631	2365	1.854E-10	0.056
GO:0023051	regulation of signaling	3620	2357	2.115E-10	0.056
GO:0001944	vasculature development	711	537	2.247E-10	0.131
GO:0000280	nuclear division	606	426	2.444E-10	-0.201
GO:0044843	cell cycle G1/S phase transition	259	219	2.765E-10	-0.262
GO:0007067	mitotic nuclear division	428	304	4.795E-10	-0.231
GO:0031967	organelle envelope	1166	770	4.838E-10	-0.147
GO:0031975	envelope	1172	774	4.926E-10	-0.147
GO:0030334	regulation of cell migration	576	474	6.727E-10	0.138
GO:0006974	cellular response to DNA damage stimulus	982	605	6.760E-10	-0.163

GOID	TERM	Number of genes	Genes in genelist	p value	Average correlation vector
GO:0044427	chromosomal part	783	539	8.766E-10	-0.172
GO:0001568	blood vessel development	665	508	1.033E-09	0.131
GO:0005743	mitochondrial inner membrane	488	314	1.080E-09	-0.216
GO:0030030	cell projection organization	1349	996	1.104E-09	0.089
GO:0051270	regulation of cellular component movement	691	559	1.172E-09	0.125
GO:0071103	DNA conformation change	246	167	1.193E-09	-0.289
GO:0043228	non-membrane-bounded organelle	4369	2896	1.707E-09	-0.089
GO:0043232	intracellular non-membrane-bounded organelle	4369	2896	1.707E-09	-0.089
GO:0007389	pattern specification process	506	402	1.873E-09	0.146
GO:0019866	organelle inner membrane	531	347	1.963E-09	-0.204
GO:0031145	anaphase-promoting complex-dependent proteasomal ubiquitin-dependent protein catabolic process	89	80	1.972E-09	-0.406
GO:0042254	ribosome biogenesis	188	138	2.023E-09	-0.305
GO:0001655	urogenital system development	373	292	2.390E-09	0.175
GO:2000145	regulation of cell motility	608	496	3.230E-09	0.130
GO:0046872	metal ion binding	4089	3375	5.902E-09	0.039
GO:0000313	organellar ribosome	60	49	6.311E-09	-0.489
GO:0005761	mitochondrial ribosome	60	49	6.311E-09	-0.489
GO:0000775	chromosome, centromeric region	214	139	7.045E-09	-0.313
GO:0006928	cellular component movement	2080	1457	7.608E-09	0.069
GO:0048646	anatomical structure formation involved in morphogenesis	1187	894	1.011E-08	0.089
GO:0043169	cation binding	4173	3440	1.014E-08	0.038
GO:0030198	extracellular matrix organization	422	352	1.068E-08	0.155
GO:0043062	extracellular structure organization	424	353	1.349E-08	0.154
GO:0048468	cell development	2228	1647	1.559E-08	0.062
GO:0009966	regulation of signal transduction	3216	2101	1.655E-08	0.054
GO:0048858	cell projection morphogenesis	913	711	1.828E-08	0.101
GO:0022603	regulation of anatomical structure morphogenesis	843	669	2.311E-08	0.105
GO:0016071	mRNA metabolic process	885	514	3.511E-08	-0.162
GO:0040012	regulation of locomotion	685	548	3.762E-08	0.116
GO:0006261	DNA-dependent DNA replication	161	106	3.896E-08	-0.335
GO:0044420	extracellular matrix part	147	117	4.034E-08	0.278
GO:0072001	renal system development	330	255	4.385E-08	0.175
GO:0042590	antigen processing and presentation of exogenous peptide antigen via MHC class I	79	77	4.441E-08	-0.373
GO:2000026	regulation of multicellular organismal development	1647	1219	5.518E-08	0.072
GO:0048514	blood vessel morphogenesis	583	445	6.481E-08	0.128
GO:0009888	tissue development	2160	1526	6.621E-08	0.063
GO:0008380	RNA splicing	525	256	6.729E-08	-0.216
GO:0051239	regulation of multicellular organismal process	2892	1958	7.054E-08	0.053
GO:0032991	macromolecular complex	5558	3799	7.678E-08	-0.077
GO:0032990	cell part morphogenesis	933	728	8.632E-08	0.096
GO:0042995	cell projection	1718	1288	8.825E-08	0.068
GO:0006260	DNA replication	388	262	1.270E-07	-0.216
GO:0002479	antigen processing and presentation of exogenous peptide antigen via MHC class I, TAP-dependent	75	73	1.294E-07	-0.375
GO:0003002	regionalization	375	312	1.412E-07	0.151
GO:0009123	nucleoside monophosphate metabolic process	624	466	1.470E-07	-0.166
GO:0000502	proteasome complex	127	64	1.726E-07	-0.406
GO:0006397	mRNA processing	610	322	1.907E-07	-0.189
GO:0009887	organ morphogenesis	1011	803	1.951E-07	0.090
GO:0007399	nervous system development	2516	1794	1.976E-07	0.055
GO:0000904	cell morphogenesis involved in differentiation	954	742	2.472E-07	0.093
GO:0001501	skeletal system development	515	417	2.506E-07	0.129
GO:0001822	kidney development	309	240	2.612E-07	0.174
GO:0051028	mRNA transport	143	102	2.885E-07	-0.313
GO:0050911	detection of chemical stimulus involved in sensory perception of smell	451	272	3.485E-07	-0.199
GO:0004984	olfactory receptor activity	418	272	3.485E-07	-0.199
GO:0051439	regulation of ubiquitin-protein ligase activity involved in mitotic cell cycle	81	75	3.661E-07	-0.374
GO:0000375	RNA splicing, via transesterification reactions	358	175	4.150E-07	-0.245
GO:0051436	negative regulation of ubiquitin-protein ligase activity involved in mitotic cell cycle	68	67	4.230E-07	-0.392
GO:0048731	system development	5637	3561	4.687E-07	0.034

GOID	TERM	Number of genes	Genes in genelist	p value	Average correlation vector
GO:0007275	multicellular organismal development	6429	4034	5.115E-07	0.031
GO:0006310	DNA recombination	273	185	5.259E-07	-0.245
GO:0040011	locomotion	1887	1323	6.062E-07	0.065
GO:0050793	regulation of developmental process	2231	1584	8.097E-07	0.056
GO:0000228	nuclear chromosome	390	308	8.327E-07	-0.192
GO:0007606	sensory perception of chemical stimulus	559	347	8.660E-07	-0.175
GO:0050907	detection of chemical stimulus involved in sensory perception	492	306	9.324E-07	-0.185
GO:0000377	RNA splicing, via transesterification reactions with bulged adenosine as nucleophile	349	170	1.044E-06	-0.243
GO:0000398	mRNA splicing, via spliceosome	349	170	1.044E-06	-0.243
GO:0007093	mitotic cell cycle checkpoint	187	163	1.186E-06	-0.259
GO:1901990	regulation of mitotic cell cycle phase transition	280	234	1.198E-06	-0.218
GO:0016477	cell migration	1277	941	1.304E-06	0.078
GO:0005643	nuclear pore	78	59	1.374E-06	-0.396
GO:0000779	condensed chromosome, centromeric region	99	75	1.395E-06	-0.378
GO:0005740	mitochondrial envelope	743	483	1.429E-06	-0.156
GO:0009161	ribonucleoside monophosphate metabolic process	606	456	1.501E-06	-0.160
GO:0007169	transmembrane receptor protein tyrosine kinase signaling pathway	873	653	1.568E-06	0.094
GO:0000819	sister chromatid segregation	73	55	1.706E-06	-0.429
GO:0044446	intracellular organelle part	9239	5593	1.710E-06	-0.067
GO:0072395	signal transduction involved in cell cycle checkpoint	72	67	2.157E-06	-0.377
GO:0051437	positive regulation of ubiquitin-protein ligase activity involved in mitotic cell cycle	73	69	2.185E-06	-0.373
GO:0016779	nucleotidyltransferase activity	154	108	2.400E-06	-0.292
GO:0005524	ATP binding	1462	1285	2.496E-06	-0.106
GO:0005509	calcium ion binding	688	583	2.953E-06	0.099
GO:0007346	regulation of mitotic cell cycle	423	349	2.971E-06	-0.180
GO:0010564	regulation of cell cycle process	535	423	3.093E-06	-0.166
GO:0007608	sensory perception of smell	482	297	3.349E-06	-0.182
GO:0005759	mitochondrial matrix	365	296	3.491E-06	-0.192
GO:0030554	adenyl nucleotide binding	1525	1336	4.061E-06	-0.103
GO:0022008	neurogenesis	1639	1211	4.168E-06	0.063
GO:0031570	DNA integrity checkpoint	172	145	4.231E-06	-0.262
GO:0030182	neuron differentiation	1394	1045	4.293E-06	0.069
GO:0051301	cell division	890	638	4.596E-06	-0.142
GO:0048870	cell motility	1374	1002	4.879E-06	0.072
GO:0051674	localization of cell	1375	1002	4.879E-06	0.072
GO:0031397	negative regulation of protein ubiquitination	115	107	4.973E-06	-0.295
GO:0022616	DNA strand elongation	44	35	5.087E-06	-0.502
GO:0001525	angiogenesis	464	366	5.140E-06	0.127
GO:0072401	signal transduction involved in DNA integrity checkpoint	71	66	5.643E-06	-0.371
GO:0072413	signal transduction involved in mitotic cell cycle checkpoint	71	66	5.643E-06	-0.371
GO:0072422	signal transduction involved in DNA damage checkpoint	71	66	5.643E-06	-0.371
GO:1902402	signal transduction involved in mitotic DNA damage checkpoint	71	66	5.643E-06	-0.371
GO:1902403	signal transduction involved in mitotic DNA integrity checkpoint	71	66	5.643E-06	-0.371
GO:1901987	regulation of cell cycle phase transition	290	243	6.052E-06	-0.207
GO:0006271	DNA strand elongation involved in DNA replication	41	32	6.300E-06	-0.522
GO:0048699	generation of neurons	1536	1141	6.404E-06	0.064
GO:0031966	mitochondrial membrane	689	452	6.497E-06	-0.155
GO:0009126	purine nucleoside monophosphate metabolic process	591	444	7.125E-06	-0.156
GO:0032879	regulation of localization	2401	1726	7.141E-06	0.050
GO:0051352	negative regulation of ligase activity	76	74	8.376E-06	-0.350
GO:0051444	negative regulation of ubiquitin-protein transferase activity	76	74	8.376E-06	-0.350
GO:0050657	nucleic acid transport	171	120	8.665E-06	-0.267
GO:0050658	RNA transport	171	120	8.665E-06	-0.267
GO:0051236	establishment of RNA localization	171	120	8.665E-06	-0.267
GO:0009593	detection of chemical stimulus	527	338	9.366E-06	-0.168
GO:0006412	translation	771	462	9.393E-06	-0.153
GO:0007507	heart development	533	405	1.008E-05	0.115
GO:0009167	purine ribonucleoside monophosphate metabolic process	590	443	1.010E-05	-0.155
GO:0010648	negative regulation of cell communication	1129	849	1.056E-05	0.078

GOID	TERM	Number of genes	Genes in genelist	p value	Average correlation vector
GO:0023057	negative regulation of signaling	1127	847	1.094E-05	0.078
GO:0000777	condensed chromosome kinetochore	90	70	1.180E-05	-0.370
GO:1903321	negative regulation of protein modification by small protein conjugation or removal	121	112	1.210E-05	-0.283
GO:0006323	DNA packaging	164	116	1.307E-05	-0.283
GO:0046930	pore complex	95	75	1.330E-05	-0.330
GO:0072431	signal transduction involved in mitotic G1 DNA damage checkpoint	69	65	1.421E-05	-0.365
GO:1902400	intracellular signal transduction involved in G1 DNA damage checkpoint	69	65	1.421E-05	-0.365
GO:1902531	regulation of intracellular signal transduction	1855	1270	1.541E-05	0.060
GO:0044452	nucleolar part	39	32	1.614E-05	-0.507
GO:0000070	mitotic sister chromatid segregation	65	47	1.623E-05	-0.438
GO:0000776	kinetochore	156	92	1.691E-05	-0.323
GO:0032559	adenyl ribonucleotide binding	1507	1318	1.692E-05	-0.101
GO:0051094	positive regulation of developmental process	971	755	1.758E-05	0.080
GO:0045333	cellular respiration	221	151	1.759E-05	-0.247
GO:0048583	regulation of response to stimulus	4468	2734	1.761E-05	0.036
GO:1901988	negative regulation of cell cycle phase transition	218	187	1.931E-05	-0.227
GO:1901991	negative regulation of mitotic cell cycle phase transition	213	182	1.990E-05	-0.229
GO:0048666	neuron development	1092	845	2.000E-05	0.074
GO:0048856	anatomical structure development	6783	4102	2.034E-05	0.026
GO:0019838	growth factor binding	137	113	2.498E-05	0.237
GO:0071363	cellular response to growth factor stimulus	822	617	2.781E-05	0.089
GO:0000077	DNA damage checkpoint	161	140	2.887E-05	-0.253
GO:0010948	negative regulation of cell cycle process	278	234	3.046E-05	-0.205
GO:1901265	nucleoside phosphate binding	2358	1976	3.089E-05	-0.086
GO:0000166	nucleotide binding	2357	1975	3.629E-05	-0.086
GO:0006977	DNA damage response, signal transduction by p53 class mediator resulting in cell cycle arrest	68	64	3.806E-05	-0.357
GO:0001882	nucleoside binding	1849	1591	4.027E-05	-0.093
GO:0009719	response to endogenous stimulus	1683	1236	4.030E-05	0.057
GO:0009968	negative regulation of signal transduction	1081	806	4.204E-05	0.077

Table B.15: Gene set enrichment results of average correlation vector for biclustering pattern Mito.CV3 found in breast cancer analysis in Section 4.2.3, showing the top 200 of 313 significant terms with adjusted p value < 0.05.

GOID	TERM	Number of genes	Genes in genelist	p value	Average correlation vector
GO:0000278	mitotic cell cycle	1169	781	8.565E-52	-0.270
GO:0044428	nuclear part	3483	2183	6.671E-49	-0.154
GO:0031981	nuclear lumen	2785	1856	9.984E-48	-0.165
GO:1903047	mitotic cell cycle process	966	674	3.552E-45	-0.271
GO:0022402	cell cycle process	1520	1000	3.459E-44	-0.218
GO:0007049	cell cycle	2122	1355	1.168E-41	-0.182
GO:0005654	nucleoplasm	1793	1266	2.632E-35	-0.171
GO:0003723	RNA binding	1808	1270	8.276E-31	-0.157
GO:0044772	mitotic cell cycle phase transition	518	416	6.279E-30	-0.282
GO:0044770	cell cycle phase transition	530	427	1.190E-29	-0.276
GO:0006396	RNA processing	993	548	2.113E-28	-0.233
GO:0044822	poly(A) RNA binding	1170	964	6.257E-28	-0.173
GO:0070013	intracellular organelle lumen	3486	2415	2.058E-27	-0.108
GO:0005694	chromosome	905	627	2.558E-25	-0.209
GO:0003676	nucleic acid binding	4689	3157	6.891E-25	-0.087
GO:0031974	membrane-enclosed lumen	3621	2527	7.151E-25	-0.101
GO:0043233	organelle lumen	3548	2472	8.385E-25	-0.102
GO:0005634	nucleus	8112	5260	1.139E-23	-0.067
GO:0006259	DNA metabolic process	1393	778	1.427E-23	-0.180
GO:0000280	nuclear division	606	426	2.355E-23	-0.248
GO:0000793	condensed chromosome	200	149	2.069E-22	-0.413
GO:0048285	organelle fission	644	447	4.184E-22	-0.236
GO:0007067	mitotic nuclear division	428	304	3.745E-21	-0.283
GO:0000775	chromosome, centromeric region	214	139	2.208E-20	-0.411

GOID	TERM	Number of genes	Genes in genelist	p value	Average correlation vector
GO:0043228	non-membrane-bounded organelle	4369	2896	3.733E-19	-0.081
GO:0043232	intracellular non-membrane-bounded organelle	4369	2896	3.733E-19	-0.081
GO:0007059	chromosome segregation	197	141	9.582E-19	-0.391
GO:0044427	chromosomal part	783	539	1.170E-18	-0.195
GO:0090304	nucleic acid metabolic process	7863	3949	1.456E-18	-0.067
GO:0005730	nucleolus	728	585	1.783E-18	-0.184
GO:0051301	cell division	890	638	3.876E-18	-0.179
GO:0006397	mRNA processing	610	322	1.306E-17	-0.243
GO:0008380	RNA splicing	525	256	1.690E-17	-0.273
GO:1901363	heterocyclic compound binding	7008	4813	2.741E-17	-0.058
GO:0097159	organic cyclic compound binding	7093	4877	1.136E-16	-0.056
GO:0006281	DNA repair	578	354	2.946E-16	-0.225
GO:0006261	DNA-dependent DNA replication	161	106	6.618E-16	-0.421
GO:0000082	G1/S transition of mitotic cell cycle	256	217	2.014E-15	-0.288
GO:0044843	cell cycle G1/S phase transition	259	219	3.689E-15	-0.284
GO:0000075	cell cycle checkpoint	275	224	3.716E-14	-0.270
GO:0006974	cellular response to DNA damage stimulus	982	605	5.410E-14	-0.158
GO:0006310	DNA recombination	273	185	3.908E-13	-0.287
GO:0000228	nuclear chromosome	390	308	5.037E-13	-0.219
GO:0000776	kinetochore	156	92	6.589E-13	-0.413
GO:0016071	mRNA metabolic process	885	514	9.443E-13	-0.164
GO:0000375	RNA splicing, via transesterification reactions	358	175	1.107E-12	-0.289
GO:0010564	regulation of cell cycle process	535	423	5.260E-12	-0.180
GO:1901990	regulation of mitotic cell cycle phase transition	280	234	6.238E-12	-0.244
GO:0000779	condensed chromosome, centromeric region	99	75	6.852E-12	-0.445
GO:0006260	DNA replication	388	262	7.869E-12	-0.232
GO:0044260	cellular macromolecule metabolic process	12514	6183	8.168E-12	-0.041
GO:0051726	regulation of cell cycle	964	723	8.637E-12	-0.135
GO:1901987	regulation of cell cycle phase transition	290	243	1.222E-11	-0.236
GO:0034660	ncRNA metabolic process	400	274	1.330E-11	-0.220
GO:0005819	spindle	287	213	1.607E-11	-0.254
GO:0051276	chromosome organization	1127	678	1.666E-11	-0.136
GO:0032993	protein-DNA complex	334	239	2.834E-11	-0.237
GO:0000377	RNA splicing, via transesterification reactions with bulged adenosine as nucleophile	349	170	3.432E-11	-0.277
GO:0000398	mRNA splicing, via spliceosome	349	170	3.432E-11	-0.277
GO:0006139	nucleobase-containing compound metabolic process	9873	5149	5.391E-11	-0.044
GO:0000819	sister chromatid segregation	73	55	5.636E-11	-0.503
GO:0032991	macromolecular complex	5558	3799	6.040E-11	-0.052
GO:0016070	RNA metabolic process	6737	3512	1.195E-10	-0.052
GO:0044451	nucleoplasm part	717	531	1.673E-10	-0.147
GO:1901988	negative regulation of cell cycle phase transition	218	187	2.215E-10	-0.258
GO:0000777	condensed chromosome kinetochore	90	70	2.299E-10	-0.435
GO:0046483	heterocycle metabolic process	10158	5298	3.116E-10	-0.041
GO:1901991	negative regulation of mitotic cell cycle phase transition	213	182	3.486E-10	-0.260
GO:0015630	microtubule cytoskeleton	1219	780	3.584E-10	-0.121
GO:0005681	spliceosomal complex	164	118	3.742E-10	-0.322
GO:0051028	mRNA transport	143	102	6.471E-10	-0.344
GO:0022613	ribonucleoprotein complex biogenesis	339	227	9.426E-10	-0.225
GO:0006725	cellular aromatic compound metabolic process	10189	5310	1.014E-09	-0.040
GO:0010948	negative regulation of cell cycle process	278	234	1.338E-09	-0.223
GO:0000070	mitotic sister chromatid segregation	65	47	1.348E-09	-0.519
GO:0071103	DNA conformation change	246	167	1.651E-09	-0.266
GO:0002682	regulation of immune system process	1544	1025	2.902E-09	0.128
GO:0034470	ncRNA processing	259	193	2.930E-09	-0.239
GO:0007346	regulation of mitotic cell cycle	423	349	3.302E-09	-0.177
GO:0010467	gene expression	7890	4156	3.746E-09	-0.044
GO:0050657	nucleic acid transport	171	120	4.229E-09	-0.306
GO:0050658	RNA transport	171	120	4.229E-09	-0.306
GO:0051236	establishment of RNA localization	171	120	4.229E-09	-0.306
GO:0022616	DNA strand elongation	44	35	7.707E-09	-0.584
GO:0006403	RNA localization	178	126	8.879E-09	-0.294
GO:0007093	mitotic cell cycle checkpoint	187	163	1.013E-08	-0.257
GO:0044425	membrane part	7949	5116	1.584E-08	0.072
GO:0044454	nuclear chromosome part	344	275	2.746E-08	-0.190

GOID	TERM	Number of genes	Genes in genelist	p value	Average correlation vector
GO:0030529	ribonucleoprotein complex	744	529	3.851E-08	-0.133
GO:0000086	G2/M transition of mitotic cell cycle	178	151	4.764E-08	-0.264
GO:0044786	cell cycle DNA replication	43	39	5.746E-08	-0.523
GO:0043234	protein complex	4612	3227	6.331E-08	-0.048
GO:1901360	organic cyclic compound metabolic process	10552	5498	7.242E-08	-0.035
GO:1902589	single-organism organelle organization	2350	1540	7.690E-08	-0.074
GO:0006271	DNA strand elongation involved in DNA replication	41	32	7.934E-08	-0.584
GO:0044839	cell cycle G2/M phase transition	180	153	9.105E-08	-0.258
GO:0042254	ribosome biogenesis	188	138	1.160E-07	-0.264
GO:0031224	intrinsic component of membrane	5833	4330	1.560E-07	0.073
GO:0003677	DNA binding	2781	1984	1.844E-07	-0.059
GO:0000226	microtubule cytoskeleton organization	393	278	2.020E-07	-0.183
GO:0016021	integral component of membrane	5650	4230	2.459E-07	0.073
GO:0006302	double-strand break repair	166	104	3.313E-07	-0.302
GO:0034641	cellular nitrogen compound metabolic process	10485	5500	4.965E-07	-0.033
GO:0034645	cellular macromolecule biosynthetic process	7021	3800	5.233E-07	-0.040
GO:0000922	spindle pole	110	86	6.944E-07	-0.330
GO:1901265	nucleoside phosphate binding	2358	1976	7.878E-07	-0.059
GO:0006955	immune response	1821	1206	8.614E-07	0.109
GO:0000166	nucleotide binding	2357	1975	8.661E-07	-0.059
GO:0043044	ATP-dependent chromatin remodeling	56	46	9.036E-07	-0.449
GO:0031577	spindle checkpoint	58	49	9.942E-07	-0.439
GO:0015931	nucleobase-containing compound transport	210	146	1.127E-06	-0.242
GO:0044446	intracellular organelle part	9239	5593	1.300E-06	-0.032
GO:0033260	nuclear cell cycle DNA replication	34	31	1.435E-06	-0.550
GO:0016887	ATPase activity	441	351	1.922E-06	-0.151
GO:0004386	helicase activity	176	132	1.953E-06	-0.252
GO:1990234	transferase complex	618	465	2.376E-06	-0.126
GO:0006399	tRNA metabolic process	193	119	3.246E-06	-0.266
GO:0000323	lytic vacuole	533	410	4.006E-06	0.165
GO:0005764	lysosome	533	410	4.006E-06	0.165
GO:0017111	nucleoside-triphosphatase activity	862	651	4.133E-06	-0.104
GO:0051239	regulation of multicellular organismal process	2892	1958	4.313E-06	0.088
GO:0009059	macromolecule biosynthetic process	7259	3922	4.592E-06	-0.036
GO:0000794	condensed nuclear chromosome	77	64	5.501E-06	-0.360
GO:0044422	organelle part	9563	5748	5.843E-06	-0.030
GO:0006996	organelle organization	3692	2303	7.470E-06	-0.051
GO:0031570	DNA integrity checkpoint	172	145	7.494E-06	-0.232
GO:0006952	defense response	1956	1285	7.940E-06	0.101
GO:0008026	ATP-dependent helicase activity	91	82	9.540E-06	-0.308
GO:0070035	purine NTP-dependent helicase activity	91	82	9.540E-06	-0.308
GO:0007017	microtubule-based process	631	427	1.082E-05	-0.131
GO:0005643	nuclear pore	78	59	1.147E-05	-0.371
GO:0050776	regulation of immune response	1013	686	1.365E-05	0.129
GO:0032549	ribonucleoside binding	1839	1583	1.510E-05	-0.061
GO:0035639	purine ribonucleoside triphosphate binding	1804	1572	1.641E-05	-0.061
GO:0043170	macromolecule metabolic process	14207	6952	1.714E-05	-0.025
GO:0001882	nucleoside binding	1849	1591	1.731E-05	-0.061
GO:0044430	cytoskeletal part	1728	1128	1.921E-05	-0.073
GO:0007126	meiotic nuclear division	191	150	2.450E-05	-0.222
GO:0006954	inflammatory response	649	514	2.515E-05	0.143
GO:0005773	vacuole	606	455	2.648E-05	0.151
GO:0031012	extracellular matrix	558	386	2.649E-05	0.162
GO:0001883	purine nucleoside binding	1838	1581	2.715E-05	-0.060
GO:0006807	nitrogen compound metabolic process	11158	5831	2.853E-05	-0.027
GO:0032550	purine ribonucleoside binding	1835	1579	2.977E-05	-0.060
GO:0016604	nuclear body	339	265	2.978E-05	-0.160
GO:0043486	histone exchange	32	25	3.144E-05	-0.564
GO:0005813	centrosome	435	321	3.357E-05	-0.147
GO:0030397	membrane disassembly	39	38	3.868E-05	-0.456
GO:0051081	nuclear envelope disassembly	39	38	3.868E-05	-0.456
GO:0031145	anaphase-promoting complex-dependent proteasomal ubiquitin-dependent protein catabolic process	89	80	4.504E-05	-0.307
GO:0031982	vesicle	3913	3061	4.538E-05	0.071
GO:0071944	cell periphery	6341	4023	5.721E-05	0.067

GOID	TERM	Number of genes	Genes in genelist	p value	Average correlation vector
GO:0007077	mitotic nuclear envelope disassembly	37	36	5.848E-05	-0.465
GO:0031988	membrane-bounded vesicle	3783	2976	5.866E-05	0.071
GO:0005615	extracellular space	1277	1073	6.057E-05	0.104
GO:0017076	purine nucleotide binding	1897	1630	6.279E-05	-0.057
GO:0016817	hydrolase activity, acting on acid anhydrides	927	693	6.496E-05	-0.092
GO:0016462	pyrophosphatase activity	920	687	7.331E-05	-0.092
GO:0032553	ribonucleotide binding	1893	1624	7.333E-05	-0.057
GO:0005576	extracellular region	5375	3709	7.669E-05	0.066
GO:0032555	purine ribonucleotide binding	1877	1611	7.815E-05	-0.057
GO:0016818	hydrolase activity, acting on acid anhydrides, in phosphorus-containing anhydrides	922	689	7.979E-05	-0.092
GO:0051321	meiotic cell cycle	202	158	8.002E-05	-0.208
GO:0002684	positive regulation of immune system process	930	620	8.781E-05	0.128
GO:0000077	DNA damage checkpoint	161	140	8.812E-05	-0.219
GO:0005886	plasma membrane	6168	3939	9.988E-05	0.066
GO:0006405	RNA export from nucleus	96	62	1.028E-04	-0.336
GO:0006353	DNA-templated transcription, termination	91	72	1.233E-04	-0.303
GO:0044459	plasma membrane part	2761	1980	1.265E-04	0.082
GO:0006364	rRNA processing	125	96	1.354E-04	-0.263
GO:0006270	DNA replication initiation	32	22	1.673E-04	-0.581
GO:0032392	DNA geometric change	74	50	1.806E-04	-0.375
GO:0005524	ATP binding	1462	1285	1.807E-04	-0.064
GO:0006200	ATP catabolic process	404	327	1.904E-04	-0.135
GO:0032508	DNA duplex unwinding	72	49	1.959E-04	-0.379
GO:0046930	pore complex	95	75	1.996E-04	-0.300
GO:0002274	myeloid leukocyte activation	142	127	2.076E-04	0.249
GO:0006323	DNA packaging	164	116	2.189E-04	-0.238
GO:0009158	ribonucleoside monophosphate catabolic process	408	331	2.271E-04	-0.134
GO:0009169	purine ribonucleoside monophosphate catabolic process	408	331	2.271E-04	-0.134
GO:0008094	DNA-dependent ATPase activity	83	67	2.322E-04	-0.319
GO:0071824	protein-DNA complex subunit organization	165	126	2.331E-04	-0.224
GO:2000145	regulation of cell motility	608	496	2.773E-04	0.135
GO:0009128	purine nucleoside monophosphate catabolic process	409	332	2.852E-04	-0.132
GO:0030334	regulation of cell migration	576	474	2.898E-04	0.137
GO:0048583	regulation of response to stimulus	4468	2734	3.246E-04	0.070
GO:0009125	nucleoside monophosphate catabolic process	411	333	3.611E-04	-0.131
GO:0006338	chromatin remodeling	135	103	3.621E-04	-0.246
GO:0071174	mitotic spindle checkpoint	45	41	3.810E-04	-0.404
GO:0044421	extracellular region part	3939	3181	3.839E-04	0.067
GO:0031055	chromatin remodeling at centromere	26	18	4.042E-04	-0.616
GO:0016072	rRNA metabolic process	134	100	4.309E-04	-0.247
GO:0051270	regulation of cellular component movement	691	559	4.495E-04	0.127
GO:0005578	proteinaceous extracellular matrix	365	316	4.667E-04	0.164
GO:0040012	regulation of locomotion	685	548	4.737E-04	0.128
GO:0008033	tRNA processing	106	77	4.769E-04	-0.285
GO:0036094	small molecule binding	2659	2219	5.002E-04	-0.043
GO:0042623	ATPase activity, coupled	298	251	5.036E-04	-0.152
GO:1903046	meiotic cell cycle process	109	80	5.062E-04	-0.281
GO:0032101	regulation of response to external stimulus	686	546	5.127E-04	0.129

Table B.16: Gene set enrichment results of average correlation vector for biclustering pattern ICT1.CV1 found in breast cancer analysis in Section 4.2.3, showing the top 200 of 680 significant terms with adjusted p value < 0.05.

GOID	TERM	Number of genes	Genes in genelist	p value	Average correlation vector
GO:0022610	biological adhesion	1342	951	2.688E-29	-0.205
GO:0007155	cell adhesion	1334	947	1.148E-28	-0.204
GO:0048583	regulation of response to stimulus	4468	2734	4.731E-26	-0.123
GO:0016477	cell migration	1277	941	3.405E-25	-0.192
GO:0040011	locomotion	1887	1323	7.986E-24	-0.161
GO:0048870	cell motility	1374	1002	8.142E-24	-0.182
GO:0051674	localization of cell	1375	1002	8.142E-24	-0.182
GO:0072358	cardiovascular system development	1116	797	1.348E-23	-0.203

GOID	TERM	Number of genes	Genes in genelist	p value	Average correlation vector
GO:0072359	circulatory system development	1116	797	1.348E-23	-0.203
GO:0006928	cellular component movement	2080	1457	7.571E-23	-0.152
GO:0001944	vasculature development	711	537	2.238E-22	-0.239
GO:0001775	cell activation	1101	799	4.184E-22	-0.195
GO:0009653	anatomical structure morphogenesis	3188	2109	4.283E-22	-0.128
GO:0051239	regulation of multicellular organismal process	2892	1958	5.201E-22	-0.132
GO:0044429	mitochondrial part	1081	707	5.569E-22	0.194
GO:0002682	regulation of immune system process	1544	1025	1.883E-21	-0.172
GO:0005739	mitochondrion	2109	1317	2.695E-21	0.140
GO:0030334	regulation of cell migration	576	474	4.175E-21	-0.245
GO:0048584	positive regulation of response to stimulus	2005	1362	6.418E-21	-0.150
GO:0001568	blood vessel development	665	508	1.194E-20	-0.236
GO:0050793	regulation of developmental process	2231	1584	4.619E-20	-0.139
GO:0051270	regulation of cellular component movement	691	559	2.324E-19	-0.219
GO:2000026	regulation of multicellular organismal development	1647	1219	2.672E-19	-0.153
GO:2000145	regulation of cell motility	608	496	4.787E-19	-0.230
GO:0009966	regulation of signal transduction	3216	2101	7.282E-19	-0.119
GO:0006955	immune response	1821	1206	1.264E-18	-0.150
GO:0031012	extracellular matrix	558	386	1.725E-18	-0.256
GO:0044459	plasma membrane part	2761	1980	2.095E-18	-0.121
GO:0048514	blood vessel morphogenesis	583	445	6.502E-18	-0.236
GO:0019866	organelle inner membrane	531	347	1.869E-17	0.249
GO:0023051	regulation of signaling	3620	2357	2.517E-17	-0.109
GO:0032993	protein-DNA complex	334	239	2.810E-17	0.301
GO:0010646	regulation of cell communication	3631	2365	3.083E-17	-0.109
GO:0040012	regulation of locomotion	685	548	4.782E-17	-0.209
GO:0005743	mitochondrial inner membrane	488	314	6.357E-17	0.258
GO:0048731	system development	5637	3561	1.182E-16	-0.092
GO:0007275	multicellular organismal development	6429	4034	2.100E-16	-0.087
GO:0007167	enzyme linked receptor protein signaling pathway	1306	921	2.787E-16	-0.161
GO:0002684	positive regulation of immune system process	930	620	3.985E-16	-0.191
GO:0071944	cell periphery	6341	4023	6.387E-16	-0.086
GO:0048856	anatomical structure development	6783	4102	1.158E-15	-0.085
GO:0070013	intracellular organelle lumen	3486	2415	1.293E-15	0.090
GO:0045321	leukocyte activation	812	587	1.872E-15	-0.192
GO:0044767	single-organism developmental process	7612	4547	1.985E-15	-0.081
GO:0003723	RNA binding	1808	1270	3.046E-15	0.121
GO:0031226	intrinsic component of plasma membrane	1430	1210	5.942E-15	-0.137
GO:0031974	membrane-enclosed lumen	3621	2527	6.656E-15	0.087
GO:0032502	developmental process	7760	4589	8.786E-15	-0.080
GO:0005886	plasma membrane	6168	3939	8.972E-15	-0.084
GO:0042127	regulation of cell proliferation	1599	1209	1.192E-14	-0.136
GO:0001525	angiogenesis	464	366	1.592E-14	-0.237
GO:0031981	nuclear lumen	2785	1856	2.268E-14	0.099
GO:0023056	positive regulation of signaling	1355	1035	2.458E-14	-0.145
GO:0044822	poly(A) RNA binding	1170	964	2.488E-14	0.134
GO:0006259	DNA metabolic process	1393	778	3.720E-14	0.152
GO:0002376	immune system process	3353	2021	7.148E-14	-0.106
GO:0006935	chemotaxis	799	595	7.175E-14	-0.184
GO:0042330	taxis	799	595	7.175E-14	-0.184
GO:0000278	mitotic cell cycle	1169	781	8.648E-14	0.149
GO:0005887	integral component of plasma membrane	1359	1171	1.224E-13	-0.134
GO:0032879	regulation of localization	2401	1726	1.442E-13	-0.113
GO:0010647	positive regulation of cell communication	1360	1041	1.487E-13	-0.141
GO:0009967	positive regulation of signal transduction	1285	981	1.561E-13	-0.145
GO:0043233	organelle lumen	3548	2472	1.800E-13	0.084
GO:0046872	metal ion binding	4089	3375	1.815E-13	-0.086
GO:0044428	nuclear part	3483	2183	1.829E-13	0.089
GO:0030335	positive regulation of cell migration	317	259	2.170E-13	-0.269
GO:0040017	positive regulation of locomotion	356	279	2.380E-13	-0.260
GO:0009986	cell surface	703	589	4.045E-13	-0.181
GO:0050776	regulation of immune response	1013	686	4.363E-13	-0.167
GO:0009605	response to external stimulus	2532	1780	4.919E-13	-0.111
GO:0046649	lymphocyte activation	694	504	6.495E-13	-0.192
GO:0005578	proteinaceous extracellular matrix	365	316	7.015E-13	-0.242

GOID	TERM	Number of genes	Genes in genelist	p value	Average correlation vector
GO:0031975	envelope	1172	774	7.200E-13	0.145
GO:0005615	extracellular space	1277	1073	7.539E-13	-0.138
GO:0031967	organelle envelope	1166	770	8.207E-13	0.145
GO:0005740	mitochondrial envelope	743	483	9.383E-13	0.183
GO:2000147	positive regulation of cell motility	328	263	9.619E-13	-0.262
GO:0043169	cation binding	4173	3440	1.000E-12	-0.083
GO:0009888	tissue development	2160	1526	1.359E-12	-0.117
GO:0035556	intracellular signal transduction	2879	1967	1.963E-12	-0.103
GO:0051272	positive regulation of cellular component movement	341	270	2.204E-12	-0.256
GO:0022603	regulation of anatomical structure morphogenesis	843	669	2.473E-12	-0.167
GO:1902531	regulation of intracellular signal transduction	1855	1270	2.732E-12	-0.123
GO:0048513	organ development	3828	2632	2.790E-12	-0.092
GO:0023052	signaling	8975	5054	2.948E-12	-0.072
GO:0044700	single organism signaling	8975	5054	2.948E-12	-0.072
GO:0005654	nucleoplasm	1793	1266	3.391E-12	0.111
GO:0009611	response to wounding	1117	886	4.067E-12	-0.146
GO:0050865	regulation of cell activation	492	377	4.161E-12	-0.214
GO:0042110	T cell activation	499	366	4.930E-12	-0.217
GO:0051094	positive regulation of developmental process	971	755	5.318E-12	-0.156
GO:0005694	chromosome	905	627	7.070E-12	0.156
GO:0006281	DNA repair	578	354	7.821E-12	0.208
GO:0045595	regulation of cell differentiation	1560	1138	7.939E-12	-0.129
GO:0048869	cellular developmental process	4670	3087	9.055E-12	-0.085
GO:0048518	positive regulation of biological process	6634	3774	9.621E-12	-0.078
GO:0007154	cell communication	9101	5120	1.450E-11	-0.070
GO:0030054	cell junction	1167	958	1.712E-11	-0.137
GO:1903047	mitotic cell cycle process	966	674	1.824E-11	0.149
GO:0006954	inflammatory response	649	514	2.319E-11	-0.183
GO:0044446	intracellular organelle part	9239	5593	3.392E-11	0.053
GO:0044707	single-multicellular organism process	9631	5555	3.852E-11	-0.067
GO:0007166	cell surface receptor signaling pathway	4618	2857	4.430E-11	-0.085
GO:0048468	cell development	2228	1647	4.763E-11	-0.107
GO:0007165	signal transduction	7988	4580	4.881E-11	-0.071
GO:0000313	organellar ribosome	60	49	4.955E-11	0.549
GO:0005761	mitochondrial ribosome	60	49	4.955E-11	0.549
GO:0060326	cell chemotaxis	251	190	5.212E-11	-0.286
GO:0009887	organ morphogenesis	1011	803	8.005E-11	-0.146
GO:0070161	anchoring junction	478	416	8.094E-11	-0.197
GO:0006952	defense response	1956	1285	8.106E-11	-0.118
GO:0031966	mitochondrial membrane	689	452	8.467E-11	0.176
GO:0050794	regulation of cellular process	16220	8000	9.863E-11	-0.058
GO:0098552	side of membrane	311	270	1.001E-10	-0.239
GO:0044815	DNA packaging complex	75	59	1.010E-10	0.496
GO:0032501	multicellular organismal process	9979	5728	1.253E-10	-0.065
GO:0008285	negative regulation of cell proliferation	655	552	1.472E-10	-0.170
GO:0030154	cell differentiation	4368	2930	1.645E-10	-0.083
GO:0009897	external side of plasma membrane	224	198	2.158E-10	-0.275
GO:0000786	nucleosome	67	54	2.893E-10	0.510
GO:1990104	DNA bending complex	67	54	2.893E-10	0.510
GO:0050789	regulation of biological process	17691	8437	3.335E-10	-0.056
GO:0044427	chromosomal part	783	539	4.038E-10	0.158
GO:0002694	regulation of leukocyte activation	460	350	4.311E-10	-0.205
GO:0008283	cell proliferation	2136	1591	4.699E-10	-0.104
GO:0005759	mitochondrial matrix	365	296	5.176E-10	0.211
GO:0050778	positive regulation of immune response	652	437	5.318E-10	-0.185
GO:0045597	positive regulation of cell differentiation	688	546	5.511E-10	-0.169
GO:0005912	adherens junction	457	402	5.538E-10	-0.194
GO:0050673	epithelial cell proliferation	325	279	6.186E-10	-0.232
GO:0072001	renal system development	330	255	6.717E-10	-0.240
GO:0048585	negative regulation of response to stimulus	1300	966	7.107E-10	-0.130
GO:0000902	cell morphogenesis	1341	1011	7.998E-10	-0.126
GO:0030198	extracellular matrix organization	422	352	8.317E-10	-0.207
GO:0001655	urogenital system development	373	292	9.139E-10	-0.225
GO:0048646	anatomical structure formation involved in morphogenesis	1187	894	9.199E-10	-0.133
GO:0065007	biological regulation	18926	8865	1.068E-09	-0.055

GOID	TERM	Number of genes	Genes in genelist	p value	Average correlation vector
GO:0030055	cell-substrate junction	388	349	1.378E-09	-0.204
GO:0044455	mitochondrial membrane part	212	128	1.409E-09	0.317
GO:0006974	cellular response to DNA damage stimulus	982	605	1.526E-09	0.144
GO:0071103	DNA conformation change	246	167	1.534E-09	0.278
GO:0043062	extracellular structure organization	424	353	1.678E-09	-0.205
GO:0005924	cell-substrate adherens junction	380	346	2.102E-09	-0.203
GO:0044422	organelle part	9563	5748	2.356E-09	0.048
GO:0032989	cellular component morphogenesis	1428	1074	2.830E-09	-0.120
GO:0016337	single organismal cell-cell adhesion	364	305	4.002E-09	-0.215
GO:0005539	glycosaminoglycan binding	193	176	4.391E-09	-0.280
GO:0019219	regulation of nucleobase-containing compound metabolic process	5589	3541	5.056E-09	-0.072
GO:0005925	focal adhesion	374	341	8.548E-09	-0.200
GO:0050678	regulation of epithelial cell proliferation	272	236	9.240E-09	-0.239
GO:0022900	electron transport chain	149	101	9.299E-09	0.345
GO:0032101	regulation of response to external stimulus	686	546	9.496E-09	-0.162
GO:0042060	wound healing	781	628	1.148E-08	-0.149
GO:0043087	regulation of GTPase activity	655	393	1.384E-08	-0.182
GO:0051249	regulation of lymphocyte activation	409	308	1.424E-08	-0.205
GO:0033124	regulation of GTP catabolic process	657	394	1.490E-08	-0.181
GO:0001667	ameboidal cell migration	285	238	1.504E-08	-0.235
GO:0023014	signal transduction by phosphorylation	790	576	1.509E-08	-0.155
GO:0007067	mitotic nuclear division	428	304	1.599E-08	0.197
GO:0007169	transmembrane receptor protein tyrosine kinase signaling pathway	873	653	1.617E-08	-0.145
GO:0050867	positive regulation of cell activation	307	243	1.758E-08	-0.229
GO:0000165	MAPK cascade	757	554	2.043E-08	-0.156
GO:0022904	respiratory electron transport chain	146	100	2.430E-08	0.340
GO:0002764	immune response-regulating signaling pathway	566	416	3.870E-08	-0.174
GO:0048519	negative regulation of biological process	5363	3322	3.898E-08	-0.072
GO:0070469	respiratory chain	114	67	4.465E-08	0.410
GO:0030030	cell projection organization	1349	996	4.556E-08	-0.118
GO:0070887	cellular response to chemical stimulus	3061	2033	4.953E-08	-0.087
GO:0098602	single organism cell adhesion	422	340	5.010E-08	-0.194
GO:0001501	skeletal system development	515	417	5.195E-08	-0.177
GO:1900542	regulation of purine nucleotide metabolic process	857	558	5.334E-08	-0.151
GO:0000775	chromosome, centromeric region	214	139	5.456E-08	0.285
GO:0001822	kidney development	309	240	5.502E-08	-0.228
GO:0007399	nervous system development	2516	1794	5.790E-08	-0.091
GO:0080090	regulation of primary metabolic process	7699	4661	5.931E-08	-0.063
GO:0048285	organelle fission	644	447	6.051E-08	0.158
GO:0043167	ion binding	6315	5058	6.834E-08	-0.060
GO:0009118	regulation of nucleoside metabolic process	712	441	7.921E-08	-0.167
GO:0022402	cell cycle process	1520	1000	8.055E-08	0.104
GO:0002253	activation of immune response	541	366	8.088E-08	-0.184
GO:0033121	regulation of purine nucleotide catabolic process	705	434	9.917E-08	-0.167
GO:0000793	condensed chromosome	200	149	9.931E-08	0.272
GO:0044770	cell cycle phase transition	530	427	1.001E-07	0.158
GO:0060429	epithelium development	1252	941	1.002E-07	-0.121
GO:0019222	regulation of metabolic process	8809	5166	1.016E-07	-0.060
GO:0043547	positive regulation of GTPase activity	605	362	1.057E-07	-0.181
GO:0002683	negative regulation of immune system process	253	205	1.107E-07	-0.241
GO:0005746	mitochondrial respiratory chain	106	62	1.114E-07	0.418
GO:0006140	regulation of nucleotide metabolic process	862	561	1.120E-07	-0.149
GO:0044772	mitotic cell cycle phase transition	518	416	1.194E-07	0.160
GO:0030811	regulation of nucleotide catabolic process	706	435	1.469E-07	-0.165
GO:0005576	extracellular region	5375	3709	1.667E-07	-0.067
GO:0048522	positive regulation of cellular process	5622	3387	1.842E-07	-0.069
GO:0005102	receptor binding	1689	1175	1.870E-07	-0.107
GO:0051056	regulation of small GTPase mediated signal transduction	606	376	1.950E-07	-0.176
GO:0048523	negative regulation of cellular process	4754	3022	1.968E-07	-0.072
GO:0034660	ncRNA metabolic process	400	274	1.973E-07	0.194
GO:0050900	leukocyte migration	362	287	2.076E-07	-0.202
GO:0022008	neurogenesis	1639	1211	2.089E-07	-0.105

Appendix C

Nanostring gene set

Table C.1: All the genes measured in the nanostring gene set described in Section 4.4.2.1 with description of groups. Also included is the PGC induction score for each gene from MitoCarta

Genes	TF network	MitoCarta	PGC induced	P53 induced	mtDNA	Control	ETC	Cytosolic Ribosome.	Mito ribosome	LFC
NRIP1	Yes	No		No	No	No	0	No	No	
PPRC1	Yes	No		No	No	No	0	No	No	
PPARGC1A	Yes	No		No	No	No	0	No	No	
PPARGC1B	Yes	No		No	No	No	0	No	No	
PPARG	Yes	No		No	No	No	0	No	No	
PPARD	Yes	No		No	No	No	0	No	No	
PPARA	Yes	No		No	No	No	0	No	No	
ESRRA	Yes	No		No	No	No	0	No	No	
ESRRB	Yes	No		No	No	No	0	No	No	
ESRRG	Yes	No		No	No	No	0	No	No	
GABPA	Yes	No		No	No	No	0	No	No	
NRF1	Yes	No		No	No	No	0	No	No	
YY1	Yes	No		No	No	No	0	No	No	
CREB	Yes	No		No	No	No	0	No	No	
MYC	Yes	No		No	No	No	0	No	No	
PRMT1	Yes	No		No	No	No	0	No	No	
TFAM	Yes	Yes	4	No	No	No	0	No	No	
TFB1M	Yes	Yes		No	No	No	0	No	No	
TFB2M	Yes	Yes		No	No	No	0	No	No	
MEF2A	Yes	No		No	No	No	0	No	No	
MYOD1	Yes	No		No	No	No	0	No	No	
FOXO1	Yes	No		No	No	No	0	No	No	
CDK7	Yes	No		No	No	No	0	No	No	
SIRT1	Yes	No		No	No	No	0	Yes	No	
FBXW7	Yes	No		No	No	No	0	No	No	
KAT2A	Yes	No		No	No	No	0	No	No	
MYBBP1A	Yes	No		No	No	No	0	No	No	
ELK1	Yes	No		No	No	No	0	No	No	
E2F1	Yes	No		No	No	No	0	No	No	
TP53	Yes	No		No	No	No	0	No	No	
SRF	Yes	No		No	No	No	0	No	No	
PPARGC1A B5 -NT	Yes	No		No	No	No	0	No	No	
ALDH5A1	No	Yes	0	No	No	No	0	No	No	Mito upper fork pos LFC
BDH1	No	Yes	16	No	No	No	0	No	No	Mito upper fork pos LFC
VAMP8	No	Yes	2	No	No	No	0	No	No	Mito upper fork pos LFC
HSD17B8	No	Yes	2	No	No	No	0	No	No	Mito upper fork pos LFC
GPT2	No	Yes	0	No	No	No	0	No	No	Mito upper fork pos LFC
PXMP2	No	Yes	2	No	No	No	0	No	No	Mito upper fork pos LFC
NTHL1	No	Yes	0	No	No	No	0	No	No	Mito upper fork pos LFC

Genes	TF network	MitoCarta	PGC induced	P53 induced	mtDNA	Control	ETC	Cytosolic Ribosome.	Mito ribosome	LFC
OGDHL	No	Yes		No	No	No	0	No	No	Mito upper fork pos LFC
AKAP1	No	Yes	3	No	No	No	0	No	No	Mito upper fork pos LFC
SLC25A10	No	Yes	0	No	No	No	0	No	No	Mito upper fork pos LFC
MRPL12	No	Yes	4	No	No	No	0	No	Yes	Mito upper fork pos LFC
DHTKD1	No	Yes	0	No	No	No	0	No	No	Mito upper fork pos LFC
TIMM8A	No	Yes	4	No	No	No	0	No	No	Mito upper fork pos LFC
SFXN4	No	Yes	0	No	No	No	0	No	No	Mito upper fork pos LFC
L2HGDH	No	Yes	4	No	No	No	0	No	No	Mito upper fork pos LFC
TSHZ3	No	Yes	0	No	No	No	0	No	No	Mito upper fork neg LFC
SLC25A24	No	Yes		No	No	No	0	No	No	Mito upper fork neg LFC
FTH1	No	Yes	1	No	No	No	0	No	No	Mito upper fork neg LFC
ME1	No	Yes		No	No	No	0	No	No	Mito upper fork neg LFC
DDAH1	No	Yes	0	No	No	No	0	No	No	Mito upper fork neg LFC
CYB5R2	No	Yes		No	No	No	0	No	No	Mito upper fork neg LFC
RAB11FIP5	No	Yes	1	No	No	No	0	No	No	Mito upper fork neg LFC
HSPB7	No	Yes	2	No	No	No	0	No	No	Mito upper fork neg LFC
TSPO	No	Yes	1	No	No	No	0	No	No	Mito upper fork neg LFC
ATP10D	No	Yes	2	No	No	No	0	No	No	Mito upper fork neg LFC
CLIC4	No	Yes	1	No	No	No	0	No	No	Mito upper fork neg LFC
HK1	No	Yes	0	No	No	No	0	No	No	Mito upper fork neg LFC
GALC	No	Yes	2	No	No	No	0	No	No	Mito upper fork neg LFC
CKMT2	No	Yes	15	No	No	No	0	No	No	Mito upper fork neg LFC
ACOT9	No	Yes	0	No	No	No	0	No	No	Mito upper fork neg LFC
ICT1	No	Yes	2	No	No	No	0	No	Yes	
MRPS25	No	Yes	7	No	No	No	0	No	Yes	
MRPL11	No	Yes	2	No	No	No	0	No	Yes	
MRPS12	No	Yes	2	No	No	No	0	No	Yes	
MRPL13	No	Yes	2	No	No	No	0	No	Yes	
MRPS26	No	Yes	2	No	No	No	0	No	Yes	
MRPS33	No	Yes	1	No	No	No	0	No	Yes	
MRPS17	No	Yes	2	No	No	No	0	No	Yes	
MRPS18B	No	Yes	2	No	No	No	0	No	Yes	
MRPS36	No	Yes	2	No	No	No	0	No	Yes	
MRPS15	No	Yes	1	No	No	No	0	No	Yes	
MRPL48	No	Yes	2	No	No	No	0	No	Yes	
MRPL27	No	Yes	1	No	No	No	0	No	Yes	
MRPL37	No	Yes	2	No	No	No	0	No	Yes	
H2AFZ	No	No		No	No	No	0	No	No	Non mito upper fork pos LFC
SNRPC	No	No		No	No	No	0	No	No	Non mito upper fork pos LFC
PPIL1	No	No		No	No	No	0	No	No	Non mito upper fork pos LFC
SNRPF	No	No		No	No	No	0	No	No	Non mito upper fork pos LFC
NUDT5	No	No		No	No	No	0	No	No	Non mito upper fork pos LFC
PAICS	No	No		No	No	No	0	No	No	Non mito upper fork pos LFC
POLR3K	No	No		No	No	No	0	No	No	Non mito upper fork pos LFC
RPA3	No	No		No	No	No	0	No	No	Non mito upper fork pos LFC
PSMA5	No	No		No	No	No	0	No	No	Non mito upper fork pos LFC
POLR2D	No	No		No	No	No	0	No	No	Non mito upper fork pos LFC
THOC4	No	No		No	No	No	0	No	No	Non mito upper fork pos LFC
RAD51C	No	No		No	No	No	0	No	No	Non mito upper fork pos LFC
EBP	No	No		No	No	No	0	No	No	Non mito upper fork pos LFC
NUP85	No	No		No	No	No	0	No	No	Non mito upper fork pos LFC
DLC1	No	No		No	No	No	0	No	No	Non mito upper fork neg LFC
PHLDB1	No	No		No	No	No	0	No	No	Non mito upper fork neg LFC
PTRF	No	No		No	No	No	0	No	No	Non mito upper fork neg LFC
AFAP1	No	No		No	No	No	0	No	No	Non mito upper fork neg LFC
AHR	No	No		No	No	No	0	No	No	Non mito upper fork neg LFC
MFGE8	No	No		No	No	No	0	No	No	Non mito upper fork neg LFC
CHST3	No	No		No	No	No	0	No	No	Non mito upper fork neg LFC
VCL	No	No		No	No	No	0	No	No	Non mito upper fork neg LFC
ZNF223	No	No		No	No	No	0	No	No	Non mito upper fork neg LFC
CCBE1	No	No		No	No	No	0	No	No	Non mito upper fork neg LFC
ARHGAP21	No	No		No	No	No	0	No	No	Non mito upper fork neg LFC
EHD2	No	No		No	No	No	0	No	No	Non mito upper fork neg LFC

Genes	TF network	MitoCarta	PGC induced	P53 induced	mtDNA	Control	ETC	Cytosolic Ribosome.	Mito ribosome	LFC
DSEL	No	No		No	No	No	0	No	No	Non mito upper fork neg LFC
NAV2	No	No		No	No	No	0	No	No	Non mito upper fork neg LFC
COL16A1	No	No		No	No	No	0	No	No	Non mito upper fork neg LFC
RPL38	No	No		No	No	No	0	No	Yes	
EIF4A3	No	No		No	No	No	0	Yes	No	
EXOSC5	No	No		No	No	No	0	Yes	No	
RPL30	No	No		No	No	No	0	Yes	No	
RPL8	No	No		No	No	No	0	Yes	No	
WDR12	No	No		No	No	No	0	Yes	No	
RPS21	No	No		No	No	No	0	Yes	No	
NHP2L1	No	No		No	No	No	0	Yes	No	
APEX1	No	No		No	No	No	0	Yes	No	
SRP68	No	No		No	No	No	0	Yes	No	
RRP1B	No	No		No	No	No	0	Yes	No	
EXOSC4	No	No		No	No	No	0	Yes	No	
NOLC1	No	No		No	No	No	0	Yes	No	
RRS1	No	No		No	No	No	0	Yes	No	
UTP18	No	No		No	No	No	0	Yes	No	
MRPL15	No	Yes	3	No	No	No	0	No	Yes	
MRPL34	No	Yes	3	No	No	No	0	No	Yes	
ATP5C1	No	Yes	3	No	No	No	V	No	No	
ATP5O	No	Yes	3	No	No	No	V	No	No	
ATP5A1	No	Yes	3	No	No	No	V	No	No	
COX5B	No	Yes	3	No	No	No	IV	No	No	
COX7B	No	Yes	3	No	No	No	IV	No	No	
COX11	No	Yes	6	No	No	No	IV	No	No	
NDUFB5	No	Yes	3	No	No	No	I	No	No	
NDUFA6	No	Yes	3	No	No	No	I	No	No	
NDUFB10	No	Yes	4	No	No	No	I	No	No	
NDUFS3	No	Yes	3	No	No	No	I	No	No	
ACTA2	No	No		Yes	No	No	0	No	No	
APAF1	No	No		Yes	No	No	0	No	No	
ARID3A	No	No		Yes	No	No	0	No	No	
BAX	No	Yes	0	Yes	No	No	0	No	No	
BID	No	Yes	2	Yes	No	No	0	No	No	
CASP1	No	No		Yes	No	No	0	No	No	
CAV1	No	No		Yes	No	No	0	No	No	
CTSD	No	No		Yes	No	No	0	No	No	
DNMT1	No	No		Yes	No	No	0	No	No	
EEF1A1	No	No		Yes	No	No	0	No	No	
FAS	No	No		Yes	No	No	0	No	No	
HIC1	No	No		Yes	No	No	0	No	No	
IRF5	No	No		Yes	No	No	0	No	No	
KRT8	No	No		Yes	No	No	0	No	No	
LGALS3	No	No		Yes	No	No	0	No	No	
LRDD	No	No		Yes	No	No	0	No	No	
MMP2	No	No		Yes	No	No	0	No	No	
PMS2	No	No		Yes	No	No	0	No	No	
PTK2	No	No		Yes	No	No	0	No	No	
PYCARD	No	No		Yes	No	No	0	No	No	
RFWD2	No	No		Yes	No	No	0	No	No	
SCD	No	No		Yes	No	No	0	No	No	
TGFA	No	No		Yes	No	No	0	No	No	
PUMA	No	No		Yes	No	No	0	No	No	
PMAIP1 (NOXA)	No	No		Yes	No	No	0	No	No	
SCD5	No	No		No	No	Yes	0	No	No	
CCDC85B	No	No		No	No	Yes	0	No	No	
ARF1	No	No		No	No	Yes	0	No	No	
SUMO3	No	No		No	No	Yes	0	No	No	
MT-CO1	No	No		No	Yes	No	IV	No	No	
MT-CO2	No	No		No	Yes	No	IV	No	No	
MT-CYB	No	No		No	Yes	No	III	No	No	
MT-ND1	No	No		No	Yes	No	I	No	No	

Genes	TF network	MitoCarta	PGC induced	P53 induced	mtDNA	Control	ETC	Cytosolic Ribosome.	Mito ribosome	LFC
MT-ND2	No	No		No	Yes	No	I	No	No	
MT-ND3	No	No		No	Yes	No	I	No	No	
MT-ND4	No	No		No	Yes	No	I	No	No	
MT-ND4L	No	No		No	Yes	No	I	No	No	
MT-ND5	No	No		No	Yes	No	I	No	No	
MT-ND6	No	No		No	Yes	No	I	No	No	

Appendix D

Materials

Below is a table of the materials used in this thesis

Table D.1: Table of materials used in this thesis.

Material	Source	Other information
	Tissue culture	
DMEM	Gibco 31966-021	
Fetal bovine serum	Gibco 10500-064	
Glutamax	Gibco 35050-038	
Normocin	InvivoGen ant-nr-2	
Trypan blue	Gibco 15250-061	
Trysin	Gibco 25200-056	0.25%
	Antibodies	
GAPDH	Santa Cruz sc-25778	
β-tubulin	Santa Cruz sc-9104	
GRP75	Santa Cruz sc-1058	1:2000
Oxphos cocktail	Novex 458199	1:1000
	Western blots	
Blotting pads	Invitrogen LC2010	
ECL	GE Healthcare PRN2106	
Ladder	BioRad 161-0375	
MES running buffer	Novex NP0002	20X
NuPAGE 10% gels	Novex NP0301BOX	1mmx10wells

Material	Source	Other information
NuPAGE LDS Sample buffer	Novex NP0007	4X
Ponceau S	Sigma P7170	
PVDF membranes	Immobilin P IPVH00010	
Transfer buffer	Novex NP0006	20X
Tween	Sigma P1379	
	Kits	
RNeasy Mini Kit	Qiagen 74106	
	Chemicals	
Antimycin A	Sigma A8674	
Carbonyl cyanide-4-(trifluoromethoxy) phenylhydrazone (FCCP)	Sigma C2920	
DMEM powder	Sigma D5030	
Glucose	Sigma G8270	
Oligomycin	Sigma 75371	
Phoshate buffered saline (PBS)	Gibco 14190-094	
Sodium pyruvate	Sigma P8574	
	Nanostring	
nCounter Master Kit	Nanostring technologies NAA-AKIT-192	
nCounter Gene Expression (GX) CodeSet	Nanostring technologies GXA-P1CS-096	
	GC-MC	
scyllo-Inositol	Sigma I8132	
Nor-leucine	Sigma N8513	
Methoxyamine hydrochloride	Sigma 226904	
Pyridine	Sigma 270970	
BSTFA + TMCS	Supleco 33155-U	99:1